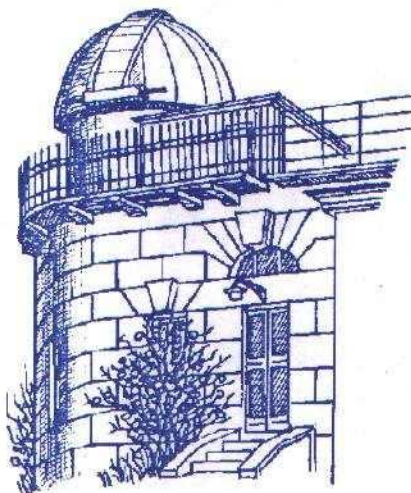


ODESSA ASTRONOMICAL PUBLICATIONS

Volume 16 (2003)



Odessa National University

ODESSA ASTRONOMICAL PUBLICATIONS

Volume 16 (2003)

(Известия Одесской астрономической обсерватории)

Special issue with the proceedings
of the conference
«Interacting Binary Stars»

Editorial Board:

V. G. Karetnikov – *Editor-in-Chief*
G. A. Garbuzov – *Associate Editor*
I. L. Andronov – *Executive Editor*

Advisory Editors:

S. M. Andrievsky, S. K. Aslanov, N. S. Komarov, N. I. Koshkin,
T. V. Mishenina, Yu. I. Zaginailo, A. I. Zhuk

Responsible for this Issue: I. L. Andronov

Technical editing: L. L. Chinarova, S. L. Strakhova

Address:

Astronomical Observatory, Odessa National University
T. G. Shevchenko Park, Odessa 65014 UKRAINE
Tel., Fax: + 038 + 0482 + 22 84 42

E-mail: astro@paco.odessa.ua
<http://www.astro.od.ua> (AO)
<http://oap16.pochta.ru>

Печатается по решению Ученого совета Астрономической обсерватории
Одесского национального университета им. И. И. Мечникова
от 15 декабря 2003 г., протокол № 10

Printed in the UKRAINE
ASTROPRINT PUBLISHING COMPANY

CONTENTS

<i>Karetnikov V. G.</i>	
Foreword	2
Contents	3
The conference «Chemical and dynamic evolution of stars and galaxies»	
<i>Andrievsky S. M.</i>	
Galactic abundance gradient	4
<i>Bisnovatyi-Kogan G. S.</i>	
Atoms in magnetic fealds: possible origin of chemical anomalies in magnetic stars	11
<i>Chernyshova I. V.</i>	
Chemical abundances and evolutionary status of some LB type stars and FBSwl	16
<i>Khan S. A., Shulyak D. V.</i>	
Model atmosphere of HD101065 with individualized abundances	18
<i>Komarov N. S.</i>	
Evolution from the nuclides to the chemical elements	23
<i>Leushin V. V.</i>	
Evolution of chemical structure extreme He-rich stars	37
<i>Lyubimkov L. S.</i>	
On the Crimea-Texas project “Surface abundances of light elements for a large sample of early B-type stars”	47
<i>Marsakov V.A., Borkova T.V.</i>	
Subsystems of the Galactic halo, their structures and compositions	52
<i>Merezhin V. P.</i>	
Correction of the scale of astrophysical quantities	61
<i>Mishenina T. V.</i>	
Element abundances in stars: connection with chemical evolution of a Galaxy ..	71
<i>Pavlenko Ya. V.</i>	
Infrered spectra of cool stars – nature and models (Review)	88
<i>Shavrina A. V., Polosukhina N. S., Tsymbal V. V., Pavlenko Ya. V., Yushchenko A. V., Gopka V. F., Veles A. A.</i>	
Some features of roAp stars spectrum	92
<i>Shustov B. M.</i>	
Galaxies and the intergalactic medium: evolutionary interrelations	97

FOREWORD

This volume of Odessa Astronomical Publications contains the contributions that have been presented by the participants of International conference "Chemical and dynamical evolution of stars and galaxies". Mentioned conference is a successor of the annual workshop "Stellar atmospheres", that was first organized in 1976. During 25 years "Stellar atmospheres" workshop was held many times in different cities of the former USSR, frequently in Odessa. An idea to transform the workshop into International conference significantly enlarging its scientific scope, and to invite astronomers which are working not only in the field of stellar, but also galactic chemistry, was proposed by Prof. Dr. N.S.Komarov (chairman of the conference).

The conference "Chemical and dynamical evolution of stars and galaxies" was held in Odessa (8-24 August 2002) and appeared to be a very fruitful. Meeting where two groups of specialists both on galactic chemodynamics and stellar physics discussed a big number of different actual problems (<http://www.conference.pochtamt.ru>).

At the concluding session all the participants made an unanimous resolution to regularly organize such conferences in the future with a periodicity of 4 years. The next conference "Chemical and dynamical evolution of stars and galaxies" has been scheduled for 2006 in Odessa.

Past conference "Chemical and dynamical evolution of stars and galaxies" was supported by INTAS. The conference was combined with the Summer International school of young astronomers "Astronomy and beyond: Astrophysics, Cosmology and Astrobiology" (12-18 August 2002).

The conference and the Summer school were organized by astronomers of Astronomical Observatory and Department of Astronomy of Odessa National University, Radioastronomical Observatory "URAN-4" of Radioastronomical Institute of Ukrainian Academy of Sciences, and members of Odessa Astronomical Society under the support from Ukrainian Astronomical Association (Kiev) and Euro-Asian Astronomical Society (Moscow).

The published in this volume reviews are systematized in the alphabetic order using the name of the first co-author. These reviews, as well as all the rest contributions (abstracts) presented at the conference, can be found at <http://oap14.pochtamt.ru/oap15.htm>.

Editorial Board expresses a hope that all the materials presented at the conference "Chemical and dynamical evolution of stars and galaxies" will be interesting for the specialists.

V. G. Karetnikov

GALACTIC ABUNDANCE GRADIENT

S.M. Andrievsky

Department of Astronomy, Odessa National University, Shevchenko Park, 65014, Odessa, Ukraine
email: scan@deneb.odessa.ua

ABSTRACT. This contribution is an overview of three papers (Andrievsky et al. 2002a; 2002b; 2002c) devoted to the metallicity distribution in galactic disc.

1. Introduction

In recent years the problem of radial abundance gradients in spiral galaxies has emerged as a central problem in the field of galactic chemodynamics. Abundance gradients as observational characteristics of the galactic disc are among the most important input parameters in any theory of galactic chemical evolution. Further development of theories of galactic chemodynamics is dramatically hampered by the scarcity of observational data, their large uncertainties and, in some cases, apparent contradictions between independent observational results. Many questions concerning the present-day abundance distribution in the galactic disc, its spatial properties, and evolution with time, still have to be answered.

A number of studies of abundance gradients in the galactic disk have been performed in recent years. The results obtained are rather disparate: from no detectable gradient to a rather significant slope of about $-0.1 \text{ dex kpc}^{-1}$.

Usually the following objects are used to derive galactic abundance gradient: hot main sequence B stars, HII regions, planetary nebulae, open clusters.

Compared to other objects supplying us with an information about the radial distribution of elemental abundances in the galactic disc, Cepheids have several advantages:

- 1) they are primary distance calibrators which provide excellent distance estimates;
- 2) they are luminous stars allowing one to probe to large distances;
- 3) the abundances of many chemical elements can be measured from Cepheid spectra (many more than from HII regions or B stars). This is important for investigation of the distribution in the galactic disc of absolute abundances and abundance ratios. Additionally, Cepheids allow the study of abundances past the iron-peak which are not generally available in HII regions or B stars;
- 4) lines in Cepheid spectra are sharp and well-defined

which enables one to derive elemental abundances with high reliability.

As it was shown in Andrievsky et al. (2002a) – Paper I, Andrievsky et al. (2002b) – Paper II the radial abundance distribution within the region of galactocentric distances from 4 to 10 kpc is best described by two distinct zones. One of them (inner: $4.0 \text{ kpc} < R_G < 6.5 \text{ kpc}$) is characterized by a rather steep gradient, while in the mid part of galactic disc ($6.5 \text{ kpc} < R_G < 10.0 \text{ kpc}$), the distribution is essentially flat (e.g. for iron the gradient is $d[\text{Fe}/\text{H}]/dR_G \approx -0.03 \text{ dex/kpc}$).

As discussed in Paper I and Paper II, such a bimodal character in the distribution may result from the combined effect of the radial gas flow in the disc and the radial distribution of the star formation rate. We note here that there are conflicting models of the galactic structure, and that possibly the metallicity gradients can help to decide which are the more likely ones. According to Sevenster (1999a; 1999b) and others (see references in Paper I) the bar extends its influence to a co-rotation radius at about 4–6 kpc. In contrast, according to Amaral & Lépine (1997) and others, the spiral arms extend from the Inner Lindblad Resonance which is at about 2.5 kpc, to the Outer Lindblad Resonance, at about 12 kpc, and the co-rotation of the spiral pattern is close to the solar galactic orbit. In the vicinity of a bar we expect to see elongated orbits of stars, and consequently, a small metallicity gradient. On the other hand, according to Lépine, Mishurov & Dedikov (2001) and Paper I an interaction between the gas and spiral waves in the disc forces the gas to flow in opposite directions inside and outside the Galactic co-rotation annulus. This mechanism produces a cleaning effect in the middle part of the disc and consequently a flattening of the metallicity distribution. At the same time, a decreased star formation rate in the vicinity of the galactic co-rotation, where the relative velocity of the spiral arms and of the gas passing through these arms is small, should also result in some decrease in the abundances.

In Andrievsky et al. (2002c) – Paper III we have begun to investigate the radial abundance distribution in the outer disc. The region of primary interest is at a galactocentric radius $R_G \approx 10 \text{ kpc}$, where according to Twarog et al. (1997) there exists a discontinuity in the metallicity distribution. Such a discontinuity can

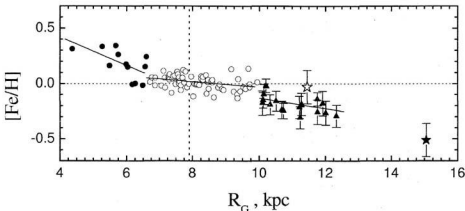


Figure 1: The radial distribution of the iron abundance. *Open circles* - the data from Paper I, *black circles* - the data from Paper II, *black triangles* - Paper III. $2\text{-}\sigma$ interval is indicated. The position of EE Mon is indicated by *filled asterisk*. The Sun is marked by the intersection of the dashed lines.

be suspected from earlier works of Janes (1979), Panagia & Tosi (1981) and Friel (1995). However, Twarog et al. (1997) were the first to clearly stress this result. Twarog et al. used photometric metallicities (interpreted to imply $[\text{Fe}/\text{H}]$) for a large sample of open clusters, and they found that galactic disc breaks into two distinct zones. Between $R_G \approx 6.5 - 10.0$ kpc they found a mean iron abundance $\langle [\text{Fe}/\text{H}] \rangle$ of ≈ 0 (i.e., the slope is very small, if present). Beyond $R_G \approx 10.0$ kpc the mean $\langle [\text{Fe}/\text{H}] \rangle$ is ≈ -0.3 . This implies a sharp discontinuity at $R_G \approx 10$ kpc.

Recently, Caputo et al. (2001) reported a similar result. Those authors calibrated BV1 data for a large sample of galactic Cepheids (galactocentric distances from 6 to 19 kpc) as a function of metallicity using non-linear pulsation models. Their results (although not very reliable on a per star basis) suggest that the derived metallicity distribution in the galactic disc can be represented either by a single gradient of $-0.05 \text{ dex kpc}^{-1}$, or by a two-zone distribution with a slope of $-0.01 \pm 0.05 \text{ dex kpc}^{-1}$ within 10 kpc and $-0.02 \pm 0.02 \text{ dex kpc}^{-1}$ in the outer region of the galactic disc. In other words, within each region the metallicity gradient is weak to non-existent, while between these regions a significant change of the metallicity/gradient does occur.

2. Radial abundance distributions: from inner to outer disc

To make the picture on galactic abundance gradients as complete as possible, one can plot data from Paper

I-III together. Figs. 1-5 display the derived dependencies between the abundances of 25 chemical elements and galactocentric distances. As the iron abundances are the most reliable we will concentrate our discussion on the iron gradient $d[\text{Fe}/\text{H}]/dR_G$.

3. Discussion

3.1. Iron abundance gradient

Distances can be separated into three zones: the inner part of the galactic disk (gradient $d[\text{Fe}/\text{H}]/dR_G \approx -0.13 \pm 0.03 \text{ dex kpc}^{-1}$), the mid part of the disk (gradient $\approx -0.02 \pm 0.01 \text{ dex kpc}^{-1}$), and a piece of outer disc. For the latter we derive a gradient $-0.06 \pm 0.01 \text{ dex kpc}^{-1}$ and a mean $[\text{Fe}/\text{H}] \approx -0.19 \pm 0.08 \text{ dex}$. The gradient for each zone was derived from a least-squares fit using the weighted data. Thus, the abundance distribution over the galactocentric distances 4-10 kpc cannot be represented by a single gradient value. More likely, the distribution is bimodal: it is flatter in the solar neighborhood with a small gradient, and becomes steeper towards the galactic center. The steepening begins at the distance about 6.5 kpc.

The transition zone at 10 kpc can be easily identified in Fig. 1. After this point the metallicity drops by approximately 0.2 dex. All the stars in the bin beyond 10 kpc are iron-deficient. The same result is seen in Fig. 3ab of Twarog et al. (1997) which shows their open cluster metallicity values as a function of galactocentric radius. It should be noted that the sample of open clusters used by Twarog et al. consists of the

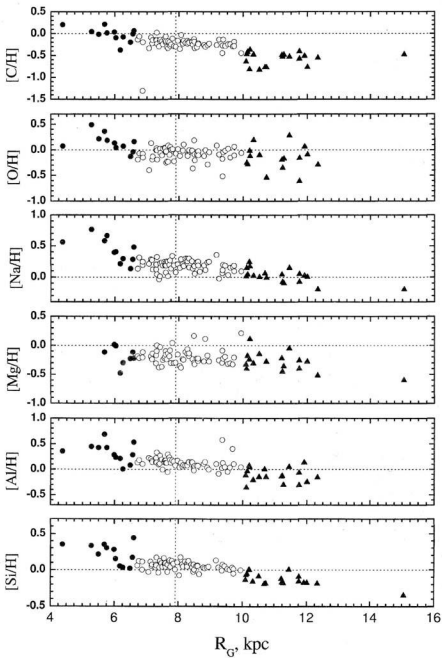


Figure 2: Same as Fig. 1, but for elements C-Si

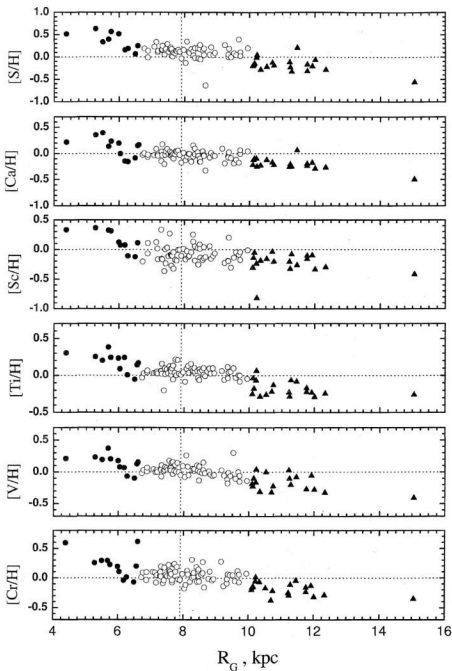


Figure 3: Same as Fig. 1, but for elements S–Cr

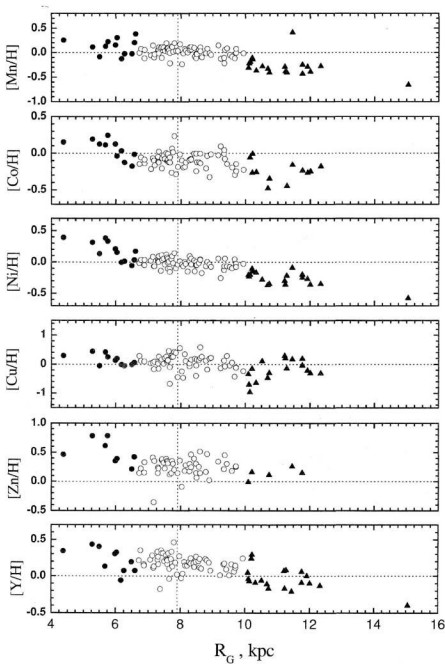


Figure 4: Same as Fig. 1, but for elements Mn–Y

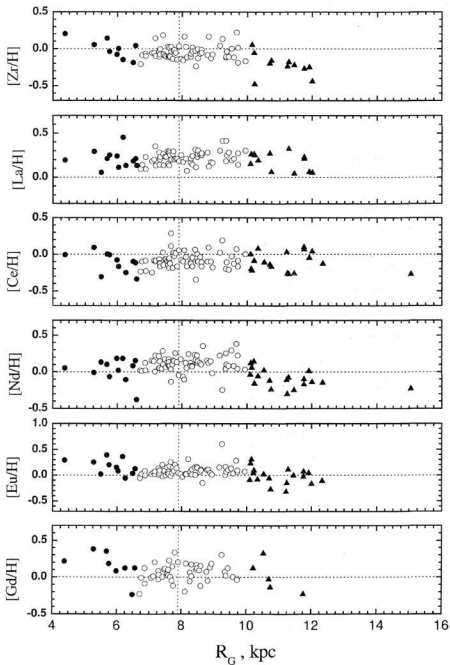


Figure 5: Same as Fig. 1, but for elements Zr–Gd

clusters with ages spanning from 1 to 5 Gyr. Thus, the youngest clusters used for the gradient study are approximately 10 times older than Cepheids. By comparing the iron abundance gradient from Cepheids with that from open clusters one would, in principle, estimate how the abundance gradient evolved with time. Nevertheless, in practice it is difficult to realize, because any conclusion will suffer from the rather high uncertainty of the open cluster data. The only we can state confidently is that the discontinuity of the metallicity distribution has really survived over several Gyrs, until now.

3.2. A possible explanation for some observed features

Recently Mishurov et al. (2002) produced a detailed model of chemical evolution of the galactic disc, taking into account the effect of co-rotation, to explain our data presented in Papers I and II. The new data presented in Paper III, suggest that the model of Mishurov et al. (2002) is basically correct, but that the co-rotation radius should be slightly shifted to about 10.5 kpc. The discontinuity in the metallicity distribution at 10 kpc is possibly explained by the gap in the gas density distribution that is associated with co-rotation (see Lépine, Mishurov & Dedikov (2001)). If we divide the Galactic disc in a large number of concentric rings, the gas from neighbouring rings tends to mix due to supernova explosions, stellar winds, cloud collisions, etc., that do not respect the frontiers between concentric rings. This mixing is equivalent to a diffusion term, and tends to smooth out metallicity gradients in the gas (and therefore, in recently formed stars). However, the gas density gap associated with co-rotation, which is observed in the 21 cm hydrogen line as discussed by Lépine, Mishurov & Dedikov (2001) is possibly a barrier that avoids contact between the gas at $R_G > R_C$ and $R_G < R_C$ and allows the existence of two distinct zones.

Acknowledgements. I would like to express my gratitude to all my colleagues with whom three basic papers on galactic metallicity gradient were published: Drs. V.V. Kovtyukh, R.E. Luck, J.R.D. Lépine, W.J. Maciel, B. Barbuy, V.G. Klochkova, V.E. Panchuk, Yu. V. Beletsky, D. Bersier, R.U. Karpischeck.

References

- Amaral L.H., Lépine J.R.D.: 1997, *MNRAS*, **286**, 885.
 Andrievsky S.M., Kovtyukh V.V., Luck R.E., Lépine J.R.D., Bersier D., Maciel W.J., Barbuy B., Klochkova V.G., Panchuk V.E., Karpischeck R.U.: 2002a, *A&A*, **381**, 32.
 Andrievsky S.M., Bersier D., Kovtyukh V.V., Luck R.E., Maciel W.J., Lépine J.R.D., Beletsky Yu.V.: 2002b, *A&A*, **384**, 140.
 Andrievsky S.M., Kovtyukh V.V., Luck R.E., Lépine J.R.D., Maciel W.J., Beletsky Yu.V.: 2002c, *A&A*, **392**, 491.
 Caputo F., Marconi M., Musella I., Pont F.: 2001, *A&A*, **372**, 544.
 Friel E.D.: 1995, *ARA&A*, **33**, 381.
 Janes K.A.: 1979, *ApJS*, **39**, 135.
 Lépine J.R.D., Mishurov Yu.N., Dedikov S.Yu.: 2001, *ApJ*, **546**, 234.
 Mishurov Yu.N., Lépine J.R.D., Acharova I.A.: 2002, *astro-ph/0203458*.
 Panagia N., Tosi M.: 1981, *A&A*, **96**, 306.
 Sevenster M.N.: 1999a, *MNRAS*, **310**, 629.
 Sevenster M.N.: 1999b, *ApSS*, **265**, 377.
 Twarog B.A., Ashman K.M., Antony-Twarog B.J.: 1997, *AJ*, **114**, 2556.

ATOMS IN MAGNETIC FIELDS: POSSIBLE ORIGIN OF CHEMICAL ANOMALIES IN MAGNETIC STARS

G.S. Bisnovaty-Kogan

Space Research Institute, Russian Academy of Sciences

Profsoyuznaya 84/32, Moscow 117810 Russia, *gkogan@mx.iki.rssi.ru*

ABSTRACT. The interaction of atomic magnetic moments with non-uniform magnetic fields may be important for the diffusion in the matter near the surface of neutron and magnetic stars. Formation of the anomalous abundance of some elements in magnetic stars is considered as an extension of the old model of Babcock (1963) and Jensen (1962). Phase transition of the second order is shown to be held in helium as a transition from diamagnetic to paramagnetic stars with increasing of magnetic field (Bisnovaty-Kogan and Höflich, 1990), efficiency.

Key words: Stars: atomic magnetic moments; magnetic stars.

1. Introduction

Chemical anomalies are observed in Ap stars, having masses $M \leq 2 M_{\odot}$ and strong magnetic fields up to 10^4 Gs. The existence of such anomalies may be connected with the following exceptional properties of these stars.

They have a small convective core $< 0.3 M_{\odot}$, and very thin convective envelope. Absence of strong convective zones make it ineffective an action of dynamo processes. The magnetic field of such stars is formed from the compression of the contracting magnetized cloud, and dynamo action on the short convective stage during star evolution to the main sequence, lasting about $5 \cdot 10^5$ years (Bisnovaty-Kogan, 2001). This property may imply a large variety of magnetic field strength and topology in Ap stars. Slow rotation observed in these stars may be connected with a large rate of a loss of stellar angular momentum due to magnetic stellar winds. Slow rotation implies negligible meridional circulation and consequently negligible mixing. It also decrease even more the action of the dynamo processes. Strong magnetic field suppresses completely the residual convection in the outer envelope. That create conditions of accumulation of slow diffusive changes of the composition in stellar layers near the photosphere.

Three types of a diffusion are considered in the literature for creation of chemical anomalies.

1. Radiative diffusion (Mishaud, 1970).

2. Accumulation of anomalies during accretion (Havnes and Conti, 1971).

3. Diffusion of paramagnetic atoms in the non-uniform stellar fields (Babcock, 1963; Jensen, 1962).

The last mechanism was considered because of a striking correlation between the anomalous abundance and magnetic moment of the corresponding atoms: the largest anomaly ($\sim 10^7$ times over the solar abundance) has the element Eu, which has the largest atomic magnetic momentum in S state, $J = 7/2$. The first models could not quantitatively explain the observed anomalies. The improvement of this model by Bisnovaty-Kogan and Höflich (1990) (see also Bisnovaty-Kogan, 1992) permitted to obtain much better quantitative agreement with observations.

2. Observational correlations.

The largest chemical anomalies correspond to elements with large atomic magnetic momentum, among which the most distinguished are, see Table 1.

Another intriguing correlation exist between the spectral class of a star where maximum anomalies for given element are observed, and the ionization potential of the corresponding atom (Ledoux and Renson, 1966), see Table 2.

The model, explaining these anomalies by motion of paramagnetic atoms in non-uniform magnetic fields, was proposed by Babcock (1963) and Jensen (1962). The "optical pumping" was used for increasing the relative population of atoms with a given orientation of their spins. The "equilibrium" abundance gradient established in the non-uniform magnetic field, which balances the diffusion under the action of a field gradient, is determined by formula

$$\frac{\nabla n}{n} \approx \frac{\mu_B \nabla B}{kT}, \quad (1)$$

where μ_B is the atomic magnetic momentum. It was noted by Babcock (1963) and Ledoux and Renson (1966), that for large observed $\nabla n/n$ very large field gradients $\nabla B > 10^{-3}$ Gs/cm are needed, which at least 100 times exceed observed field gradients in solar spots.

Table 3: Elements abundances in the star β CrB, according to Ledoux and Renson (1966).

Element	Mg	Si	Ca	Sc	Ti	V	Cr	Mn
Abundance of elements relative to solar $\frac{[X]}{[X_{\odot}]}$	1.6	3.4	1.4	2.5	7.7	2.5	30	40
Element	Fe	Co	Ni	Sr	Zr	Ba	La	
Abundance of elements relative to solar $\frac{[X]}{[X_{\odot}]}$	7	10.5	1.8	40	90	4.5	620	
Element	Ce	Pr	Nd	Sm	Eu	Gd	Dy	
Abundance of elements relative to solar $\frac{[X]}{[X_{\odot}]}$	880	535	150	192	1440	890	3800	

Let us suppose for simplicity that outside the spot the composition is normal $X_{\rho, \text{Eu}}^{(0)} \approx 7.9 \cdot 10^{-10}$ by mass, and $X_{n, \text{Eu}}^{(0)} \approx 4.4 \cdot 10^{-12}$ by number of atoms, $A_{\text{Eu}} = 152$. The concentration of Eu in the spot increases in time due to diffusion and according to (5-7), is equal to

$$\begin{aligned}
 X_{\rho, \text{Eu}} &\approx X_{\rho, \text{Eu}}^{(0)} + \frac{m_{\text{Eu}} L_{\text{Eu}}}{m_t} \\
 &\approx X_{\rho, \text{Eu}}^{(0)} \left[1 + 7 \frac{\hbar}{kT} \frac{|e|B}{m_e c} \frac{v_H \chi_{\text{Eu}} \text{Eu}}{n \sigma_{\text{coll}} R^2 \theta^2} \left(\frac{R_s \nabla B}{B} \right) t \right] \\
 &\approx X_{\rho, \text{Eu}}^{(0)} \left[1 + 3 \cdot 10^{-14} \frac{B \chi_{\text{Eu}} \text{Eu}}{T^{1/2}} \left(\frac{\nabla_{300}}{n_{13} \theta_{0.1}^2} \right) t \right], \quad (8)
 \end{aligned}$$

where $n_{13} = n/10^{13} \text{ cm}^{-3}$, $\theta_{0.1} = \theta/0.1 \text{ rad}$, $\nabla_{300} = R_s \nabla B / 300 B$. $\nabla_{300} = 1$ at $B = 10^4$ corresponds to the magnetic field gradient in solar spot (Babcock, 1963). When $B = 10^4 \text{ Gs}$, $T = 5000 \text{ K}$, $\chi_{\text{Eu}} \text{Eu} = 0.001$, and $t = 3 \cdot 10^{16} \text{ s} \approx 10^9$ years we return to (8) in the spot

$$\frac{X_{\rho, \text{Eu}}}{X_{\rho, \text{Eu}}^{(0)}} \approx 130 \quad \text{for} \quad n_{13} = \nabla_{300} = \theta_{0.1} = 1. \quad (9)$$

Note that the main contribution to the diffusion flux comes from layers with $n < 10^9 \text{ cm}^{-3}$. Smaller spots, larger field gradients may give even larger Eu concentrations. The value from (9) is about 10^3 times larger than Babcock (1963) estimated for the same ∇B .

If an atom of Eu changes its spin direction during its motion to the poles, it does not reach the magnetic poles, and starts to move in opposite direction. But this motion does not lead to hot region, atoms are not ionized, and the equilibrium concentration gradient is formed which prevents the motion from the poles (see Fig.1). At $n < 3 \cdot 10^8 \text{ cm}^{-3}$ the spin does not change its direction due to small overturn cross-section (3), and Eu flux goes directly to the poles.

4. He atoms in a very high magnetic fields: second order phase transition.

The magnetic field has a large influence on the atomic structure when the energy level of the electron in the magnetic field E_B exceeds the binding energy E_b of the electron in the atom. For hydrogen we have (Landau and Lifshits, 1963)

$$E_b = \frac{m_e c^2}{2\hbar^2}, \quad E_B = \hbar \frac{|e|B}{2m_e c}, \quad (10)$$

and these energies are equal at characteristic magnetic field

$$B_* = \frac{m_e^2 |e|^3 c}{\hbar^3} = 2.35 \cdot 10^9 \text{ Gs}. \quad (11)$$

When the atomic $J \neq 0$ the atom is paramagnetic with a positive susceptibility, like H or Eu. The ground energy level of this atom deepens and its binding energy increases with increase of B . The ground state of He atom has $J = S = L = 0$, and in it is diamagnetic with a negative susceptibility. The ground energy level of this atom goes up with B , making it less bound. The first excited state of He with excitation energy $E_{\text{ex}} = 19.82 \text{ eV}$, $S = J = 1$ and with atomic structure 2S_1 , has paramagnetic properties. With increasing of B the binding energy of the diamagnetic ground level decrease, and the binding energy of the first excited state (paramagnetic) increases. As was obtained by Gadiyak et al. (1982) the binding energies of the ground and the first excited state become equal at $B_* = 0.7 B_c = 1.7 \cdot 10^9 \text{ Gs}$ (see Fig.4). At $B > B_c$ the ground state of the atom is already paramagnetic with nonzero spin. It was noted by Bisnovatyi-Kogan and Höflich (1990), that the phase transition of the second order happens at $B = B_c$, when the neutral helium change its property from diamagnetic to paramagnetic ground state.

calculations are given by Bisnovaty-Kogan and Höflich (1990).

2.3. Structure of non-LTE atmosphere.

The density and temperature profiles in non-LTE atmosphere shown in Fig.2 from Bisnovaty-Kogan and Höflich (1990) resembles closely at the photosphere to the corresponding LTE model of Kurutz (1979) in all layers except the very inner regions, because in normal atmospheres convection results in slightly less steep temperature gradient. The minimum temperature is somewhat lower because of the stronger cooling due to metal lines. In the very outer regions the relative abundance of EuI is higher by more than an order of magnitude than the LTE value due to reduction of the radiation field. The fraction χ_{EuI} of the neutral EuI is of the order of $10^{-4} - 10^{-3}$ over a large fraction of the atmosphere (see Fig.3 from Bisnovaty-Kogan and Höflich, 1990), and is sufficient to explain our effect. The concentration of EuI may increase due to increase of a local electron density n_e , which in the layers $\log \tau_{5000} = -8 - 10$ is determined mainly by ionization of abundant elements with low ionization potential like Na ($I=5.138$ eV, $X_{p,Na,\odot} = 4.4 \cdot 10^{-5}$), K ($I=4.339$ eV, $X_{p,K,\odot} = 4.4 \cdot 10^{-6}$), for solar abundances.

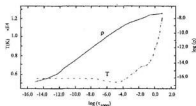


Figure 2: Temperature and density profile as a function of $\tau(5000$ Angström) for an atmosphere with $T_{eff}=7600$ K, and $\log g = 4$. Element abundances are taken which can be regarded as typical for Ap stars (see text).

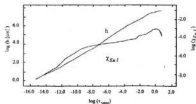


Figure 3: χ_{EuI} and atmosphere height h as a function of $\tau(5000$ Angström).

EuI lines have not been observed in the spectra of Ap stars, probably, because they are strongly blended by

other lines. Lines of atomic CaI with $I=6.11$ eV, close to EuI with $I=5.67$ eV, have been observed in the spectrum of A2.6 star TX Leo (Leushin and Topil'skaya, 1988).

3. Diffusion flux of Eu atoms into the polar regions.

Consider diffusion of Eu atoms under the action of the magnetic field gradient, taking into account collisions with the H atoms. Collisional cross-section and the cross-section of a spin overturn during collision are written as

$$\sigma_{coll} \approx 10^{-16} \text{cm}^2, \tag{3}$$

$$\sigma_{\uparrow\downarrow} \approx 10^{-3} \alpha^2 \sigma_{coll} \approx 10^{-23} \text{cm}^2$$

Eu atoms in S state with a spin projection $\sigma = \frac{7}{2}$ is drifting in the direction of increasing of the magnetic field to the magnetic poles. The diffusive flux of Eu atoms is equal to (Lifshits and Pitaevski, 1979)

$$\vec{j}_{EuI} = D \left(\frac{n_{EuI} \vec{F}}{kT} - \nabla n_{EuI} \right) \text{cm}^{-2} \text{s}^{-1}. \tag{4}$$

Here n_{EuI} is the concentration of Eu atoms, $F = \frac{7}{2} \hbar \nabla \omega_B$ is the force acting on the paramagnetic Eu atom in a non-uniform magnetic field, $\omega_B = \frac{g \mu_B B}{\hbar}$ is a cyclotron frequency, $D \approx \frac{v_H^2 \lambda}{n \sigma_{coll}}$ is a diffusion coefficient for Eu atoms, $n = n_H + n_{He}$, v_H is the thermal velocity of hydrogen. Without ionization the concentration gradient balances the magnetic force and in equilibrium, when brackets in (4) are equal to zero we have the Babcock-Jensen result (1). If Eu atoms are ionized during the move along the magnetic field lines, when they enter the hot regions near the magnetic poles, the term ∇n_{EuI} does not prevent continuous diffusion. The total flux of Eu atoms in this case is equal to

$$\vec{L}_{EuI} = 2\pi R_s \bar{n}_{EuI} \frac{7}{2} \hbar \frac{\nabla \omega_B}{kT} \frac{v_H}{n \sigma_{coll}} (\text{s}^{-1}), \tag{5}$$

where \bar{n}_{EuI} (cm^{-2}) is the surface density of the Eu atoms of the star reverse layer, R_s is a radius of the star.

Let θ be the angle size of the polar spot (or of the surface of a spherical layer) with anomalous composition. The surface area of the spot is

$$S \approx 2\pi R_s^2 (1 - \cos \theta) \approx \pi R_s^2 \theta^2. \tag{6}$$

The total mass of the spot over the reverse layer, corresponding to the mass over the layer where EuI lines are formed, is equal to

$$m_t = \bar{\rho} S \approx \bar{\rho} \pi R_s^2 \theta^2. \tag{7}$$

Table 1: Properties of elements showing strong chemical anomalies

Element	Eu	Cr	Mn
Atomic shell structure	$4f^7 6s^2$	$3d^6 4s$	$3d^5 4s^2$
Atomic state	$^8S_{7/2}$	7S_3	$^6S_{5/2}$

Table 2: Elements showing strongest chemical anomalies versus spectral class of a star

Element	Eu	Sr	Cr	Mn
Spectral class corresponding to maximum overabundance	A8 - A3	A8 - A5	A2	B8
T_{eff} (K)	7580 - 8720	7580 - 8200	8790	11900
I_{ion} (eV)	5.67	5.695	6.766	7.44

2. The model

The modification of the Babcock-Jensen model suggested by Bisnovaty-Kogan and Höflich (1990) is based on the fact, that atoms moving in the magnetic field towards magnetic poles enter a region with greater densities and temperatures, where they are inevitably ionized. It means that concentration gradient of neutral atoms preventing farther diffusion will, not be installed and the real gradient of element concentration (including atoms and ions) may be much greater than follows from (1). Due to ionization there is a continuous flux of paramagnetic atoms to the regions of the magnetic poles, see Fig.1.

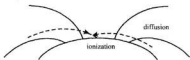


Figure 1: Schematic picture of the magnetic diffusion into polar region.

2.1. Neutral atoms in Ap stars.

Let us investigate Eu anomalies, and find first the concentration of Eu atoms in the surface layers of Ap stars with the effective temperature $T_{eff} = 7600$ K, characteristic for (A7-A8) type stars. In LTE equilibrium the concentration is determined by Saha formula

for ground states (Mihalas, 1978)

$$\frac{n_a}{n_i} \approx 2.07 \cdot 10^{-16} n_e \frac{g_a e^{I_{ion}/kT} T^{-3/2}}{g_i} = 2 \cdot 10^{-17} n_e \quad (2)$$

for $I_{Eu} = 5.67$ eV, $g_a=8$, $g_i=9$, and $T = 6000$, which can be regarded as a representative value above the photosphere of A8 - A3 stars (Kurutz, 1979). Taking corresponding $n_e = 5 \cdot 10^9 - 5 \cdot 10^{13}$, we obtain $\frac{n_a}{n_i} = 10^{-7} - 10^{-4}$. This value is too small to produce the observed anomalies due to diffusion of atoms. But the condition of LTE is violated in the regions above the photosphere, so the degree of ionization may be less in reality.

2.2. Non LTE treatment of upper layers.

Non-LTE model of the atmosphere of the star with $T_{eff} = 7600$ K, $\log g = 4$ was constructed by Bisnovaty-Kogan and Höflich (1990), using a method of Höflich and Wehrse (1987). The properties of the star were close to those of the star β CrB, which element abundances (Ledoux and Renson, 1966) have used in calculations (see Table 3). Other abundances were presumed to be solar. The non-LTE atmosphere was constructed for optical depths $\log \tau$ between -15 and 1.2. Up to 20 lower levels were allowed to deviate from LTE for H, He, C, N, O, Na, Mg, K, Ca and Eu. All radiative and collisional bound-bound and bound-free transitions were included in the statistical equations. Having in mind a suppression of the convection by the strong magnetic field, only radiative energy transport was taken into account in the atmosphere. Farther details of physical conditions used in

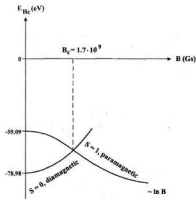


Figure 4: Semi-quantitative behaviour of energy of the He atomic levels (ground and first excited states) in a magnetic field. The point $B = B_c$ corresponds to the second order phase transition.

The motion of He atoms in the non-uniform magnetic field may create an inverse population of He atomic states, leading to laser-like radiation. It may happen during accretion of He atoms onto a neutron star, having $B \gg B_c$, or in the more exotic situation with an ejection of atomic He from the neutron star surface. Matter velocities at accretion and ejection are very large (sub-relativistic), so the He atoms become excited in both cases, giving finally the strongly collimated pulse of ultraviolet radiation.

Acknowledgements. This work was partially supported by RFBR grant 02-02-16900.

References

- Babcock M.W.: 1963, *ApJ*, **137**, 690.
 Bisnovaty-Kogan G.S.: 1992, in "Chemical evolution of stars and galaxies" (in Russian), ed. A.G.Massevich, Kosmosinform, p.130.
 Bisnovaty-Kogan G.S.: 2001, "Stellar Physics", vol.2, Springer, Heidelberg.
 Bisnovaty-Kogan G.S., Höflich P.: 1990, *Ap. and Space Sci.*, **168**, 293.
 Gadiyak G.V., Lozovik Yu.E., Mashchenko A.I. and Obrecht M.S.: 1982, *J. Phys. B: At. Mol. Phys.*, **15**, 2615.
 Havnes O., Conti P.: 1971, *A&A*, **14**, 1.
 Höflich P., Wehrse R.: 1987, *A&A*, **185**, 107.
 Jensen E.: 1962, *Nature*, **194**, 668.
 Kurutz R.L.: 1979, *ApJ Suppl.*, **40**, 1.
 Landau L.D. and Lifshits E.M.: 1963, *Quantum mechanics* (in Russian), Nauka, Moscow.
 Ledoux P., Renson P.: 1966, *Ann. Rev. A&A*, **4**, 293.
 Leushin V.V., Topil'skaya G.P.: 1988, in *Proc. Int. Meeting "Magnetic Stars"*, Nauka, Moscow.
 Lifshits E.M., Pitayevski L.P.: 1979, *Physical kinetics* (in Russian), Nauka, Moscow.
 Mihalas D.: 1978, *Stellar atmospheres*, Freeman and Co., San Francisco.
 Mishaud G.: 1970, *ApJ*, **160**, 641.

CHEMICAL ABUNDANCES AND EVOLUTIONARY STATUS OF SOME λ Bootis TYPE STARS AND FBSwl

I.V. Chernyshova

Astronomical Observatory, Odessa National University,
T.G. Shevchenko park, 65014, Odessa, Ukraine e-mail: chernyshova@mail.ru

ABSTRACT. Comparative analysis of chemical abundances in the atmospheres of λ Bootis type stars and FBSwl (field blue stragglers weak lined) is presented. Evolutionary status of these metal deficient stars is discussed.

Key words: chemically peculiar stars, A-dwarfs, F-dwarfs, synthetic spectra, abundance, λ Bootis

among stars brighter than $m_v = 8^m$. Their δm_1 values indicate abundances in the interval $-0.9 < [Fe/H] < -0.4$. A spectroscopic investigation of this group of metal-deficient F dwarfs to clarify their nature was recommended. Bond (1970) and Gray (1988) suggested that FBS possibly are cool representatives of the λ Bootis class of young stars with weak metallic lines.

1. Introduction

Group of λ Bootis type stars consists of Population I, metal poor (except C, N, O and S elements which have almost solar abundance), non-magnetic, late B to early F-type dwarfs. They fall into two classes with normal (NHL) and peculiar (PHL) hydrogen profiles with weak cores and broad but often shallow wings, have a weak $\lambda 4481$ lines and high $v \sin i$. Some of them have IR excesses and strong absorption features in IUE spectra. According to Venn and Lambert (1990) accretion theory, the chemical peculiarity of λ Bootis stars originates from the presence of a circumstellar shell (most likely a remnant of the star formation). Depleted gas from the circumstellar envelope consist of CNO and S elements is accreted by the star while elements with higher condensation temperature accumulate in the dust grains.

A-component ($V=6.^m71$, A-type) of unusual visual binary system VW Ari (HD15165, BDS 1269) wide known as multiperiodically pulsating star (probably of δ Sct-type) having non-radial modes. This star shows the spectrum typical for very metal deficient star and high $v \sin i$ value, while B-component ($V=8.^m33$, F-type) possesses a solar-like chemical composition and slow rotation (Andrievsky *et al.* 1995). Such a strange difference in the chemical composition of both components could appear due to the peculiar evolution of VW Ari A as a λ Boo-type star (Chernyshova *et al.* 1998).

Olsen (1980) had applied Strömberg photometry to predict spectral classifications of faint stars and finding lists of potentially interesting objects. He has identified a category of early F type metal-poor dwarfs (so called "week-lined field blue stragglers" (FBSwl))

2. Observation and abundance analysis

In our works Paunzen *et al.* (1999) and Andrievsky *et al.* (2002) we determined accurate LTE abundances for 7 well established λ Bootis stars and 20 candidates to λ Bootis type stars. We compared abundances of our candidates with two MK standard stars and abundance pattern from Paunzen *et al.* (1999). Details of observations of 19 FBSwl are presented in Andrievsky *et al.* 1995, 1996. High resolution and high S/N CCD spectra have been obtained at six sets. The effective temperatures and surface gravities were estimated using the Strömberg photometric indices checked with additional calibrations in the Geneva system. We obtained LTE abundances and rotational velocities by using method of synthetic spectra with help of programs STARS (Tsymbal 1996) and WIDTH9, the atmosphere models of Kurucz and atomic data from the Vienna Atomic Lines Database (Kupka *et al.* 1999).

3. Obtained results

All metals show moderate deficiency on FBS and moderate or strong deficiency on 7 λ Bootis type stars and VW Ari A. C and O are in little deficiency on all stars. Most of the stars show normal abundance of sodium. VW Ari A show distribution of elements like typical λ Bootis type star. Take into account normal hydrogen profile of star we can call it NHL type star (of course if all other main features of λ Bootis type stars will be found on this star).

After our detailed abundance analysis for test of membership of twenty λ Bootis type stars candidates we are able to confirm or establish the member-

ship for nine objects (HD23258, HD36726, HD40588, HD74911, HD84123, HD91130, HD106223, HD111604 and HD290799). Six stars (HD90821, HD98772, HD103483, HD108765, HD201184 and HD261904) can be definitely ruled out as being member of the λ Bootis group whereas no ambiguous decision can be drawn for another five stars (HD66684, HD105058, HD120500, HD141851 and HD294253).

The results of investigation of chemical abundances of FBSwl were published in Andrievsky *et al.* (1995, 1996) and Chernyshova (1999). Although most of FB-Swl show slight metal deficit and some of them show abundance pattern similar to λ Bootis type stars. So we can add them to the list of candidates of λ Bootis stars.

4. Conclusions

Future investigations of λ Bootis should concentrate on establishing homogeneity of the group of λ Bootis (candidates should show the most of common properties), clarification of the main physical processes responsible for its phenomenon by analysing of parameters (abundance pattern, behaviour in the infrared etc.), improving theory of λ Bootis forming by taking all observational results and evolutionary status of group's members into account. Precise IR spectroscopic and photometric observation of λ Bootis is necessary for understanding the physico-chemical processes of accretion and diffusion in their circumstellar gas and dust discs and chemical anomalies on a surfaces, possible discovering of binaries among them.

References

- Andrievsky S.M., Chernyshova I.V., Pausen E., Weiss W.W., Korotin S.A., Beletsky Yu.V., Handler G., Heiter U., Korotina L., Stutz C., Weber M.: 2002, *A&A*, **396**, 641
- Andrievsky S.M., Chernyshova I.V., Usenko I.A., Kovtyukh V.V., Panchuk V.E., Galazutdinov G.A.: 1995, *PASP*, **107**, 219
- Andrievsky S.M., Chernyshova I.V., Kovtyukh V.V.: 1996, *A&A*, **310**, 277
- Andrievsky S.M., Chernyshova I.V., Klochkova V.G., Panchuk V.E.: 1998, *Contrib. Astron. Obs. Skalnaté Pleso*, **27**, 446
- Bond H.E. 1970, *ApJS*, **22**, 117
- Chernyshova I.V., Andrievsky S.M., Kovtyukh V.V., Mkrtichian D.E. 1998, *Contrib. Astron. Obs. Skalnaté Pleso*, **27**, 332
- Chernyshova I.V.: 1999, *Chem. Evol. from Zero to High Redshift*, Proc. of the ESO Workshop (eds. J.R. Walsh, M.R. Rosa) Berlin: Springer-Verlag, 63
- Gray R.O. 1988, *AJ*, **95**, 220
- Kupka F., Piskunov N.E., Ryabchikova T.A., Stempels H.C., Weiss W.W. 1999, *A&AS*, **138**, 119
- Olsen E.H. 1980, *A&AS*, **39**, 205
- Pausen E., Andrievsky S.M., Chernyshova I.V., Klochkova V.G., Panchuk V.E., Handler G.: 1999, *A&A*, **351**, 981
- Tsybmal V. 1996, In: *Model Atmospheres and Spectrum Synthesis*, Adelman S.J., Kupka F., Weiss W.W. (eds.), ASP Conf. Ser., **108**, 198
- Venn K.A., Lambert D.L.: 1990, *AJ*, **363**, 234

MODEL ATMOSPHERE OF HD101065 WITH INDIVIDUALIZED ABUNDANCES

S.A. Khan, D.V. Shulyak

Department of Astronomy, Tavrian National University after V.I. Vernadskiy

ABSTRACT. We have calculated the model atmosphere of extremely peculiar α Ap star HD101065. The line opacity with individualized abundances has been executed by «line-by-line» method. Due to lack of data for the REE lines we scaled D.R.E.A.M. data base by ten. The synthetic spectrum and indices in photometric system $uvby$ have been calculated as: $b-y = 0.713$, $m_1 = 0.336$, $c_1 = -0.121$. We had obtained good agreement between an observation and modelling.

Key words: peculiar star, model atmosphere, individualized abundances, HD101065.

1. Introduction

At present time observed spectra of stars are main sources of the information for stellar astrophysics. Because of most of the radiation originates in outer layers of a star, named stellar atmosphere, we have to build sufficient atmosphere model for proper analysis of stellar spectra.

The evolution of atmospheric models was closely related to the evolution of our conception of the energy transfer in outer layers of stars and the historical progress of the computer power. From 70's great necessity appeared to create the opacity tables and the spectral lines lists. The most important projects became the works of Kurucz, OPACITY and OPAL projects (1988-96), VALD (1995-99) [1,2]. For the cool stars it is very important to consider molecular sources of opacity, that is why a number of authors created lines lists of molecules: H_2O , TiO_2 , TiO , OH , CH , H_2 and other. Lately, more attention was paid to the lists of REE lines among which we want especially note the D.R.E.A.M. database of REE lines [3].

Currently there are several methods of opacity calculation. The main methods are: OPDF and OS. The most actively used OPDF (Opacity Distribution Function) method. The OPDF method is realised in ATLAS9 [4] code of Kurucz. It should be noted that using of OPDF method is complicated because it requires calculation of opacity distribution function each time for given abundances, sets

of temperatures, pressures and microturbulence velocities. It is possible to make calculations more easier by using the set of pre-calculated OPDF tables for different abundances, for example the abundances scaled to solar composition (Kurucz, 1992-93) [5]. Thus, set of tables makes possible quick calculation atmosphere models with tabulated values of T_{eff} , $\lg g$ and metallicity $[A]$ for normal stars. Though, in case of chemically peculiar (CP) stars it is impossible to take into account wide range of potential abundances. Therefore, stars of this kind require calculations of individual OPDF tables (Piskunov, Kupka, 1998-2001) [6] or use of other opacity calculation method, such as Opacity Sampling method.

The main idea of Opacity Sampling (OS) method lies in fitting the number of points along frequency in given range so as mean statistical dependency of the absorption coefficient in spectral lines is reproduced satisfactory. Points upon the frequency are chosen either with fixed step or randomly (Monte-Carlo method). By increasing the number of points we can achieve convergence in atmosphere structure to approach, which is got if opacity is calculated by direct method for great number of points. Using of OS technique leads to less calculation time in comparison to OPDF method only an average resolution of 4000 or less, that is fully insufficiently for CP stars modelling. OS technique realised in ATLAS12, Phoenix, SAM12 and other codes.

The methods described above have generic deficiency. These methods do not allow efficient calculations of models with stratified abundances. The fact is that stratification of the abundances with depths leads to changing of absorption coefficient with depths for given wavelength range. Consideration of stratification by OPDF technique is very difficult and time-consuming, by the OS technique is not trustworthy enough because of its statistical character.

Till present time the guess about chemical homogeneity of atmosphere along depth did not call in question. Though indications had appeared of possible stratification due to help of high quality

spectra. Especially, taking into account that nature of such phenomenon has been determined – diffusion of atoms under the influence of radiative field or magnetic field.

The method which allows to avoid limitations described above is the direct method of opacity calculation. It allows to calculate the model atmosphere with individualized and stratified abundances. Though this method is simple by its ideology it was very difficult to employ it till recently because of insufficient computer power.

2. Calculations

In present work we made the model atmosphere calculations by LLModels code (V. Tsymbal, D. Shulyak) [7], which computes opacity by direct method. The LLModels code was created on base of the ATLAS9 code of Kurucz and code of calculation of synthetic spectrum from set of programs STARSF of Tsymbal [8]. Modelling is performed with guesses of plane-parallel structure of atmosphere and LTE for early and intermediate type of stars.

The absorption coefficient in lines is calculated for each wavelengths point including opacities produced by neighbouring lines. The step of calculations must be small enough to provide accurate lines profiles calculations (approximately 300-400 thousands of points in field of radiation maximum of a star). This leads to the full account of frequency and depths dependencies of the line absorption coefficient. This method is named line-by-line method, further in article we will use this term.

The calculation of opacity in continuum is performed with 1A step. We found that using of 1A step does not change atmosphere structure in comparison with calculations with the same step as in lines opacity computing. The hydrogen lines are also calculated with 1A step excluding the range $\pm 50\text{\AA}$ from the center of hydrogen lines where calculations are performed with the same step as in lines opacity calculations.

The computing of correction to integral of density in column unit is performed by same method as in TCORR subroutine of ATLAS9 code. Whereas using of rosseland mean tables is unwarranted for stars with stratified abundances we have applied different approach. The equation of hydrostatic equilibrium is resolved at $t_{\text{top}}, k_{\text{top}}$ set instead of $t_{\text{rom}}, k_{\text{rom}}$. Owing to the fact that obtained values are interpolated backward to standard set of rosseland depths and opacities it is necessary to provide agreement between values of physical arguments, which used in following iterations. Therefore, absorption coefficients for current set of temperatures and pressures are calculated for wavelength 5000Å excluding lines opacities.

We performed elimination of spectral lines which don't make significant contribution to lines opacity for speed-up of calculation. The criteria of selection is:

$$\frac{a_l}{a_c} \leq x,$$

where a_l, a_c are coefficients of absorption in line and continuum respectively, x is a criteria of selection. The testing calculation shows that using criteria 10^{-2} is well enough for accurate model calculation.

We used LOWLINES.DAT lines list of Kurucz [9] which includes more than 31 millions lines for elements up to fifth ionization stage. It should be noted that for hot stars it is necessary to add HILINES.DAT list which includes about 10 millions lines up to ninth ionization stage.

The elimination of spectral lines allows considerably decrease computing time of a atmosphere model. Thus, for example, using criteria 10^{-4} and 10^{-2} reduces the number of lines needed for opacity calculation by a factor 20 and 100 respectively.

In process of lines selections it is appropriate to use prepared Kurucz solar scaled model or to calculate the model using ATLAS9. Here, values of $T_{\text{eff}}, \lg g$ should be chosen at the nearest parameters values of the sought model. Scale parameter [A] – metallicity should be chosen so as abundances correspond or slightly increase expected or known mean abundances in investigated star.

The method was approved on Vega. We have calculated atmosphere model for Vega with ATLAS9 (OPDF), ATLAS12 (OS) and «line-by-line» codes. The $T-t_{\text{rom}}$ relation, synthetic fluxes and colours didn't show any significant differences among various opacity techniques and observed values. The accounting of faint spectral lines (criteria of selection 10^{-4}) in opacity calculation doesn't show any distinctions (more than error of calculation) in comparison with criteria 10^{-2} .

3. Model atmosphere of HD101065

The HD101065 star (Przybylski's star) is often called the most unusual roAp star. At the 32 IAU colloquium in 1975 Przybylski attracts attention to spectral features of this star. He notes deficiency or strong weakening of iron peak lines and points to serious restriction in selection of model atmosphere. First lines identifications works were made by Przybylski [10, 11], Warner [12], Wegner and Petford [13]. They confirmed excess of rare-earth elements (+4 dex). Cowley used method of wavelength coincidence statistics to show the presence of weak Fe lines [14].

The main problem in model atmosphere calculation lies in the difficulty of the effective temperature determination. The presence of strong opac-

ity caused by great number of REE lines made impossible correct finding of the effective temperature by use of observed photometry values. The considering of REE opacities was heavy due to the lack of atomic data for REE lines. The analysis of hydrogen lines [15] gives value of $T_{\text{eff}} = 7500\text{K}$. Observed photometric indices in 6-colours system leads to conclusion that effective temperature is about 6000K . This disagreement could be well explained by influence of strong opacity in REE lines which leads to changes in atmosphere structure.

The most detailed abundance analysis of HD101065 is performed by Cowley and Mathys [16] in wavelengths range 3900–6500Å. They point the presence of doubly ionized rare-earth elements (Pr III, Nd III, Ce III) that indicate unusual structure of model atmosphere. The last work devoted to analysis of abundances of HD101065 was made by Cowley and others [17]. As this work presents the most detailed analysis at present time we are describing its major results below.

Cowley derived abundances for 54 elements (including a lot of rare-earth elements). The fundamental parameters of model atmosphere were derived as: $T_{\text{eff}} = 6600\text{K}$, $\lg g = 4.2$. He showed, that convection plays no significant role in the temperature structure through strong blanketing and magnetic field. The magnetic broadening of spectral lines might be roughly approximated with a microturbulence velocity $u_{\text{micro}} = 1 \text{ km s}^{-1}$ for iron peak lines and $u_{\text{micro}} = 2 \text{ km s}^{-1}$ for rare-earth elements. Cowley used model atmosphere with individualized abundances calculated by the method of Piskunov and Kupka [6] which based on the OPDF method.

The considering of absorption in REE lines was complicated because trustworthy atomic data are known only for 13000 lines of neutral and once ionized rare-earth elements. That is why to compensate for missing line opacities caused by the incompleteness of rare-earth line lists Piskunov [6] and Cowley [17] increased the abundances of iron peak elements by 1.5 dex. It should be noted that described procedure is just empirical operation. The increasing value of iron peak elements was determined with best agreement between observations and theoretical study.

In present work we attempted to calculate model atmosphere of HD101065 with consideration of opacity caused by REE lines. The parameters of atmosphere: effective temperature, acceleration of gravity and abundances were taken from Cowley's work: $T_{\text{eff}} = 6600\text{K}$, $\lg g = 4.2$, microturbulence $u_{\text{micro}} = 2 \text{ km s}^{-1}$; the range of optical depths: from -8 to $+2$ with step 0.1.

We used LOWLINES.DAT lines list of Kurucz, which includes more than 31 millions lines for elements up to fifth ionization stage. In selection of lines which have significant influence on opacity

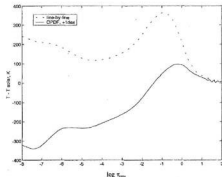


Figure 11: Temperature difference between a model atmosphere for HD101065 with individualized abundances and model with solar abundances. The difference between a model with scaled metallicity (+1 dex) and solar abundance model is displayed as well.

we used model calculated by ATLAS9 code of Kurucz. Cowley work shows that abundances of non rare-earth elements in atmosphere of HD101065 are near or less than solar ones, that is why we used OPDF tables for $[A] = 0$. The abundances were taken from Cowley's work. The criteria of selection of spectral lines was picked up as 10^{-3} . Thus, about 280 thousands of spectral lines were selected in range 500–30000Å of the maximum radiation of the star.

The addition of Kurucz preselected list by data about REE lines was made by using D.R.E.A.M. database, which includes more than 56 thousands lines of CeII, DyIII, ErIII, HoIII, LaII, LuII, LuIII, NdIII, PrIII, TbIII, ThIII, TmII, TmIII, YbII,

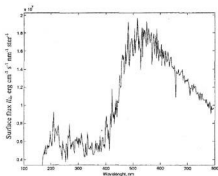


Figure 12: Synthetic fluxes for model atmosphere HD101065 with individualized abundances. Strong absorption features in the 400nm region smoothes the Balmer jump.

YbIII, YbIV, calculated with known Cowan's code [18]. Unfortunately, at present time D.R.E.A.M. includes data of a quarter of all rare-earth elements. Granting this fact and possible stages of elements ionization we scaled database by ten. Resulting list has been united with preselected Kurucz's list LOWLINES.DAT and used in further calculations of opacity. The total number of lines is about 850 thousands.

Then we calculated model atmosphere of HD101065 with individualized abundances. Fig. 1 shows temperature difference between a model atmosphere for HD101065 with individual composition and a corresponding model with solar abundance. For comparison, the difference between a model with scaled solar abundance (+1 dex) is also shown in Fig. 1. It should be noted that all models have been calculated with the same fundamental parameters.

The HD101065 model with specific chemical composition is quite different from the scaled abundance model. Its enhanced opacity leads to higher temperatures than the solar abundance model. Unlike, the heating found for the model with scaled solar abundances is less than 100K in layers deeper than $t_{\text{opt}} = -1.4$.

Fig. 2 shows synthetic fluxes for calculated model with individual chemical composition. It also shows that the Balmer jump is smooth out because of a strong absorption features in the 400 nm. It is a common knowledge that index c_1 of photometric system $uvby$ mensurates the height of the Balmer jump. Conducted calculations show that $c_1 = -0.121$, the observed data [19] is $c_1 = -0.012$.

Table 1 gives a summary of the $uvby$ photometric indices. The observed data are adduced accordingly to the reference [19]. The data from Cowley paper [17] are also represented in Table 1. The table shows that calculated indices are well agreed with observed ones with consideration that HD101065 is extremely peculiar star that significantly differs from usual CP stars.

Table 1: Comparison between the observed Strömgen indices and calculated ones

	Observations	Cowley's values	«line-by-line» model
$b-y$	0.452	0.387	0.713
m_1	0.430	0.582	0.336
c_1	-0.012	0.298	-0.121

4. Conclusions

Conducted computations of HD101065 model atmosphere showed that accounting of opacity caused by lines is extremely important in model atmosphere calculations of peculiar stars. This fact becomes especially important for stars with un-

usual abundances (extremely peculiar stars), for which it is impossible to make correct model atmosphere by scaling abundances to solar ones. In general case the task of analysis of CP stars is essentially nonlinear. We must consider not only individual abundances for opacities calculations but also possible stratification with depth. The used line-by-line code of opacity calculation allows to make such computing.

The executed work shows that model atmosphere of HD101065 calculated only with individualized abundances presents a large step towards precision analysis of this star, although it should be noted that calculated colours are still not in excellent agreement with observations.

Acknowledgement. We are grateful to A. Shavrina for stimulating this work, as well as V. Tsymbal for useful discussions.

References

- Piskunov N.E., Kupka F., Ryabchikova T.A., Weiss W.W., Jeffery C.S. VALD: The Vienna Atomic Line Data Base // *Astronomy & Astrophysics Supplement Series.* - 1995. - v.112. - N 3. - p.525-535.
- Kupka F., Piskunov N.E., Ryabchikova T.A., Stempels H.C., Weiss W.W. VALD-2: Progress of the Vienna Atomic Line Data Base // *Astronomy & Astrophysics Supplement Series.* - 1999. - v.138. - N 1. - p.119.
- Biemont E., Palmeri P., Quinet P. D.R.E.A.M. Database on Rare Earth at Mons University, <http://www.umh.ac.be/~astro/dream.shtml>
- Kurucz R.L. CD-ROM N13, 1993 // Smithsonian Astrophysical Observatory.
- Kurucz R.L. CD-ROM N14, 1993 // Smithsonian Astrophysical Observatory
- Piskunov N., Kupka F. Model atmospheres with individualized abundances // *The Astrophysical Journal.* - 2001. - v. 547. - N 2. - p.1040-1056.
- Tsymbal V., Shulyak D. Line-by-line opacity stellar atmosphere models // *Scientific conference «Chemical and dynamic evolution of stars and galaxies».* Odessa, 18-24 august, 2002.
- Tsymbal V. STARSP: A Software System for the Analysis of the Spectra of Normal Stars // *ASP Conference Series.* - 1996. - v.108. - p.198-199.
- Kurucz R.L. CD-ROM N1, 1994 // Smithsonian Astrophysical Observatory.
- Przybylski A. A G0 Star with High Metal Content // *Nature.* - 1961. - v. 189. - p. 739.
- Przybylski A. // *Nature.* - 1966. - v. 210. - p. 20
- Warner B. // *Nature.* - 1966. - v. 211. - p. 55.
- Wegner G., Petford A.D. Abundance analysis of Przybylski's star (HD 101065) // *MNRAS.* - 1974. - v.168. - p. 557.

- Cowley C.R., Cowley A. P., Aikman G., Grosswhite H. Element identification in Przybylski's star // *Astrophysical Journal*. – 1977. – v. 216. – N 1. – p. 37.
- Kurtz D., Wegner G. The nature of Przybylski's star - an AP star model inferred from the light variations and temperature // *The Astrophysical Journal*. – 1979. – v.232. – N 1. – p.510
- Cowley C.R., Mathys G. Line identifications and preliminary abundances from the red spectrum of HD 101065 (Przybylski's star) // *Astronomy & Astrophysics*. – 1998. – v. 339. – N 1. – p.165.
- Cowley C.R., Ryabchikova T., Kupka F., Bord J.D., Mathys G., Bidelman W.P. Abundances in Przybylski's star // *MNRAS*. – 2000. – v.317. – N 2. – p. 299.
- Quinet P., Palmeri P., Bi'emont E. On the use of the Cowan's code for atomic structure calculations in singly ionized lanthanides // *JQSRT*. – 1999. – v.62, p. 625 – 646
- Hauck B., Mermilliod M. Uvbyb photoelectric photometric catalogue // *Astronomy & Astrophysics Supplement Series*. – 1998. – v.129. – N 3. – p.431-433.

EVOLUTION FROM THE NUCLIDES TO THE CHEMICAL ELEMENTS

N.S. Komarov

Astronomical Observatory, Odessa National University,
Odessa 65014 Ukraine, e-mail: astro@paco.odessa.ua

ABSTRACT. The chemical evolution of Universe and it's objects (from grains to black holes) were of main goal of recent reviews and investigations. The evolution of chemical elements and their isotopes (early nuclides) discussed as indicator of evolution of Universe from Big Bang to now. The problem of determination of contents of chemical elements and their isotopes in atmospheres of cool giants to use method of the models of atmospheres and the synthetic spectra is discussed briefly. The determination of fundamental characteristics of cool stars (the effective temperature T_{eff} , surface gravity $\lg g$, metallicity $[Fe/H]$) are discussed too. The evolution of all nuclides heavier ${}^4\text{He}$ (with the exception, possibly, of most lightest nuclides - ${}^6\text{Li}$, ${}^7\text{Li}$, ${}^9\text{Be}$, ${}^{10}\text{B}$, ${}^{11}\text{B}$) are caused of these stars.

Key words: fundamental characteristics-stars, abundances-stars, nucleosynthesis-stars, evolution-stars.

Introduction

The interpretation of the «earth» Mendeleev's table and/or the distribution of contents of chemical elements and their isotopes in different objects of Universe must be accounted with theory of the origin and evolution of these objects. The evolution of the Universe may be looked as evolution of nuclides, and then as evolution of chemical elements and their isotopes! The first nuclides were formed in result of the Big Bang. The accuracy of determination of contents of chemical elements and their isotopes in various objects our Universe is the key in our understanding of evolution of all objects Universe after Big Bang. The answer on question about origin of nuclides heavier ${}^4\text{He}$ is basic for understanding of evolution us of surroundings. Why haven't stars without heavy elements? What is the distribution of nuclides from its masses (mass of chemical element from Mendeleev's table is of weighted mean value on all stable isotopes of this element plus electrons) or what Mendeleev's table is at other objects of the Universe? What the «cos-

mic», «normal», «standard» or «solar» of contents of all nuclides must be adopted?

The main results of determination of content of chemical elements in the atmospheres of the cool giants of only oxygen sequence of the Galaxy disk and their fundamental characteristics are given in this brief review. A brief survey of results is presented. The conclusion are making possible about evolution of the contents of chemical elements in the atmospheres of cool stars at transition stages from main sequence (MS) to red giant (FRGB), from the upper boundary of a giant branch to the horizontal one, and eventually, at the stage of asymptotic giant branch (AGB). The velocity of stellar evolution, efficiency of mixing depends on initial mass of the stars and primordial chemical composition of progenitor matter.

The full description about it was made by Trimble (1975, 1991), Geheren (1988), Lyubimkov (1995), Komarov (1999). The current «standard» distribution of contents of nuclides usually are comparing with theoretical predictions in results nuclear reactions (synthesis or decay), of theory stellar and galactic evolution, theory of Big Bang and so on. The distribution of nuclides should be exchanged in time and therefore it is very interesting to investigate contents of chemical elements and their isotopes in various objects of Galaxy and Universe having of various ages.

«Cosmic», «Normal», «Standard» and «Solar» abundance

The lightest nuclides have arisen in result of Gamow's Big Bang. The Big Bang hypothesis support of four pillars:

1) The Hubble expansion. It can be proved of redshift of spectra lines in galaxies and supernovae. In spite of the numerous attempts are determining the Hubble constant, its actual value remains one of the fundamental problems in cosmology. However, now, the most probable value for this constant is $H_0 = 59 \pm 6 \text{ km(sMpc)}^{-1}$.

2) The relict radiation. It is Plank function with temperature equal 2.726 ± 0.010 K at 95% confidence level. The fluctuations of radiation are present. Small spatial anisotropy could indicate that the matter wasn't distributed homogeneously when microwave background radiation originated, and small deviations with respect to the black body spectrum should indicate the presence of high energy sources in the primordial Universe. You cannot make galaxies without disturbing the microwave background and without chemical elements.

3) The abundance of light nuclides. The predicted cosmological abundance of light nuclides depends mainly on the universal baryonic density. Common particles at that epoch include: photons, neutrons, electrons, and quarks. After another phase, the quark condenses into ordinary particles: neutrons and protons. Then we finally enter into a regime where there is a direct comparison with our observations of galaxies and stars. So, the light elements with observed abundance ~75% for H and ~25% for He in weight fit with the cosmological predictions with only the one value the baryon density $\Omega_b = 0.05 \pm 0.03$. Two paths are for formation of ${}^4\text{He}$:

a) The deuterium nucleus collides with proton to form ${}^3\text{He}$, then a neutron to form ${}^4\text{He}$.

b) The deuterium collides first with a neutron to form ${}^3\text{H}$ (tritium), then with a proton to form ${}^4\text{He}$.

4) The kind of neutrinos. The Big Bang model predicts that the contents of light nuclides would fit only if there were no more than three families of neutrinos. This was exactly what was observed at Large Electron-Proton collider. So, the light elements with abundance ranging from 76% for H to 10^{-10} for Li all fit with the cosmological predictions with the one adjustable parameter being the baryon density $\Omega_b = 0.05 \pm 0.03$.

The density of particles was dropped to value $\sim 10^6$ grsm $^{-3}$ after 1s of the Big Bang ($T = 10^{10}$ K, dimension of Universe was increased to 10^4 km, or 10 ly). The thermodynamic equilibrium of neutrino with other particles can't more to stay in this condition. This neutrino began to move in Universe freely. The electrons and protons have been stop to form in a few second (energy below 10^6 eV). The protons and neutrons began coupling in the 100 s after Big Bang ($T = 10^8$ K, and dimension 100 ly) in lightest nuclides H, D, ${}^3\text{He}$, ${}^4\text{He}$ and ${}^7\text{Li}$ (more heavier nuclides can't formed in result absent of stable nuclides with masses number 5 and 8). Besides H, the nuclides ${}^4\text{He}$ had been appeared in main, which consists of nearly 1/4 baryonic mass of Universe. This process call of first nucleosynthesis, but relative distribution in Universe of lightest nuclides is good test of model of Big Bang. The final step to the formation of nuclides was capture of the suit-

able number of free electrons to form neutral atoms! However, the remaining electrons still had plenty of energy. The Universe was obscured. The cooling was continued about 3×10^5 years. Temperature was decreased to 10^4 K diameter of Universe had of dimension 10^9 ly, the nuclides have been surrounded of electronic envelopes and first light atoms H and He (first of chemical elements) have been formed. The average energy of photons was became a few eV in this time and it was not enough to destroy of atoms. At that moment, Universe became transparent to radiation because it became without free electrons. When the temperature was decreased to 3000 K of gravitation forces between atoms was became to exceed of other forces. The gravitation was acted on fluctuation of density in spatial distribution of atoms (mainly H and He) was led to accretion of matter and was formed of large scale structures - proto-galaxies. In latter, the stars and stellar systems - galaxies (the dimension 10^6 light yrs after Big Bang and $T \sim 10^4$ K) were formed on this base.

The other nuclides were formed in result of nucleosynthesis in core stars and their subsequent development. Most the reactions occur during of the evolution of the star, but some are formed in the shock wave that accompanies a supernovae explosion (in example, e-process). The atoms of these newly formed elements are injected into the interstellar medium at high velocity, and by processes that are not well understood, many of them, such silicon and iron atoms, become constituents of tiny interstellar dust grains. The interstellar shocks can then act to destroy these particles. The charged grains move on a spiral in the post-shock magnetic field and are actually accelerated as the post-shock gas (a process called betatron acceleration). The refractory grain such as graphite and silicates destroy in shock with $V > 100$ kms $^{-1}$. The compression and cooling behind shock waves may be trigger of the formation of galaxies as well as stars. During the era of galaxy formation, the propagation of huge shock waves - driven by the collective effect of supernovae in "seed" galaxies - or possibly by super-conducting loops of cosmic string, may have swept up and compressed by hydrogen gas to galactic proportions, and triggered the collapse of protogalactic gas clouds. In addition, the shock waves can produce H_2 , enabling the nearly pure hydrogen gas to cool significantly below 10^4 K and thereby form stars.

Some stars observe as supernovae in result of super explosions. The interstellar shocks driven by supernovae may determine the structure of the interstellar medium (ISM). A five-phase model of the ISM has been developed.:

- most of the volume of the ISM is hot ($T = 10^6$ K) gas that has been shocked by supernova blast waves;

- most the mass of the ISM is in cold ($T < 100\text{K}$) clouds;

- clouds are surrounded by warm envelopes that are heated to $T = 800\text{K}$ and are partially ionized of radiation.

- the cold, warm, and hot phases are all at about the same pressure;

- inside non-radiating blast waves, evaporation of the clouds and their envelopes injects material into the hot gas phase; after the blast waves become radiating, the hot gas cools and returns to the warm and cold phases.

The meteorites contain dust grain with pre-solar (other stellar systems or interstellar medium) matter, which formed from nuclides forming in result nuclear reactions in cores of stars of various types. Then they have reached of stellar atmospheres in result of mixing. The pre-solar, may be interstellar medium, contains SiO_2 and SiC grains. The individual grain have of different isotopic contents Al, O, Si and C. The major effect is due to galactic heterogeneity. The many grains contains isotopes of noble gases and the elements Ba, Nd, Sm and Dy. The contents of nuclides of Sr, Zr and Mo in single SiC grains had been measured (Zinner&Amari, 1999). The meteorites give important information on nucleosynthesis, and stellar evolution, and the evolution of the Mendeleev's table of the Galaxy. The contents of isotopes in the various grains are completely different from those found in the Solar System. These grains represent true stellar material and preserved the isotopic abundance of their primordial sources. The analysis of different dust grains show that their matter was been formed from stars giant. So, pre-solar grains give information on the isotopic abundance of individual stellar sources and on their evolution status (red giant or asymptotic giant branches). Variations in the $^{16}\text{O}/^{17}\text{O}$ ratio reflect differences in stellar mass but variations in the $^{16}\text{O}/^{18}\text{O}$ ratio can only be explained by differences in the original isotopic ratio of the stars. The presence of large ^{26}Mg excesses from the decay of ^{26}Al in many grains is observed. Since ^{26}Al is produced at the higher temperatures of shell burning of H and these nuclides was formed in AGB-stars. The part dust grains was formed in time burst supernovae and novae stars.

The meteoritic SiC have of pre-solar origin from carbon stars.

The heave elements show that nuclides were produced in result of the s-processes (Kr, Sr, Zr, Mo, Xe, Ba, Nd, Sm and Dy).

This evolution is going about 10^9 years. The contents of chemical elements in atmospheres of various types of stars can provide some information about cosmic contents of nuclides from Gamow's Big Bang to now. They can give information about

nuclear processes, about evolution of stars and of Galaxy. The stars may be divided on two main groups - unevolved and evolved. In first group stars' of elemental abundances in their atmospheres has probably not affected by nuclear reactions in appointed stage of evolution, but in second group - vice versa. We investigated of evolved stars for testing of theories of nucleosynthesis, of stellar evolution and chemical evolution of Galactic disk. For it is necessary to know of the distribution of chemical elements from mass number in the atmospheres of stars with different masses. They have passed through this or that stage of evolution.

The distribution contents nuclides from atomic number Z , or number of neutrons N , or upon mass number $A = N + Z$ (atomic weight) is of source for testing of theories of their evolution. The information about distribution of nuclides is of Earth crust, meteorites, atmosphere of Sun with corona and solar wind, atmospheres of planets, soil of Moon, atmospheres of stars, interstellar medium and so on. The distribution of chemical elements in atmospheres of Sun can be taken from Anders&Grevesse (1989), Rykaljuk (2000), Grevesse&Sauval (1998), but distribution of isotopes was taken according to their distribution in Earth crust and meteorites Anders&Grevesse (1989), Cameron (1986), Grevesse&Sauval (1998). The contents of nuclides relate to the progenitor matter of solar system. The initial distribution was taken to account nuclear decay which may to bring to change of abundances of parent and daughter nuclides. This distribution of elemental abundance is adopted as "cosmic", "normal", "standard" one. The solar abundances of some nuclides are different from "normal" one (Tabl. I). The distribution of nuclides have of characteristic properties: the contents of nuclides exponentially decrease of with the growth of mass number to $A = 100$, and than observe a considerable slowing down; large fluctuations in abundances of light elements; peaks of abundances of nuclides with definite of mass numbers.

The analysis of contents of chemical elements in atmospheres of stars shows that have of stars with different from "solar" contents of elements (for example, stars of Population II of the Galaxy, stars of the RCrB-type, peculiar, metallic, zirconium, carbon and so on stars). It should be noted, however, that at the same time the contents of elements of interstellar medium in regions HII around newly formed stars and in planetary nebulae (old objects) is close to that of the solar system. Moreover, elemental contents in other galaxies and quasars (at oldest objects of the Universe) don't differ almost from solar one. The theory of formation and evolution of nuclides, and then of chemical elements and all their isotopes (stable and non-stable) must explain all this.

Table 1: The abundances of nuclides and chemical elements

Z	El	A	process	An&Gr 1989	An&Gr 1989	Cam 1986	Ryk 3000	Gr&Sau 1998	Gr&Sau 1998
1	H	1	U	12.00	12.00	12.00			
		1.0079		12.00	12.00	12.00	12.00	12.00	
	D	2	U? _l	7.53		7.22			
2	He	3	U?	7.14		7.08			
4			U,H	10.99	[10.99]	10.83			
		4.00280		10.99	[10.99]	10.83	10.92	[10.93±0.04]	
3	Li	6	l	2.19		2.22			
		6.941		3.31	1.16	3.32	1.08	1.10±0.10	3.31±0.04
3		7	l,H,U?	3.28		3.32			
4	Be	9	l,U?	1.42	1.15	1.65	1.15	1.40±0.09	1.42±0.04
5	B	10	l,U?	1.83		1.83			
		10.81		2.89	(2.6)	2.53	2.3	[2.55±0.30]	2.79±0.05
		11	l,U?	2.43		2.43			
6	C	12	He, α	8.55		8.62			
		12.011		8.56	8.60	8.62	8.57	8.52±0.30	
		13	H	6.60		6.67			
7	N	14	H	8.05		7.94			
		14.0067		8.05	8.00	7.93	7.94	7.92±0.06	
		15	H	5.62		5.50			
8	O	15.9994		8.93	8.93	8.84	8.86	8.83±0.06	
		16	He	8.93		8.84			
		17	H	5.51		5.54			
		18	He,N	6.23		6.15			
9	F	19(18.9984)	H	4.48	4.56	4.41	4.56	[4.56±0.3]	4.48±0.06
10	Ne	20	He,s	8.06		7.94			
		20.179		8.09	[8.09]	7.99	7.63	8.08±0.06	
		21	He,N,s	5.44		5.42			
		22	He,N,s	6.92		7.02			
11	Na	23(22.9897)	C,s	6.31	6.31	6.35	6.32	6.33±0.03	6.32±0.02
12	Mg	24	He,C, α	7.48		7.50			
		24.305		7.59	7.58	7.60	7.6	7.58±0.05	7.58±0.01
		25	C,s	6.58		6.60			
		26	C,s	6.63		6.65			
13	Al	27(26.98154)	C,s	6.48	6.47	6.50	6.47	6.47±0.07	6.49±0.01
14	Si	28	O, α ,s	7.52		7.54			
		28.085		7.55	7.55	7.58	8.0	7.55±0.05	7.56±0.01
		29	O,s	6.22		6.25			
		30	O,s	6.05		6.07			
15	P	31(30.97378)	O,s	5.57	5.45	5.39	5.48	5.45±0.04	5.56±0.06
16	S	32	O, β ,s	7.24		7.25			
		32.06		7.27	7.21	7.27	7.23	7.33±0.11	7.20±0.06
		33	O,Si,s	5.14		5.15			
		34	O,Si,s	5.89		5.90			
		36	N,Si,s	3.57		3.41			
17	Cl	35	O,Si,s	5.13		5.13			
		35.453		5.27	5.5	5.25	5.50	[5.5±0.3]	5.28±0.06
		37	O,Si,s	4.51		4.64			
18	Ar	36	O,Si, β ,s	6.48		6.53			
		38	O,Si,s	5.76		5.80			
		39.948		6.56	[6.56]	6.60	6	[6.40±0.06]	
		40	s	2.97		3.96			
19	K	39	O,Si,s	5.10		5.09			
		39.098		5.13	5.12	5.12	5.15	5.12±0.13	5.13±0.02
		40	O,Si,s	1.20		2.26			
		41	O,Si,s	3.96		3.96			
20	Ca	40	O,Si, α	6.33		6.36			
	Ca	40.08		6.34	6.36	6.37	6.45	6.36±0.02	6.35±0.01
		42	Si,s	4.15		4.18			

Z	El	A	process	An&Gr 1989	An&Gr 1989	Cam 1986	Ryk 2000	Gr&Sau 1998	Gr&Sau 1998
		43	Si,s	3.47		3.53			
		44	Si,s,α	3.99		4.69			
		46	NSi	1.93		1.89			
		48	NSi	3.61		3.63			
21	Sc	45(44.9559)		3.09	3.10	3.07	3.06	3.17±0.10	3.10±0.01
22	Ti	46	E	3.84		3.85			
		47	E	3.80		3.82			
		47.90		4.93	4.99	4.96	5	5.02±0.06	4.94±0.02
		48	E,α	4.80		4.82			
		49	E	3.67		3.70			
		50	E,NSi	3.67		3.68			
23	V	50	E	1.42		1.36			
		50.9414		4.02	4.00	3.98	4	4.00±0.02	4.02±0.02
		51	E	4.02		3.98			
24	Cr	50	E	4.32		4.31			
		51.996		5.68	5.67	5.68	5.7	5.67±0.03	5.69±0.01
		52	E	5.61		5.60			
		53	E	4.56		4.66			
		54	E	4.06		4.06			
25	Mn	55(54.9380)	E	5.53	5.39	5.54	5.4	5.39±0.03	5.53±0.01
26	Fe	54	E	6.27		6.29			
		55.847		7.51	7.67	7.53	7.6	7.50±0.05	7.50±0.01
		56	E,s	7.47		7.49			
		57	E,s	5.85		5.86			
		58	E,s	4.96		5.05			
27	Co	59(58.9332)	E,s	4.91	4.92	4.92	4.94	4.92±0.04	4.91±0.01
28	Ni	58	E,s	6.08		6.09			
		58.70		6.25	6.25	6.26	6.3	6.25±0.04	6.25±0.01
		60	E,r	5.66		5.67			
		61	E,r	4.30		4.33			
		62	E,r	4.80		4.82			
		64	E,r	4.25		4.29			
29	Cu	63	E,s	4.11		4.15			
		63.541		4.27	4.21	4.31	4.06	4.21±0.04	4.29±0.04
		65	E,r	3.76		3.80			
30	Zn	64	E,s	4.34		4.36			
		65.38		4.65	4.60	4.68	4.45	4.60±0.08	4.67±0.04
		66	E,s	4.10		4.12			
		67	E,s	3.27		3.28			
		68	E,s	3.93		3.94			
		70	E,r	2.45		2.47			
31	Ga	69	E,s	2.91		2.94			
		69.72		3.13	2.88	3.16	2.8	2.88±0.10	3.13±0.04
		71	E,s	2.73		2.75			
32	Ge	70	E,s	2.94		2.96			
		72	E,r	3.07		3.08			
		72.59		3.63	3.41	3.64	3.4	3.41±0.14	3.63±0.04
		73	E,r	2.52		2.53			
		74	E,r	4.19		3.20			
		76	E,r	2.52		2.53			
33	As	75(74.9216)	s,r	2.37	-	2.37	-	-	2.37±0.02
34	Se	74	p	1.29		1.34			
		76	s	2.30		2.36			
		77	s,r	2.23		2.28			
		78	s,r	2.72		2.77			
		78.96		3.34	-	3.40	-	-	3.41±0.03
		80	s,r	3.04		3.10			
		82	r	2.31		2.36			
35	Br	79	s,r	2.33		2.24			
		79.904		2.63	-	2.54	-	-	2.63±0.04

Z	El	A	process	An&Gr 1989	An&Gr 1989	Cam 1986	Ryk 2000	Gr&Sau 1998	Gr&Sau 1998
		81	s,r	2.32		2.23			
36	Kr	78	p	0.74		0.74			
		80	s,p	1.55		1.55			
		82	s	2.27		2.25			
		83	s,r	2.27		2.25			
		83.80		3.21	-	3.19	-	-	3.31±0.08
		84	s,r	2.96		2.95			
		86	r	2.45		2.43			
37	Rb	85	s,r	2.26		2.22			
		85.4675		2.41	2.60	2.36	2.6	2.60±0.15	2.41±0.02
		87	r	1.85		1.84			
38	Sr	84	p	0.67		0.68			
		86	r	1.92		1.93			
		87	r	1.77		1.75			
		87.62		2.93	2.90	2.94	2.9	2.97±0.07	2.92±0.02
		88	r	2.84		2.85			
39	Y	89(84.9054)	s,r	2.22	2.24	2.26	2.2	2.24±0.03	2.23±0.02
40	Zr	90	s,r	2.32		2.37			
		91	s,r	1.66		1.70			
		91.22		2.61	2.60	2.65	2.68	2.60±0.02	2.61±0.02
		92	s,r	1.85		1.89			
		94	r	1.85		1.90			
		96	r	1.06		1.11			
41	Nb	93(92.9064)	s,r	1.40	1.42	1.53	1.86	1.42±0.06	1.40±0.02
42	Mo	92	p	1.13		1.38			
		94	p	0.93		1.13			
		95	s,r	1.16		1.37			
		95.94		1.96	1.92	2.18	2.09	1.92±0.05	1.97±0.02
		96	s	1.18		1.40			
		97	s,r	0.94		1.15			
		98	s,r	1.34		1.55			
		100	r	0.94		1.16			
43	Tc	[97]	s,r			-0.6			
44	Ru	96	p	0.57		0.60			
		98	p	0.10		0.13			
		99	s,r	0.93		0.96			
		100	s	0.93		0.96			
		101	s,r	1.06		1.09			
		101.01		1.82	1.84	1.85	1.85	1.84±0.07	1.83±0.04
		102	s,r	1.32		1.35			
		104	r	1.09		1.12			
45	Rh	103(102.9055)	s,r	1.09	1.12	1.18	1.34	1.12±0.04	1.10±0.04
46	Pd	102	p	-0.29		-0.33			
		104	s	0.74		0.73			
		105	s,r	1.05		1.04			
		106	s,r	1.13		1.13			
		106.4		1.70	1.69	1.69	1.56	1.69±0.04	1.70±0.04
		108	r	1.12		1.12			
		110	r	0.77		0.76			
47	Ag	107	s,r	0.96		0.94			
		107.868		1.24	(0.94)	1.24	0.9	(0.94±0.25)	1.24±0.04
		109	r	0.92		0.93			
48	Cd	106	p	-0.14		-0.15			
		108	p	-0.29		-0.29			
		110	r	0.86		0.85			
		111	r	0.87		0.87			
		112	r	1.14		1.15			
		112.40		1.76	1.86	1.77	2	1.77±0.11	1.76±0.04
		113	r	0.85		0.85			
		114	r	1.22		1.23			

Z	El	A	process	An&Gr 1989	An&Gr 1989	Cam 1986	Ryk 300	Gr&Sau 1998	Gr&Sau 1998		
49	In	116	r	0.64		0.64					
		113	p,s	-0.55		-0.52					
		114.82		0.82	(1.66)	0.85	1.7	(1.66±0.15)	0.82±0.04		
50	Sn	115	r	0.80		0.84					
		112	p	0.12		0.12					
		114	p	-0.04		-0.04					
		115	p,s,r	-0.33		-0.31					
		116	s	1.30		1.30					
		117	s,r	1.02		1.03					
		118	s,r	1.52		1.52					
		118.69		2.14	2.0	2.14	2	2.0±(0.3)	2.14±0.04		
		119	s,r	1.07		1.02					
		120	s,r	1.65		1.66					
51	Sb	122	r	0.80		0.82					
		124	r	0.90		0.92					
		121	s,r	0.80		0.83					
		121.75		1.04	1.0	1.07	1	1.0±(0.3)	1.03±0.07		
		123	r	0.67		0.92					
		120	p	-0.81		-0.66					
		122	s	0.65		0.78					
		123	s	0.19		0.34					
		124	s	0.91		1.05					
		125	s,r	1.09		1.23					
52	Te	126	s,r	1.51		1.66					
		127.80		2.24	-	2.39	-	-	2.24±0.04		
		128	r	1.74		1.89					
		130	r	1.77		1.93					
		127(126.9045)	s,r	1.51	-	1.68	-	-	1.51±0.08		
		124	p	-0.69		-0.56					
		126	p	-0.74		-0.60					
		128	s	0.57		0.68					
		129	s	1.66		1.78					
		130	s	0.87		0.97					
53	I	131	s,r	1.56		1.67					
		131.30		2.23	-	2.34	-	-	2.17±0.08		
		132	s,r	1.64		1.76					
		134	r	1.22		1.35					
		136	r	1.13		1.275					
		133(132.9054)	s,r	1.12	-	1.17	2.1	-	1.13±0.02		
		54	Xe	130	p	-0.77		-0.74			
				132	p	-0.79		-0.76			
				134	s	0.59		0.80			
				135	s,r	1.03		1.07			
136	s			1.10		1.15					
137	s,r			1.26		1.31					
137.34				2.21	2.13	2.26	2.01	2.13±0.05	2.22±0.02		
138	s,r			2.06		2.11					
55	Cs	138	p	-1.85		-1.89					
		138.9055		1.20	1.22	1.14	1.32	1.17±0.07	1.22±0.02		
		139	s,r	1.20		1.14					
		136	p	-1.11		-1.06					
56	Ba	138	p	-0.99		-0.95					
		140	s,r	1.58		1.60					
		140.12		1.61	1.55	1.65	1.68	1.58±0.09	1.63±0.02		
		142	r	0.65		0.70					
57	La	141(140.9077)	s,r	0.78	0.71	0.83	0.76	0.71±0.08	0.80±0.02		
		142	s	0.91		0.91					
		143	s,r	0.56		0.56					
58	Ce	144	s,r	0.85		0.85					
		144.24		1.47	1.50	1.47	1.38	1.50±0.06	1.49±0.02		
		142	s,r	0.56		0.56					
59	Pr	142	s	0.91		0.91					
		143	s,r	0.56		0.56					
60	Nd	144	s,r	0.85		0.85					
		144.24		1.47	1.50	1.47	1.38	1.50±0.06	1.49±0.02		

Z	El	A	process	An&Gr 1989	An&Gr 1989	Cam 1986	Ryk 2000	Gr&Sau 1998	Gr&Sau 1998
		145	s,r	0.39		0.39			
		146	s,r	0.71		0.71			
		148	r	0.23		0.23			
		150	r	0.22		0.22			
62	Sm	144	p	-0.54		-0.55			
		147	s,r	1.42		1.14			
		148	s	0.02		0.01			
		149	s,r	0.11		0.10			
		150	s	-0.16		-0.17			
		150.4		0.97	1.00	0.95	0.86	1.01±0.06	0.98±0.02
		152	r	0.39		0.38			
		154	r	0.32		0.31			
63	Eu	151	s,r	0.22		0.23			
		151.96		0.54	0.51	0.55	0.61	0.51±0.08	0.55±0.02
		153	s,r	0.26		0.27			
64	Gd	152	p	-1.62		-1.50			
		154	s	-0.59		-0.47			
		155	s,r	0.24		0.37			
		156	s,r	0.38		0.51			
		157	s,r	0.27		0.39			
		157.25		1.07	1.12	1.20	1.14	1.12±0.04	1.09±0.02
		158	s,r	0.47		0.59			
		160	r	0.41		0.54			
65	Tb	159(158.9254)	s,r	0.33	-0.1	0.46	-0.1	(-0.1±0.3)	0.35±0.02
66	Dy	156	p	-2.10		-2.14			
		158	p	-1.87		-1.90			
		160	s	-0.48		-0.50			
		161	s,r	0.43		0.42			
		162	s,r	0.56		0.35			
		162.50		1.15	1.1	1.14	1.1	1.14±0.08	1.17±0.02
		163	s,r	0.55		0.54			
		164	s,r	0.60		0.59			
67	Ho	165(154.9304)	s,r	0.50	(0.26)	0.54	-	(0.26±0.16)	0.51±0.02
68	Er	162	p	-1.90		-1.93			
		164	p,s	-0.84		-0.87			
		166	s,r	0.48		0.46			
		167	s,r	0.31		0.30			
		167.26		0.95	0.93	0.94	0.83	0.93±0.06	0.97±0.02
		168	s,r	0.38		0.40			
		170	r	0.13		0.11			
69	Tm	169(167.26)	s,r	0.13	(0.00)	0.12	0.28	(0.00±0.15)	0.15±0.02
70	Yb	168	p	-1.94		-1.99			
		170	s	-0.57		-0.64			
		171	s,r	0.10		0.03			
		172	s,r	0.29		0.21			
		173	s,r	0.16		0.08			
		173.04		0.95	1.08	0.88	0.8	1.08±(0.15)	0.96±0.02
		174	s,r	0.45		0.38			
		176	r	0.05		-0.02			
71	Lu	175(174.97)	s,r	0.11	(0.76)	0.11	0.76	0.06±0.10	0.13±0.02
		176	s	-1.47		-1.40			
72	Hf	174	p	-2.05		-1.93			
		176	s	-0.54		-0.48			
		177	s,r	0.01		0.07			
		178	s,r	0.18		0.24			
		178.49		0.74	0.88	0.81	0.85	0.88±(0.08)	0.75±0.02
		179	s,r	-0.12		-0.06			
		180	s,r	0.29		0.35			
73	Ta	180	p	-4.05		-4.04			
		180.9479		-0.13	-	-0.12	-	-	-0.13±0.02

Z	El	A	process	An&Gr 1989	An&Gr 1989	Cam 1986	Ryk 300	Gr&Sau 1998	Gr&Sau 1998
74	W	181	sr	-0.13		-0.12			
		180	p	-0.22		-1.82			
		182	sr	0.10		0.47			
		183	sr	-0.17		0.21			
		183.85		0.68	(1.11)	1.05	1.18	(1.11±0.15)	0.69±0.03
		184	sr	0.17		0.53			
75	Re	186	r	0.13		0.51			
		185	sr	-0.18		-0.15			
		186.207		0.27	-	0.28	-0.3	-	0.28±0.03
76	Os	187	sr	0.06		0.12			
		184	p	-2.36		-2.33			
		186	s	-0.42		-0.48			
		187	s	-0.42		-0.52			
		188	sr	0.51		0.54			
		189	sr	0.59		0.62			
		190	sr	0.80		0.84			
		190.2		1.38	1.45	1.41	1.45	1.45±0.10	1.39±0.02
77	Ir	192	r	1.00		1.03			
		191	sr	0.95		1.00			
		192.22		1.37	1.35	1.43	1.45	1.35±(0.10)	1.37±0.02
78	Pt	193	sr	1.17		1.23			
		190	p	-2.21		-2.17			
		192	s	-0.42		-0.38			
		194	sr	1.20		1.24			
		195	sr	1.21		1.25			
		195.95		1.68	1.8	1.72	1.75	1.8±0.3	1.69±0.04
79	Au	196	sr	1.08		1.13			
		198	r	0.54		0.58			
80	Hg	197(196.9665)	sr	0.83	(1.01)	0.90	0.95	(1.01±0.15)	0.85±0.04
		196	p	-1.73		-1.93			
		198	s	0.08		-0.09			
		199	sr	0.31		0.12			
		200	sr	0.45		0.26			
		200.59	sr	1.09	-	0.90	1.9	-	1.13±0.08
		201	sr	0.21		0.19			
		202	sr	0.56		0.37			
		204	r	-0.08		-0.07			
		203	sr	0.29		0.32			
		204.37		0.82	(0.9)	0.85	0.9	(0.9±0.2)	0.83±0.04
82	Pb	205	sr	0.67		0.70			
		204	s	0.34		0.28			
		206	sr	1.33		1.27			
		207	sr	1.37		1.31			
		207.2		2.05	1.85	1.99	1.93	1.95±0.08	2.06±0.04
83	Bi	208	sr	1.82		1.76			
		209(208.9804)	sr	0.71	-	0.72	1.9	-	0.71±0.04
90	Th	232(232.0381)	r	0.08	0.12	0.23	0.2	-	0.09±0.02
		235	r	-0.62		-0.62			
92	U	238(238.02)	r	-0.49	(<-0.47)	-0.12		(<-0.47)	-0.50±0.04

A remarkable complication arises due to scanty number of stable isotopes (islands of stability) among the set of unstable isotopes (the sea of non-stability). Therefore, the distribution of nuclides to a greater extent must be modified as a result of radioactive decay. The process may be different under these or those conditions (up to no decay all, example neutron). The chemical composition of atmospheres of the stars of first evolution stage is not contaminated with stellar nucleosynthesis products, whereas that of the second evolution stars can be diluted with products of nucleosynthesis and to differ from abundance progenitor matter. The atoms of these newly formed elements are injected into the interstellar medium at high velocity, and by processes that are not well understood, many of them, such silicon and iron atoms, become constituents of tiny interstellar dust grains. The interstellar shocks can then act to destroy these grains by collisions with high velocity atoms and by collisions with other dust particles. The stars of the Galactic disk are objects second or third stars' of generation.

The testing of theories of nucleosynthesis and stellar evolution, chemical and dynamical evolution of the Galaxy is the one from problem of modern astrophysics. The testing was based upon data of abundances of chemical elements and their isotopes in diverse object of the Galaxy. In particular, for this goal necessary to know the almost precision about the contents of chemical elements and their isotopes in the atmospheres of stars different masses which have passed through this or that stage of evolution. The cool giants and super-giants are of the convenient object for such investigation. They are the brightest objects of stellar population in the Galaxy and in their spectra a great number of absorption and/or emission lines various chemical elements and their compounds are detected (even for stars with extreme iron deficiency).

According to the present concepts of theory of stellar evolution, the star's time stay at a certain stage (in this at that locus of H-R diagram) considerably depends of its mass, initial chemical composition and nucleosynthesis processes. The belonging of stars to various types of population of the Galaxy, to different types of clusters and dynamic groups gives an excellent possibility of tracing evolution of chemical composition of their atmospheres.

The contents of chemical elements in stellar atmospheres

In this paper we shall to spoke about results of investigation of chemical composition in the atmospheres of cool giants of oxygen sequence of the Galaxy thick and thin disks which have been

obtained at Astronomical Observatory of Odessa National University.

The stars-giant in the Galaxy disk are at various stages of evolution – the first and subsequent giant branches (FRGB and other), blue and red parts of the horizontal branch (BHB and RHB), the asymptotic giant branch (AGB), the post-asymptotic giant branch (post-AGB). These stars have located in the regions H-R diagram, which will penetrate each other. If the mixing of atmospheres of stars with products of elements nucleosynthesis hold true, that the contents of nuclides in atmospheres of stars in common with their known fundamental characteristics can provide information about evolution status of stars, about its of mass and about chemical composition of progenitor matter (Sweigart et al., 1989).

The existence of three stages of possible deep mixing is supposed:

- on a stage MS, or at an exist on a stage FRGB,
- on a stage AGB (in time burning H and He in layers sources),
- on a stage of thermal flares of He.

The simplest interpretation of spectral classification of stars makes necessary to suggest a difference between chemical compositions in the atmospheres of cool giants stars. It are stars with excess or deficiency of elements of iron group, with various ratio of abundances of carbon and oxygen elements with even and odd Z , with excess or deficiency of elements of s -process and so on.

A great number of works have been issued recently on the determination of contents of chemical elements and their isotopes in the atmospheres of stars, and other fundamental characteristics, by using spectra with a high signal-noise ratio ($S/N=300$) and the method of model atmospheres and of synthetic spectra. We shall consider in brief the results of survey given in literature.

The stars of the main sequence (MS) of the Galaxy disk in the solar vicinities have the following contents of elements CNO - group relative to the Sun:

$$[C/H] = -0.23, [N/H] = 0.38, [O/H] = -0.03,$$

where $[El/H] = \log(El/H)^* - \log(El/H)_\odot$, and $\log(El)$ is the abundance of element in the scale of $\log H=12.0$. The ratio of contents of isotopes ^{12}C and ^{13}C range from 4 to 90 (The average value $^{12}C/^{13}C = 22.5$ whereas that of $^{12}C/^{13}C$ for the solar atmosphere is equal ~ 90). The values $^{12}C/^{13}C$ from 20 to 30 have of stars with $M > 2M_\odot$. The ratio swiftly decrease for stars with more little mass according to observations and that contradicts of theory. To explain this effect it is necessary to suppose unknown mechanism of mixing. During further evolution of stars with $M < 1.5M_\odot$ they proceeds in sequence of spectral types M-MS-S-SC-C (R or N).

The progenitors of G-M giant stars are F-G dwarf stars with masses ranging from $0.8 < M/M_{\odot} < 3.0$. Therefore, the products of nucleosynthesis in their atmospheres should be expected as the parent matter in atmosphere of stars-giant diluted with products nuclear synthesis? Indeed, the average ratio abundances is equal $C/N=0.9$ for open clusters of the Hyades and Praesepes (Mishenina et al., 1990, Komarov & Basak, 1992) while for the Sun $C/N=4.8$, but for star-dwarfs of Hyades was found $C/N=(C/N)_{\odot}$. The average value $C/N=2.3$ is obtained for cool giant stars of Galaxy field (Komarov, 1999). It means that the content N grows while content C decrease. It should be noted that theory of evolution of single star predicts ratio $C/N=2.0$ after mixing. The ratio of isotopes $^{13}C/^{12}C$ for atmospheres of cool star-giants are much less than the solar (earth) one. The ratio contents of nuclides due to convection and circulation, He-flares deeply penetrating convection and loss mass can be changed on the stellar atmospheres. It was obtained that $C/N=2.3$, i.e. the content of nitrogen was found to enhance while that of carbon to decrease, incidentally, for metal deficient stars and for those with $M < 1M_{\odot}$ the ratio $(C/N)^*=(C/N)_{\odot}$, whereas $(N/Fe)^* > (N/Fe)_{\odot}$ and $(C/Fe)^* < (C/Fe)_{\odot}$ for all the giants (Kjaergaard et al., 1987). At the same time the total abundance of C, N, O elements for dwarf stars and giant stars of Hyades cluster is nearly identical. The carbon and essential nuclides were synthesized in the interior of giant stars, and then were injected into the space by means of violent supernova explosions, or continuously, although with much less efficiency via stellar winds. The atmospheres of star-giants must be carbon poor, nitrogen rich at the constant oxygen abundance in comparison to the contents of these elements in the atmospheres of dwarf stars.

The light elements Li, Be and B are easily destructed at low temperatures (nearly from 2×10^6 to 5×10^6) that must decrease abundance these elements in atmospheres giant stars especially Li. These nuclides can't be formed during of stellar evolution (during of the processes nuclear synthesis), excluding may be, 7Li . However, content of 7Li in some star-giant exceeds the cosmological content! The contents of 7Li in meteorites and the solar atmosphere differ by nearly two orders. Now it is necessary to determine of contents of these elements in atmospheres oldest of Galaxy stars with big deficiency of metal.

The contents of chemical elements had obtained for the atmospheres of field giant stars and it is in good agreement with that of dwarf stars in the region of metallicity $-2.4 < [Fe/H] < 0.35$. The elements of the α -process are overabundant in the atmospheres of metal deficient stars, but Na and Al are

in deficiency relative to elements α -process (Gratton et al., 1987). It should be noted that "excess" of some elements relative to the solar abundance could be result from either hyperfine structure of atomic lines or isotopic shift. The excess in contents is observed not only for Na, but also for Al and Si. The overabundances increase with luminosity of stars. The observed anomalies provide evidence that, in addition to the CNO hydrogen-burning cycle, the MgAl and NeNa cycles operate of main-sequence phase. The anomalies in contents of s-process elements, also observed in the atmospheres of field stars, testify to the presence of a substantial number of neutrons. The anomalies in contents of s-process elements are absent from giant of the young Hyades cluster. The readers can to write of capital reviews by Gehren (1988).

Therefore, the structure of a lower level of every line of absorption is necessary to carefully analyze in determining elemental abundance. The contents of chemical elements can be in several times overestimate. It is necessary to take account of relative contents of all stable isotopes at determination of content a certain chemical element. The isotopic shift for the elements of iron group is unlikely to occur since isotopes ^{54}Cr , ^{55}Mn , ^{56}Fe , ^{58}Co , ^{59}Ni are primarily observed. For elements with odd Z the hyperfine structure of atomic levels is probable. Abundance ratios of isotopes of elements C, O, Ng, Al, Si, Ca, Ti, Zr can differ from those of the Earth and give information about nucleosynthesis process of addition of α -particles and neutrons.

The structure of a red giant can exist only at absence of full mixing between outer and inner layers. However, as was shown above, the $^{13}C/^{12}C$ isotopic ratio for giant stars is considerably less than that of the Earth (the Sun). The interest represent of metal-poor red giants with $[Fe/H] < -2$ which are likely to be stars with low mass ($M < 0.8M_{\odot}$) and which have originated from a cloud with mass $10^3 > 10^6 M_{\odot}$. Massive stars have of short lifetimes and they supply the cloud with different metals and products of the CNO-cycle. Variations in intensity bands of CN, CH and NH indicate that red giants originated from progenitor matter with various ratios of nucleosynthesis products. In this respect, rather illustrative is the Cas A object - a remnant of the supernovae flared up approximately 350 year ago. The clouds are found with a primary oxygen abundance $[H/O] = -3.7$, $[He/O] < -1.9$ and $[C/O] < -2.1$. The lines of S, Ar and Ca elements are visible in various clouds. This means that the star is in the pre-supernovae stage of evolution has layer structure, and thickness of corresponding layers depend on initial mass of the star.

The determination of contents of chemical elements of cool stars is associating with the prob-

lem of determining fundamental characteristics, i.e. of effective temperatures T_{eff} , of gravities on the surface (g), of metallicities ($[Fe/H]$), of microturbulent velocities (V_t), with that of calculation of model atmospheres adequate to the structure of atmospheres of real stars, with that of determining physical-chemical parameters of radiation and of collision of atoms and molecules Ridgway et al. (1980), Komarov et al. (1985), Korotina et al. (1992), Komarov (1999).

The value of microturbulent velocity V_t in the first approximation was estimated from the curve of growth for absorption lines FeI. The value V_t was revised by the method of model atmospheres by means of calculation of abundance $\log(Fe)$, the values V_t being diverse. The correlation between $\log(Fe)$ and W_λ was found, and the value V_t was selected when there was no correlation between $\log(Fe)$ and W_λ . The influence of rotation and macroturbulence on the profile of absorption lines was taken into account by the convolution of a synthetic spectrum with the apparatus function of a spectral device. It is suggested that broadenings of a profile of the line due to rotation and macroturbulence are small as compared to those caused by the apparatus function of the device.

For cool stars it is difficult to select relatively pure absorption lines by taking no account of a synthetic spectrum and its convolution with the apparatus function of the device as the apparatus function of a spectral device. The apparatus function of a spectral device was taken the Gaussian with a half-width equal to spectral resolution. For selecting pure and weakly blended absorption lines the calculation of synthetic spectra were carried out. The models atmospheres was taken from the grid (Bell et al., 1978) with parameters T_{eff} , $\log g$, $[Fe/H]$ corresponding to K0 III and K5 III stars, but namely (5000, 3.00, 0.0) and (4000, 1.50, 0.0) respectively.

The fundamental characteristics and chemical composition of same stars γ Tau, δ Tau, ϵ Tau (clusters of Hyades), α Tau, γ Sge their were found from spectrograms with reciprocal dispersion to be not worse than 5.6 Å/mm with the wavelength range 5360–6700 Å. In the same detail chemical composition of stars BS 3427 and BS 3428 of open clusters Hyades and Praesepe was investigated Komarov et al. (1985), Komarov et al. (1985), Mishenina et al. (1986), Gopka et al. (1990), Gopka et al. (1990), Komarov et al. (1992).

The chemical contents in the atmospheres of cool giant stars of oxygen sequence depends from belonging of stars to various stages of star evolution (Korotina et al., 1989; Korotina et al., 1992). It is related to our possibility of only rough estimating mass of field of stars and in even such assumption there arises a question on reliability

of the results. We judge of evolutionary status of a star from its position in the H-R diagram but at the same locus of H-R diagram can be located stars proceeding different stages of evolution affected by distinctions in masses and initial chemical composition of pro-star medium. The best position of stars seemed to be those belonging to the open clusters or dynamical groups because of a possibility of estimating their age. But here we come across a paradox. As is known (Korotina et al., 1989, Korotina et al., 1992) relative quantity of stars of G5 III – K0 III spectral types with "standard" chemical composition must be small but that of stars in K2 III – K5 III range with "standard" chemical composition is predominant. However, in the most nearby open Hyades and Praesepe clusters K0 III giant stars have "standard" abundance (except for some elements C, O, Na) whereas in the most well studied dynamical group the α Boo star (K2 IIIp) is certain to be metal-deficient. In the analysis and comparisons of results obtained various authors the abundances should be given relative to hydrogen in the same star rather than relative to abundance in the solar atmospheres. From our data the elemental contents in atmospheres of star giants belonging to the thick disk and thin of Galaxy are obtained.

The quality of determination of contents of chemical elements and their isotopes in atmospheres of stars must be connected with problems of possible influence of fundamental characteristics of atmospheres of stars as well as of effects:

- non-LTE;
- rotation;
- chromosphere, corona and wind;
- starspotting;
- fluorescence;
- nonthermal of transfer of energy.

The elemental contents of ~120 of cool giant stars in vicinity of Sun have been determined. The method of model atmospheres and of synthetic spectra was used. It should be noted that many elements show discrepancies in content determined absorption lines of atoms and ions. For us, astrophysics-observers, the following question is of importance:

"At what stage does the mixing of interstellar medium with matter, as having passed through the stellar evolution stage, take place."

As is well known, the basic suppliers for newly synthesized nuclides into the interstellar medium are of the outburst of supernovae types SNI, SNIi, possibly, of outburst of novae N . The stars being on the AGB are as a result of outflow of matter (stellar wind and super-wind). Massive, short-living stars $M > 8M_\odot$ synthesize oxygen, elements of a -process and light Z -odd and N -even elements

(Na, Al). The SNI-type stars with $M \sim (1+3)M_{\odot}$ are the source of elements iron-group. These stars are evolved slower than those of SNIi-type. SNI-type stars are basic suppliers of these elements into the interstellar medium because during the outburst a complete fragmentation of the star takes place. The AGB-stars determine the content of heavy elements s-processes, as well as elements CNO-group and their isotopes (for example, the values of ratios of isotopes $^{12}\text{C}/^{13}\text{C}$ vary in the atmospheres cool stars from 4 to 90). The stars of the given metallicity can have various contents of other elements, in particular, elements of α -process. The AGB-stars have of a degenerate CO-nucleus and two thin layer sources of He and H. The He flares occurs. This promotes to the mixing of interstellar medium with newly formed stable and unstable nuclides, which passed through nucleosynthesis, with matter of stellar atmospheres. These stars have M from 1 to $8 M_{\odot}$.

In the Astronomical Observatory of Odessa National University the new data about temperature, gravity, microturbulent velocity, radius, mass and total luminosity of ~ 1500 G-, K-, M star-giants are obtained (Korotina et al., 1989, Korotina et al., 1992, Komarov et al., 1996). The metallicities of star-giants belonging to 27 open clusters and moving groups of various ages were determined. The dispersion of metallicities for old stars amounts from 0.0 to -0.5 dex, but for young stars amounts from 0.1 to -0.1 dex. It is assumed that the division of star-giants in vicinity Sun into two groups corresponds to their division into two ages' groups or into two star formation flashes localized in time. The processes of mixing in interstellar medium have been increased in the course its evolution. It should be noted that T_{eff} of these stars for the same spectral type increases with growth metallicity. It is shown that their luminosities are increased with growth metallicity too. The distribution of stars for various intervals of metallicities and for various intervals of space velocities was studied. It was found that for stars with slow space velocities $V_{\text{sp}} < 60 \text{ km s}^{-1}$ (stars of Galactic disk) have maximum in distribution for $[\text{Fe}/\text{H}] = -0.2$ dex. The distribution of stars from metallicities with $V_{\text{sp}} > 60 \text{ km s}^{-1}$ is nearly constant.

The contents of chemical elements in atmospheres of K-supergiants belonging in the Small Magellan Cloud were determined. The all investigated of stars have a deficit in the contents of iron on a comparison with the solar ones. For all stars the same method was used. All stars have close photometric and spectral characteristics. The variations of the contents of iron $[\text{Fe}/\text{H}]$ at selected stars SMC, on all probability, reflect differences primordial of chemical structure of an inter-

stellar medium. The interest represents the contents of elements of α -process in our case the contents of elements Ca, Si. In our Galaxy in atmospheres of stars with a deficit of metals have the enrichment contents of these elements. At investigated stars SMC, on the contrary, the small deficit in the contents Si, Ca to relative iron are observed. The values $[\text{Si}/\text{Fe}]$ vary from -0.5dex up to -0.1dex. The contents Ca is more close the contents one for stars with solar content of iron (Komarov et al., 2001).

We began of investigation of contents of nuclides to use of molecules-hydrides namely Mg, Ca, Zr and etc. The new molecular characteristics of radiation have been used. The stars belongs thick (old?) and thin (young?) disks of Galaxy. It should be noted, the production of nitrogen is dominated by primary processes at low metallicity and secondary processes at high metallicity for spiral galaxies and vice versa. The production of carbon increases with increasing metallicity. The masses depend neither from the spectral type nor from the metallicity. The most impressive result is that of cool star-giants in the spectral region from G5 to K5 have masses statistically less than solar one, and consequently, these have the ages compared with that of a globular clusters. The determination of contents of elements and their isotopes in atmospheres cool giant stars was made (Komarov et al., 1985a, Komarov et al., 1985b, Gopka et al., 1990a, Gopka et al., 1990b, Komarov&Basak, 1992, Komarov et al., 1994, Komarov, 1999, Kovtyukh et al., 2000, Komarov et al., 2001) to use of model atmospheres Bell et al. (1978), Kurucz (1993) and codes of Tsymal (1994, 1995).

Conclusion

The accretion of small satellite galaxies appears to have been important in the formation of the halo, thick and thin discs of the Galaxy. The disrupting Sgr dwarf galaxy and the recent discovery of a young, metal-poor component of the halo indicate that this is a continuing process. The Milky Way is large disk galaxy. Its main components are the rapidly rotating thin and thick disks, the very slowly rotating metal-poor halo, the bulge, and the dark corona. The contents of chemical elements in atmospheres of stars belonging of thin disk gives information about the later stage of evolution.

The differences in the relative contents of nuclides of a Mg for cold stars - giants of thin and thick disks of a Galaxy are within the limits of errors of their determination. The study of the relative contents of nuclides of a Mg, and nuclides of other elements, and for the greater number of star-giants of thick and thin disks of

a Galaxy is necessary for final conclusions. As shown early, in processes of enrichment of atmospheres of stars by products of nuclear fusion (s-process) can happens at the stage of transition from MS on a branch of the star-giants.

We believe that cool star-giants in vicinity of Sun don't belong to one group. They belong of thick and thin disks of Galaxy. Therefore, the contents of light as well as heavy nuclides in their atmospheres must be studied by the same method, same observable material, same input physics and same physical approximations. The conclusion about evolution of chemical elements and their isotopes in stellar stage of evolution may be made only in this a case.

References

- Anders E., Grevesse N.: 1989, *Geoch. Cosmoch. Acta*, **53**, 197.
- Bell R.A., Eriksson R., Gustafsson B., Nordlund A.: 1978, *Astron. Astrophys. Suppl.*, **34**, 229.
- Cameron A.J. Contents of chemical elements and nuclides in solar system. 1986, *The nuclear Astrophysics* /ed. D.D. Clayton, D.N. Schramm, **33** (Rus.).
- Gehren T.: 1988, *Rev. in Modern Astronomy*, **1**, 52.
- Gopka V.F., Komarov N.S., Mishenina T.V., Juschenko A.V.: 1990a, *Astron. Zhurnal*, **67**, 1204.
- Gopka V.F., Komarov N.S.: 1990b, *Astronom. Zhurnal*, **67**, 1211.
- Gratton R.G., Sneden C.: 1987, *Astron. Astrophys.*, **178**, 179.
- Grevesse N., Sauval A.J., Standard Solar Composition. *Space Science Reviews*, 1998, **85**, 161-174.
- Kjargaard P., Gustafsson B., Wolker G.A.K., Hulftgwist L.: 1987, *Astron. Astrophys.*, **178**, 145.
- Komarov N.S., Mishenina T.V.: 1985a, *Kinematika i fizika nebesnykh tel*, **1**, 77.
- Komarov N.S., Mishenina T.V., Motrich V.D.: 1985b, *Astron. Zhurnal*, **62**, 740.
- Komarov N.S., Basak N.Yu.: 1992, *Astron. Astrophys. Trans.*, **3**, 179.
- Komarov N.S., Basak N.Ju., Gorbaneva T.V., Kantzen L.E.: 1994, *Odessa Astron. Publ.*, **7**, 143.
- Komarov N.S., Korotina L.V., Shevchuk T.V.: 1996, *Kinematika i fizika nebesnykh tel*, **26**, 3
- Komarov N.S.: 1999, The cool stars-giant, *Astroprint*, Odessa, 213 p. (Rus.)
- Komarov N.S., Zgonyajka N.S., Vasil'eva S.V.: 2001, *Kinematika i fizika nebesnykh tel*, **17**, 471.
- Korotina L.V., Dragunova A.V., Komarov N.S.: 1989, *Astrofizika*, **21**, 9.
- Korotina L.V., Komarov N.S.: 1992, *Astron. Zhurnal*, **69**, 1188.
- Kovtyukh V.V., Komarov N.S., Andrievsky S.M., Dulapchi I.F.: 2000, *Odessa Astron. Publ.*, **12**.
- Kurucz R.L.: 1993, CD-ROM N18, *Smithsonian Astrophys. Obs.* Cambridge, MA
- Lyubimkov L.S. The chemical content: the methods and results of analysis. 1995, *Astroprint*, Odessa, 324 p. (Rus.)
- Mishenina T.V., Panchuk V.E., Komarov N.S.: 1986, *Izvestia SAO*, **28**, 1.
- Ridgway S.T., Joyee R.R., White N.M., Wing H.F.: 1980, *Astrophys. J.*, **235**, 126.
- Rykaljuk: 1998, The elected problems of astronomy and astrophysics, L'vov, 58.
- Sweigart A.V., Greggio L., Renzini A.: 1989, *Astrophys. J. Suppl.*, **69**, 911 p.
- Trimble V.: 1975, *Reviews of Modern Physics*, **47**, N4, 976 p.
- Trimble V.: 1991, *Astrophys. Rev.*, **3**, 1.
- Tsybmal V.V.: 1994, *Odessa Astron. Publ.*, **7**, 146.
- Tsybmal V.V.: 1995, *ASP Conference Ser.*, **108**, 198.
- Zinner E., Amari S.: 1999, *Asymptotic Giant Branch Stars*, I.A.U. Symposium **191**, 59-68.

EVOLUTION OF CHEMICAL STRUCTURE EXTREME HE-RICH STARS

V.V. Leushin

Special astrophysical observatory of RAS, N. Archiz, Russia
leushin@sci.lebedev.ru

1. Introduction

Abundances of chemical elements observed in various astrophysical objects now are, in general, the result of nucleosynthetic processes occurring in the Universe (primordial and stellar nucleosynthesis). So, the nuclei consisting of integer number of α -particles (^{12}C , ^{16}O , ^{20}Ne , ...) are the most stable and abundance. Intermediate nuclei (^{14}N , ^{18}F , ...) are not synthesized in the process of helium burning and their abundances do not exceed the value which was at the moment when hydrogen stopped burning.

A theory of element nucleosynthesis, beginning from hydrogen and ending with transuranium nuclei, is studied sufficiently well and only in some details differs from that clear and correct scheme presented by Burbidge et al. (1957). However, along with the examples of exact agreement with the presented scheme of nucleus synthesis, there are some cases which deviate from the scheme of nucleus evolution given in that paper. The observation indicate a few stars with very high helium content and with anomalies in heavy element abundances. As a rule, all of them have low iron abundance, predomination of nitrogen in comparison with carbon and oxygen and great neon fraction (Rolleston, Dufton, Fitzsimmons, 1994; Conlon, Dufton, Keenan, 1994; Drilling, Jeffery, Heber, 1998). These and similar anomalies can be produced by mixing of matter between different stellar layers at the stage of layer source (van Winchel, 1997; Marigo, Bressan, Chiosi, 1998).

The most stars where the results of such mixing are observed as chemical anomalies in the atmospheres are the main components of the binary systems (ν Sgr, β Lyr, KS Per...). The characteristics and evolutionary features of these systems are rather close. These systems represent just that rare case of stellar evolution when the star allows the products of nuclear reactions occurred in its internal regions to be studied. Quantitative investigation of processes, which transform the initial chemical composition of the star into the one currently observed, is possible only when the stellar structure and its evolution status are sufficiently known.

The brightness of the stars abovementioned is high enough for photoelectrical and spectroscopical investigations, nevertheless the correctness of determination of their fundamental parameters and evolution status is rather low.

In this paper we analyse their evolutionary status in order to draw some conclusions on internal processes which determine the chemical anomalies presently observed in stars of this type. From our point of view these anomalies are caused by the followings: i) nucleosynthetic processes in the internal layers of the stars; ii) diffuse and convective mixing of matter in the contacting layers; iii) ejection of the surface matter into the interstellar medium. The primary of the system is a helium star which is in the stage of carbon burning in the shell source before neon burst in O-Ne-Mg core. The observed helium stars could be formed in the systems in the process of evolution of their main components after hydrogen burning in the core and after expansion and expulsion of the hydrogen envelope as a result of filling their Roche lobes.

2. Chemical composition of some helium-rich stars

In Table 1 the observed surface abundances of chemical elements of some typical helium-rich stars, their effective temperatures, and surface gravities are presented in comparison with solar ones (Anders, Grevesse, 1989; Harris, Lambert, 1984; Harris et al., 1987, 1985, 1988; Leushin, Topilskaya, 1988; Cameron, 1986; Leushin, 2000; Leushin, 2001).

The abundances of elements in these stars are normalized to the unit without allowance for the contribution of elements heavier than ^{20}Ne . In spite of this neglecting the main regularities in relative abundances are observed sufficiently clear. First of all this is redistribution for same stars of C, N and O abundances as a result of CNO-cycle processes. Then the characteristic feature of these stars is the increase of the total abundance of the elements of CNO group as compare to the solar one. The exception from the general tendency are some stars,

in particular V652 Her and HD 144941, in which the measure abundance of CNO elements is essentially lower than the solar one. β Lyr and ν Sgr are the most bright and well studied among the stars of this group. But since β Lyr is currently at the beginning of the stellar evolution stage studied, the main attention we pay to consideration of the processes mentioned above in ν Sgr.

Table 1: The abundances of light elements in the atmospheres of some helium-rich stars

Star	T_{eff}	$\lg g$	H	He	C	N	O	Ne
KS Per	11000	1.1	10^{-4}	0.99	$4 \cdot 10^{-4}$	0.004	10^{-5}	0.001
β Lyr	12000	2.5	0.16	0.81	0.024	0.001	0.005	-
ν Sgr	13500	1.5	10^{-4}	0.930	0.014	0.023	0.002	0.009
HD 168476	14000	1.5	10^{-4}	0.79	0.032	0.012	0.003	-
LSS 4300	14700	1.4	0.001	0.89	0.01	0.022	-	-
HD 124448	15750	3.7	10^{-3}	0.85	0.029	0.009	0.004	-
BD+102179	16250	3.6	10^{-4}	0.79	0.1	0.009	0.002	-
	16800	2.6	0.001	0.85	0.026	0.001	0.001	-
LSS 3184	23300	3.4	10^{-4}	0.98	0.009	0.002	0.001	-
V652 Her	23500	3.7	0.01	0.98	10^{-4}	0.008	0.001	-
BD-9 4395	22700	2.6	0.001	0.98	0.013	0.001	0.001	-
HD 144541	23200	3.9	0.01	0.98	$5 \cdot 10^{-3}$	$3 \cdot 10^{-3}$	10^{-4}	-
Sun	5600	4.3	0.71	0.265	0.004	0.001	0.007	0.002

The stage of fast evolution, in which ν Sgr is at present, is associated with the filling of Roche lobe and small energetic efficiency of nuclear reactions in its interior at considerable luminosity excess. Besides, investigations of chemical composition indicate almost complete loss of hydrogen envelope of the star. Since the hydrogen abundance in the atmosphere of the primary is less than 10^{-4} by mass, then we deal with the remnant in which hydrogen has already burned and the component has passed the stage of purely helium star.

In accordance with the results of numerous calculations (Seidel, 1929; Leushin & Topilskaya, 1987; Dudley & Jeffery, 1990, 1993), the fundamental parameters of the main component of ν Sgr are as follows:

$$M = (2.5 \pm 0.4) M_{\odot},$$

$$R = (40 \pm 5) R_{\odot},$$

$$\lg(L/L_{\odot}) = 4.6 \pm 0.1,$$

$$T_e = (13500 \pm 150) \text{K},$$

$$\lg g = 1.5 \pm 0.1.$$

The structure of helium star with a mass of about $2.5 M_{\odot}$ is very compact. Its radius does not exceed $0.4 - 0.6 R_{\odot}$, its effective temperature should be close to 80 000 K (Paczynski, 1970; 1971). Therefore, the observed values of temperature (10000-13500 K) and radius ($40 - 50 R_{\odot}$) are caused by the envelope. The size of the star is defined by chemical composition and mass of this envelope.

If the hydrogen abundance is considerably less (in case of ν Sgr, $X=10^{-4}$), then the radius of hydrogen envelope cannot have sizes of $40 - 50 R_{\odot}$ as in ν Sgr. And a thin hydrogen envelope won't give a necessary optical depth for decrease of helium core temperature to the observed value. And therefore, the

observed now filling of Roche lobe cannot be caused by the first expansion of the star after hydrogen burning and formation of helium core.

According to Schonberner and Drilling (1983) the currently observed primary of ν Sgr is at the second stage of Roche lobe filling and mass loss (BB case). At the first phase of mass loss the primary has released almost all hydrogen envelope. The remained hydrogen forms a very rarefied envelope of small mass ($M_{\text{H}}/M < 0.1$) over the extended pure helium envelope reaching the sizes of $40 - 50 R_{\odot}$.

The observed characteristics of the primary of ν Sgr impose very strong restrictions on the evolution scenery. In the case of passive role of the secondary, the evolution scenery of the system is defined only by the primary component.

Mass of the secondary is currently $4 M_{\odot}$, that corresponds to a star at the initial main sequence with an effective temperature of $1.5 \cdot 10^4 - 2 \cdot 10^4$ K (Chin and Stothers, 1991). In this case luminosity of the secondary in the optical range is about 0.01 of the total luminosity of the system, therefore its spectrum is not observed in the visible range. And in ultraviolet the picture is vice versa. The luminosity of the primary companion in ultraviolet is weakened by strong absorption caused by anomalous chemical composition of its atmosphere. At the same time because of the high effective temperature the secondary contributes strongly to luminosity in this spectrum region.

Since $4 M_{\odot}$ is mass of the component at the present time (this occurred possibly after the first filling of the Roche lobe by the primary and getting of a part of the envelope onto the secondary)

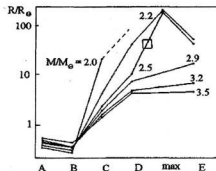


Figure 1: The size of the helium envelope as a function of evolution stage for helium stars of different masses. The letters indicate the evolution stages: A-B - nucleus helium burning in the convective core, B-C - compression of carbon-oxygen core, C-D - carbon burning in the convective core, D-E - neon burning in the core. The square shows the position of the primary component of ν Sgr.

then the initial mass of the secondary could be less than that observed now. All this confirms the above mentioned assumption that evolution of ν Sgr was defined up to now only by the primary component.

Fig. 1 shows helium envelope radius as a function of evolution stage and mass of the star itself (Habets, 1986a,b). According to evolution calculations helium stars with masses less than $2M_{\odot}$ do not reach the stage of carbon burning in the convective envelope (stage D), their radii decrease at the final stages of evolution as compared to the more massive stars. Helium stars within the mass interval $2.2M_{\odot} < M < 2.9M_{\odot}$ evolve to the stage of neon burning in the core (stage E). Between the stages D and E, their radii have maximal values ($\approx 250R_{\odot}$). At further mass increase of helium stars the maximum achieved radius, as well as towards small masses, decreases sharply. Therefore, the observed for ν Sgr radius of the primary ($R=40R_{\odot}$) imposes restrictions on both component mass ($M=2.5M_{\odot}$) and its evolution stage (see Fig. 1, position of the primary is shown with the square). Thus, the observed values of mass and radius of the primary of ν Sgr are in good agreement with the theoretically calculated ones for the evolved helium star with the initial mass within $2.0-2.5M_{\odot}$. Such a helium star could originate in the binary system in the process of evolution of normal component with the initial mass $7-8M_{\odot}$ after hydrogen burning in the core, expansion and release of hydrogen envelope as a result of Roche lobe filling. In this case, the mass of the remained helium core will be $2.5M_{\odot}$. The duration of the process of helium star formation is 40-60 million years (Chin and Stothers, 1991; Maeder and Meynet, 1988; 1989). Further evolution of helium remnant with $2.5M_{\odot}$ mass is calculated in detail up to the stage of neon burning in O-Ne-Mg core (Habets, 1986a).

From the observed values of luminosity and effective temperature the primary enters the evolutionary track of a helium star with mass $2.5M_{\odot}$ to the point that corresponds to C-O-Ne core with the layer burning sources of carbon and helium and before the neon flare in the core. The mass of helium shell above the upper zone of nucleus burning is equal approximately to one solar mass. The living time of the component from the time when it released the hydrogen envelope is about 2.5-2.7 million years, and the duration of the observed phase with the radius that fills the Roche lobe is less than 50000 years. Some other stars presented in Table 1 pass the similar evolution. The differences in chemical contents He-rich stars are connected with distinctions in initial values of dynamic characteristics of binary systems. The dynamic characteristics cause distinctions in evolutionary processes inside a star and result in variations of observable abundances.

Table 2: The contents of light elements in atmosphere of ν Sgr and Sun

Element	On number of atoms		On weight	
	ν Sgr	Sun	ν Sgr	Sun
H	-3.40	-0.05	-4.00	-0.15
He	-0.01	-1.00	-0.03	-0.58
C	-2.31	-3.50	-1.85	-2.40
N	-2.15	-4.12	-1.64	-2.95
O	-3.41	-3.28	-2.70	-2.15
Ne	-2.76	-3.90	-2.05	-2.70
Fe	-3.80	-4.50	-2.05	-2.75

Compositions of more abundant elements in the atmosphere of the primary of the system ν Sgr in comparison with the data for the solar atmosphere are listed in Table 2 (Leushin, Topilskaya, 1988).

High abundance of elements of CNO group (0.040 in mass) in comparison with the solar (0.012) and especially high neon abundance (to 0.01) demand extended stages of nucleus burning at least up to neon synthesis.

Moreover, if the initial chemical composition, suffered evolutionary nucleus changes, was similar to the solar one then the observed excess of the total abundance of CNO-elements demands corresponding nucleus processes. And if carbon increase as a factor of 3.5, as compared to that in the Sun, can be explained by conversion of ^4He into ^{12}C , then nitrogen increase as a factor of 20 is a more complicated problem, since nitrogen is synthesized at hydrogen burning in CNO cycle only from carbon and at rather high temperatures from oxygen also. During this cycle carbon converts into nitrogen, but the total abundance of CNO elements does not change transforming into equilibrium quantity at which relation of nitrogen and carbon is $^{14}\text{N}/^{12}\text{C} = 10^2-10^3$. Thus, nitrogen abundance can not be higher than the total abundance of C, N and O. The following stages of nucleus evolution (up to iron formation) change abundances of He, C, O, Ne and so on, while nitrogen abundance remains practically unchanged.

The two above mentioned peculiarities in abundances of light elements in the atmosphere of the primary of ν Sgr do not agree with theoretical calculations of stellar evolution. The modern evolution theories state that rather intensive mixing of zones of various nucleus burning and those free from burning do not exist. According to the theoretical calculations the products of nucleus burning remain in those layers where the reactions of this type occurred, and the element in the star are located in layers (Masevich, Tutukov, 1988; de Jager, 1984; Haiashi et al., 1962). Therefore, if we observe in the primary the shell consisting of helium, that is formed from hydrogen in CNO cycle reactions, then there must not be

higher neon abundance than in the initial matter. As a rule, chemical composition of the initial matter for the stars, being formed, is solar in which neon abundance is equal to 0.002, and the total abundance of CNO elements is 0.012. At the same time for ν Sgr these values are essentially higher.

We could understand a great carbon overabundance in ν Sgr, if we observe a layer in which helium burning process had begun converting helium into carbon in triple α -process. However, here, as it was mentioned above, along with the carbon overabundance we observe essentially higher nitrogen and neon abundances. And what is more the total value of C, N, O and Ne abundances is essentially higher than the initial one. The data on C, N, O and Ne elements are obtained with a good accuracy and need careful considerations.

We may suppose that the matter observed in the ν Sgr and other stars atmospheres was originated due to at least two nucleus burning sources. If in the period of the first expansion of the component, helium core compression and helium flare the core is convective, and at the same time at the boundary of the core hydrogen is burning in the envelope, then there occurs exchange (mixing) of matter between zones of helium and hydrogen burning. In this case in the region of hydrogen burning additional synthesis of nitrogen is possible from carbon thrown there from the zone of helium burning. This process is simultaneous and increased carbon and nitrogen abundances sharply accelerate hydrogen burning with all circumstances that follows after this.

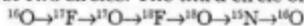
If at the moment of this exchange there occur expansion and release of the outer layers (that are not in reactions) either on the component or out of the system, then we can observe just that part of the star where hydrogen burning in CNO cycle takes place, and in the region with carbon overabundance. The fact, that oxygen abundances in the Sun and ν Sgr are similar and neon abundance is sharply increased, imposes restrictions on mixing rate and on temperature of helium burning in the core.

3. Nucleus reactions of CNO cycle and triple α -process

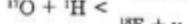
Below we consider possible theoretical scheme of formation of the observed chemical composition of the helium-reach stars. Main attention at calculations is paid to CNO cycle in the zone of hydrogen burning. The zone of helium burning is interesting in our case only from the view point of chemical composition of the matter which is diffused from this zone. The triple α -process is the main nucleus reaction here. Generation of nuclei that follow after carbon is taken into consideration only for oxygen

^{16}O and ^{20}Ne , since the formation rate of other nuclei (^{24}Mg , ^{28}Si and etc.) are negligibly small.

The theory of CNO cycle, beginning from Bethe (1939) is described in detail many times. The total scheme of nucleus reactions of hydrogen burning in high temperature reactions represents some connected circles: CN, NO, OF, FNe... with formation of α -particles from protons in each of them. For our calculations we used all the reactions of the first two circles. The third circle of CNO cycle

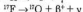
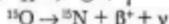
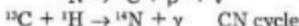


is not closed here, since the reaction in the second channel at interaction of ^{17}O with proton

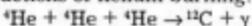


which gives ^{18}F and leads to formation of this circle, has a very low rate. And slow reactions in the third circle cause small corrections of the results of the first two circles. The same can be said according to all following circles.

Except hydrogen reactions we included into calculations helium reactions, that is, triple α -process and neutron formation reactions from the nuclei of ^{12}C . Thus, for calculations of chemical evolution we use the following set of reactions. Reactions of CNO cycle:



Reactions of helium burning:



The fact that all these reactions proceed both forward and backward is taken into consideration.

The rates of the given reactions are taken from data by Leng (1978), Fowler, Cauglan, Zimmerman (1975) and NACRE - <http://pntpm.ulb.ac.be/nacre.htm> (Angulo et al., 1999). The character of cross sections of the calculated nucleus reactions and the physical conditions in the system investigated indicate that the process of hydrogen burning, continuing for rather a long time, takes place at equilibrium values of concentrations ^{12}C , ^{13}C , ^{14}N and ^{15}N , which grows very slowly due to burning of ^{16}O (three last reactions of CNO cycle, which we took into considerations). The nuclei of ^{14}N formed from oxygen transform simultaneously into equilibrium concentrations of the above mentioned

four isotopes. Such character of hydrogen burning process allows us to use equilibrium conditions for calculations at different stages.

For each moment of time the quantity of ^{14}N originated from ^{16}O is calculated. Then, the equilibrium ratios of isotopes of the CN cycle are re-counted taking into account this change. Just the same procedure (analogous set of equations) was used for calculations of equilibrium relations of isotopes in two circles of CNO cycle (CN and NO). In this case we obtain additionally equilibrium concentrations ^{18}O , ^{17}O and ^{17}F . Equilibrium in this circle is reached during the time comparable with the time of hydrogen burning and therefore this procedure can be used only for control of calculations.

The evolution of mass nucleus concentrations are determined by the following equations:
 $dX_i/dt = A_i(\pm \sum < b_j > X_j) / A_i \pm \sum < b_j k > X(j) / A_i X(k) / A_{i0}$
 where $X(i)$ is the mass concentration of the i -th element, A_i is the atomic weight of the corresponding nucleus. The first sum in the right part is taken from all j for one-particle nucleus reactions, the second - from j and k for two-particle reactions.

The final value of mass concentration of each element at the time moment $T - X_i(t)$, in accordance with the above mentioned, is defined by numerical integration in time ($X_i(t)$ - the initial value of concentration).

We carried out a number of calculations of chemical composition changes caused by CNO cycle. An interval of the used temperatures is $(15 - 50) \cdot 10^8 \text{ K}$, an interval of densities $5 - 100 \text{ g/cm}^3$. The initial chemical composition is close to the solar one; $X(\text{H})=0.7$, $X(\text{C})=0.005$, $X(\text{N})=0.001$, $X(\text{O})=0.009$. Some results of these calculations are given in Tables 2 and 3. Thus the time of hydrogen burning (decrease of its abundance to 0.02 in mass) under stationary conditions (constant temperature, density and absence of mixing) from $1.5 \cdot 10^8$ years (for $T=50 \cdot 10^8 \text{ K}$ and $\rho=100 \text{ g/cm}^3$) to 10^3 years (for $T=15 \cdot 10^8 \text{ K}$ and $\rho=5 \text{ g/cm}^3$). Almost all the time the burning proceeds at equilibrium in the CN cycle, which is attained for a much shorter time (0.15 years in the first case and $2.7 \cdot 10^6$ years in the second).

Table 2: The time (in sec) of entering to the equilibrium hydrogen burning in CN cycle

$\rho, \text{ g/cm}^3$	$T, \text{ K}$				
	0.015	0.020	0.030	0.040	0.050
5	$8 \cdot 10^3$	$5 \cdot 10^3$	10^1	$2 \cdot 10^6$	10^6
10	$4 \cdot 10^3$	$3 \cdot 10^3$	$5 \cdot 10^0$	$6 \cdot 10^6$	$5 \cdot 10^6$
20	$2 \cdot 10^3$	$1.5 \cdot 10^3$	$3 \cdot 10^0$	$4 \cdot 10^6$	$2 \cdot 10^6$
25	$1.5 \cdot 10^3$	10^3	$1.5 \cdot 10^0$	$3 \cdot 10^6$	$1.8 \cdot 10^6$
50	$9 \cdot 10^2$	$6 \cdot 10^2$	10^0	$2 \cdot 10^6$	10^6
100	$4 \cdot 10^2$	$4 \cdot 10^2$	$6 \cdot 10^0$	10^6	$5 \cdot 10^6$

Table 3: The time (in sec) of hydrogen burning in CN cycle up to $X(\text{H})=2 \cdot 10^{-2}$

$\rho, \text{ g/cm}^3$	$T, \text{ K}$				
	0.015	0.020	0.030	0.040	0.050
5	$3 \cdot 10^{20}$	$6 \cdot 10^{17}$	10^{15}	10^{13}	$5 \cdot 10^{11}$
10	10^{20}	$3.5 \cdot 10^{17}$	$4 \cdot 10^{14}$	$6 \cdot 10^{12}$	$2.5 \cdot 10^{11}$
20	$5 \cdot 10^{19}$	$1.5 \cdot 10^{17}$	$2 \cdot 10^{14}$	$2 \cdot 10^{12}$	10^{11}
25	$3 \cdot 10^{19}$	10^{17}	$1.5 \cdot 10^{14}$	$1.8 \cdot 10^{12}$	$9 \cdot 10^9$
50	$1.5 \cdot 10^{19}$	$6 \cdot 10^{16}$	10^{14}	10^{12}	$7 \cdot 10^9$
100	10^{19}	$3 \cdot 10^{16}$	$3.5 \cdot 10^{13}$	$4 \cdot 10^{11}$	$4.5 \cdot 10^9$

In the process of hydrogen burning the abundances of the main isotopes change by two steps.

At the first stage all carbon is converted to nitrogen, at the second stage, covering all the period of hydrogen burning, oxygen is gradually transformed to nitrogen and to equilibrium concentrations of ^{13}C , ^{13}C , ^{14}N and ^{15}N . The character of these changes is presented in Table 4 and Fig. 2.

4. The internal structure of the stars during the mixing stage

The data from Tables 2-4 show that some variants of calculations can not be realized by the present moment in our Universe, since the time of these processes exceeds the age of the Universe. At the same time under certain physical conditions, which exist, in particular, in the star

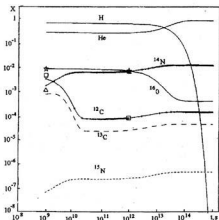


Figure 2: Dynamics of nucleosynthesis in the star at $T=3 \cdot 10^8 \text{ K}$, $\rho=25 \text{ g/cm}^3$ and initial chemical composition: $X(\text{H})=0.7$, $X(\text{CNO})=0.015$ before termination of hydrogen burning. The signs show the initial and equilibrium values of ^{12}C , ^{14}N , ^{16}O abundances.

under study, for all the stages of the CNO cycle to be realized short time intervals are required that can well fall in time within the corresponding stages of evolution of the star.

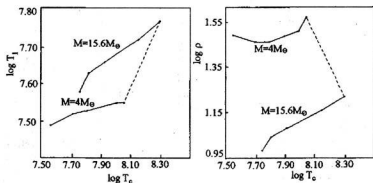


Figure 3: Temperature T_1 and density ρ of the hydrogen shell source for stars of different masses as a function of temperature T_c at the centre (from calculations of Haiashi et al., 1962).

Table 4: Mass abundance of different isotopes after hydrogen burning in the layer above the helium core

T_p , K	t , s	H	He	^{12}C	^{13}C	^{14}N	^{15}N	^{16}O	^{17}O	
ρ , g/cm 3										
0.015	5.0	.1E+22	.53E-08	.98E+00	.39E-04	.12E-04	.10E-01	.53E-06	.18E-02	.23E-02
	20.0	.1E+21	.49E-03	.98E+00	.40E-04	.12E-04	.10E-01	.53E-06	.18E-02	.24E-02
	100.0	.1E+20	.22E-01	.96E+00	.39E-04	.12E-04	.10E-01	.53E-06	.19E-02	.24E-02
0.020	5.0	.5E+19	.16E-11	.98E+00	.83E-04	.26E-04	.13E-01	.60E-06	.12E-02	.50E-04
	20.0	.5E+18	.17E-04	.98E+00	.84E-04	.26E-04	.13E-01	.60E-06	.12E-02	.51E-04
	100.0	.1E+18	.17E-04	.98E+00	.84E-04	.26E-04	.13E-01	.60E-06	.12E-02	.51E-04
0.030	5.0	.1E+16	.48E-02	.98E+00	.17E-03	.52E-04	.13E-01	.55E-06	.47E-03	.15E-06
	20.0	.1E+16	.11E-08	.98E+00	.16E-03	.52E-04	.13E-01	.55E-06	.46E-03	.15E-06
	100.0	.2E+15	.11E-08	.98E+00	.16E-03	.52E-04	.13E-01	.55E-06	.46E-03	.15E-06
0.040	5.0	.5E+14	.87E-08	.98E+00	.25E-03	.78E-04	.13E-01	.49E-06	.27E-03	.42E-07
	20.0	.2E+13	.40E-01	.94E+00	.25E-03	.79E-04	.14E-01	.49E-06	.28E-03	.43E-07
	100.0	.1E+13	.49E-03	.98E+00	.25E-03	.79E-04	.14E-01	.49E-06	.27E-03	.43E-07

The stars presented in Table 1 may be conditionally divided into three groups with general evolution scenarios: the first group – ν Sgr and LSS 4300 in which overabundance of N and general increase of elements of CNO group are observed. They formed their chemical abundances before the stars lost its hydrogen envelope in the period of evolution when the layer hydrogen burning above the helium core was in progress. At the same time helium burning took place in the core, which began shortly after the onset of the core compression. During the compression time, according to theoretical calculations of evolution, the temperature at the centre rises from a few tens million degrees to hundreds million degrees, the central density being increased by more than 3 orders (see, for instance, Maeder and Meynet, 1988; Chin and Stothers, 1991). At the same time, physical characteristics in the region of shell, source of hydrogen burning at the boundary of helium core change much less.

Fig. 3 shows the relationship between temperature and density of the layer source and temperature at the centre, which grows as a result of

compression (Haiashi et al., 1962). As it is seen from these data the temperature varies here by a factor of 1.1-1.5, while the density changes even less. Helium flash at the centre (and hence termination of the core compression, which caused the temperature and density to increase) for stars of different masses occurs with the parameters shown by the dashed lines in Fig. 3.

Thus for a star of $7M_{\odot}$ the parameters of the layer source must be close to the following: $T=40-10^8$ K and $\rho=20$ g/cm 3 . Since the temperature and density inside the helium core decrease rather slowly and at the boundary the decrease rate of these quantities rises sharply, then the depth of the layer source is very small and its mass is $10^{-4}-10^{-6}M_{\odot}$.

According to our assumptions, it is this layer that entraps matter enriched in carbon from the helium burning zone. On the one hand, this carbon, when transforming to nitrogen, changes the abundance of the CNO group elements, and on the other hand, accelerates transformation of hydrogen to helium, increasing thus energy release in the layer. This additional energy release can stimulate instability of the inner parts of the star, mix-

ing and thermal pulsations (Marigo et al., 1998). The dependence of the chemical composition of the core region upon the time (derived for $T=180 \cdot 10^6$ K and $\rho=3.15 \cdot 10^3$ g/cm³) is shown in Fig. 4. From this region additional carbon is supplied to the layer source of hydrogen burning amount.

The whole period of formation of the observed chemical composition by the mechanism considered here takes, depending on the adopted physical conditions (first of all on the values of mixing parameters), from 5 to 10 million years (47–57 million years of evolution from the initial main sequence) (Maeder, Meynet, 1988; 1989; Chin and Stothers, 1991). The temperature at the centre changes in this period from $100 \cdot 10^6$ to $200 \cdot 10^6$ K, the central density $\rho_c=2.7 \cdot 10^3$ – $7.0 \cdot 10^3$ g/cm³. The decrease in temperature and density within the helium core is smooth and slow enough and can be described by a polytrope, but at the boundary the temperature and density undergo an abrupt change. The temperature at the boundary of the hydrogen layer source drops from a few tens million to a few hundreds thousand degrees, the density decreases from hundreds to tens of g/cm³.

The carbon-oxygen-neon core at the final stage of helium burning has a mass of 1 – $1.3M_{\odot}$; this core is surrounded by a helium shell of 1 – $1.2M_{\odot}$, at the upper boundary of which nuclear hydrogen burning in the layer takes place. The mass of this layer is 10^{-4} – $10^{-6}M_{\odot}$. Thus a star with a mass of $7M_{\odot}$ has a very complex He-C-O-Ne core of a total mass of 2.1 – $2.6M_{\odot}$ surrounded by a hydrogen envelope of 4.9 – $4.4M_{\odot}$. The observed component of

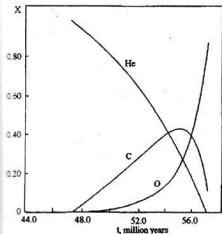


Figure 4: Variation of chemical composition of the core region of the star with the temperature $2 \cdot 10^8$ K and $\log g=3.5$ when carbon is synthesized from helium.

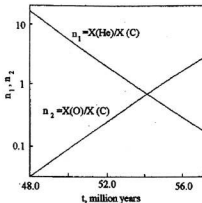


Figure 5: He/C and O/C ratios as a function of time for the core region of a star of $7M_{\odot}$.

ν Sgr is exactly this core, that remained after loss of the whole hydrogen envelope. Apparently, evolution run of LSS 4300 is the same that we propose for ν Sgr. The initial stage of identical process is, apparently, observed in β Lyr, which has not lost yet its hydrogen envelope.

The helium star with a mass of $2.5M_{\odot}$ evolves very fast, expanding the envelope (now helium) up to 40–50 solar radii, i.e. it is transformed to the observed component of ν Sgr. The chemical composition of the observed atmosphere of the primary is formed precisely in the considered period in down the hydrogen envelope, in the layer of hydrogen burning above the He-C-O-Ne core. And if at this moment there exists faint mixing between the helium burning and hydrogen burning zones, then we can get a chemical composition with the above described peculiarities.

The physical structure of the considered stars in the stage of formation of the observed chemical composition was responsible for the non-uniform distribution of elements along the star radius. The varying abundances of the He, C, and O nuclei in the helium core are shown in Fig. 4 for $T=1.8 \cdot 10^8$ K and $\lg \rho=3.5$. At these temperature, and density values helium burns in the core of a star with $M=7M_{\odot}$. The ratios between mass concentrations $X(\text{He})/X(\text{C})$ and $X(\text{O})/X(\text{C})$ for such a core, depending on time, are presented in Fig. 5. The nitrogen abundance in the core is constant and is within $-X_{\text{e}}(\text{N}) + X_{\text{e}}(\text{C}) = X(\text{N}) = X_{\text{e}}(\text{N}) + X_{\text{e}}(\text{C}) + X_{\text{e}}(\text{O})$ depending on the amount of oxygen converted to nitrogen in hydrogen burning in the CNO cycle. The zero indicates the initial values of concentrations of the corresponding elements. The chemical composition of the helium envelope is defined by the conditions in the CNO cycle and the results of calculation for the corresponding parameters.

Initial abundances of elements in the zone of shell hydrogen burning depend on the time of the CNO cycle action up to the moment of mixing with the matter from the core and on the initial conditions. Thus for the modeling of the chemical composition that is produced in the zone of the shell source of hydrogen with the presence of mixing, it is necessary to allow for the content of three zones mentioned. The initial chemical composition of the mixture in the zone of hydrogen burning is calculated proceeding from the following assumptions.

a) Matter in the zones of hydrogen and helium burning can be taken in any stage of transformation, i.e. hydrogen abundance can be varied from the initial ($X=0.7$) to the final ($X=0$); the same refers to helium (from $Y=0.285$ to $Y=0$).

b) The ratio between the isotopes of C and N in the zone of hydrogen burning is taken equilibrium. The oxygen abundance is defined by the amount of burned hydrogen.

c) The chemical composition of matter from the helium burning zone is determined by the parameters: $n_1 = X(^4\text{He})/X(^{12}\text{C})$ and $n_2 = X(^{16}\text{O})/X(^{12}\text{C})$. The nitrogen abundance here is fixed and is equal to «equilibrium» for the CNO cycle in the zone of hydrogen burning.

d) The portion of matter brought to the zone of hydrogen burning (M_2) is determined by the parameter $n_3 = M_2/M_1$ where M_1 is the mass of matter in the hydrogen burning zone.

e) The portion of matter dredged up from the helium burning zone (M_3) that is mixed with matter of the helium shell, is determined by the parameter $n_4 = M_3/M_2$.

Then the initial chemical composition in the hydrogen burning zone is produced in two stages in the following manner:

i) Mixing of matter of the core and helium shell.
ii) Diffusion of matter with the formed composition to the hydrogen burning zone. The composition of the helium shell is determined by the parameters:

CNO – total initial mass concentration of the CNO group elements,

$X_0(\text{O})$ – amount of oxygen unburned in the CNO cycle which is determined by appropriate calculations.

Then the mass concentrations in the shell will be the following:

$$\begin{aligned} X(\text{He})_{\text{env}} &= 1 - \text{CNO}, \\ X(\text{C})_{\text{env}} &= 0, \\ X(\text{N})_{\text{env}} &= \text{CNO} - X_0(\text{O}), \\ X(\text{O})_{\text{env}} &= X_0(\text{O}). \end{aligned}$$

The mass concentrations at the centre of the star:

$$\begin{aligned} X(\text{He})_{\text{cnc}} + X(\text{C})_{\text{cnc}} + X(\text{N})_{\text{cnc}} + X(\text{O})_{\text{cnc}} &= 1, \\ X(\text{He})_{\text{cnc}} &= n_1 X(\text{C})_{\text{cnc}}, \\ X(\text{C})_{\text{cnc}} &= (1 - X(\text{N})_{\text{cnc}})/(n_1 + n_2 + 1), \\ X(\text{N})_{\text{cnc}} &= \text{CNO} - X_0(\text{O}), \\ X(\text{O})_{\text{cnc}} &= n_2 X(\text{C})_{\text{cnc}}. \end{aligned}$$

After mixing in the helium shell the chemical composition will be:

$$\begin{aligned} X(\text{He})_{\text{env}} &= (1 - \text{CNO} + n_4 X(\text{He})_{\text{cnc}})/(1 + n_4), \\ X(\text{C})_{\text{env}} &= n_4 X(\text{C})_{\text{cnc}}/(n_4 + 1), \\ X(\text{N})_{\text{env}} &= \text{CNO} - X_0(\text{O}), \\ X(\text{O})_{\text{env}} &= (X_0(\text{O}) + n_4 X(\text{O})_{\text{cnc}})/(1 + n_4). \end{aligned}$$

In the core and in the shell it is sufficient to take into account only the main isotopes – ^4He , ^{12}C , ^{14}N and ^{16}O . Matter with the obtained composition is dredged up from the shell to the hydrogen burning zone in different stages, then is mixed and transformed in the nuclear reactions. The final composition in the hydrogen burning zone is calculated for all isotopes taking into account the relation:

$X(^1\text{H}) + X(^4\text{He}) + X(^{12}\text{C}) + X(^{13}\text{C}) + X(^{14}\text{N}) + X(^{15}\text{N}) + X(^{16}\text{O}) + X(^{17}\text{O}) = 1$.
The corresponding concentrations are:

$$\begin{aligned} X(^1\text{H}) &= X(^1\text{H})/(1 + n_3), \\ X(^4\text{He})_{\text{layer}} &= (X(^4\text{He}) + n_3 X(^4\text{He})_{\text{env}})/(1 + n_3), \\ X(^{12}\text{C})_{\text{layer}} &= (X(^{12}\text{C}) + n_3 X(^{12}\text{C})_{\text{env}})/(1 + n_3), \\ X(^{13}\text{C})_{\text{layer}} &= X(^{13}\text{C})/(1 + n_3), \\ X(^{14}\text{N})_{\text{layer}} &= (X(^{14}\text{N}) + n_3 X(^{14}\text{N})_{\text{env}})/(1 + n_3), \\ X(^{15}\text{N})_{\text{layer}} &= X(^{15}\text{N})/(1 + n_3), \\ X(^{16}\text{O})_{\text{layer}} &= (X(^{16}\text{O}) + n_3 X(^{16}\text{O})_{\text{env}})/(1 + n_3), \\ X(^{17}\text{O})_{\text{layer}} &= X(^{17}\text{O})/(1 + n_3). \end{aligned}$$

Thus changing the input parameters n_1 , n_2 , n_3 and $X_0(\text{O})$, one may change the rate and degree of mixing in different stages of helium burning in the core and hydrogen burning in the shell.

5. Structure extreme He-rich Stars and Conclusions

Using the above described model of chemical composition change in different stellar zones, we can simulate the process of formation of the observed abundances of light elements in the atmospheres of the considered stars. Varying the model parameters, we can obtain the agreement with the results of observations of elements in different helium-rich stars. The procedure described was used in details in calculations for obtaining agreement with the chemical composition of the most unique star ν Sgr. For this purpose we made a series of calculations of nucleosynthesis with different parameters of mixing. Since there can be numerous variants of such calculations, we restricted their number, proceeding from the most likely assumptions.

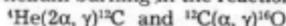
The carbon-oxygen core with a mass of $1.3M_{\odot}$ is surrounded by a helium envelope with a mass of $1.2M_{\odot}$. At the bottom of this envelope helium is burning, while at the upper boundary (in the layer with a mass of $10^{-4} - 10^{-6}M_{\odot}$) hydrogen burning occurs. Above is the hydrogen envelope with a mass $4.5M_{\odot}$.

Since the mass of the helium envelope is sufficiently large, and the mixing between the core and this shell must not be very intensive for the inhomogeneity in the core and the star as a whole to be preserved, we have considered the variants when

Table 5: Concentration of elements in different zones of the star with varied parameters of mixing

Model			Mass concentration of elements								
			X_0			X			X_c		
n_1	n_2	n_4	C	N	O	C	N	O	C	N	O
1	0.2	0.5	0.068	0.015	0.028	0	0.056	0.007	0.021	0.043	0.017
2	0.2	0.07	0.050	0.015	0.010	0	0.045	0.002	0.004	0.043	0.00
2	0.25	0.25	0.060	0.015	0.013	0	0.050	0.003	0.012	0.043	0.005
2	0.026	0.33	0.062	0.015	0.013	0	0.052	0.004	0.015	0.043	0.006
2	0.27	0.4	0.065	0.015	0.014	0.001	0.054	0.004	0.018	0.043	0.007
2	0.3	0.5	0.07	0.015	0.015	0.001	0.057	0.004	0.023	0.043	0.007

a mass of 0.05–0.5 of the helium envelope mass is dredged up to the helium shell. At the same time, since the mass of the hydrogen burning shell is small, then the ratio between the shell mass and the mass dredged up was supposed to be equal to unity. Besides, we varied the chemical composition of matter transferred from the helium burning zone ($n_1=X(\text{He})/X(\text{C})$ and $n_2=X(\text{O})/X(\text{C})$). The value of n_1 varied from 10 to 0.5. A certain stellar evolution stage (at the stage of shell helium burning) and a definite value of n_2 correspond for each selected value of n_1 , that proceeds from the relation between n_1 and n_2 and the time shown in Fig. 6. These relations have been obtained from the calculation results of helium burning in the reactions



at a temperature $T=1.8 \cdot 10^8$ and $\tau=3.15 \cdot 10^8$ (the temperature and density correspond to a star with a mass of $M=7M_\odot$ in the period of helium burning). We may be found many variants for which the total number of the CNO elements or the nitrogen abundance will coincide with those observed in ν Sgr, none of the variants with the equilibrium distribution of N and C ($X(\text{N})/X(\text{C})=5.5$) alone can give the carbon - nitrogen ratio ($X(\text{N})/X(\text{C})=0.043/0.012=3.3$) observed in ν Sgr. Thus to explain the observed chemical composition, we make another assumption that the reaction products of the shell hydrogen source after hydrogen completely burned out continued mixing with matter of the helium envelope enriched in carbon.

Table 5 shows the distributions of C, N and O in stars close in mass to those observed in ν Sgr, which can be obtained as a result of varying mixing parameters.

As it was mentioned above, n_1 in Table 5 characterizes the composition of matter dredged up from the shell helium source to the helium envelope and therefore the evolutionary stage. The amount of this matter is characterized by the value of n_2 . The mass ratio of the corresponding element in the helium envelope after mixing is denoted by parameter X_0 , while for the shell hydrogen source after mixing and hydrogen burning by X . At last, X_c is the mass ratio of the element after the final mixing of hydrogen burning products in the layer with matter from the helium envelope.

The parameter n_4 denotes the mass proportion, mixed into matter of the layer hydrogen source after the termination of hydrogen burning.

A comparison of the C, N and O abundances observed in the atmosphere of ν Sgr

$$(X(\text{C})=0.012, X(\text{N})=0.043, X(\text{O})=0.008)$$

with the data from Table 5 shows that within the accuracy the observed values are in good agreement with the theoretical, the fit being the best when

$$X_0(\text{C})=0.012, X_0(\text{N})=0.043, X_0(\text{O})=0.005,$$

here $n_1=2$, $n_2=0.25$ and $n_4=0.25$.

Besides, for $n_1=2$, $n_2=0.26$ and $n_4=0.33$ the corresponding calculated abundances are

$$X_c(\text{C})=0.015, X_c(\text{N})=0.043, X_c(\text{O})=0.006,$$

which is also close enough to the observed values.

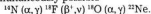
Thus it can be stated that the observed abundances of the C, N and O elements in the atmosphere of ν Sgr were generated about five million years ago in a star that had not lost its thick hydrogen envelope. This moment came approximately after $52 \cdot 10^6$ years of evolution of the star with the initial mass $7M_\odot$ from the main sequence. By that time the amount of helium in the shell helium source was still twice that of synthesized carbon ($n_1=2$). About a quarter of the core mass ($n_2=0.25-0.26$) containing He, C and O ($X(\text{He})/X(\text{C})=2$, $X(\text{O})/X(\text{C})=0.21$) was mixed with the helium envelope and the mixture, having been dredged up to the shell hydrogen source, was momentarily (for about 1000 years) converted to helium and nitrogen. Then the products of nuclear hydrogen burning were mixed with matter of helium envelope again after hydrogen had been depleted. The amount of mass dredged up from the helium envelope was 0.25–0.3 of the hydrogen shell source mass. Just at this moment hydrogen envelope release completed and chemical composition of the star became such as we observe now.

The problem neon also is solved within the framework of the offered model. Neon is one of most abundant (after helium and nitrogen) elements in the atmosphere ν Sgr. Neon is formed as a result of reactions helium with carbon and oxygen



in a core of a star, and then arise from the mixing in those layers of a star, which are now observed in result of losses of an envelope. In this case we

should assume, what in a core of ν Sgr during helium burning in three α -process the carbon promptly turned to oxygen, and last in neon. The formation of neon in a nuclear chain with nitrogen is simultaneously possible



Taking into account, that in ν Sgr the large contents of nitrogen, we should assume, that the generation neon goes simultaneously with generation of nitrogen. The mixing between hydrogen-burning and helium-burning zones results in that generated in a helium-burning zone the carbon having got in shell a source burning of hydrogen will be transformed to nitrogen. Substance enriched by nitrogen in turn getting in a helium-burning zones increases quantity neon, which then is again arise the top layers. Thus, the simultaneous enrichment and nitrogen and neon is created.

Such situation is possible in another He-rich stars. The change of parameters of mixing at different stages of evolution can result in various features of observable abundances.

The work is executed at support of the RFBR grants.

References

- Anders E., Grevesse N., 1989, *Geochim. et Cosmochim. Acta.*, **53**, 197
- Angulo C., Arnould M., Rayet M., et. al., 1999, *Nucl. Phys. A656*, 3
- Bethe H.A., 1939, *Phys. Rev.*, **55**, 434
- Brown R.E., 1962, *Phys. Rev.*, **125**, 347
- Burbidge E.M., Burbidge G.R., Fowler W.A. and Hoyle F., 1957, *Rev. Mod. Phys.*, **29**, 547
- Chin Chao-wen and Stothers R.B., 1991, *Astrophys. J. Suppl. Ser.*, **77**, 299
- Conlon E.S., Dufton P.L., Keenan F.P., 1994, *A&A*, **290**, 897
- Drilling J.S., Jeffery C.S., Heber U., 1998, *A&A*, **329**, 1019
- Dudley R.E., Jeffery C.S., 1990, *Mon. Not. R. Astron. Soc.*, **247**, 400
- Dudley R.E., Jeffery C.S., 1993, *Mon. Not. R. Astron. Soc.*, **262**, 945
- Duvignau H., Friedjung M. and Hack M., 1979, *Astron. Astrophys.*, **71**, 310
- Fowler W.A., Caughlan G.R., Zimmerman B.A., 1975, *Annu. Rev. Astron. Astrophys.*, **13**, 69
- Habets G.M.H.J., 1986a, *Astron. Astrophys.*, **165**, 95
- Habets G.M.H.J., 1986b, *Astron. Astrophys.*, **167**, 61
- Hack M., Pasinetti E., 1962, *Contr. Oss. Astr. Milano Merate*, **215**, 3
- Hack M., Flora U. and Santin P., 1980, in: M. Plavec, D. Popper, R. (eds.) *Close Binary Stars*, Ulrich, Dordrecht: Reidel, 271
- Haiashi C., Hoshi R., Sugimoto D., 1962, *Suppl. Progr. Of Theor. Physics*, **22**, 1
- Harris M.J., Lambert D.L., 1984a, *Astrophys. J.*, **281**, 739
- Harris M.J., Lambert D.L., 1984b, *Astrophys. J.*, **285**, 674
- Harris M.J., Lambert D.L., Goldman A., 1987, *Mon. Not. R. Astron. Soc.*, **224**, 237
- Harris M.J., Lambert D.L., Smith V.V., 1985, *Astrophys. J.*, **292**, 620
- Harris M.J., Lambert D.L., Smith V.V., 1988, *Astrophys. J.*, **325**, 768
- Hellings P., de Loore C., Burger M., and Lamers H.J.G.L.M., 1981, *Astron. Astrophys.*, **101**, 161
- Jager de C., 1984, *The brightest stars*, M.: Mir, 494
- Kameron A., 1986, in: Barns Ch., Kleyton D., Shramm D. (eds.) *Yadernaya fizika*, M.: Mir, 31
- Lee T.A., Nariai K., 1967, *ApJ.Lett.*, **149**, 193
- Leng K., 1978, *Astrofizicheskie formuly*, M.: Mir
- Leushin V.V., 2000, *Bull. Spec. Astrophys. Obs.*, **50**, 35.
- Leushin V.V., 2001, *Pis'ma v Astron. Zurn.*, **27**, 746
- Leushin V.V., Topilskaya G.P., 1985, *Astrofizika*, **22**, 121
- Leushin V.V., Topilskaya G.P., 1987, *Astrofizika*, **26**, 195
- Leushin V.V., Topilskaya G.P., 1988a, *Astrofizika*, **28**, 363
- Leushin V.V., Topilskaya G.P., 1988 b, *Astrofizika*, **28**, 554
- Maeder A. and Meynet G., 1988, *Astron. Astrophys. Suppl. Ser.*, **76**, 411
- Maeder A. and Meynet G., 1989, *Astron. Astrophys.*, **210**, 155
- Marigo P., Bressan A., Chiosi C., 1998, *A&A*, **331**, 564
- Masevich A.G., Tutukov A.V., 1988, *Evolutsiya zvezd: teoriya i nablyudeniya*, M.: Nauka, 280
- Merezhin V.P., 1986, *Trudy gor. Astron. Obs. KSU*, **50**, 52
- Morrison K., 1988, *Mon. Not. R. Astron. Soc.*, **233**, 621
- Nariai K., 1967, *Publ. Astr. Soc. Pacific*, **19**, 564
- Paczynski B., 1970, *Acta Astron.*, **20**, 47
- Paczynski B., 1971, *Acta Astron.*, **21**, 1
- Parthasarathy M., Comachin M., Hack M., 1986, *Astron. Astrophys.*, **166**, 237
- Rao N.K., Venugopal V.R., 1985, *Astron. Astrophys.*, **6**, 101
- Reeves H., 1970, in: Aller L., McLafflin D.B. (eds.) *Vnutrennee stroenie zvezd*, M.: Mir, 13
- Rolleston W.R.J., Dufton P.L., Fitzsimmons A. 1994, *A&A*, **284**, 72
- Schonberner D., Drilling J.S., 1983, *Astrophys. J.*, **268**, 225
- Seydel F.L., 1929, *Publ. Astr. Soc. Pacific*, **6**, 278.
- Snezhko L.I., 1969, *Science Notic., Ser. Astr. Sverdlovsk*, No. 70, 163.
- Wilson R.E., 1914, *Lick Obs. Bull.*, **8**, 132.
- van Winckel H., 1997, *A&A*, **319**, 561

ON THE CRIMEA-TEXAS PROJECT "SURFACE ABUNDANCES OF LIGHT ELEMENTS FOR A LARGE SAMPLE OF EARLY B-TYPE STARS"

L.S. Lyubimkov

Crimean Astrophysical Observatory, p. Nauchnyj, Crimea, Ukraine

1. Introduction

Empirical data on the chemical composition of stars provide a unique possibility for testing and correcting modern theories of stellar evolution. Light chemical elements, namely He, C, N and O, in surface layers of young massive stars are of special interest. Actually, their abundances change significantly in stellar interiors during the hydrogen-core burning which is realized in stars of interest through the CNO cycle. If some mixing exists between interiors and surface layers of the stars, appreciable changes of surface abundances of these elements should take place, too. This process can have a noticeable influence on all subsequent evolutionary stages of the stars. Moreover, when these massive stars explode as Type II supernovae at the end of their evolution and eject matter into the ambient interstellar medium (ISM), the mass of ejected elements seems to be strongly dependent on the mixing during this early evolutionary phase known as the main sequence (MS) phase. Since supernova explosions are the main source of ISM enrichment by many elements, this early mixing should be taken into consideration in models of the Galaxy's chemical evolution.

Observational manifestations of the mixing in late O- and early B-type MS stars were reviewed in detail elsewhere (see, e.g., Lyubimkov 1996, 1998; Maeder & Meynet 2000). It should be noted that the first hints of the mixing came more than 25 years ago from studies of the surface helium abundance in hot MS stars (Lyubimkov 1975, 1976; see also Lyubimkov 1988). It was shown that this value increases as the stellar age increases. Later a significant increment was found for the surface nitrogen abundance (Lyubimkov 1984). These data on the He and N enrichment of surface layers of O and B stars during the MS phase were unexpected for the theory of that time. However the present-day theory recognizes a reality of this process and suggests the stellar rotation as a source of the mixing (see, e.g., Meynet & Maeder 2000; Heger & Langer 2000).

Two important details remain incomprehensible from the viewpoint of the theory. First, an interesting dependence of the surface helium abundance He/

H on age was found for hot MS stars that are components of close binaries. The dependence seems not to be monotonic; in fact, the initial abundance He/H is unchanged for the first half of the MS lifetime, but then it increases abruptly by about two times (Lyubimkov 1996). There are also some hints of similar non-monotonic increment of He/H for single B stars (Lyubimkov 1998). Second, one can expect that, according to the theory, there are correlations between the He and N abundances at the end of the MS phase, on the one hand, and rotational velocities of the stars, on the other hand. However, all attempts to find such correlations were unsuccessful.

Unfortunately, available data on the He, C, N and O abundances in O and B stars were insufficient in order to understand more in detail the process of mixing and, in particular, to solve two above-mentioned problems. It was necessary to increase strongly the number of the stars observed and to raise an accuracy of the abundances derived. Therefore the project "Surface abundances of light elements for a large sample of early B-stars" was presented as a result of collaboration between the Crimean Astrophysical Observatory (Ukraine) and the University of Texas at Austin (USA). Permanent members of the Crimean team are L.S. Lyubimkov, T.M. Rachkovskaya, S.I. Rostopchin and D.B. Poklad. The American team is presented by Prof. D.L. Lambert. Our general goal was to provide new comprehensive observations for a large sample (about 100) of early B-type MS stars and to complete a thorough analysis of CNO-cycle elements, namely He, C, N and O. A brief description of main results is given below.

2. Observatory

High-resolution spectral observations of 123 B0-B5 stars, which are likely to be in the MS phase, were implemented in 1996-1998 at two observatories, namely the Crimean Astrophysical Observatory (CrAO) and the McDonald Observatory (McDO) of the University of Texas. The 2.6-m telescope and the coude spectrograph with a 1024x256 CCD were used at the CrAO, while the 2.7-m telescope and coude 2D Echelle spectrometer with 2048x2048 CCD

were employed at the McDO. All details of the observations and reductions of spectra are described in Lyubimkov et al. (2000, hereinafter Paper I).

There were some limitations when B stars were selected for the observations. The limitations arise from the locations of the stars on the sky, their visual magnitudes and their physical properties. The electronic version of the Bright Star Catalogue (Hoffleit & Warren 1991) has been used for the selection.

In particular, we tried to observe only normal B stars. Spectroscopic binaries, Be stars and variable stars were usually excluded. Nevertheless, 16 of 123 stars from our list were found to show hints of H α emission, duplicity or pulsations, so they are not normal. We measured for these 16 stars the equivalent widths of H I and He I lines, but excluded them from further analysis.

Furthermore, we selected rather bright and, therefore, rather near B stars. Two reasons can be given for our selection. First, unlike faint stars, spectra of high quality can be obtained for bright stars. Second, one may expect for distant stars that their initial helium abundance Y and metal abundance Z (by mass) differ from the Y and Z values for stars in the star neighbourhood. Further analysis will demand the use of evolutionary tracks for determinations of masses and ages of the stars. The tracks depend on Y and Z ; therefore, generally speaking, it is impossible to use one and the same set of the tracks both for near stars and for distant ones. The B stars with the visual magnitudes I 6.7 have been included in our list.

One of our goals was to search for possible correlation between the He, C, N and O abundances and the observed rotational velocities $v \sin i$. So, we selected B stars with a wide range of $v \sin i$ values, from 0 to about 300 km/s where this value is known. For many observed stars the rotational velocities were unknown; they are determined for the first time in this project.

Other details of the star selection, as well as the full list of 123 programme stars are presented in Paper I.

3. Hydrogen and helium lines

Equivalent widths W of two Balmer lines, H β and H γ , and ten He I lines were measured for 123 programme stars, as well as of the He II 4686 line for the hottest ones. The Balmer lines are used as a good indicator of the surface gravity $\log g$, whereas the He I lines are used for determination of the helium abundance He/H, the microturbulent parameter V , and the projected rotational velocity $v \sin i$.

All measurements of the equivalent widths have been implemented by the Crimean team. Two hydrogen lines were measured independently by two members of the team, whereas helium lines were measured independently by three members. When comparing different sets of the W values, we obtained a good agreement. The averaged W values are employed in further analysis.

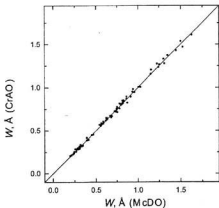


Figure 1: Comparison of the mean He I equivalent widths measured from the CrAO and McDO spectra for 14 common stars.

It is interesting that there were 14 common stars, for which all these lines have been observed both at the CrAO and at the McDO, so we were able to compare the equivalent widths derived from two sets of spectra. Such comparison for He I lines is presented in Fig. 1. A very good agreement is seen between the CrAO and McDO data; in fact, there is no systematic difference, and the accidental scatter is within ± 5 per cent. The measured equivalent widths, as well as their detailed analysis can be found in Paper I.

4. Basic parameters

As mentioned above, 16 of 123 programme stars are not normal, so our further analysis included 107 remaining stars. We determined basic parameters of these stars, first of all their effective temperatures T_{eff} and surface gravities $\log g$. Both parameters were derived simultaneously on the basis of standard $T_{\text{eff}} - \log g$ diagrams. Two colour indices were used as good indicators of T_{eff} , namely the index Q in the UBV photometric system and the index $[c_1]$ in the wby system. As is known, both values are independent of interstellar extinction. As far as $\log g$ is concerned, equivalent widths W of the above-mentioned Balmer lines, i.e. H β and H γ , as well as the b -index were used as good indicators of this parameter.

In Fig. 2 the $T_{\text{eff}} - \log g$ diagrams are shown as examples for two B stars, namely HR 8797 (B0.5 IV) and HR 6588 (B3 IV). Various curves here are the loci from the theoretical models, which predict the observed value for each of the considered parameters, i.e. for two equivalent widths and three photometric indices. For the hotter star, HR 8797, we also display in Fig. 2 the curve that corresponds to the He II 4686 line. It should be noted that all computed values in our analysis are based on Kurucz's (1993) model atmospheres.

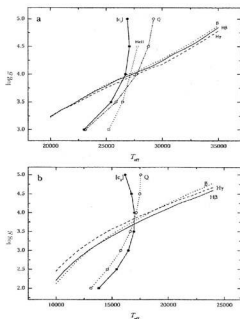


Figure 2: Diagrams for the T_{eff} and $\log g$ determination for the stars (a) HR 8797 (B0.5 IV) and (b) HR 6588 (B3 IV).

Furthermore, we found the interstellar extinction in the V band, i.e. the A_V value, basing on the *ubv* photometry. Using three derived parameters, namely T_{eff} , $\log g$ and A_V , one can evaluate the distance d of the stars (note that the masses M are necessary as well; they were determined from evolutionary tracks, see below). We found the d values and compared them with distances obtained from the *Hipparcos* parallaxes (ESA 1997). The comparison is presented in Fig. 3. The upper panel shows the two sets of d values with their errors. In the lower panel the relative difference between our and the *Hipparcos* data including common errors of both sets is displayed. When taking into account uncertainties in the d values, one may see that agreement between the two sets is rather good. In particular, the scatter in the lower panel is mostly within ± 50 per cent and can be explained, as a rule, by errors of the d determination.

In Fig. 4 the T_{eff} and $\log g$ values derived for programme stars are compared with the evolutionary tracks of Claret (1995). One may see that most of the stars correspond really to the MS phase. About ten stars have very likely recently completed this phase. Three stars are marginally below the Zero Age Main Sequence (ZAMS), but the uncertainty in their surface gravity would allow them to be on the ZAMS. Interpolating among the tracks we estimated the masses M of the stars.

Furthermore, using the M values, we determined the radius R and luminosity L . The age t was evaluated as well from Claret's computations.

The derived values of T_{eff} , $\log g$, d , M and other parameters for 107 stars are presented and discussed in Lyubimkov et al. (2002, Paper II). Interpolating among Kurucz's (1993) model atmospheres, we found for each star the model atmosphere according to its T_{eff} and $\log g$ values. These models were used in further analysis of the He, C, N and O abundances.

5. Helium abundances and microturbulent parameters

Non-LTE analysis of HeI lines in spectra of 102 programme stars was implemented in order to determine the helium abundance He/H, the microturbulent parameter V_t and the projected rotational velocity $v \sin i$ (five stars of 107 were omitted). A determination of He/H and V_t was based on the equivalent widths measured in Paper I; the lines 4471 and 4922 were used as indicators of He/H and the lines 4713, 5016, 5876 and 6678 were used as indicators of V_t . The velocities $v \sin i$ were found from profiles of the same lines.

The He/H- V_t diagram for the star HR 8797 is shown in Fig. 5 as an example. An idea of such diagram is similar to the well-known $T_{\text{eff}} - \log g$ diagram (see Fig. 2); various curves here are the loci from the theoretical models, which predict the ob-

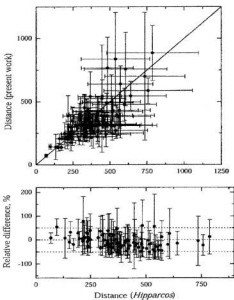


Figure 3: Comparison of our distances d (pc) with the *Hipparcos* d values.

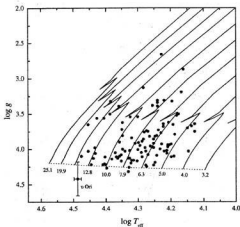


Figure 4. Location of programme stars on the evolutionary diagram. Claret's (1995) evolutionary tracks are shown for stars with masses M from 3.2 to $25.1M_{\odot}$. Dotted line corresponds to the ZAMS.

served equivalent widths of the used helium lines. This diagram allow to obtain simultaneously both parameters, He/H and V_t , basing on the different dependence of the lines on the microturbulent parameter V_t . The 4471 and 4922 curves, on the one hand, and the 4713, 5016, 5876 and 6678 curves, on the other hand, show a number of intersections; their averaged coordinates give He/H and V_t for the star. In particular, for HR 8797 the parameters $\text{He}/\text{H}=0.131$ and $V_t=13.8$ km/s were obtained. The He/H and V_t values for 102 stars are presented in Lyubimkov et al. (2003, Paper III).

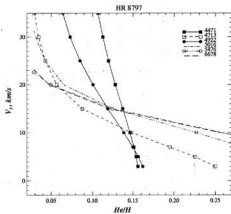


Figure 5: Diagram for the He/H and V_t determination for the star HR 8797.

Two of 102 stars were found to be the helium-weak stars. Since one of our objectives was a search of possible correlations of He/H and V_t with stellar masses M , we divided the remaining 100 stars into three groups as follows. Group A includes the stars with relatively low masses between 4.1 and $6.9M_{\odot}$, 42 objects in all (M_{\odot} is the solar mass). Group B contains the stars of intermediate masses between 7.0 and $11.2M_{\odot}$, 46 objects in all. Group C includes the most massive stars with M between 12.4 and $18.8M_{\odot}$, 12 objects in all.

We analyzed a relation between the microturbulent parameter V_t and the relative age t/t_{ms} for each group separately (here t_{ms} is the MS lifetime). In group A the parameter V_t seems to be small for all stars independently of t/t_{ms} . The V_t values vary within the 0-5 km/s region, as a rule. Similar low velocities V_t were found for stars of group B with the relative ages $0.0 < t/t_{\text{ms}} < 0.8$, however the evolved stars with $0.8 < t/t_{\text{ms}} < 1.02$ showed a large scatter of V_t from 0.3 to 11.0 km/s. For most massive stars of group C, in contrast with group A and B, a strong correlation between V_t and t/t_{ms} was obtained. Actually, for the non-evolved stars with $t/t_{\text{ms}} < 0.3$ the V_t values varied from 4 to 7 km/s, whereas for the most evolved stars with $t/t_{\text{ms}} > 0.8$ the high velocities V_t in the 16 to 23 km/s range were found.

It is interesting that, when $V_t > 7$ km/s, the $V_t(\text{HeI})$ values determined from HeI lines are systematically overestimated as compared with the $V_t(\text{OII}, \text{NII})$ values derived from OII and NII lines. Moreover, this discrepancy tends to increase as V_t increases, so the most marked difference takes place for hottest evolved B giants. One may suppose that the velocity gradient due to mass loss is very likely to exist in atmospheres of such giants, like O and B supergiants. This effect can be a principal cause of overbroadening of HeI lines as compared with weaker OII and NII lines (see Paper III for details).

We analyzed as well a relation between the helium abundance He/H and the relative age t/t_{ms} . A correlation was found for each of the groups A, B and C, so the helium abundance tends to increase with the age. For instance, Fig. 6 displays this relation for stars of group A. The straight line drawn by the least squares method shows that the He/H value increases from 0.105 to 0.134 during the MS phase when t/t_{ms} varies from 0 to 1. Therefore, the mean helium enrichment of atmospheres of the 4.1-6.9 M_{\odot} stars is 28 per cent.

The most pronounced helium increment was found for most massive stars, i.e. for group C. When using the $V_t(\text{HeI})$ values derived from HeI lines, we obtained for this group the mean He enrichment of 43 per cent, while when the $V_t(\text{OII}, \text{NII})$ values based on OII and NII lines are employed, the He abundance increases on the average by 2.2 times. It should be noted that the He/H values based on the $V_t(\text{OII}, \text{NII})$ scale are in better agreement with the

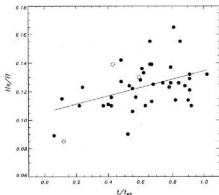


Figure 6: The helium abundance as a function of the relative age for stars of group A. The straight line is drawn by the least-squares method.

theory (see Paper III). There is a possibility that such massive single stars, like massive components of binaries, keep their initial He abundance unchanged during the first half of the MS lifetime.

6. Rotational velocities

A determination of the projected rotational velocities $v \sin i$ for 102 programme stars was based on analysis of profiles of the same HeI lines; the individual parameters He/H and V_1 were taken into consideration for each star. The non-LTE profiles computed for the various $v \sin i$ values were fitted to the observed ones to derive $v \sin i$. It is important that a difference in $v \sin i$ for various HeI lines was found to be small. The averaged rotational velocities are presented in Paper III; they vary from 5 to 280 km/s. It should be noted that for many stars the $v \sin i$ values have been not determined earlier.

The theoretical models of rotationally mixed stars predict a strong dependence of the helium enrichment during the MS phase on the rotational velocity. Unfortunately, spectral observations of stars allow to obtain only the projected rotational velocity $v \sin i$, but not directly the equatorial velocity v . Nevertheless, a comparison of the derived He/H values with $v \sin i$ would be useful for a check of the theory.

We compared He/H with $v \sin i$ for stars with relative ages $t/t_{ms} > 0.7$, i.e. close to the MS termination. When the abundances He/H are based on the $V_1(OI, NII)$ scale, there is an obvious trend: the stars with the greater velocities $v \sin i$ tend to have the higher final abundances He/H.

Therefore, a qualitative agreement with the theory takes place.

7. Concluding remarks

A significant part of the project is already implemented. Actually, high-resolution spectra of more than 100 early B stars were obtained. A number of basic parameters was determined including the effective temperatures T_{eff} , surface gravities $\log g$, masses M , ages t etc. A detailed non-LTE analysis of HeI lines was effected to find the helium abundance He/H, microturbulent parameter V_1 and rotational velocity $v \sin i$. Relations between He/H and V_1 , from the one hand, and M , t/t_{ms} and $v \sin i$ from the other hand, were constructed. It was confirmed that there is the helium enrichment during the MS phase, which correlates with the masses M and rotational velocities $v \sin i$. It is necessary to note that from the outset we tried to get a highest accuracy on each stage of this work.

At present we are implementing a last stage of the project, i.e. an analysis of CII, NII and OII lines on the basis of non-LTE computations. Our goal is an accurate determination of the C, N and O abundances and a search for correlations with M , t/t_{ms} and $v \sin i$.

References

- ESA, 1997, *The Hipparcos and Tycho Catalogues*, ESA SP-1200. ESA, Noordwijk.
- Heger A., Langer N., 2000, *Ap.J.*, **544**, 1016.
- Hoffleit D., Warren W.H., Jr, 1991, *The Bright Star Catalogue*, 5th revised edn. ADS, Srasbourg (electronic version).
- Kurucz R.L., 1993, CD-ROM 13.
- Lyubimkov L.S., 1975, *Pis'ma Astron. Zh.*, **1**, #11, 29.
- Lyubimkov L.S., 1976, *Izv. Krym. Astrofiz. Obs.*, **55**, 112.
- Lyubimkov L.S., 1984, *Astrofizika*, **20**, 475.
- Lyubimkov L.S., 1988, *Astrofizika*, **29**, 479.
- Lyubimkov L.S., 1996, *Astrophys. Space Sci.*, **243**, 329.
- Lyubimkov L.S., 1998, *Astron. Zh.*, **75**, 61 (also *Astron. Rep.*, **42**, 52).
- Lyubimkov L.S., Lambert D.L., Rachkovskaya T.M., Rostopchin S.I., Tarasov A.E., Poklad D.B., Larionov V.M., Larionova L.V., 2000, *Mon. Not. Roy. Astron. Soc.*, **316**, 19 (Paper I).
- Lyubimkov L.S., Rachkovskaya T.M., Rostopchin S.I., Lambert D.L., 2002, *Mon. Not. Roy. Astron. Soc.*, **333**, 9 (Paper II).
- Lyubimkov L.S., Rostopchin S.I., Lambert D.L., 2003, *Mon. Not. Roy. Astron. Soc.* (in press, Paper III).
- Maeder A., Meynet G., 2000, *Ann. Rev. Astron. Astrophys.*, **38**, 143.
- Meynet G., Maeder A., 2000, *Astron. Astrophys.*, **361**, 101.

SUBSYSTEMS OF THE GALACTIC HALO, THEIR STRUCTURES AND COMPOSITIONS

V.A. Marsakov, T.V. Borkova

Space Research Department at Rostov State University, Russia
e-mail: marsakov@ip.rsu.ru; borkova@ip.rsu.ru

ABSTRACT. It is shown that general populations of globular clusters and metal-poor field stars are components at least of three subsystems occupying different volumes in the Galaxy. The thick disk and proto-disk subsystems are genetically associated with the Galaxy. The age distributions of these two subsystems do not overlap. It is argued that heavy-element enrichment and the collapse of the proto-galactic medium occurred mainly in the period between the formation of the proto-disk halo and thick disk subsystems. The largest third subsystem has no metallicity gradient, most of its objects have retrograde motion in the Galaxy, some of them have unusually low content of α -elements, and their ages are comparatively low in average, supporting the hypothesis that the objects in this subsystem had an extragalactic origin.

Quite recently the Milky Way was supposed to form from single proto-galactic cloud. However, recently published observations demonstrate that some galactic objects have obvious extragalactic origin. In particular, the most direct evidence is provided by the Sagittarius dwarf spherical galaxy, which is now in the process of tidal destruction in the halo (Ibata et al. 1994). There are five globular clusters associated with this galaxy. Furthermore, one of the most significant results was the discovery of a large clump of field stars, which is part of the tidal tail of the Sgr galaxy (Ivesic et al. 2000). It should be noted that the existence of several populations among globular clusters (GC) and high velocity field stars belonging to different subsystems of the Galaxy follows from the discreteness of their distributions on metallicity and angular momentum. Even the earliest metallicity functions revealed a gap near $[\text{Fe}/\text{H}] = -1.0$, which divides the populations of these objects into two discrete groups: a metal-poor, spherically symmetric, slowly rotating halo subsystem and a metal-rich, rather rapidly rotating, thick-disk subsystem (Marsakov & Suchkov 1977, 1978, Zinn 1985). Halo globular clusters were further shown to sepa-

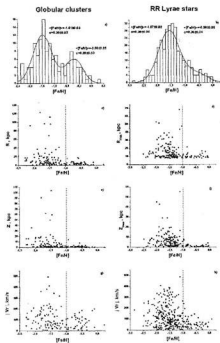


Figure 1: Relations between metallicity and other parameters of GCs and field RR Lyraes. A Sharp jump near $[\text{Fe}/\text{H}] = -1$ is seen in all panels.

rate into two groups with different horizontal-branch (HB) morphologies. These subgroups, whose distributions are both spherical, differ in their kinematics and the spatial volume they occupy (Mironov & Samus 1974, Zinn 1993). Halo clusters, which have redder HBs for a given metallicity (i.e., with horizontal branches showing a considerable number of stars on the low-temperature side of the Schwarzschild gap) are predominantly outside the solar circle, have a large velocity disper-

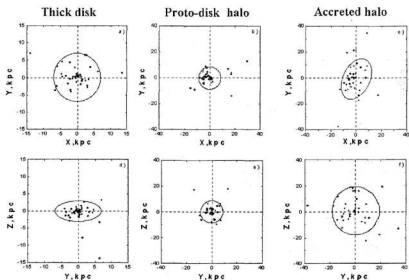


Figure 2: The spatial distributions for metal rich GCs (the first column), metal-poor GCs with extremely blue HBs (the second column), and metal-poor GCs with reddened HBs (the third column). The closed curves are upper envelopes drawn by eye.

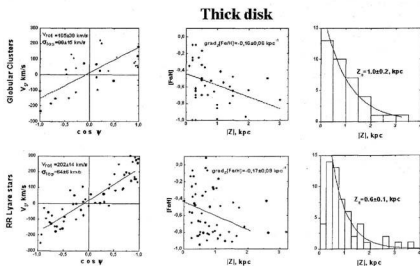


Figure3: Properties of metal-rich populations. The first column shows the kinematical diagrams, where ψ is the angle between the line of sight on the object and the vector of rotation about Z-axis, and V_S is objects line-of-sight velocity relative to an observer at rest at the position of the Sun. The straight lines are regression fits, whose slopes yield the subsystem's rotation rate. The second column shows the relations between metallicity and distance from the Galactic plane. The slope of the regression line yields the metallicity gradient. The third column shows the distributions of GCs and field RR Lyrae stars in Z. The curves approximate the histograms with an exponential laws with scale heights Z_s .

Table: Characteristic parameters of subsystems RR Lyrae field stars and globular clusters

Parameter	Thick disk		Proto-disk halo		Accreted halo	
	RR Lyrae	GC	RR Lyrae	GC	RR Lyrae	GC
Number	30	37	68	30	76	47
$\langle [Fe/H] \rangle$	-0.57 ± 0.05	-0.56 ± 0.05	-1.54 ± 0.04	-1.71 ± 0.05	-1.59 ± 0.04	-1.60 ± 0.07
$\sigma_{[Fe/H]}$	0.28 ± 0.03	0.28 ± 0.03	0.36 ± 0.03	0.26 ± 0.03	0.29 ± 0.03	0.35 ± 0.05
$\langle \Theta \rangle$, km/s	198 ± 9	165 ± 38	104 ± 10	77 ± 33	-40 ± 12	-23 ± 54
σ_{Θ} , km/s	51 ± 7	88 ± 15	84 ± 7	129 ± 19	101 ± 8	140 ± 18
$\langle e \rangle$	0.23 ± 0.03	0.13 ± 0.04	0.54 ± 0.03	0.53 ± 0.06	0.75 ± 0.03	0.59 ± 0.06
$limR_{max}$, kpc	13	7	18	10	40	20
$limZ_{max}$, kpc	2	3	10	10	22	20
Z_{α} , kpc	0.74 ± 0.05	1.0 ± 0.02	3.1 ± 0.1	2.5 ± 0.5	6.4 ± 0.5	8.5 ± 1.5
$grad_1 [Fe/H]$, kpc^{-1}	-0.03 ± 0.04	-0.01 ± 0.02	-0.00 ± 0.01	-0.03 ± 0.02	-0.00 ± 0.01	-0.03 ± 0.01
$grad_2 [Fe/H]$, kpc^{-1}	-0.23 ± 0.10	-0.16 ± 0.06	-0.02 ± 0.01	-0.03 ± 0.02	-0.00 ± 0.01	-0.03 ± 0.01
$\langle \mathcal{D} \rangle$, Gyr		12.5 ± 0.5		15.5 ± 0.5		13.8 ± 0.3
$\sigma_{\mathcal{D}}$, Gyr		1.4 ± 0.3		0.8 ± 0.2		1.4 ± 0.2
$\sigma_{[Mg/Fe]}$	0.26 ± 0.02		0.35 ± 0.02		0.29 ± 0.03	
$\sigma_{[Mg/Fe]}$	0.17 ± 0.01		0.14 ± 0.02		0.15 ± 0.02	

sion, lower rotational velocities, and smaller ages than clusters with blue HBs, which are concentrated inside solar circle. (Da Costa & Armandroff 1995). This difference can be explained if the older proto-disk halo subsystem shares a common origin with the thick-disk, whereas the clusters of another subsystem - accreted halo - were captured by the Galaxy from intergalactic space during later stages of its evolution (Zinn 1993).

The presence of two populations with different histories in the low-metallicity halo was suggested by Hartwick (1987). He argued that two components were needed to model the dynamics of field RR Lyrae variables with metallicities $[Fe/H] < -1$: one spherical and somewhat flattened inner component, that is dominant at galactocentric distances less than radius of the solar circle. Study of a large sample of stars in a deep survey in the direction of the North Galactic Pole demonstrates that stars further than 5 kpc from the plane of the disk tend to have retrograde orbits (Majewski 1992). (A retrograde rotation is a pretty convincing argument for an origin largely independent of the Galaxy.) Further evidence for the presence of objects with an extragalactic origin among field stars is the identification of objects with relatively young ages and low abundances of heavy elements (so that they should have been older, according to abundance age indicators). The subsystem of accreted globular clusters sometimes is named the "young halo" for precisely this reason. On average, high-velocity field subdwarfs with highly eccentric orbits ($e > 0.85$) are younger than subdwarfs with similar metallicities but less eccentric orbits (Carney 1996). Carney derived the isochrone ages of subdwarfs based on Stromgren photometry. Hanson et al. (1998), who also used abundances of α -elements as age indicators, likewise concluded that metal-poor red giants in retrograde

orbits were relatively young. ($[\alpha/Fe]$ is known to be low for younger objects formed from matter already enriched in the injects of type Ia supernovae, whereas the higher relative abundances of α -elements in older stars are due to type II supernovae.) However, observations of field RR Lyrae stars and blue horizontal-branch stars were used in (Lauden 1998) to estimate the number ratios of these objects in different directions from the Sun. Blue horizontal-branch giants dominate among stars close to the Galactic center and Galactic plane, whereas the numbers of variable stars and giants were approximately the same at greater distances. These stars have similar metallicities, suggesting that the inner, bluer population of the Galaxy is older than the outer population.

Thus, the existence of two subsystems in the metal-poor halo is no doubt, but it is very difficult to identify all objects, which are the debris of dwarf galaxies, with direct observations. Fortunately, all reliable identified accreted globular clusters possess a distinctive inner feature: the morphology of their horizontal branches. Therefore, to determine characteristics of different halo subsystems we suppose that the Galaxy accretes only metal-poor globulars, which have reddened HB for a given metallicity. And on the contrary, only metal-poor globulars with extremely blue HB belong to the proto-disk halo subsystem. Objects of this subsystem formed together with the Galaxy as a whole. When protogalactic cloud appreciable contracted, metal-rich globular clusters was born and formed younger, something flattening thick disk subsystem.

Objects belonging to the thick disk can be reliably distinguished based on metallicities. Figure 1a shows the distribution of heavy-element abundance for all Galactic globular cluster from catalogue with spectroscopic determination of $[Fe/H]$ of Harris (1996). The solid curve shows an approximation of the his-

togram using a superposition of two Gaussian curves with parameters estimated using a maximum-likelihood method. It is seen that the entire globulars population can be divided into two metallicity groups, separated by a well-defined gap at $[Fe/H] = -1.0$. The metallicity function of field RR Lyrae stars in Fig. 1b can also be described by two normal curves at high confidence level. The mean values and dispersions of the metallicities in the groups coincide with the corresponding parameters for globular clusters within the errors (see Table). The breakdown of both (the globular clusters and the field stars) populations into two subsystems separated by $[Fe/H] = -1.0$ is further supported by the fact that diagrams in Fig. 1 (c-d, e-f) demonstrate an abrupt change of spatial locations and velocity distribution when the metallicity crosses precisely this boundary value of $[Fe/H]$. Note that we can observe only nearest field stars and therefore in Figures 1c and 1e we use calculated orbital parameters (apogalactic distances and the maximum distance of the orbit from the Galactic plane) for determination of spatial distributions. The present spatial distribution of globular clusters in Fig. 2a,d demonstrates that subsystem of metal-rich ($[Fe/H] > -1.0$) objects is concentrated toward both the center and the Galactic plane, and its shape can be very roughly described as an ellipsoid of revolution slightly flattened along the Z-axis. The flattening is caused by rapid rotational velocity of this subsystem (see Fig. 3a,d). Present position of metal-rich globulars and field stars indicate high negative vertical metallicity gradients (Fig. 3b,e) and relatively small scale heights. Taking into consideration coincidence of main characteristics of metal rich globulars and field RR Lyraes (see Fig. 3 and Table) we have to conclude that both populations belong to the same subsystem of the Galaxy, named the thick disk.

Let us now consider the metal-poor objects. Figures 2b-e,c-f show the spatial distributions of the two groups that selected according to horizontal branch color. We can see that the globular clusters of our proto-disk halo are appreciable concentrated toward the galactic center, and their galactocentric distribution is enclosed by a sphere of radius ≈ 9 kpc. The distribution of intended accreted clusters in the YZ plane fits well inside a circle of radius ≈ 19 kpc. The accreted clusters occupy a much smaller area in the XY plane, and their distribution can be described by an elongated figure with semi-axis equal to 18 and 10 kpc. The semi-minor axis is perpendicular to the Z-axis and makes an angle of about 30° to the X-axis. That is subsystem of the metal-poor clusters with reddened horizontal branches occupy a slightly flattened spherical value which is a factor of ≈ 2 larger than for the clusters with extremely blue HB.

Properties of these subsystems of metal-poor globular clusters differ also. Kinematical diagrams in

Fig. 4a,d show that subsystem of globular clusters with extremely blue horizontal branches exhibits a fairly well defined prograde rotation, whereas subsystem of clusters with reddened horizontal branches indicates retrograde rotation (see Table). Hence most clusters with reddened HB are really accreted objects. Metallicity gradients for both subsystems were negligible but non-zero. Fig. 4c,f shows that scale heights of these subsystems differ dramatically.

It is much more difficult to identify field stars that have an extragalactic origin, i.e. those belonging to the accreted halo. According to the hypothesis that the proto-galaxy collapsed monotonically from the halo to the disk, suggested by Eggen et al. (1962), stars genetically related to the Galaxy cannot have retrograde orbits. Only the oldest halo stars may be an exemption, since they could have retrograde orbits due to the natural initial velocity dispersion of proto-stellar clouds. On the other hand, some stars formed from extragalactic fragments and captured by the Galaxy may have prograde orbits. In any case, such stars should have fairly large peculiar spatial velocity relative to the Local Standard of Rest. We used for this study the largest catalogue of RR Lyrae variables compiled by Dambis & Rastorguev (2001). The catalogue contains 262 stars with published photoelectric photometry, metallicities, radial velocities, and absolute proper motions. The diagram in Fig. 5a shows that there is a transition from prograde to retrograde orbits around the galactic center near $V_{pec} = 280$ km/s. We also can see in the rest diagrams in Fig. 5 that all orbital parameters demonstrate the break of their relations and abrupt increase in their dispersions in the vicinity the same threshold peculiar velocity. Fig. 5f shows that RR Lyraes with velocities near the threshold lever might have any orbital inclination up to orthogonal to the galactic plane, whereas the range of "permitted" inclinations continuously becomes narrower when velocity moves away from this threshold level in both sides. For this reason, we adopt $V_{pec} > 280$ km/s as the critical value for distinguishing stars of the accreted halo. We suppose that stars with lower peculiar velocities have a galactic origin and belong to the proto-disk halo, and to the thick disk halo subsystems. Apparently, this kinematical criterion is not entirely unambiguous: some stars of proto-disk halo may have larger peculiar velocities. Evidence for this is provided, in particular, by the increase in the star density immediately to the right of the threshold level in our diagrams. However, we decided to retain a simple criterion, in order not to artificially coiffeuse the situation.

The spatial velocities of the stars can be used to obtain estimates for a numbers of characteristics for subsystems, if we can first reconstruct the star's galactic orbits. The orbital elements were computed using the Galactic model of (Allen & Santillan 1991),

Globular Clusters

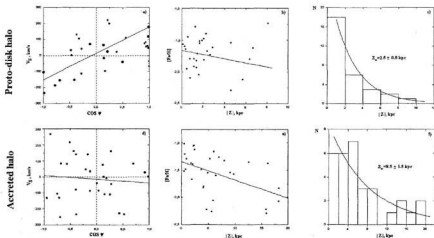


Figure 4: Properties of metal-poor subsystems of GCs with blue HBs (top row), and with redder HBs (bottom row). Notations are the same as in Fig. 3.

RR Lyrae

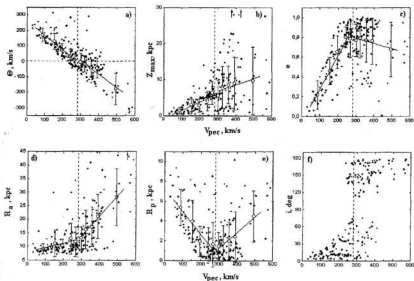


Figure 5: Relations between peculiar velocity and other characteristics of the RR Lyrae. The large open circles with error bars are mean values and dispersions of the corresponding parameters in narrow intervals of V_{pec} . The straight lines are the least-square fits for the stars lying both on the left and on the right of $V_{pec} = 280$ km/s (the vertical dotted lines).

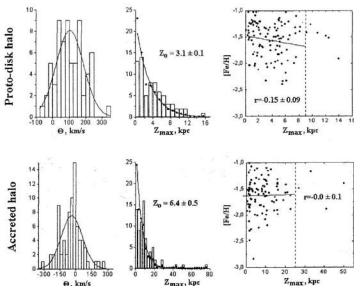


Figure 6: Properties of metal-poor subsystems of RR Lyrae with low peculiar velocity (top row) and high peculiar velocity (bottom row). The first column shows histograms in the rotation velocities. The second column shows the distribution of Z (see text for details), and the curves approximate the reconstructed distributions with exponential law. The third column shows relations between maximum height above the galactic plane and metallicity.

which includes a spherical bulge, disk, and extended massive halo. Fig. 6 (see also Table) shows that the vertical metallicity gradients (Fig. 6 c-f) and the distributions of RR Lyrae stars in the two metal-poor subsystems as a function of their rotation velocities and distances to the Galactic plane differ drastically. (Note, that to compute the scale height using Z_{\max} we must first to reconstruct the "real", instantaneous Z -distribution for all stars according to probability density of its location at different Z . The filled dots in the histograms (Fig. 6c,f) are the reconstructed distributions in Z .)

Age is one of the most uncertain parameters. In particular, Hipparcos data requires substantial revision of GC distances. As a result, the ages of even the most metal-poor (i.e., oldest) clusters do not exceed ≈ 10 Gyr (see, e.g., Reid 1997). However, we adopted the old scale here, because the refinement of the age-scale zero point based on the new data is probably now only in its initial stage, and we are primarily interested in relative parameters. The data of the comparative catalogue of homogeneous age dating of 63 globular clusters by Borkova & Marsakov (2000) shows, that the globulars of different subsystems have different ages also. Fig. 7a demonstrates the age distribution of globular clusters, which have a com-

mon origin with the Galaxy. It is seen that age distributions of the thick disk and proto-disk halo clusters do not overlap. It follows from Fig. 7a and from the Table the age dispersion for the proto-disk halo clusters is nearly equal to the error in ages themselves. The thick disk cluster ages exhibit a much larger scatter. In other words, the halo clusters formed almost simultaneously, whereas the corresponding processes in the thick disk required at least several billion years. The age gap between subsystems, if any, might be swamped by the errors in the estimated ages. From the comparison of Fig. 7b and 7a it is seen that the ages of the clusters with reddened horizontal branches (Fig. 7b) demonstrate large spread, and mean age of their age distribution is smaller than that for the proto-disk halo clusters.

Figure 8 demonstrates that field stars of different subsystems differ also in content of α -elements. As a surrogate of α -elements content may be accepted magnesium abundance. We compile all known to us published spectroscopic determination of $[Mg/Fe]$ with non-LTE models, led these data into the united scale, and compute stellar spatial velocities using Hipparcos parallaxes (it is used only stars with error of parallax $< 25\%$). In any interstellar cloud star formation process en-

Clobular Clusters

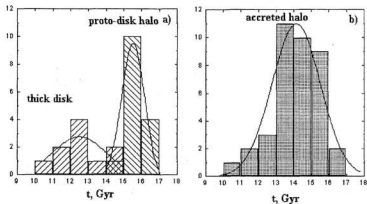


Figure 7: The age distribution of the globular clusters of (a) Galactic origin and (b) accreted by the Galaxy. Different shadings are used to show the thick disk and prot-disk halo clusters. The curves are Gaussian fits to the corresponding histograms. Data was taken from (Borkova & Marsakov, 2000).

rich their gas with the ejecta from Type II, then Type Ia supernovae, and each would yield a distribution similar to Figure 8. Wyse & Gilmore (1988) has discussed the possible utility of $[\alpha/\text{Fe}]$ as a chronometer. If the model for Type Ia supernovae are a good quite, once there has been a burst of star formation it should take roughly 1 Gyr for the first Type Ia supernovae to appear, although timescales ranging from 0.5 to 3 Gyr have been suggested by Yoshii et al (1996). Thus, the simplest interpretation of Fig. 8 is that the Galaxy took only about ~ 1 Gyr to rise from primordial chemical abundances to $[\text{Fe}/\text{H}]=-1$. According to the chemical evolution calculations of Travaglio et al (1999) the thick disk population formed in the early Galaxy during an interval of ~ 1.1 Gyr to 1.6 Gyr after the beginning of the protogalactic collapse. (Note, that this time interval is in some disagreement with age dispersion for the thick disk clusters, determined with the help of theoretical isochrones (see Fig. 7a).) Gilmore & Wise (1998) have suggested that the very low $[\alpha/\text{Fe}]$ values for metal-poor stars could be produced by very slow, perhaps episodic, star formation. Only small galaxies, whose chemical enrichment history was quite different from that of the Galaxy, might be recognized by unusual locations in this diagram. Nissen & Schuster (1997) noted that while some of the halo stars followed the same trend in $[\alpha/\text{Fe}]$ as did the disk stars, some of the halo stars were clearly deficient in $[\alpha/\text{Fe}]$. These deficiencies also seemed to be related to the maximum distance these stars from the galactic plane, their maximum distance

from the Galactic center, and their high spatial velocities. This last point is illustrated in our Fig. 8. We can see in the diagram that overwhelming number of fast metal-poor stars ($V_{\text{pec}} > 280$ km/s) have magnesium content that appear to be appreciably lower than those of majority of stars having similar metallicities (see also Table). Probably, some victims have star formation that was slow enough to permit inclusion of SN Ia ejecta into the star-forming gas, and also produce relatively low metallicity. Thus, the content of α -elements can be used as additional inner criterion for distinguishing accreted objects.

Here, we compare the characteristics of the metal-poor subsystems. The parameters of the corresponding halo subsystems differ somewhat. In particular, the metallicity dispersion of the proto-disk halo derived from the globular clusters is lower than that of the outer halo. The field stars show the opposite pattern (see Table). However, the differences are comparable to the formally computed uncertainties, indicating that any conclusions about differences between these parameters have low statistical significance. The vertical gradients in the proto-disk halo for both the RR Lyrae stars and the globular clusters almost coincide, but the radial gradients differ (see Table). In the accreted halo, both gradients are absent for the field RR Lyrae stars but are non-zero for the clusters. However, both gradients for the globular clusters in the accreted halo are due exclusively to metal-richer objects close to the galactic center ($R \sim 7$ kpc). Distant RR Lyraes were not included in

Nearest field stars

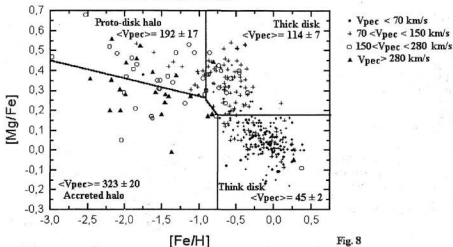


Fig. 8

Figure 8: Abundance ratio $[Mg/Fe]$ versus $[Fe/H]$ for nearby field stars. Drawn by eye straight lines divide panel into four sections, which mainly occupied stars of different subsystems of the Galaxy. Mean peculiar velocities of stars into each panel are denoted (km/s). Ranges of star's peculiar velocities are denoted.

our sample. In any case, values of all corresponding gradients coincide within the uncertainties. In this study, we have identified the halo subsystems based on spatial velocity. Therefore, the differences between the proto-disk halo and accreted halo in any kinematical parameter for field stars should be more prominent. The velocity dispersions for the subsystems of globular clusters are obviously overestimated due to the larger distance uncertainties and, as a result, are much higher than the values for field RR Lyrae stars. The radial size of the proto-disk halo is approximately a factor of 1.8 larger for the field stars than for the clusters, whereas the two scale were the same within the errors. Recall that we can estimate the radial sizes of RR Lyrae subsystems only from their maximum distances from the galactic center, which leads to appreciable overestimates of these sizes. Note, that in order to obtain correct estimates of sizes of galactic subsystems based on data for nearby stars, it is necessary to take into account the kinematical selection effect, which leads to a deficiency of stars with large R_x and Z_{max} in the solar neighborhood.

Thus, we can see generally good agreement between characteristics of corresponding subsystems of field RR Lyrae stars and Galactic globular clusters distinguished using different criteria. This evidences for that populations of both the clusters and the field stars are not uniform and compose

three different subsystems of the Galaxy: the metal-rich thick-disk, related to it by its origin the inner proto-disk halo, and the outer accreted halo. Analysis of these patterns suggests the following scenario for the early evolution of our Galaxy. The first stellar objects were formed when the proto-galactic cloud had already collapsed to the size of the modern Milky Way. The proto-disk halo formed over a short time interval. The radial and vertical metallicity gradients in this oldest known Galactic subsystem provide evidence that the first heavy-element enrichment of the gas-dust medium took place before the clusters and field stars of this subsystem formed. Both, the spatial and chemical characteristics change abruptly as we move to the thick-disk subsystem. The formation of stars in these subsystems was apparently separated by a substantial time lag, which shows up only as a gap in the age distribution. This time lag enabled the gas and dust clouds to become appreciable enriched in heavy elements (which had time to mix) and to collapse to much smaller sizes before the new generation of stars and clusters began to form. As a result, a rather flat, metal-rich, thick-disk subsystem formed. The appreciable collapse of the proto-disk cloud after the formation of the halo subsystem resulted in an increase of the rotational velocity and a rapid flattening of the future subsystem. Strong negative vertical metallicity gradient in the thick-disk tes-

tify to continuing collapse of this subsystem to the Galactic plane in their formation time. Differences in age, metallicity, and spatial distributions indicate that heavy-element enrichment and collapse of the proto-Galaxy occurred mainly in period between the formation of the proto-disk halo and thick disk subsystems. The collected result indicate that outer halo subsystem is characterized by a large size an absence of appreciable metallicity gradients, predominantly large orbital eccentricities, a large number of objects on retrograde orbits, and, on average, younger ages for its objects, supporting the hypothesis that object in this subsystem had an extragalactic origin.

More detail about subsystems of metal-poor populations of the Galaxy can be seeing in (Borkova & Marasakov, 2000, 2002).

References

Allen A., Santillan A., 1991, *Rev. Mex. Aston. Astroph.*, **22**, 225
 Borkova T.V., Marsakov V.A., 2000, *Astron Zh*, **77**, 750 (2000, *Astron. Rep.*, **44**, 665)
 Borkova T.V., Marsakov V.A., 2002, *Astron Zh*, **79**, 510, (2002, *Astron Rep.*, **46**, 460)
 Carney B.W., 1996, *PASP*, **108**, 900
 Da Costa G.S., Armandroff T.F., 1995, *AJ*, **109**, 2533
 Dambis A.K., Rastorguev A.S., 2001, *AstL*, **109**, 2533
 Eggen O.L., Lynden-Bell D., Sandage A., 1962, *ApJ*, **136**, 748

Hanson R.B., Sneden C., Kraft R.P., and Fulbright J., 1998, *AJ*, **116**, 1286
 Harris W.E., 1996, *AJ*, **112**, 1487 (rev. 22 June 1999)
 Hartwick F.D.A., 1987, in *the Galaxy*, Ed. By G. Gilmore and B.Carwell (Dordrecht), p.281
 Ibata R.A., Gilmore G., Irvin M.J., 1994, *Nature*, **370**, 194
 Ivesic Z., et al 2000, *AJ*, **120**, 963
 Lauden A.C., *AJ*, 1994, **108**, 1016
 Majewski S.R., *ApJ*, 1992, **78**, 87
 Marsakov V.A., Suchkov A.A., 1977, *Astron Zh*, **54**, 1232 [*Sov Astron*, **21**, 700]
 Marsakov V.A., Suchkov A.A., 1978, *Astron Zh*, **55**, 472 [*Sov Astron*, **22**, 700]
 Mironov A.V., Samus N.N., 1974, *Perem.Zvezdy*, **19**, 337
 Nissen P.E., Schuster W.J., 1997, *Aap*, **251**, 457
 Reid I.N., 1997, *AJ*, **114**, 161
 Travaglio C., Galli D., Gallino R., et. al, 1999, *ApJ*, **521**, 691
 Wise R.F.G., Gilmore G., 1988, *AJ*, **95**, 1404
 Yoshii Y., Tsujimoto T., Nomoto K., 1996, *ApJ*, **462**, 266
 Zinn R., 1985, *ApJ*, **293**, 424
 Zinn R., 1993, in *The Globular Clusters-Galaxy Connection*, Ed. By H. Smith and J. Brodee, *ASP Conf. Ser.*, **48**, 38

CORRECTION OF THE SCALE OF ASTROPHYSICAL QUANTITIES

V.P. Merezhin

Tatarstan Academy of Science, N. Bauman Str. 20, Kazan 420503, Russia
e-mail: vpvega@ant.kcn.ru

ABSTRACT. To construct the correct scale of astrophysical quantities a simple procedure of determination of self-consistent and interdependent with each other mean values of basic characteristics for every spectral subclass is offered.

Key words: Stars: the scale of astrophysical quantities.

1. Introduction

It is not necessary to explain anybody how useful the scale of astrophysical quantities turns out to be in different astronomic investigations. But the following question is to the point: are the scales' data and the approach used to construct them reliable? As investigations show, there are grounds to raise such question. So, when comparing with each other the already existing scales of the same luminosity class, the following peculiarities are revealed:

1) distinctions in the mean values according the very spectral subclass of one scale turn out to be essential towards another one, and evidently exceed the errors of determination of basic characteristics themselves.

2) strange and illegitimate behavior of some values, derivatives (combinations) of basic characteristics, along spectral sequence from hot stars to cold ones.

3) absence of precise and single-valued connection between such values as mass of a star and its luminosity.

The list of only just these peculiarities gives us a reason to doubt in the reliability of data the existing scales have. That's why, to construct a correct scale it is necessary to study out the reasons that cause an uprise of these peculiarities, and to find the ways of their removal. Right this is the aim of the present article.

In this case we'll not touch the ways that determine basic characteristics of individual stars (they are well-known) and the approach of the scale construction as a whole (every investigator uses his

own methods with this purpose (see e.g. Allen, 1997; Strajzys and Kuriliene, 1981), but we'll consider only several details of this problem. In particular, we'll analyze the procedure of stars selection with the purpose of sample formation and the receipt with its help the mean values of basic characteristics for the given subclass. Under the sample we understand a collection of stars having the same MK-characteristics. Further, to shorten the notation we'll write "the mean values of basic characteristics" implying by this that these values refer to the given spectral subclass of the given luminosity class.

2. Heterogeneity of the sample. Near values of basic characteristics.

Let refer to the analysis of the first peculiarity. Usually, to construct the scale of astrophysical quantities of the given luminosity class, investigators concentrate their attention on the receipt of one or at least two mean values of some basic characteristics, attracting with this purpose such types of stars whose corresponding characteristic (or characteristics) is determined unhesitatingly. However, in practice everything is more complicated. For example, to construct the scale of effective temperatures, the stars with surely determined absolute power distributions in their spectra and angular diameters are usually attracted (see, e.g. Morton and Adams, 1968; Hayes, 1978). However, the number of such well-known stars is in fact not great, and it is often not enough to consider the obtained values as the reliable and typical for the given subclass. This remark remains reasonable also for the mean values of other basic characteristics. It is necessary to add that the selection of stars into the sample is not strict. Essentially, except MK-characteristics there are no any other criteria controlling such selection.

The pictures 1 and 2 taken from Merezhin (2001) will help us to judge either the obtained mean values of basic characteristics are typical for the given spectral subclass or not. As an example, here are presented histograms for effective tempera-

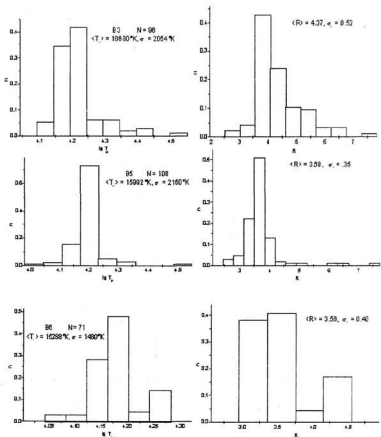


Figure 1: Distributions of T_e and R inside spectral subclass are shown. The luminosity class is V (see text).

ture T_e and radius R (picture 1), as well as mass M and absolute star magnitude M_v (picture 2) inside spectral subclass for stars of V luminosity class. To demonstrate this we confine ourselves by subclasses B3, B5 and B6. The total amount of stars (N) participated in the formation of mean values T_e , R , M and M_v is indicated at pictures for each sample. It is possible to find the algorithm of construction of such histograms in the quoted article, and we'll not recur to it here. When constructing these histograms, the only criteria according to which we reckoned the star in one or another spectral subclass was its MK-characteristics obtained directly by the observational data.

As it is shown on pictures 1 and 2, the spread in values of every from quantities T_e , R , M and M_v , inside of any from the presented subclasses, turns out to be a considerable one and noticeably exceeds the interval of $3\sigma_Q$ width that in fact determines the reliability of $\langle Q \rangle$'s mean value,

where Q is any of quantities under consideration, and σ_Q is an average square error of determination of $\langle Q \rangle$ value. If take into account the value of σ_Q determination error itself of Q characteristic, then the difference between its minimum and maximum values denominated in this measure turns out to be very large inside the given subclass. So, for subclass B3 the determination error σ_{T_e} of $\langle T_e \rangle$ value is equal to $\pm 2054 \text{ K}$, and determination error σ_M of $\langle M \rangle$ value is $\pm 1.27 M_\odot$. Then, as it shown on pictures 1 and 2 the difference between minimal and maximum values of T_e inside B3 subclass turns out to be equal to -18500 K ($-9\sigma_{T_e}$), and the difference between minimum and maximum values of mass $-12.7 M_\odot$ ($-10\sigma_M$).

It is clear that because of big variation of basic characteristics values and small amount of stars attracted to such determinations, it is rather problematically to consider the received value as a typical one for the given subclass. At least we can

advance two arguments supporting the justness of this remark. The last remark is equally related to any from characteristics considered here and to the effective temperature as well. Firstly, errors of determination of basic characteristics which are inevitably contained in every star, will influence on the mean value formation. Secondly, values of characteristics of the same stars received by different investigators are noticeably differ from each other, and this may tell on the mean formation. Such differences are conditioned by the usage of different methods of observation and determination of basic characteristics of individual stars, by dissimilarity of ways of attaching the observational data to different standards and calibrated dependencies, by the use of different standards and calibrated dependencies and methods of observational data processing. However we shouldn't think that the contribution of this component will be meaningful, and the differences between the characteristics values of the same stars received by different investigators will be dramatic. As investigations show, these differences do not usually fall outside the intervals equalled in the trebled value of determination error of characteristics themselves. This is conditioned by the following circumstance – in spite of the variety of methods of observation and determination of basic characteristics, methods of observational data processing and their attaching to standards and calibrated dependencies, all of them do not differ from each other in principle, and eventually lead to similar results. Nevertheless, when the number of stars in a sample is not big, this circumstance should be taken into account.

The appearance of variation of basic characteristics inside spectral subclass is the statement of a well-known fact that the stars having even equal MK-characteristics can differ from each other in their basic characteristics (Underhill, 1982). This variation as it follows from the data on pictures 1 and 2 turns out to be considerable, and it should be taken into account when constructing the scale of astrophysical quantities. In principle, except stars which are the typical representatives of the given spectral subclass, there in a sample can be presented episodic stars, such as: a) the very evolved objects; b) the durable variable stars which happened to be in the given subclass temporarily at some phase of the sparkle and evolution changing; c) the stars having though cognate MK-characteristics but yet slightly different from the standard ones; d) the objects having values of MK- and basic characteristics as if similar with the standard ones only through the influence of the perturbing factors on their pressure-temperature field structure (e.g., rotation and turbulence) and others. Investigations show that the analogous spread

in values of any from basic characteristics is detected in other not represented here spectral subclasses of V luminosity class, and in IV and III luminosity classes of stars as well.

It is clear that in order to correct the above-stated and to find the stable solution, the sample should contain if possible a big number of members that is computing in some tens. However, according to the objective and subjective reasons such approach fails to be realized in practice. That's why a big variety of stars types inside spectral subclass from one hand, and their small number participating in formation of the mean value, as well as highhandedness in their selection and the absence of strict selection criteria from the other hand, are the main sources of appearance of the peculiarity that was the first to be enumerated in the previous paragraph.

3. Quantities g_{dyn} and v_{cr} as the indicators of the reliability of determination of the mean values of basic characteristics. Mass-luminosity correlation

We can judge about the reliability of the obtained values with the help of derivatives of basic characteristics by studying their behavior according to changes in characteristics that form these derivatives. As the behavior of derivatives is known beforehand, its bare change will serve us as the evidence of the fact that the derivatives together with the mean values of basic characteristics are not correct. In other words, it is possible to choose such values that will serve as the indicators which allow to judge about the reliability of the data from the scale of astrophysical quantities.

As an example, let limit ourselves by studying the behavior of such derivatives as dynamic grav-

ity $g_{dyn} = \left(\frac{G \times M}{R^2} \right)$ and critical rotation velocity v_{cr} .

These are the functions of M and R characteristics, and therefore they give us a possibility to judge about the reliability of $\langle M \rangle$ and $\langle R \rangle$ values determination. If we are dealing with the single stars, then as it is known (see, e.g., Sinnerstad, 1980) their mass is estimated according to the evolutionary tracks. The effective temperature and the absolute star value (or its luminosity) are attracted with this purpose. Then due to g_{dyn} and v_{cr} quantities we can judge indirectly about the reliability of $\langle T_{eff} \rangle$ and $\langle M \rangle$ (or $\langle L \rangle$) values determination.

In order to get the formulae for estimating velocity v_{cr} , let use a well-known expression (Huang and Struve, 1963).

$$\frac{\Omega_{cr}^2}{2 \times \pi \times G \times \rho} = 0.36075 \quad (1)$$

If $\rho = \frac{M}{4\pi R_{cr}^3 \times 0.180373}$, $v_{cr} = \Omega_{cr} \times R_{cr}$ and $R_{cr} = \frac{3}{2} \times R_p$, then after small transformations we find the necessary formulae

$$v_{cr} = 2.10873 \times 10^{-4} \times \sqrt{\frac{M}{(1-\beta) \times R}}, \quad (2)$$

where Ω_{cr} denotes the critical rotation angular velocity; R_{cr} is the critical radius; ρ is the mean density; and G is the constant of gravitation.

When deducing the formulae (2) we used the correlation $R_p = R_0 \times (1 - \beta) \times \left(\frac{v}{v_{cr}}\right)^2$ taken from Maeder and Peytremann (1970) that ties together polar radius R_p of the rotating star with radius R_0 of the non-rotating star of the same mass. The constant β is equal to 0.030 if $M > 2M_\odot$, and is equal to 0.024 when $M < 2M_\odot$ and where M_\odot is mass of the Sun.

Table 1: The variation of g_{dyn} and v_{cr} quantities along the spectral sequence. The luminosity class V

Sp	Our scale		The scale of Strajzys and Kuriliene		Popper's scale		Renewed scale	
	g_{dyn}	v_{cr}	g_{dyn}	v_{cr}	g_{dyn}	v_{cr}	g_{dyn}	v_{cr}
O5-5.5	5660	554	8083	756	-	-	4509	518
O6-6.5	5702	525	7543	698	-	-	6698	549
O7-7.5	6596	537	7370	651	9942	617	6675	545
O8-8.5	6918	528	7545	615	10301	610	7196	538
O9.5	7738	557	9742	728	6903	509	7274	538
B0	8338	558	10413	720	6375	482	7592	523
B1	8452	489	10173	642	7714	490	8119	473
B2-2.5	8821	485	11680	620	8702	477	9280	470
B3	9996	483	11415	565	12220	463	10366	449
B4	10758	448	12262	480	10590	440	10679	434
B5	10882	463	13169	445	16079	468	10923	429
B6	10913	455	12232	420	13211	424	11135	425
B7	11313	410	11684	397	-	-	11921	421
B8	11289	408	11955	388	15457	409	12366	416
B9-9.5	10278	370	10656	362	11781	377	12938	396
A0	10621	361	11693	358	15334	391	14219	382
A1	10441	356	13107	366	10203	349	14357	378
A2	14127	374	14378	370	20794	393	14754	378
A3	14792	376	16502	379	13551	364	14938	377
A4-5	16428	376	17280	375	12793	358	15684	372
A7	17489	375	18950	375	37847	272	18107	378
F0	18328	371	19859	366	11822	329	15704	353
F2	20133	374	18534	354	11865	326	21262	376

Let consider now a well-known to us behavior of g_{dyn} and v_{cr} quantities along spectral sequence, viz.: gravity g_{dyn} must rise and velocity v_{cr} must decrease from hot stars to cold ones. The results of this analysis are shown in Table 1 within spectral range from O5 to F2 for the stars of V luminosity class according to the data of our scale, the scale of Strajzys and Kuriliene (1981) and the Popper's scale (1980) of masses and radiuses.

Everybody can get acquainted in details with the method of constructing the scale of Strajzys and Kuriliene in the work of reference. Popper's data were received on the ground of measuring M and R values of the components of close binary stars. As for our scale, we can mark the following. In order to construct this scale we attracted 152 stars with the reliable photometric and spectrophotometric data. The stars' values T_e , M , and B.C. were determined according to D -test (Merezhin and Shaimukhmetova, 1992) with the help of Kuruts' data (1979). The radiuses were measured under the formula (Allen, 1977)

$$\lg M = a_r M_{bol} + b_r \quad (3)$$

and masses were derived from the evolutionary tracks of Maeder and Megret (1978). The quantities T_e , R , M , M , and B.C. of every star were used then to obtain their mean values.

Taking into account a smooth course of changing of characteristics R and M along spectral sequence from hot stars to cold ones, we have a right to anticipate the analogous change of g_{dyn} and v_{cr} quantities along the same sequence. However, it is not so. As it follows from the data of Table 1 (see columns No. 2, 4 and 6) for gravity g_{dyn} , though generally it is detected a tendency to the increase in its value from hot stars to cold ones, nevertheless change of g_{dyn} value along spectral sequence evidently bears an irregular character. We see that change is not smooth, and in some sections of the sequence a change of gravity g_{dyn} turns out to be antithetic the general tendency. The same behavior is discovered at the velocity v_{cr} (see columns No. 3, 5 and 7). It is clear that such strange and illegitimate behavior of g_{dyn} and v_{cr} quantities is impossible to be explained by the action of some perturbing factors, it is evidently conditioned by the fact that we have incorrect knowing of $\langle R \rangle$ and $\langle M \rangle$ values in separate sections of spectral sequence. This fact is confirmed by the circumstance that the character of irregularity and its amplitude are not constant and are changed from one scale of astrophysical quantities to another. It is important to underline that irregularity is kept regardless of the method the quantities $\langle R \rangle$ and $\langle M \rangle$ were determined - either it was made together with the formula (3) by the use of evolutionary tracks or with the help of close binary stars. As investigations show such peculiarity of behavior of g_{dyn} and v_{cr} quantities is observed in all scales of V, IV and III luminosity classes without exception. Let us nominally call this behavior of derivative quantities as the internal inconsistency of astrophysical quantities. Right this inconsistency conditions the second peculiarity.

In the light of the above-stated the third peculiarity finds its own explanation. It is completely connected with mass-luminosity correlation and

allows to judge about the reliability of $\langle M \rangle$ and $\langle L \rangle$ values determination. As investigations show (see, e.g. Schwarzschild, 1961) there are strong reasons confirming the existence of connection between the star's mass and its luminosity. Usually this dependence is presented as a linear correlation (Aller, 1955)

$$\lg M = a_1 \times \lg L + b_1 \quad (4)$$

or (Schwarzschild, 1961; Aller, 1955)

$$\lg M = a_2 \times M_{bol} + b_2 \quad (5)$$

where a_i and b_i ($i = 1, 2$) are the coefficients subjected to determination. Here quantities M and L are expressed in the sun measures.

As investigations show such form of dependence between quantities M and L (or M and M_{bol}) is kept up to the III luminosity class, and only a_i and b_i values undergo changes from one luminosity class to another. Not going into details of the problem as a whole, let consider only such part of the problem that refers to a_i and b_i values determination. As it is well known (see, e.g., Demircan and Kanraman, 1991) the quantities $\langle M \rangle$ and $\langle L \rangle$ take part in their determination.

Table 2: The values of a_i and b_i coefficients according to the literature and our data

№	a_i	b_i	References
1	0.298	+0.030	Deich (1962)
2	0.262	+0.056	Russell and Moor (1940)
3	0.255	-0.013	Parenago and Masevich (1951)
4	0.260	-0.022	Our scale
5	0.270	-0.019	Demircan and Kanraman (1991)
6	0.255	-0.002	Demircan and Kanraman (1991)
7	0.320	-0.013	Eggen (1956)
8	0.300	-0.145	Svechnikov (1969)
9	0.258	+0.021	McCluskey and Kondo (1972)
10	0.263	+0.011	Heintz (1973)
11	0.358	-0.220	Kopal (1978)
12	0.272	-0.046	Cester et al. (1983)
13	0.240	-0.001	Griffins et al. (1988)

Let refer to the data of table 2, where a_i and b_i values are cited for the stars with measurable mass values, and where are indicated the references to the works from which these data were taken. As the literature data show, the errors of a_i and b_i coefficients determination are on the average equal to ± 0.010 and ± 0.012 , respectively. To demonstrate graphically the spread in a_i and b_i values received by different investigators, let use the scale where the units of measurement are σ_a and σ_b themselves. The measurements received by different investigators, e.g. a_i value, in such scale noticeably differ from each other, and the spread in their values goes within the interval of $\approx 12\sigma_a$ width. Much bigger differences are detected when estimating b_i coefficient. In this case the spread in

its values goes within the interval of $\approx 23\sigma_b$ width. The cited values of the intervals' width evidently exceed the admissible limits of the intervals correspondingly equal to $3\sigma_a$ and $3\sigma_b$, that in fact determine the reliability of the found a_i and b_i values. Here: σ_a and σ_b are the errors of determination of a_i and b_i values, respectively.

So we can state that a_i and b_i values received by different investigators differ noticeably from each other. Besides, b_i value in some cases is positive, and in others is negative. This allows to make a conclusion about the instability of the received solutions and about the unreliability of determination of $\langle M \rangle$ and $\langle L \rangle$ values, as well as about the absence of clear connection between M and L quantities.

4. Correction of the scale of astrophysical quantities

As it follows from the above-stated, a traditional approach used to construct the scale of astrophysical quantities requires to be corrected. To fulfill this correction let refer to pictures 1 and 2. These pictures suggest us one of the possible variants of its realization. We suppose that the correction should be made in two steps. The first one concerns the sample as a whole itself. We just add that it is not necessary to impose any rigid restrictions on its formation. For the sample to be a respectable one, a selection of members must be rather mild, and any stars having even peculiarities in their spectra can be present there. (Here the similarity of MK-characteristics of the sample members have still a great importance. In this case such factor as subjectivity in stars selection is excluded). But the stars with a very quick change of shine can be the exception.

To analyze the sample at the second step, we can offer the following algorithm. Let us have the sample, for each member of which there are known its basic characteristics. Then, for each characteristic Q from the total set of Q quantities we choose its maximum and minimum values and determine a width of the interval inside which all existing Q values of the sample under investigation must be located. Thereafter, this interval is divided to equal sections and we construct a histogram in the same way as it was made in the second paragraph of the present article. The length of a section is determined a priori with consideration of all members in the sample and the correctness of determination of Q characteristic under investigation. For example, we can take quantity σ_Q as a length of such section. These histograms will not differ in their form from those shown on pictures 1 and 2. That is why we return to these pictures again. We see that a certain similarity of distributions' forms of characteristics presented here is noticeably detected. Each distribution has the maximum.

Namely, the major and considerable part of stars from their whole collection of the given sample is centralized at a comparatively narrow section of each histogram. It is clear that the stars having close to each other values of Q characteristics are grouped near the maximum of distribution. On this basis we consider that:

(a) stars grouping near the maximums of distributions for different basic characteristics can be referred to the typical representatives of the given spectral subclass;

(b) stars distant far from the maximum in the same distributions are rather not typical; and according to different reasons they accidentally happened to be in the sample under investigation.

As an example, let analyze the sample of spectral subclass B3. If we refer to the distribution according to the effective temperature, then we may consider the stars having T_e values inside 14125 K < T_e < 17783 K interval to be typical for this subclass. While the stars whose temperatures must have either T_e < 14125 K or T_e > 17783 K values should be referred to (b) group. The analysis of distribution according to radius leads us to the conclusion that the stars found inside the $3.6R_{\odot}$ < R < $4.6R_{\odot}$ interval should be reckoned in (a) group, and the objects having R , R < $3.6R_{\odot}$ or R > $4.6R_{\odot}$ values should be referred to (b) group. For distributions according to mass and absolute star value, the stars with M and M_v values existing inside intervals $5.0M_{\odot}$ < M < $7.0M_{\odot}$ and $-1^m.00$ < M_v < $-1^m.80$ should be referred to (a) group, and the stars whose M and M_v values turns out to be either M < $5.0M_{\odot}$ or M > $7.0M_{\odot}$, as well as either M_v < $-1^m.00$ or M_v > $-1^m.80$ are referred to (b) group. It is not difficult to make the analogous analysis for the stars of B5 and B6 spectral subclasses.

Naturally, to find the mean values of any from basic characteristics it is better to use the stars which can be considered typical for the given spectral subclass with more certainty. It follows from the above-stated that more suitable to this aim are the stars grouping near the maximums of distributions. Then, as one of the selection criteria it is possible to use a narrow section near the maximum of distribution of Q characteristic which allows to separate typical stars from accidental ones in the sample under investigation. To obtain the mean values of basic characteristics, there should be used only the stars of (a) group, and the stars of (b) group can not be taken into consideration and can be excluded from the further analysis. We expect that in this case the objects grouping at a comparatively narrow but rather noticeable section of distribution admit us to get constant solutions with small errors. Length of a section can be changed at the investigator's will. It is clear that such criterion is impossible to be considered as a

strictly well-founded one. That's why, in order to be sure in the correctness of partition of stars of the sample to (a) and (b) groups, it is preferably to use at one time several distributions for different basic characteristics. In perfect case we expect that the same stars will be grouping in each of such distributions near the maximum.

The last remark requires an additional explanation. As practice shows, the appearance of the same stars near the maximum of distribution for each from T_e , R , M and M_v quantities for B3, B5 and B6 subclasses is really observed in most cases. However, sometimes it is detected that in the same distribution the objects according to one of these quantities turns out to be near the maximum, and according to the other ones – not at all. In the last case basic characteristics of these objects are either wrong determined or they are just not typical representatives for the given subclass. That's why, to correct the indefiniteness they can be attributed to (b) group and excluded from the further analysis. Namely, we have a possibility to enforce the control for the sample members selection.

The reliability of determination of the mean values of basic characteristics after the use of every from the specified steps must be executed by indicators. By way of control it is suggested here to use even such indicators as dynamic gravity and critical rotation velocity. Right smooth increase and decrease of g_{dyn} and v_{cr} quantities along spectral sequence from hot stars to cold ones without any irregularities, will indicate us that the obtained mean values of characteristics are correct. However, such selection of indicators is not obligatory. In principle, it is possible with this purpose to attract other indicators derived from basic characteristics having a well-known behavior along spectral sequence, or very attractive peculiarities according to which it would be also possible to judge about the reliability of the obtained results. All this will strengthen the reliance in the data of astrophysical quantities scale.

It is clear that if investigator takes into consideration all stars of the sample, the mean value of any basic characteristic found by him, must differ from the analogous mean value of the same characteristic obtained by the correction procedure. The mean derived by traditional approach will be dislocated to the right or to the left from the mean determined by the correction procedure. The extent of dislocation (according to the module) is determined as a difference between the mean values obtained by two approaches. It depends upon a width of the interval inside which the whole set of values of basic characteristic Q (which we have in our disposition) is located. The direction of dislocation will depend on what kind of "tail" from the maximum of distribution, from the right or left sides, is more extended.

Table 3: In good repair scale of astrophysical quantities for the luminosity classes V + IV

Sp	N(n)	$\langle T_e \rangle$	$\langle T_s \rangle$	$\langle R \rangle$	$\langle R' \rangle$	$\langle M \rangle$	$\langle M' \rangle$	$\langle \lg L \rangle$	$\langle \lg L' \rangle$	$\langle M_s \rangle$	$\langle M_s' \rangle$
O5	8(3)	41155	39505	11.36	12.43	26.67	25.44	5.52	5.53	-5.64	-5.58
O6	15(5)	37049	37464	10.10	9.40	21.24	21.61	5.24	5.20	-5.32	-5.38
O7	10(3)	36117	37450	9.14	9.30	20.12	21.08	5.11	5.19	-5.15	-5.36
O8	18(7)	32903	34720	8.43	8.40	17.95	18.54	4.88	4.97	-4.59	-4.90
O9	20(7)	32380	30900	8.60	8.32	17.58	18.38	4.83	4.76	-4.48	-4.22
B0	32(9)	29234	29669	7.87	7.54	15.71	15.76	4.61	4.60	-3.98	-4.02
B1	59(15)	24968	24627	6.58	5.77	11.44	9.87	4.18	4.04	-3.30	-3.19
B2	31(9)	21459	23170	5.48	5.43	8.90	9.44	3.76	3.88	-2.47	-2.90
B2.5	29(8)	19782	18625	4.66	4.58	7.56	7.50	3.48	3.36	-2.09	-1.84
B3	96(42)	18680	18297	4.37	4.07	6.97	6.27	3.32	3.22	-1.68	-1.77
B4	38(14)	16650	16430	3.90	3.69	5.78	5.31	3.02	2.94	-1.38	-1.22
B5	108(54)	15992	15598	3.69	3.53	5.41	4.97	2.90	2.82	-0.98	-1.09
B6	71(30)	15288	14508	3.56	3.40	5.05	4.70	2.80	2.66	-0.80	-0.78
B7	42(12)	13618	13156	3.33	3.11	4.29	4.21	2.54	2.42	-0.57	-0.50
B8	46(14)	12566	12798	2.94	2.92	3.64	3.85	2.29	2.31	-0.38	-0.44
B9	49(15)	11078	10703	2.70	2.52	3.07	2.90	2.00	1.88	0.06	0.16
B9.5	25(9)	10294	9986	2.45	2.29	2.71	2.56	1.78	1.67	0.34	0.45
A0	23(9)	9840	9620	2.32	2.15	2.59	2.40	1.66	1.55	0.52	0.64
A1	15(5)	9454	9423	2.29	2.09	2.39	2.39	1.58	1.49	0.80	0.79
A2	16(7)	9112	9176	2.22	2.03	2.29	2.03	1.49	1.42	1.07	1.09
A3	13(5)	8796	8971	2.07	1.99	2.15	2.16	1.36	1.36	1.29	1.20
A4-5	9(4)	8446	8545	1.82	1.85	1.97	1.96	1.18	1.22	1.68	1.52
A7	8(3)	8007	7878	1.75	1.65	1.81	1.80	1.06	0.98	1.92	2.03
F0	6(2)	7320	7165	1.58	1.66	1.57	1.58	0.81	0.82	2.30	2.46
F2	4(3)	6674	6552	1.57	1.39	1.39	1.39	0.64	0.51	3.34	3.46

In principle, b_1 and b_2 coefficients in the formulae (4) and (5) must be absent in order not to break the equality when $M=1$ and $L=1$. Otherwise, the disruption of mass-luminosity correlation takes place. If the coefficient is really $b_i \neq 0$, then as it is not difficult to make sure, the Sun turns out to be 10^6 times brighter than it should be judging by its mass. In other words, the mean star of V luminosity class that has a mass equal to that of the Sun, will be weaker than the Sun for 2^{m-5-b_i} stars quantities, as well as will have rather less dimensions and more density than the Sun has (Russell and Moore, 1940). That's why it would be interesting to ascertain the situation with coefficients b_1 and b_2 and their physical sense. However, we are not succeed yet in finding any concrete recommendations to solve this problem in the frames of the suggested correction procedure. Nevertheless, we hope that the solution of the problem will be found in case the exactness of $\langle M \rangle$ and $\langle L \rangle$ values determination will increase.

Of course, from the formal point of view the offered approach is impossible to be considered as a perfect one. But it can be quite acceptable in practice. Having even the unrepresentative sample of stars which the investigator succeeded to attract with the purpose of constructing the scale of astrophysical quantities, the correction procedure, as it seems to us, is still necessary to be held. Otherwise, it will be difficult in future to depend upon the obtainment of the reliable and steady results.

In principle, we can assure in reliability and steadiness of the results which are obtained by the correction procedure, in the following way: It is necessary to take other stars that did not participate in the construction of astrophysical quantities scale, and to construct a new scale with them according to the methodic described above. Eventually we should come to the results identical to those obtained earlier by the other set of stars. Our assurance is grounded on a quite obvious position that we should always obtain equal mean values of basic characteristics regardless of the set of stars we use. That is quite understandable as the selfsame set of mean values of basic characteristics should always answer the objects having equal MK-characteristics in the frames of the given luminosity class and the given subclass.

5. Results

To demonstrate the correction procedure let refer to the stars of V and IV luminosity classes. We'll limit ourselves by constructing a scale in the spectral range from O5 to F2. Let unite the stars of these luminosity classes for the sample to be representative. The results of these investigations are presented in Table 3 where there are the data obtained by traditional (in columns No. 3, 5, 7, 9 and 11) and other methods offered by us (in columns No. 4, 6, 8, 10 and 12). In the last case when constructing the histograms it was used one of the

criteria of dividing the members of a sample to (a) and (b) groups, viz. we choose the section near the maximum of distribution which extension for each from T_e , lgL , R , M and M_v characteristics changed according to the number of N members of the sample and according to the exactness of their determination. It is natural that under such division a number of stars n participated in formation of the mean value, turns out to be visibly less than number N . In column No. 2 of table 3 a number of members of each sample found in group (a) is indicated in round brackets. As investigations show, the higher is the exactness of basic characteristic determination in practice and the more stars are in the sample, the narrower can be chosen the section near the maximum to find the mean value. We will nominally call the scale of astrophysical quantities received by the use of the correction procedure – the renewed scale.

The way of obtaining basic characteristics of stars that were used to construct the scale of astrophysical quantities, was traditional (Merezhin, 1994 a, b). Namely, the magnitude V , the color indicators U-B and B-V of the UVB system, the excess of color E (B-V) and the angular diameter D were in the first place collected for each member of the sample according to the published data. All these data are necessary for us to derive an absolute energy distribution in the spectrum of the used star. The quantities V , U-B and B-V were mainly taken from Mermilliod and Nicolet (1977). A standard energy distribution in the spectrum of a star with MK-characteristics A0V and $V=0$ were obtained according to data of Vega's absolute calibration performed by Arkharov (1989). Then, using D -test (Merezhin and Shaimukhametov, 1992) there were received the self-consistent and interdependent with each other T_e , M_v and B.C. values that form a reliable base to find other basic characteristics of a star. In cases when the data for D -test usage were not enough, we used the traditional ways of determination of the quantities we are interested in. As a result, a homogeneous set of data was received, because all basic characteristics of stars were found by the same means and according to the single methodic.

Let now refer to the analysis of the data of table 3. As it follows from these data, the correction procedure of the scale doesn't bring any essential changes into the scale of astrophysical quantities, although the mean values of basic characteristics of the renewed scale differ slightly from the analogous values obtained in the frames of the traditional approach. So, $\langle T_e \rangle$ value obtained by the use of all stars of the sample ($N=108$) turns out to make 15992K for spectral subclass B5, while $\langle T_e \rangle$ value with the use of stars of only (a) group ($n=54$) makes 15598K. For the same subclass the quantities

$\langle R \rangle$ and $\langle R' \rangle$ are equal to $3.69R_\odot$ and $3.53R_\odot$, and $\langle M \rangle$ and $\langle M' \rangle$ quantities are equal to $5.05M_\odot$ and $4.97M_\odot$, respectively. For the absolute star value its mean values $\langle M_v \rangle$ and $\langle M_v' \rangle$ are equal to $-0^m.98$ and $-1^m.09$, respectively. We see that the differences in the mean values of basic characteristics received by two different ways are really insignificant and their values are within the errors of determination of these mean values. So, the values of differences $\langle T_e \rangle - \langle T_e' \rangle$, $\langle R \rangle - \langle R' \rangle$, $\langle M \rangle - \langle M' \rangle$ and $\langle M_v \rangle - \langle M_v' \rangle$ are equal to 394°K , $0.16R_\odot$, $0.08M_\odot$ and $+0^m.11$, respectively. Comparing these values of differences with those σ_T , σ_R , σ_M and σ_{M_v} values cited for that subclass on pictures 1 and 2, we assure in the validity of our remark.

It should seem that such small distinctions in the mean values obtained by two different ways do not deserve a special attention. However, if we analyze the behavior of g_{dyn} and v_{er} quantities along spectral sequence from hot stars to cold ones in the renewed scale of astrophysical quantities, then the advantage of the offered approach is easily traced. Let refer to the data of Table 1 where the quantities g_{dyn} and v_{er} obtained by the renewed scale are presented in columns No. 8 and 9. We see that in spectral range from O5-5.5 to A7 the behavior of the gravity g_{dyn} along spectral sequence from hot stars to cold ones turns out to be habitual. A deviation from such behavior is revealed only near F0 subclass. The change of the velocity v_{er} along the same sequence is habitual in spectral range from O6-6.5 to A4-5. Interruptions in the behavior of the last is observed at very hot (subclass O5-5.5) and cold (subclasses A7, F0 and F2) stars. It's to the point to underline that the normal behavior of g_{dyn} and v_{er} quantities at a big expansion along spectral sequence from hot stars to cold ones which we observe, results automatically from the data of the renewed scale.

The following two arguments give us an occasion to assert that the mean values found by the correction procedure are still more correct as compared with those values of the same means determined by traditional method. Let consider the first one. We see that errors of determination of the mean values $\langle T_e \rangle$, $\langle M \rangle$, $\langle R \rangle$ and $\langle lgL \rangle$ are much less than errors of determination of the mean values $\langle T_e' \rangle$, $\langle M' \rangle$, $\langle R' \rangle$ and $\langle lgL' \rangle$. So for B1 subclass we received: root-mean-square errors σ_T , σ_M , σ_R and σ_L in determination of $\langle T_e \rangle$, $\langle M \rangle$, $\langle R \rangle$ and $\langle lgL \rangle$ values turn out to be equal to $\pm 2595\text{K}$, $\pm 2.04M_\odot$, $\pm 1.22R_\odot$ and ± 0.30 , while root-mean-square errors σ_T' , σ_M' , σ_R' and σ_L' in determination of $\langle T_e' \rangle$, $\langle M' \rangle$, $\langle R' \rangle$ and $\langle lgL' \rangle$ are equal to $\pm 325\text{K}$, $\pm 0.65M_\odot$, $\pm 0.10R_\odot$ and ± 0.06 , respectively. For B9 subclass we found that: $\sigma_T = \pm 650\text{K}$, $\sigma_M = \pm 0.32M_\odot$, $\sigma_R = \pm 0.35R_\odot$ and $\sigma_L = \pm 0.17$ for quantities $\langle T_e \rangle$, $\langle M \rangle$, $\langle R \rangle$ and $\langle lgL \rangle$; and $\sigma_T' = \pm 160\text{K}$, $\sigma_M' = \pm 0.15M_\odot$, $\sigma_R' = \pm 0.06R_\odot$ and $\sigma_L' = \pm 0.03$

for quantities $\langle T_*^* \rangle$, $\langle M^* \rangle$, $\langle R^* \rangle$ and $\langle \lg L^* \rangle$, respectively. That is, in both subclasses under consideration the values of errors of determination σ_T , σ_M , σ_R and σ_L turn out to be much more than the values of errors of determination σ_T^* , σ_M^* , σ_R^* and σ_L^* . The second argument is a habitual behavior of dynamic gravity and critical rotation velocity along spectral sequence from hot stars to cold ones inside the renewed scale of astrophysical quantities.

As investigations show, when the sample is thin, it is practically impossible to use the correction procedure. In this case the maximum is faintly observed, and this fact complicates the selection of stars to (a) group. As a result we get the uncertain mean values. Therefore, the only one device required to obtain the reliable mean values of any from basic characteristics is to increase a number of stars in every sample. In our case this remark concerns O5-5.5, A7, F0 and F2 subclasses. Practice shows that when the sample includes 25-30 members, the procedure of selection leads already to the correct results.

Using the data from columns No. 7 and 9 of Table 3, by filling them with polynomial of the first order, we find that the values of a_1 and b_1 are equal to 0.2612 (± 0.001) and -0.0260 (± 0.003), but using data of columns 8 and 9 we get that $a_1 = 0.2593$ (± 0.005) and $b_1 = -0.0160$ (± 0.013). We see that the distinctions in values of a_1 and b_1 coefficients of the renewed and not renewed scales are not essential. Then, in order to establish the reasons of the coefficient b_1 's appearance in the relation (4), let fulfill the following simple calculations. Let refer to the data of columns No. 8 and 10 of Table 3 and consider the following two examples. Let $\langle \lg L^* \rangle$ values to be higher and $\langle M^* \rangle$ values to be lower than the true values of $\langle \lg L^* \rangle$ and of $\langle M^* \rangle$, respectively (example No. 1). According to the second example, we suppose that $\langle \lg L^* \rangle$ values are lower, and $\langle M^* \rangle$ values are higher the true values of $\langle \lg L^* \rangle$ and $\langle M^* \rangle$, respectively. Then, if $\langle \lg L^* \rangle$ and $\langle M^* \rangle$ values presented in Table 3 differ from the true ones $\langle \lg L^* \rangle$ and $\langle M^* \rangle$ for 10% only, we get $a_1 = 0.2603$ and $b_1 = -0.0734$ and $a_1 = 0.2592$ and $b_1 = 0.0387$ for the first and second examples, respectively. We see that the values of a_1 coefficient remain in both cases invariable, while the values of coefficient b_1 noticeably differ from each other. So, it even changes the sign when transferring from one example to another.

Further, if $\langle \lg L^* \rangle$ and $\langle M^* \rangle$ values presented in Table 3 differ from the true ones $\langle \lg L^* \rangle$ and $\langle M^* \rangle$ for 5% only, we find that $a_1 = 0.2594$ and $b_1 = -0.0445$ and $a_1 = 0.2592$ and $b_1 = 0.0102$ for the first and second examples, respectively. We see that in this case the situation with a_1 and b_1 coefficients doesn't differ notably from the previous one. But it suffers from evident changes if $\langle \lg L^* \rangle$ and $\langle M^* \rangle$ values presented in Table 3 differ from the true

ones $\langle \lg L^* \rangle$ and $\langle M^* \rangle$, e.g. for 1-2% only. In the last case we have $a_1 = 0.2593$ and $b_1 = -0.0302$ and $a_1 = 0.2593$ and $b_1 = -0.0034$ for the first and second variants, respectively. We also see that in both examples the quantity b_1 remains negative.

These examples allow to make the following conclusion. In principle, if deviations of quantities $\langle \lg L^* \rangle$ and $\langle M^* \rangle$ from the true values $\langle \lg L^* \rangle$ and $\langle M^* \rangle$ are not great, then it is not difficult to obtain the elimination of b_1 coefficient in the relation (4) by variation of values of these quantities. However, as it seems to us, the following argument binds us with the necessity of the obligatory presence of the last in mass-luminosity correlation. As calculations show, the quantity a_1 remains practically invariable even under considerable deviations of the mean values $\langle \lg L^* \rangle$ and $\langle M^* \rangle$ from their true values, while b_1 quantity suffers from essential changes even under small deviations in the mean values under consideration. Then the appearance of coefficient b_1 in the relation (4) is conditioned by not only incorrect knowing of $\langle \lg L^* \rangle$ and $\langle M^* \rangle$ values, but also by the presence of different perturbation effects inside the stars. Right their presence brings to the disruption of mass-luminosity correlation and leads to the necessity of introducing the mean star of the given luminosity class. For example, the rotation effect can play the role of one of them. It is known (see, e.g., Sackman and Anand, 1970) that the presence of the angular moment the star has, brings to the deceleration of the nuclear reactions rate and the lowering of its luminosity as compared with non-rotating star of the same mass. It is clear that we should expect even though a weak disruption of mass-luminosity correlation. To confirm this, we can present the fact already established by the observations. So, as investigations show (see, e.g., Krat, 1962), mass-luminosity correlation is not implemented by the secondary components of close binary systems. It is stipulated by the non-standard evolution of stars entering a pair.

6. Conclusion

The offered correction procedure of the scale of astrophysical quantities is not burdensome to our mind. It doesn't change the approach to the scale's construction as a whole, but improve the exactness of finding the mean values of basic characteristics. It is realized by attraction of a big number of stars with the already known values of basic characteristics and their thorough selection. To check the reliability of the obtained mean values it is offered to attract the indicators with their already known behavior. Right the correctness of their behavior in the frames of the constructed scale of astrophysical quantities allows to judge about the reliability of the results.

References

- Allen, C.W.: 1977, *Astrophysical Quantities*. Mir Publishers, Moscow, 280
- Aller, L.X.: 1955, *Astrophysica, v. I, Foreign Literature Publishers*, Moscow, 22
- Cester, B., Ferluca, S., Boehm, C.: 1983, *Ap. Sp. Sci.* **96**, 125
- Deich, A.N.: 1962, in: A.A. Mikhilov (ed.), *The Course of Astrophysics and Astronomy*, Physt-Math. Publishers, Leningrad-Moscow, Vol. II, 53
- Demircan, O., Kanraman, G.: 1991, *Ap. Sp. Sci.* **181**, 313
- Griffiths, S. C., Hicks, R. B., Milone, E. F.: 1988, *J. R. As. Soc. Can.* **82**, 1
- Hayes, D. S.: 1978, in: *The Absolute Calibration of the HR Diagram: Fundamental Effective Temperatures and Bolometric Corrections*. The HR Diagram IAU № 80, 65
- Heintz, W. D.: 1973, in: *Double Stars*. Reidel Dordrecht, Holland
- Huang, Su-Su and Struve, O.: 1963, in *Stellar Atmospheres*, J.L. Greenstein (ed.), *Stellar Rotation and Atmospheric Turbulence in Stellar Atmospheres*, Foreign Literature Publishers, Moscow, p.323
- Eggen, O.: 1956, *A. J.* **60**, 401
- Kopal, Z.: 1978, *Dynamics of Close Binary Systems*. Dordrecht: Reidel D.
- Krat, V.A.: 1962, in: A.A. Mikhilov (ed.), *The Course of Astrophysics and Astronomy*, Physt-Math. Publishers, Leningrad-Moscow, Vol. II, 96
- Kurucz, R.L.: 1979, *Ap. J. Suppl.* **40**, 1
- McCluskey, G. E. Jr., Kondo Y. 1972, *Ap. Sp. Sci.* **17**, 134
- Maeder, A., Megnet, G.: 1988, *Publ. De l'Observatoire de Geneva, Series C., Pre-publications, Fascicule*, **30**, 1
- Maeder, A., Peytremann, E.: 1970, *As. Ap.* **5**, 120
- Merezhin, V.P.: 1994a, *Ap. Sp. Sci.* **215**, 83
- Merezhin, V.P.: 1994b, *Ap. Sp. Sci.* **218**, 223
- Merezhin, V. P.: 2000, *Ap. Sp. Sci.* **275**, 217
- Merezhin, V.P., Shaimukhametov, R.R.: 1992, *Kinem. Phys. Selestial Bodies* **8** № 6, 54
- Mermilliod, J.C., Nicolet, B.: 1977, *As. Ap. Suppl.* **29**, 259
- Morton, D.C., Adams, T.F.: 1968, *Ap. J.* **151**, 611
- Parenago, P.P., Masevich, A.G.: 1951, *Tr. Gos. Astron. Institut P.K.Schternberg* **20**, 1
- Popper, D. M. : 1980, *Ann. Rev. As. Ap.* **18**, 115
- Russell, H. N., Moor, Ch. E.: 1940, *The Masses of the Stars*. Chicago
- Sackman, I.-J., Anand, P.S.P.: 1970, *As. Sp. Sci.* **8**, 76
- Sinnerstad, U.: 1980, *As. Ap. Suppl.* **40**, 395
- Schwarzschild, M.: 1961, *Structure and Evolution of Stars*, Foreign Literature Publishers, Moscow, 242
- Svechnikov, M.A.: 1969, *Catalogue of Orbital Elements, Masses and Luminosities of Close Double Stars*, Publishers of Sverdlovsk State Univ., Sverdlovsk
- Straj is, V., Kuriliene, G.: 1981, *Ap. Sp. Sci.* **80**, 353
- Underhill, A. : 1982, in: *B Stars with and without Emission Lines / Ed. Underhill A.* Monograph series on Nonthermal Phenomena in Stellar Atmospheres. Washington. NASA.

ELEMENT ABUNDANCES IN STARS: CONNECTION WITH CHEMICAL EVOLUTION OF A GALAXY

T.V. Mishenina

Astronomical Observatory, Odessa National University,
Shevchenko Park, Odessa, 65014, Ukraine

ABSTRACT. Abundances of 17 elements in the atmospheres of 100 stars belonging to different population of the Galaxy were determined. The comparing of the obtained results with the predictions of current chemical evolution models was made.

1. Introduction

The introduction of efficient high-resolution spectrographs on modern telescopes and the development of theoretical interpretation of spectra allow to define very accurately the chemical composition of stars and to test the theories of nucleosynthesis and chemical galactic evolution.

One of the important questions of modern astrophysics is the investigation of enrichment of the chemical elements and then the construction of an adequate model of the chemical and dynamic evolution of the Galaxy. The individual elements are produced at various events and on different timescales, and the observed abundances may be used to decode the galactic evolution. However, the chemical enrichment is realised by the return of new elements into the interstellar medium (ISM) through slow and fast mass loss phenomena, whose relative importance is controlled by several parameters, like the initial stellar mass distribution, the physics of stellar winds, star formation rates, stellar lifetimes, the metal dependency of the nucleosynthesis, the galactic gas flows, the mixing processes in the ISM etc. As we cannot get this information directly from observations, it is necessary to use models of galactic evolution taking into account all these processes in detail.

The goal of this work is the determination and the analysis of several element abundances in atmospheres of the stars belonging to various subsystems of the Galaxy and the choice of sources of the contributions in the element abundances by the comparison of the observations with the predictions of some galactic models.

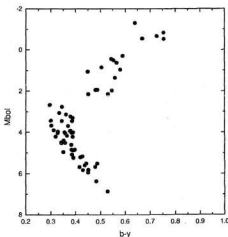


Figure1: The diagram of M_{bol} vs $b-y$ for program stars

2. Observations

For the decision of the task we selected 100 stars (dwarfs, giants and subgiants) in a range of metallicity $-3 < [Fe/H] < 0.3$ (Fig. 1). The observations were taken from the library of spectra were collected at the Haute Provence Observatory (Soubiran et al., 1998). They had been made with the 193 cm telescope equipped ELODIE spectrometer ($R = 42\,000$), the spectral range is 4400-6800 Å, signal-to-noise ratios are more 100. Spectra were previously reduced (Kats et al., 1998), the further processing of spectra (continuum level location, measuring of equivalent widths etc) was carried out by us using the DECH20 software (Galazutdinov, 1992). Equivalent widths EWs of lines were measured by means of a Gaussian fitting.

We have compared our EWs with those defined by other authors (Mishenina, Kovtyukh, 2001; Mishenina et al., 2002a, b). The agreement is sufficiently good.

3. Stellar parameters

The basic characteristics of investigated stars are given in the papers (Mishenina, Kovtyukh, 2000; Mishenina, et al., 2002a, b). The spectral classes Sp, stellar magnitude V and colour index (B-V) are taken from a database SIMBAD, parallax – from the observation of Hipparcos (ESA 1997). Bolometric magnitudes M_{bol} are calculated with use bolometric corrections from the paper of Alonso et al. (1995). Use of direct methods of definition of effective temperature T_{eff} is possible only for the limited number of stars. The used photometric and spectral methods are burdened by some additional errors. The photometric methods base on theoretical or empirical spectral calibrations and require the account of the interstellar reddening. The spectral methods require the reliable damping constant and account of probable influence of the departures from the local thermodynamic equilibrium (NLTE) require the account interstellar reddening, spectral. Therefore for T_{eff} determination we used the following iterative procedure. As the first approach, we adopted T_{eff} determinations given in the paper of Soubiran et al. (1998), they are based on a statistical method using the large number of lines in a spectrum and calibration of effective temperature T_{eff} , taken from the reference sources with certain weight. Then T_{eff} was specified on conditions that the iron abundance determined on any line is independent on its low level energy E_{low} . As the control of a choice T_{eff} we carried out the comparison of the observational profile of the H α lines with the theoretical calculations of the H α lines under the program STARS (Tsymbal, 1996).

The surface gravity $\log g$ was determined on the assumption of the ionisation balance for iron lines and then it was specified under the standard formula:

$$\log g = 4 \log T_{eff} + 0.4 M_{bol} + \log(M/M_{star}) - 12.5,$$

where the following parameters for the Sun $T_{eff} = 5770$ K and $\log g = 4.40$ are accepted.

Microturbulent velocity V_t was determined on conditions that the iron abundance determined with Fe I lines is independent on its equivalent widths EWs. As a metallicity of star [Fe/H] the iron abundance determined with the oscillator strengths from Gurtovenko, Kostyk (1989) on the program of Kurucz WIDTH9 is accepted.

The accuracy of definition of parameters is equal: $\Delta T_{eff} = \pm 100$ K, $\Delta \log g = \pm 0.3$ dex, $\Delta V_t = \pm 0.2$ km/s, $\Delta [Fe/H] = \pm 0.1$ dex. The parameters of atmospheres of studied stars are given in Tab. 1. The comparing of our studies with results of some recent works was made in paper (Mishenina, Kovtyukh, 2001; Mishenina, et al., 2002a,b). The agreement between parameters of atmospheres determined by other and

us authors is within the limits of determination errors. The available divergences are caused, first of all, by the various methods of parameter definitions that were used by the authors.

In order to distinguish disk stars (D) from halo stars (H) by kinematic criteria, we determined the spatial velocities and galactic orbital parameters of our target stars. The first group of stars (D) includes objects with disk-like kinematic, (nearly-circular orbits, not reaching extreme distances from the plane and with a significant component of rotational velocity. Thick-disk stars dominate this group. The second group (H) includes all stars whose orbits reach larger distances from the galactic plane; they have larger values of eccentricities or retrograde rotational velocities. All other stars fall into an intermediate group (I) corresponding to the overlap between the thick disk and the halo (Mishenina, et al., 2002a).

Lithium. The change of any element abundance with age or with distance in the Galaxy represents undoubted interest for the theories of chemical evolution of the Galaxy and nucleosynthesis. But the lithium occupies the special place, both by amount of papers on Li abundance determination, and on that role, which it plays in building of an adequate picture of the Universe. Lithium is one of few elements formed as a result of the Big Bang and its cosmological abundance can characterize baryon-proton ratio and the baryon contribution to density of the Universe. Li abundance characterizes also physical and nuclear processes occurring inside stars.

The lithium is destroyed in nucleosynthesis at rather low temperatures (near $2.5 \cdot 10^8$ K) and its abundance in stellar atmospheres varies already at stages Pre Main Sequence and Main Sequence (Iben, 1965; D'Antona, 1991). Since Spite & Spite (1982) revealed that the lithium in evolved stars of Population II shows comparable surface abundances (for stars with T_{eff} beyond 5800 K, [Fe/H] < -1.4), many Li abundance investigations were made that confirmed this result. In recent works the obtained value of $\log A(Li)$ is equals to 2.1 (Pilachowski et al., 1993), 2.32 (Thorburn et al., 1994), 2.24 (Bonifacio & Molero, 1997), 2.40 (Gratton et al., 2000). The primordial abundance of Li according to the big bang models is $3 \cdot 10^{-8}$ on mass (Walker et al., 1991). That value is close to those observed in dwarfs and subdwarfs.

Lithium abundances for the stars of our target were derived from a fitting of observational data with a synthetic spectra computed by STARS code (Tsymbal, 1996) in LTE assumption using the detailed structure of the lithium feature at 6707 Å. Atomic and molecular line list was taken from Mishenina & Tsymbal (1997). The calculations of NLTE (Carlsson et al., 1994) departures show that the 6707 lines are slightly affected by it.

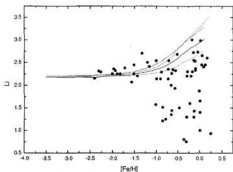


Figure 2: Comparison of Li dwarf observations ($T_{\text{eff}} > 5600$ K) with theoretical models of Timmes et al. (1995, ApJS 98, 617) (the calculated Li abundance is shown as the solid line, the dotted lines show factors of two variation in the ν -process yields) and Romano et al. (1999, A&A 352, 117) (dashed line).

The study of behaviour of the Li abundance for stars with $T_{\text{eff}} > 5600$ K, and $\log g > 3$ on various metallicities allows to estimate the contribution of various sources of the Li production in enrichment of interstellar medium (ISM). The lithium abundance raises with $[\text{Fe}/\text{H}]$ increasing and it shows the larger dispersion on $[\text{Fe}/\text{H}] > -1.3$ (see Fig. 2, and also Reboles et al., 1988; Chen et al., 2000).

Lithium evolution has already been studied in detail by several authors and some sources of the Li-production were considered. The model of chemical evolution of D'Antona and Matteucci (1991) considered classical novae and AGB stars as additional sources of Li-production. In the later model of Matteucci et al. (1995) the neutrino-process nucleosynthesis from Type II SNe and hot bottom burning in intermediate mass AGB was taken. Abia et al. (1995) has accepted the Li production from low mass AGB stars (C-stars) and Galactic cosmic ray (GCR) nucleosynthesis. We have compared our Li determination $\log A(\text{Li})$ to the calculation of lithium evolution (Timmes et al., 1995) (Fig. 2). The authors used simple standard model, which accepted, that halo and disk are parts of the same system distinguished only on age. Timmes et al. (1995) have considered two sources of the Li - production: as a product of homogeneous Big Bang (Walker et al., 1991) and synthesized Li in processes of neutrino capture in massive stars (at $[\text{Fe}/\text{H}] > -1$). As to iron, it is delivered with two main sources - supernovae SN II and SN Type Ia. The analysis of the metallicity in the solar neighbourhood shows that of 1/3 the Solar System iron abundances arise from SN II and 2/3 from SN Ia. The calculated Li abundance is displayed as the solid line, and the dashed lines show factors of two variations in the ν -process yields.

Our result is a higher (0.1 dex on the average) than Li abundance, predicted by the model. Probably, it is result of errors of Li abundance definition or there is a consequence more high cosmological value of Li abundance (larger than 2.1 dex). Models of Li dilution, taking into account various transport mechanisms (Pinsonneault et al., 1992; Proffitt, Michaud, 1991; Chaboyer, Demarque, 1994) also requires more larger primordial lithium abundances than $\log(\text{Li}) = 2.1$. Certainly, it may be also due to unreliable choice of sources of Li-production or preconditions of model of chemical evolution.

Ryan et al. (2001) carefully studied the abundance and evolution of Li in galactic halo and disk. They draw attention to a choice of effective temperature of stars. Higher temperature conducts to the larger Li abundance. Ryan et al. (2001) also have carried out the comparison of the evolution of Li as a function of $[\text{Fe}/\text{H}]$ with the predictions of several models of galactic evolution that is taking into account various sources of Li-production and their combination (primary nucleosynthesis, reactions cosmic ray spallation, nucleosynthesis in supernovae through ν -process, nucleosynthesis in AGB stars and novae). The main distinctions between models arise at a stage of a disk (on $[\text{Fe}/\text{H}] > -1$), where AGB stars and novae begin to bring the remarkable contribution to Li enrichment with interstellar medium (ISM). For halo star evolution the essential processes are primary nucleosynthesis, ν -process, and reaction of GCR spallation. We have compared our data to model Romano et al. (1999), taking into account the above-mentioned processes. This model gives the good agreement with our data (see Fig. 2, dashed line) and we may conclude, that the main sources of Li enrichment of halo stars are Li-production as a result of the Big Bang, reaction of cosmic ray spallation and α -process in massive supernovae.

Carbon. The main nuclear source of carbon is helium hydrostatic burning in massive stars (He burning before explosion, the yield depends on presupernovae model - convective criterion, processes of hashing, expiration of masses and rate of nuclear reactions) and in stars of intermediate and low masses. The supernovae Type II and Type Ia are the main producer of carbon at earlier stage of the Galaxy, then the longer lived intermediate- and low-mass stars play important role, and also at the same time metal-rich Wolf-Rayet stars eject the carbon in ISM by stellar wind.

Our determinations of the carbon abundance were made on C I lines 4817, 5052, 5380 Å. These lines are weak and they are invisible at $[\text{Fe}/\text{H}] < -1$. Therefore our $[\text{C}/\text{Fe}]$ data present the small region of metallicity. For metal-poor stars the carbon abundance are determined on molecular CH lines in ul-

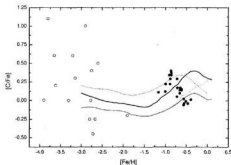


Figure 3: The trend of $[C/Fe]$ vs $[Fe/H]$. Our $[C/Fe]$ - black circles, open circles - $[C/Fe]$ (Ryan et al., 1991, AJ 102, 303); Norris et al., 2001, ApJ 561, 1034). The dashed lines show the calculations of Timmes et al. (1995) with two factors variation in the iron yields from massive stars, dotted line shows the results when Type Ia supernovae are excluded; solid line - Liang et al. (2001, A&A 374, 936).

tra-violet (UV) range, CO lines in infra-red (IR) range, on atomic CI and [CI] lines, at that [CI] lines no effects the departures from LTE. As a whole, $[C/Fe]$ determinations for unevolved stars show the larger dispersion from -0.5 up to $+0.5$ dex (Tomkin et al., 1992; Carretta et al., 2000; Gratton et al., 2000) and the average relation $[C/Fe]$ roughly solar at $[Fe/H] > -2.5$. At $[Fe/H] < -2.5$ there are the larger scattering of $[C/Fe]$ (from -0.7 to $+1.1$) with some tendency of growth of observed $[C/Fe]$ with $[Fe/H]$ increasing (Ryan et al., 1991; Norris et al., 2001).

The different sources of carbon-production were used in several chemical evolution models. So in model Timmes et al. (1995) the carbon yields from Supernovae II (Woosley, Weaver 1995) and the yields from stars of intermediate- and low- masses independent from metallicity (Renzini, Voli, 1981) was accepted, at that the main contribution was made the intermediate- and low- mass stars. The model Timmes et al. (1995) unsatisfactorily described observable trend of $[C/Fe]$ with $[Fe/H]$, particularly, at low metallicities (Fig. 3, our $[C/Fe]$ - black circles, open circles - $[C/Fe]$ (Ryan et al., 1991; Norris et al., 2001). The dashed lines show the calculations of Timmes et al. (1995) with two variations in the iron yields from massive stars, dotted line shows the results when Type Ia supernovae are excluded. Chiappini et al., (1997) have received similar result by two-infall model. The carbon yields from the intermediate- and low- mass stars as the main source of carbon was also considered by Oberhummer et al. (2000). Marigo (2001) has analysed the carbon yields, but dependent from metallicity for the same stars.

Other source of carbon contribution to the chemical enrichment of the ISM was proposed in model Prantzos et al. (1994). The authors have assumed, that after during the near 1-2 Gyr of the halo phase, the massive stars by means of a stellar wind enriched by carbon with ISM during the further galactic evolution. Gustaffson et al. (1999), having considered evolution of carbon in a Galactic disk, have accepted, that the main source - the stellar wind from rich metal massive stars. Later Gustaffson, Ryde (2000) have concluded, that a source of carbon still is not clear. Hou et al. (2000) have united sources of carbon; they have accepted a star wind from massive stars both star of intermediate- and low-masses. Goswami, Prantzos (2000), having applied our new model considering halo and a disk as two independent systems, have concluded, that the C yields from SN II (Woosley, Weaver 1995) are not sufficient reflect an observational picture and that there are other sources, for example, Wolf-Rayet stars or intermediate- and low mass stars.

Liang et al. (2001) using the standard infall model was explored the origin of carbon by 8 different models of stellar nucleosynthesis yields. They have shown that at early stages of a Galaxy, the massive stars are the main source of carbon, then the contribution from the longer lived intermediate- and low-mass stars and from the metal-rich WR stars grows. Unfortunately, the modern nucleosynthesis calculations do not allow selecting precisely the main carbon sources. We have carried out the comparison the $[C/Fe]$ data with of Liang et al. (2001) (Fig. 3, solid line) model, using as the basic sources of carbon production the intermediate- and low-mass stars (with the yields dependent from metallicity, Marigo, 2001) and the stellar wind from massive stars (Portinari et al., 1998). Noted, the authors do not examine observational increase of $[C/Fe]$ (up to $+1$) at $[Fe/H] < -2.5$. We suppose, that this growth may be explain by the contribution from Supernovae II type, and the larger dispersion of $[C/Fe]$ values at these metallicity by unhomogeneous early Galaxy.

Oxygen. The oxygen abundance does not change during burning hydrogen in traditional CNO cycle, and so both the dwarfs and the giants can be indicators of enrichment by oxygen of ISM. However, globular cluster giants show remarkable (up to 1.5 dex) scattering of $[O/Fe]$ and anticorrelation of oxygen abundance with the sodium and aluminium abundance. On it we shall stop later.

Overabundance of oxygen to iron relative to solar $[O/Fe]$ in stars with deficiency of metals was revealed Conti et al. (1967). The values of oxygen excess have evoked significant discussion that remains undecided till now. The question is that the oxygen abundance determined on forbidden $[O I]$

lines, IR triplet OI lines and molecular features (OH lines) will not be come to an agreement among themselves (Nissen, Edvardsson 1992; Fulbright, Kraft 1999). The $[O/Fe]$ value determined on lines [OI] 6300, 6360 AA is equal to near 0.4 dex (Spite, Spite 1986; Barbuy, 1988; Spissman, Wallerstein, 1991) and it is lower, than in case of use of IR triplet lines at 7770 AA, $[O/Fe] = 0.9$ dex (Abia, Rebolo, 1989; Cavallo et al., 1997). Furthermore the last determinations show the trend of $[O/Fe]$ with metallicity decreasing. The first attempt to improve this situation was made by Kiselman (1991). Using NLTE calculations, he found the encouraging result – NLTE corrections were achieved 0.4dex. However, further attempts of the NLTE calculations (Tomkin et al., 1992; Takeda, 1994; Mishenina et al., 2000) have resulted in lower values of NLTE departures (up to 0.2 dex) and it has not removed the contradictions for these two groups of lines. The subsequent attempt to rule the situation has touched the change of a scale of effective temperatures for metal-poor stars (King, 1993). Later it was confirmed and accepted in works Gratton et al., 2000; Carretta et al., 2000.

But the oxygen abundance study using UV molecular lines have shown more high $[O/Fe]$ which is agree to results on IR triplet lines (Tomkin et al., 1992, Boesgaard et al., 1999, Israelian et al., 1998). The situation is complicated by the fact, that at $[Fe/H] < -2.0$ the analysis of the giants [O I] lines and of the dwarfs IR triplet lines are used. At the same time the definitions of oxygen abundance on these two groups of lines for dwarfs with $[Fe/H] > -1.5$ has given the similar result (Spite, Spite, 1991). Tomkin et al have assumed, that the neglect of convection can be responsible for the

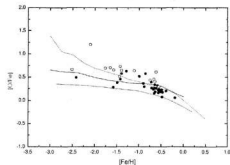


Figure 4: The trend of $[O/Fe]$ vs $[Fe/H]$ (black circles – this work, open circles – Mishenina et al. 2000, A&A 353, 978). Lines represent of models: Timmes et al., 1995 (solid); Shustov et al. (1997, A&A 317, 397) (dash-dotted); Chang et al. (1999, A&A 350, 38) (dashed); Qian, Wasserburg (2001, ApJ 549, 337) (dotted).

discrepancy. We have determined O abundance using the models with convection (Castelli et al., 1997) for metal poor giants ($T_{\text{eff}} < 4600$ K) and without convection (Kurucz, 1993). We found the small difference (0.05), which has not removed the observation contradictions.

And, at last, the application of 3D models gives one more chance to solve this problem within the framework of stellar atmosphere modelling (Asplund et al., 1999). However, Israelian et al., (2001) find for a star BD+23 3130 ($[Fe/H] = -2.43$) high oxygen abundance ($[O/Fe] = 0.78$), using three indicators of oxygen in frameworks of one-dimensional models, and they assumed that is not a problem of theoretical modelling of atmospheres. The question still remains open. Therefore the interpretation of a trend $[O/Fe]$ with $[Fe/H]$ by the theories of chemical evolution of the Galaxy has some uncertainty.

In our work the average value of $[O/Fe]$ was obtained from [OI] lines and it is $+0.46 \pm 0.12$ (8 stars) in the region of $-1.5 < [Fe/H] < -0.7$. At metallicities from -0.7 to -0.3 the $\langle [O/Fe] \rangle$ is $+0.17 \pm 0.09$ (15 stars). These values are lower than those were defined from IR triplet lines (Cavallo et al., 1997, Mishenina, et al., 2000) and from OH ultraviolet lines (Boesgaard et al., 1999; Israelian et al., 1998). But our present result carried out at $[Fe/H] > -1.5$ and it was quite concordance with our preceding one (see Fig. 4). All remain intricate in case of cool giants. Just for these stars the forbidden oxygen lines is detectable in their spectra at low metallicities. In our example of stars there is star BD+30 2611 with the low O abundance ($[O/Fe] = +0.19$ from our determination), its low O abundance was noticed by Kraft et al. (1992), King (1997) and Gratton et al. (2000). As see from Fig. 4, and also see (Carretta et al., 2000; their Fig. 3) the scatter in $[O/Fe]$ is wide at $[Fe/H] < -1$ from both [OI] lines and IR triplet lines. This may be as the result of determination errors or the prestellar medium scatter of oxygen abundance.

In the given research we used [OI] lines, as the spectra, examined by us, have no IR spectral region. We receive average value $\langle [O/Fe] \rangle = +0.46 \pm 0.12$ (8 stars) in a range $-1.5 < [Fe/H] < -0.7$ and $\langle [O/Fe] \rangle = +0.18 \pm 0.09$ (17 stars) in a range $-0.7 < [Fe/H] < -0.3$. The mean value of $[O/Fe]$ does not contradict the tendency of growth $[O/Fe]$ on lower $[Fe/H]$. The average value of $[O/Fe]$, obtained in this work for dwarfs and in the paper of Mishenina, et al. (2000), for halo stars $\langle [O/Fe] \rangle = +0.53 \pm 0.08$ (4 stars) and disk $\langle [O/Fe] \rangle = +0.24 \pm 0.12$ (16 stars).

Hydrostatic burning of He in massive supernovae SN II (Woosley, Weaver, 1995) is the main source of oxygen. These calculations of the O yields are used in models of chemical evolution. We have carried out the comparison $[O/Fe]$ data with several chemical evolution models (Timmes et al. 1995; Shustov et al., 1997; Chang et al., 1999). $[O/Fe]$

near 0.4–0.5 dex was accepted in these models and it is lower, than those obtained with permitted IR triplet lines and UV molecular lines. The model which is taking into account loss of heavy elements into intracluster medium (Shustov et al., 1997) better, than other considered models, are reproduced the run of oxygen with $[Fe/H]$, however, on low $[Fe/H]$ is not achieved the values of $[O/Fe]=1$ dex and more. Three components model of Qian, Wasserburg (2001) supposing, that the first massive stars $M > 100 M_{\odot}$ produce oxygen in an early Galaxy, reflects well enough the observation data. It is necessary to note, that there is also other opportunity to explain the larger dispersion at low metallicity, it may be due to homogeneous of the earlier Galaxy. Among stars the poor metals observe stars, which show low enough value of $[O/Fe]$. So in our example there is a star BD+30 2611 c by very low value of $[O/Fe]=+0.19$ (our definition), such low value was marked also Kraft et al. (1995); King (2000); Gratton et al. (2000). As see from Fig. 4 the larger scatter of $[O/Fe]$ is observed at low $[Fe/H]$.

Using our $[O/Fe]$ and executed by us early, including recalculation NLTE of $[O/Fe]$, obtained in work Cavallo et al. (1997) we have estimated the scattering of $[O/Fe]$ values for stars with $[Fe/H] < -1$ and $[Fe/H] > -1$, it is equal ± 0.29 (43 stars) and ± 0.17 (33 stars), correspondingly. Thus the determination errors are equal correspondingly ± 0.19 and ± 0.15 . Thus, observation dispersion for stars with $[Fe/H] > -1$ is caused, for the most part, of measurement errors, but in case of stars with $[Fe/H] < -1$ parts of an errors may be due to ungemogenous prestellar matter.

Sodium. Sodium is synthesized during hydrostatic burning of carbon and partially, during hydrogen burning shell through the NeNa cycle.

The observational situation for sodium abundance in metal-poor stars is not quite clear. Pila-chowski et al. (1996) studied halo stars and found a slight mean deficiency $\langle [Na/Fe] \rangle = -0.17 \pm 0.22$ and a slight tendency for $[Na/Fe]$ to increase with advancing evolutionary stage. Investigation of Na abundance of halo stars on extreme orbits (Stephens, 1999) exhibits the $[Na/Fe]$ decrease (up to -0.7 dex) at $[Fe/H]$ from -1 to -2. Study of thick disk stars displays mildly enhanced Na with an average $\langle [Na/Fe] \rangle$ is 0.087 ± 0.014 , there is a mild trend with metallicity (Prochaska et al., 2000). The determination of Na abundance was carried out by Carretta et al. (2000). They found for stars with $[Fe/H] < -0.6$, that the average $\langle [Na/Fe] \rangle = -0.09 \pm 0.19$.

Lines of a doublet Na I 6154 and 6160 AA, and line 5682 A, (other component of this doublet is blended by telluric spectrum line) were chosen for definition of the sodium abundance. Not LTE departures for 6154 and 6160 AA lines are insignificant, but it is more important for a 5682 A line as was

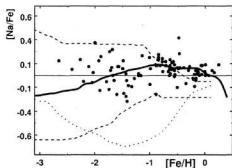


Figure 5: The trend of $[Na/Fe]$ vs $[Fe/H]$ Our $[Na/Fe]$ data – black circles; dotted line – Timmes et al. (1995); solid line – Samland (1998, ApJ 496, 155); dashed lines – Goswami, Prantzos (2000, A&A 359, 191).

shown earlier for stars of various types (Mashonkina et al., 2000; Korotin, Mishenina, 1999; Baumuller et al., 1998; Gratton et al. 1999), but for D of Na I lines, they achieve -0.5 dex (Baumuller 1998).

We determined Na abundance with taking into account the NLTE corrections (Mishenina et al., 2002b). NLTE calculations were made under the program MULTI (Carlsson, 1986), modified (Korotin, Mishenina, 1999). In our case the corrections for 6154, 6160 lines are slightly and they are higher (up to 0.2 dex) for 5682 line.

Let's consider the behaviour of $[Na/Fe]$ with $[Fe/H]$ and compare it to the predictions of models of chemical evolution of the Galaxy (Timmes et al., 1995; Samland, 1998; Goswami, Prantzos, 2000) (Fig. 5). All these models as the main source of Na production consider massive stars and a Na yields take from nucleosynthesis calculations of Woosley, Weaver (1995). The authors specify, that on $[Fe/H] > -1.0$ some synthesis of sodium in intermediate mass stars can occur in the hydrogen burning shell through the neon-sodium cycle (Denissenkov, 1989). Mass loss of the stellar envelopes would enrich the interstellar medium. However, they did not take into account in model calculation. Note, that the important question concerning synthesis of Na is a question on that, primary it is an element or secondary. In the first case it synthesizes directly burning carbon and the Na yields is independent from metallicity. In a case of its production during neutron or proton capture the Na yields depends on neutron excess (Woosley, Weaver, 1995) and, correspondingly, from metallicity (Samland, 1998). In last case Na abundance should demonstrate deficiency in relation to iron in metal-poor stars.

As see from a Fig. 5., the calculations of Timmes et al. (1995) (dotted line) and Goswami, Prantzos

(2000) (dashed lines) do not reproduce an observation run of $[\text{Na}/\text{Fe}]$ with $[\text{Fe}/\text{H}]$. At that Timmes (1995) consider the Na yields independent from $[\text{Fe}/\text{H}]$ and accepting, that halo and disk are parts of the same system, differing only on age. Goswami, Prantzos (2000) take the Na yields dependent from metallicity and considers halo and disk, as two independent subsystems. It is interesting, that in case of the Na yields independent from metallicity (upper dashed line), the behaviour $[\text{Na}/\text{Fe}]$ in model Goswami, Prantzos (2000) is similar to the behaviour of alpha-elements (Mg, Si), this case is marked by the authors as not realistic. Model Samland (1998) (solid line) better describes the trend of Na with $[\text{Fe}/\text{H}]$, than other models. This model using the metal dependency of stellar nucleosynthesis, and taking into account the large number of free model parameters (gas flows in the galaxy, mixing processes in ISM, energy release of supernovae etc.), have a great influence on the distribution of chemical elements, and, in particular, Na.

The average values of $[\text{Na}/\text{Fe}]$ for stars with $[\text{Fe}/\text{H}] > -1$ is equal to 0.07 ± 0.09 (60 stars) and slightly larger than for stars with $[\text{Fe}/\text{H}] < -1$, it is equal -0.02 ± 0.14 (38 stars). NLTE corrections reduce the dispersion (in LTE assumption the sigma is ± 0.14 and ± 0.20 , accordingly), but the scattering is larger for stars of lower metallicity. We suppose that the larger dispersion is due to the larger determination errors at $[\text{Fe}/\text{H}] < -1$, though the Na dispersion in prestellar medium can also do its part for total dispersion.

Aluminium. The aluminium is a product of hydrostatic burning of carbon and neon in massive stars, and partially, hydrogen burning in MgAl a cycle. Al a yield is strongly effect to influence of a shock wave depends on model pre-supernovae and power of a shock wave.

The Al abundance determination is made in LTE approach with lines Al I 6696, 6698 AA. For these lines NLTE corrections do not exceed 0.15 dex (Baumuller, Gehren, 1997). At $[\text{Fe}/\text{H}] = -1.0$ – -1.5 lines of aluminium weaken in stellar spectra depending on temperature and surface gravity of a star. The obtained values of $[\text{Al}/\text{Fe}]$ are in the good concordance with those obtained in some papers (Edvardsson et al., 1993; Baumuller, Gehren, 1997; Prochaska et al., 2000) for stars with $[\text{Fe}/\text{H}] > -1.5$.

To examine the evolution of aluminium at lower metallicities we have taken the result of works (Ryan et al., 1996b; Norris et al., 2001). These determinations are carried out on a resonance line of Al I 3961.5, very effected to influence of NLTE departures (-0.65 on $[\text{Fe}/\text{H}] = -3$, Baumuller, Gehren, 1997). If to correct $[\text{Al}/\text{Fe}]$ data for NLTE, we shall get $[\text{Al}/\text{Fe}]$ on 0.2 – 0.3 over solar relation at $[\text{Fe}/\text{H}] > -1.5$ and on -0.2 – -0.3 below solar relation with a wide scatter at $[\text{Fe}/\text{H}] \sim -3$. As $[\text{Al}/\text{Fe}]$ data were found without the NLTE departures the comparison observation data to calculation of models

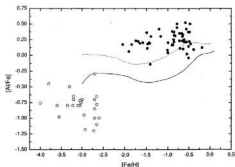


Figure 6: The trend of $[\text{Al}/\text{Fe}]$ vs $[\text{Fe}/\text{H}]$. Our $[\text{Al}/\text{Fe}]$ – black circles, open circles – $[\text{Al}/\text{Fe}]$ (Ryan, 1991; Norris et al., 2001). The solid and dashed lines show the calculations of Timmes et al. (1995) with two factors of variation in the iron yields from massive stars.

of chemical evolution is not enough correct. We carry out such comparison as a first approximation. In a fig. 6 the comparison $[\text{Al}/\text{Fe}]$ with models (Timmes et al., 1995 – solid line, our $[\text{Al}/\text{Fe}]$ – black circles, open circles – Ryan et al., 1996b; Norris et al. (2001) is displayed. We see underproduction of aluminium at higher $[\text{Fe}/\text{H}]$, especially if to take into account the NLTE corrections. The calculations of Goswami, Prantzos (2000) for aluminium yields independent from metallicity predict the trend of $[\text{Al}/\text{Fe}]$ with $[\text{Fe}/\text{H}]$ similarly the trend of alpha-elements (with $[\text{Al}/\text{H}]$ overabundance up to 0.5 on $[\text{Fe}/\text{H}] \sim -3$). The authors consider this model only for illustration. Samland (1998), using Al yields dependent from metallicity and enlarged on the factor 5, achieves the quite good concordance between observational data and model calculation. Additional source of Al can be Al-production through AlMg cycle. There is another source of Al-production. There is another source of Al-production. The origin of a radioactive isotope ^{26}Al became interesting problem with the discovery of an excess of ^{26}Mg in the Allende meteorite (Lee et al., 1977). The presence of array line due to the decay of ^{26}Al in ^{26}Mg in the Galaxy pointed to the production of ^{26}Al in a Galaxy at present time, since the half-life of ^{26}Al is $7.2 \cdot 10^5$ years.

As a whole, the theories of nucleosynthesis and chemical evolution do not yet describe the trend of $[\text{Al}/\text{Fe}]$ with $[\text{Fe}/\text{H}]$.

α -elements. The so-called α -elements are formed due to capture of α -particles in the processes of hydrostatic neon and oxygen burning. Oxygen, magnesium, silicon, sulfur, calcium and titanium traditionally belong to this group (though Ti is an element of iron peak). Supernovae SN II and, partially, SN Ia are producer of silicon and calcium.

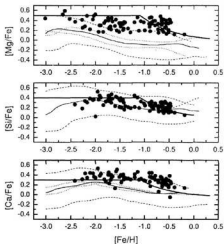


Figure 7: Our relative abundance of the 6-elements, Mg, Si, Ca and the tracks for these elements computed by Timmes et al. (1995) (thin solid line) and by Pagel&Tautvaišienė (1995, MNRAS 276, 505) (thick solid line).

The Si, Ca yields depend on pre-supernovae model and power of a shock wave.

We carried out Mg, Si, Ca abundance determination using the lines of neutral atoms of these elements and LTE approximation. Some authors (Gratton et al., 1999; Thevenin, Idiart, 1999; Shimanakaya, Mashonkina, 2000) have estimated the departures from LTE for lines of Mg. The NLTE corrections for Mg I lines (for example, Shimanakaya, Mashonkina 2000) have not change the trend of $[Mg/Fe]$ with $[Fe/H]$ and the average value of $[Mg/Fe]=0.45\pm 0.05$. Estimations of the departures from LTE for lines Mg at $[Fe/H]< -0.6$.

The effects of non-LTE for Fe and Mg lines were investigated by Gratton et al. (1999). They shown that the size of the model atom impact on results of non-LTE computations. Using 60-level model of the iron atom, they found negligible departures from the LTE in high gravity stars and slightly pronounced in low gravity stars, which is evidently due to the less efficient thermalization by collisions in giants. Non-LTE corrections for Fe lines are very small in dwarfs, and only small corrections (<0.1 dex) are expected for giant stars. The main non-LTE effect for Mg is overionization, but for high excitation lines these corrections are small in cool dwarfs ($T_{\text{eff}} \leq 6000\text{K}$) and larger in warmer dwarfs (-0.15 dex). Corrections are larger also in giants due to collisions less efficiently complete.

In Fig.7 we plotted our $[Mg/Fe]$, $[Si/Fe]$ and $[Ca/Fe]$ vs $[Fe/H]$ abundances together with the

tracks computed by Timmes et al. (1995) and by Pagel, Tautvaišienė (1995). The thick solid line represents the results of Pagel, Tautvaišienė (1995). The thin solid line corresponds to the data from Timmes et al. (1995), the dashed line shows variation of the iron yield by a factor of two and dotted line reflects variation in an exponent by 0.3 in the initial mass function. For $[Si/Fe]$ vs $[Fe/H]$ and for $[Ca/Fe]$ vs $[Fe/H]$ plots observations are in the reasonable agreement with both models, and $[Mg/Fe]$ vs $[Fe/H]$ – with the model of Pagel, Tautvaišienė (1995), as one can see from Fig. 7. But, the discrepancy between the tracks for Mg of two models is evident, «for reasons which are not yet clear» (Pagel, Tautvaišienė, 1995). Both models assume that magnesium is a pure product of massive supernovae SNI. The best fit the model of Timmes et al. (1995) to the $[Mg/Fe]$ observations may be a systematic reduction of the iron yields from massive stars by a factor of two and a small magnesium contribution originating from another source (Timmes et al., 1995).

The model of Goswami, Prantzos (2000) describes well the behaviour of α -elements, except Mg. Samland (1998) accepts, that the main source of Mg are massive stars (SN II) and 1.5% of Mg – production come out from SN Ia. The complicated model of Samland (1998) describes well the trend of $[Mg/Fe]$ vs $[Fe/H]$.

Iron. The main nuclear source of iron is explosive nucleosynthesis in supernovae SN II and SNIa. 2/3 of solar abundance of iron is a product of explosion of white dwarfs in double systems (SN Ia), supernovae SN II is producteur of 1/3 of iron solar abundance.

The abundance of iron relative to solar one $[Fe/H] = \lg(Fe/H) \text{ star} - \lg(Fe/H) \text{ star}$ is used as parameter metallicity of a star.

The iron abundance was obtained on similar set of lines for all study stars, in LTE approximation. From 50 up to 150 lines depending on metallicity were used in our analysis. The influence of NLTE effects on the neutral and ionized iron lines was investigated in some works (Thevenin, Idiart, 1999; Gratton et al., 1999; Schukina, Bueno, 1998). Unfortunately, the construction of complex model of atom (as iron, for example) is difficult task, especially in absence of physical parameters with satisfactory accuracy.

Other problem concerning the iron abundance in metal-poor stars, there is a diffusion of atoms of iron, which can result in lower iron abundance in giants (Chaboyer et al., 2001). The observation of dwarfs and giants in globular clusters do not support this assumption – Fe abundance in dwarfs and giants coincide among themselves.

***n*-capture elements.** Two main mechanisms are responsible for the production of these elements: the *r*-process (for rapid neutron capture and the *s*-process for slow neutron capture depending on the magnitude of the neutron flux available, and in some cases the *p*-process (Burbidge et al., 1957). The *r*- and *s*-process syntheses are supposed to occur at different stages of star's lifetime. The *r*-process nuclei are synthesized in massive stars, that explode as Type II supernovae (SNe) (Cowan et al., 1991). The *s*-process is traditionally divided into two types: the weak *s*-component and the main *s*-component. The weak *s*-component is responsible for the production of lighter elements (Sr, Y, Zr) during the core He burning in massive stars (Lambd et al., 1977; Raiteri et al., 1991). The main *s*-component elements (heavier than Ba) can be synthesized during the thermal pulses in the AGB phase of intermediate- and low-mass stars (Iben, Renzini, 1982; Hollowell Iben, 1989). In the works concerning *n*-capture elements determinations (Spite, Spite, 1978; Gilroy et al., 1988) the pattern of an element relative to iron ratio has been found not to follow that of α - or iron-peak elements at $[\text{Fe}/\text{H}] < -2$. Truran (1981) speculated that for low metallicity stars this might be due to the dominant role of the *r*-process. Later Gratton Sneden (1994) found that the relative contribution of the *s*-process is smaller in the metal-poor stars than in the solar system but that it is not at all negligible, even in stars as metal-poor as $[\text{Fe}/\text{H}] = -2.5$. McWilliam et al. (1995) confirmed the slump for $[\text{Sr}/\text{Fe}]$, $[\text{Ba}/\text{Fe}]$ vs $[\text{Fe}/\text{H}]$ at a unique metallicity, about of $[\text{Fe}/\text{H}] = -2.4$ early detected by Spite, Spite (1978). This observation implies that a distinct phase of nucleosynthesis occurred before the Galaxy reached $[\text{Fe}/\text{H}] = -2.4$. McWilliam et al. (1995), Ryan et al. (1996) found also that the dispersions in some heavy element abundances (Sr for example) represent a scatter in the original stellar compositions at $[\text{Fe}/\text{H}] < -2.5$. This signature may have arisen from the weak *s*-process in massive stars or by *r*-processing. McWilliam (1998), Sneden et al. (1998), Burris et al. (2000) confirmed the significant scatter in *n*-capture elements at low metallicities.

In our study Sr, Y, Ba, La, Ce, Nd and Eu abundance analysis was carried out in the LTE approximation using the oscillator strengths $\log g$ from the paper of Gurtovenko, Kostyk (1989). Oscillator strengths from this source for some of the elements (including Ba, Eu) allow for the effect of hyperfine structure.

Non-LTE calculations for Ba were performed in the work by Mashonkina et al. (1999). They showed that corrections are small for subordinate lines (< 0.08 dex) and increase to 0.20 for the Ba II resonance line $\lambda 4554 \text{ \AA}$. Departure from the

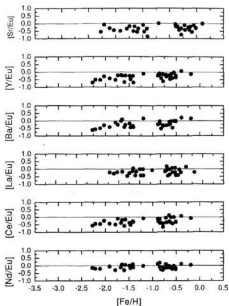


Figure 8: Relative abundances of Sr, Y, Ba, La, Ce, Nd to Eu versus $[\text{Fe}/\text{H}]$.

LTE gets stronger with lower metallicity, depends on temperature and microturbulence but is insensitive to surface gravity and EW. However, the observed underabundance of Ba at the considered low metallicities is 1–1.5 dex, and this amount can't be removed completely by accounting for these corrections only. Therefore, we consider our analysis to be quite robust against non-LTE effects.

The study of the trends of relative abundances vs $[\text{Fe}/\text{H}]$ is important to investigate of the influence of the *n*-capture elements in enrichment of the Galaxy (Mishenina, Kovtyukh 2001). Investigation of *r*-, *s*-processes in the Solar System was carried out by Kappeler et al. (1989) and Raiteri et al. (1991). They conclude that more than 90% of Eu should come from the *r*-process. Relative abundances of Sr, Y, Ba, La, Ce, and Nd to Eu may indicate the efficiency of the *s*-process at the epochs of different metallicities (see Fig. 8). $[\text{Nd}/\text{Eu}]$ exhibits larger contribution of the *r*-process than other elements. $[\text{Y}/\text{Eu}]$, $[\text{Ba}/\text{Eu}]$ and $[\text{Ce}/\text{Eu}]$ show trend with $[\text{Fe}/\text{H}]$ that may be the evidence of the *s*-process enrichment growth with increasing metallicity. Mashonkina et al. (1999), by direct determination of the odd-to-even isotopic ratio from the Ba II resonance line, showed at the instance of two stars that they have been formed from material whose barium content originated mainly in the *s*-process ($[\text{Fe}/\text{H}] > -2.2$). This result agrees with our conclu-

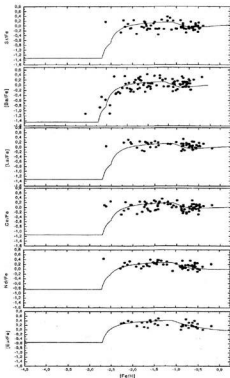


Fig. 9. Relative abundances of Sr, Y, Ba, La, Ce, Nd, and Eu versus $[Fe/H]$ and the tracks for these elements computed by Pagel & Tautvaišienė (1997, MNRAS 288, 108) (solid line).

sion. Relative abundances to iron of $[Sr/Fe]$, $[Y/Fe]$, $[Ba/Fe]$, $[La/Fe]$, $[Ce/Fe]$, $[Nd/Fe]$, $[Eu/Fe]$ vs $[Fe/H]$ and comparison with the tracks of the model of Pagel Tautvaišienė (1997) are given in Fig. 9. The run of $[Ba/Fe]$ vs $[Fe/H]$ confirms the well-known jump of Ba abundances at $[Fe/H]$ about of -2.5 dex (Spite Spite, 1978). Unfortunately, the lack of more stars in our sample with metallicities < -2.5 does not permit to trace the behavior of Ba abundances at earlier times and check if there is a plateau at $[Fe/H] < -2.5$ predicted by the model of Pagel Tautvaišienė (1997). But inside the available range of metallicities $-0.5 > [Fe/H] > -2.5$ agreements with these model calculations is pretty good. These theoretical abundances have been computed assuming two separate time delays in s-elements production of the order of 37 Myr and 2.7 Gyr, corresponding to progenitor masses of about 8 Msolar and 1.5 Msolar respectively. Now, let's compare our results with the chemical evolution theory of Travaglio et al. (1999), which considers AGB stars of different masses

and low mass SN as the sources of production of r- and s-elements. Ba, La, Ce, Nd, and Eu that contain species of very different origin (mostly r-process production for Eu and s-process for Ba) were analyzed by these authors. Fig. 10 represents the behavior of these elements among the three populations of the Galaxy (the solid line corresponds to thin disk, the dotted line - thick disk, the dashed line - halo). For La, Nd, and Eu the agreement between observations is good, while for Ce and, especially, Ba it clearly breaks down. The model of Travaglio et al. (1999) predicts the appearance of s-enrichment at lower $[Fe/H]$ than it follows from our observation data (for Ba, for example). It may be due to that at $[Fe/H] < -2.5$ the inhomogeneous models of chemical evolution are required. Analysis of our data and matching with various evolutionary models testifies to s enrichment at $[Fe/H] > -2.5$ by a wind from AGB stars of small masses. Some our target stars show that r-process contributes into Ba, Y and Ce abundances at $[Fe/H] < -2.0$. Sr shows larger scatter. McWilliam et al. (1995), Ryan et al. (1996) found larger dispersion in $[Ba/Fe]$ and $[Sr/Fe]$ at lower metallicities ($[Fe/H] < -2.5$) and have interpreted it as the evidence of the formation of our Galaxy at early times by mergers of the fragments with various proper enrichments (Searle, Zinn, 1978). Recently, the inhomogeneous chemical evolution models have been constructed by Raiteri et al. (1999) - for the run of $[Ba/Fe]$ vs $[Fe/H]$, by Travaglio et al., (2000) - for the run of $[Eu/Fe]$ vs $[Fe/H]$ and Tsujimoto et al. (2000) - the run of $[Ba/Mg]$ vs $[Mg/H]$, $[Eu/Mg]$ vs $[Mg/H]$. We compared our $[Eu/Fe]$ vs $[Fe/H]$ data with the calculations of the inhomogeneous chemical evolution models by (Travaglio et al., 2000 (schematically, Fig. 11, 12). A Monte Carlo model by Travaglio et al. (2000) is based on the idea of fragmentation and coalescence between interstellar gas clouds, taking into account the effects of local enrichment and mixing of the halo gas, and accentuating on elements like Eu produced by r-process from low-mass SN. In case of Eu production from high-mass SN (15-25M), the time delay in the enrichment of Eu with respect to Fe will be too small and it is not enough to explain the observed spread in $[Eu/Fe]$ at $-3.5 < [Fe/H] < -2.5$. Our data are overlapped with the model dots partially in common region of $[Fe/H]$. Never the less, inhomogeneous models are very perspective for the interpretation of the behavior of r- and s-elements at early times of galactic evolution (at $[Fe/H] < -2.5$).

Cooper and zinc. Cu and Zn, two elements immediately following the iron peak. The first schematic description of the chemical evolution of Cu and Zn was proposed by Sneden et al. (1991), who suggested that they might be ascribed mainly to the weak s-process. Their conclusions were sub-

sequently questioned by Raiteri et al. (1992) and by Matteucci et al. (1993). In this last work evidence was presented in favor of a large contribution from relatively long-lived processes, tentatively identified as Type Ia supernovae. Contrary to this, Timmes et al. (1995), using the copper and zinc yields of Type II supernova explosion from Woosley, Weaver (1995), suggested that these elements might be synthesized in significant amounts by the major nuclear burning stages in massive stars. These contrasting explanations one meets when an incomplete picture of stellar yields and a simplified chemical evolution scheme have to be used for interpreting the data.

The 5105.54, 5218.20, 5782.12 Å lines of Cu I were used for abundance definition (Mishenina et al., 2002a). Synthetic spectra were calculated taking into account the hyper-fine structure of Cu I components (Steffen, 1985). The abundance of zinc was obtained from the 4722.16, 4810.53, 6362.35 Å lines of Zn I. We used the EWs of these lines and Oscillator strengths for Zn I lines were taken from Gurtovenko, Kostyk (1989). The abundance definition was made in LTE assumption. Concerning Cu and Zn, computations of NLTE-effects on their abundances are complex and so far a good estimate of NLTE-corrections has not been presented. A posteriori, obtaining different abundances from lines with different low-level excitation potentials can be an empirical demonstration that departures from LTE are present. In the case of Cu, the lines 5105 Å and 5782 Å occur from meta-stable levels $E_{low} = 1.39$ and 1.64 eV, respectively, unlike the line at 5218 Å $E_{low} = 3.82$ eV. We have estimated that the discrepancy in Cu abundance, as determined from the lines at 5105 Å and at 5218 Å, is $<[Cu/H]_{5105} - [Cu/H]_{5218}> = 0.04 \pm 0.10$. The difference is well within the uncertainty of the estimate, and does not provide reasons for assuming that departures from LTE are of any importance. Unfortunately, Zn I lines have similar potentials and we cannot perform a similar analysis for the Zn abundance. We can however note that we used solar oscillator strengths for Zn I lines from Gurtovenko, Kostyk (1989), which implicitly include departures from LTE. We thus consider that our results can be affected only marginally by NLTE-effects.

Our values of $[Cu/Fe]$, $[Zn/Fe]$, and $[Cu/Zn]$ are shown as a function of $[Fe/H]$ in Fig. 13, and compared to abundances available in the literature. In the figure we prefer to use different points for measurements of the same star made by different authors, instead of making averages: in this way the scatter related to the heterogeneous composition of the database can be better appreciated. The trends for Cu and Zn are remarkably different, suggesting that differences in the dominant stellar

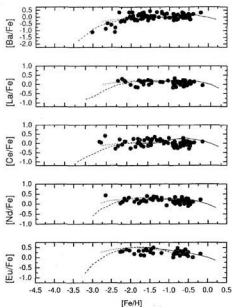


Figure 10: Relative abundances of Ba, La, Ce, Nd, and Eu versus $[Fe/H]$ and the tracks for these elements computed by Travaglio et al. (1999, ApJ 521, 691) (the solid line corresponds to thin disk, the dotted line – thick disk, the dashed line – halo).

mechanisms controlling the production of these elements must exist. Observational trends of $[Cu/Fe]$, $[Zn/Fe]$, and $[Cu/Zn]$ versus $[Fe/H]$ are shown. Symbols are for: H stars, D, and I stars from this work; Sneden et al. (1991); Westin et al. (2000); Hill et al. (2002) and Cowan et al. (2002). Thin dotted lines connect the points representing observations of the same stars by different authors. Error bars for individual objects are shown only when reported in the original papers. Fig. 14 shows indeed that fitting their relative trends requires at least a polynomial function with a quartic term. The line in the figure has no special meaning other than minimizing the sigma of the fit; it however shows that any reasonably accurate interpolation curve must necessarily assume relationships more complex than expected from purely primary or purely secondary processes. A purely secondary element would have a linear trend with slope +1. On the contrary, in the region where an almost linear trend exists ($-2 < [Fe/H] < -0.5$) the observed slope is about 0.6. Hence, already in early times of galactic evolution (the halo phases) Cu cannot be considered as a purely secondary element. In such phases it might be explained as the superposition of (at least) two independent processes, one of primary and one of

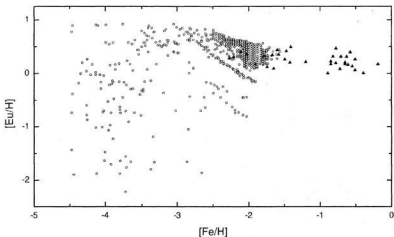


Figure 11: $[Eu/Fe]$ versus $[Fe/H]$, the filled triangles represent our data, the small open circles correspond schematically to the calculations of Travaglio et al. (2001, ApJ 549, 346). The r -process yields of Eu are derived from SN II in the mass range $8-10 M_{\odot}$.

secondary origin. A parabolic relation does in fact hold for the Cu abundance data in the shown metallicity interval, and Cu can have contributions from both primary and secondary processes in short-lived (i.e. massive) stars. The importance of secondary mechanisms can be quantitatively estimated by considering Cu production compared to the s -only isotope $80Kr$. This nucleus is known to be produced at about 12% of its abundance in the

main component of the s -process (Arlandini et al., 1999) and to have possibly a 10% p -process contribution. The rest is due to neutron captures in massive stars. Let us use for these last the recent models by Hoffman et al. (2001), where the overproduction of isotopes up to $A=100$ is given. Those models have to produce $80Kr$ at the 78% level of its solar abundance, then summing over the isotopes of Cu one gets for this element a contribution from sec-

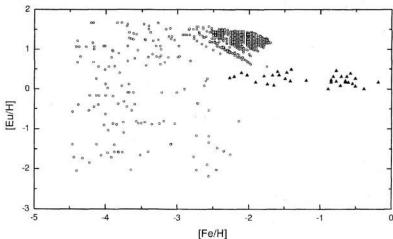


Figure 12: $[Eu/Fe]$ versus $[Fe/H]$, the filled triangles represent our data, the small open circles correspond schematically to the calculations of Travaglio et al. (2001). The r -process yields of Eu are derived from SN II in the mass range $15-30 M_{\odot}$.

ondary processes in massive stars of about 23% (assuming no primary contribution from the same stars).

Below $[Fe/H] = -2.5$, $[Cu/Fe]$ reaches an apparent plateau (though this conclusion is uncertain due to the limited data) around -0.6 dex. As 70% of iron comes later from type Ia Supernovae, this implies a primary contribution by population II massive stars of $10^{66} \pm 0.3$, which gives a total contribution as small as 7.5%. From the recent work by Heger et al. (2002) we also see that pre-galactic very massive stars cannot give remarkable contributions to Cu.

We can also exclude that the primary massive star contribution be dominated by the r -process. The comparison with Ba (Fig. 15), which galactic evolution in early phases is due to r -process (Travaglio et al., 1999) confirms it. Summing up, inspection of the observed data, comparisons with other elements and isotopes of known origin, and a very rough scheme for the chemical enrichment of the galactic halo allows us to predict that Cu receives a primary contribution by massive stars of about 7.5% of its abundance, while something around 25% should come from secondary processes in the same stars (slow neutron captures, or the weak s -process). Another 5% have been already attributed to the main s -component from AGB stars of long lifetime. We cannot avoid the suggestion that the remaining part (formally 62.5%) comes from the less known processes we have so far neglected, i.e. explosive nucleosynthesis in Type Ia supernovae. A similar reasoning can be repeated for Zn, which however shows a trend very close to Fe itself, so that the conclusion is more straightforward. Attributing 3% of its production to the main s -process component in AGB stars, the rest should come either from primary nucleosynthesis in massive stars (30%), or from Type Ia supernovae (something around 67%, like for Fe). The massive star yield cannot be dominated by the r -process, but some contribution from this last remains possible. For this «test» we make use of a metallicity distribution and a Star Formation Rate previously obtained (Travaglio et al., 1999) through an evolutionary model suitable for reproducing a large set of Galactic and extragalactic constraints (for details on the code see Ferrini et al., 1992; for its application to galactic heavy element enrichment see also Travaglio et al., 2001). The model considers the Galaxy as divided in three zones, halo, thick disk and thin disk. For Cu and Zn, we simply mimic the input stellar yields by imposing the tentative production sites derived in the previous section for the primary and secondary contributions in massive stars, in Type Ia supernovae and in AGB stars. Fig. 15 and Fig. 16 show the resulting chemical enrichment, through plots of $[Cu/Fe]$, $[Zn/Fe]$, $[Cu/Zn]$ and $[Cu/Ba]$, $[Zn/Ba]$ versus $[Fe/H]$. Chemical evolution predictions for Ba are from

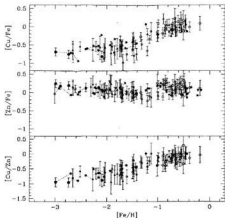


Figure 13: Observational trends of $[Cu/Fe]$, $[Zn/Fe]$, and $[Cu/Zn]$ versus $[Fe/H]$ are shown. Symbols are for: H stars (open triangles), D (open circles), and I stars (open squares) from this work; Sneden et al. (1991, A&A 246, 354) (stars); Westin et al. (2000, ApJ 530, 783), Hill et al. (2002, A&A 387, 560), and Cowan et al. (2002, ApJ 572, 861) (filled circles). Thin dotted lines connect the points representing observations of the same stars by different authors. Error bars for individual objects are shown only when reported in the original papers.

Travaglio et al. (1999). Being an outcome of the very crude estimates previously discussed, the results illustrated by the figures are not bad, and confirm that our suggestions for the stellar yields should be roughly correct. However, while they can interpret the general trends, they cannot explain the spread of abundances at very low metallicity. This is in particular related to the oversimplification of attributing massive star yields of Cu and Zn to generic explosive phenomena, in the absence of a criterion for distinguishing different processes occurring in different masses. In the galactic evolution results presented by Travaglio et al. (1999), the r -process was attributed to moderately massive (8-10 Msolar stars, ejecting their nucleosynthesis contribution after some delay compared to the typical products of very massive objects; this was adopted as a possible explanation for the delay in the appearance of Eu and Ba with respect to oxygen and iron (Travaglio et al., 1999). Making use of this same separation of massive star yields in two groups with different time scales for enrichment, we might improve our suggestions on the origin of Cu and Zn, trying to disentangle their r -process contribution from the rest. Actually, if the r -process becomes well mixed in the Galaxy only after $[Fe/H]$ has reached the value -2.5 or so, we can tentatively interpret the

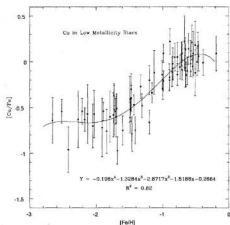


Figure 14: $[Cu/Fe]$ vs $[Fe/H]$: filled squares are the observations of Fig. 12. The fit (continuous line) shows that the dependency of $[Cu/Fe]$ on $[Fe/H]$ is more complex than implied by purely primary or purely secondary mechanisms.

scattered Cu and Zn abundances in very metal-poor stars as an indication that these last were born out of clouds selectively contaminated by different supernova types, sometimes carrying the signature of the r -process, sometimes that of NSE

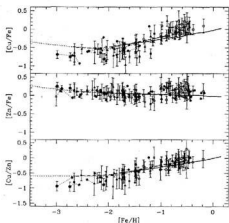


Figure 15: Galactic evolution of $[Cu/Fe]$, $[Zn/Fe]$, $[Cu/Zn]$ according to the chemical evolution prescriptions described in the text (including primary processes from massive stars, secondary processes from SNI, s -processes from AGB stars, and SNIa contributions). Symbols are the same as in Fig. 12.

or other explosive nucleosynthesis phenomena, in a poorly mixed early Galaxy.

Results and conclusions

We have determined the stellar parameters and abundances of 17 chemical elements in the atmospheres of 100 stars of various metallicities. The comparison of obtained data with current chemical evolution model was made. In summary, we found the following results.

Lithium. The main sources of Li enrichment of ISM are the Li yields as a result of the Big Bang, the reaction of cosmic ray spallation and ν -process in massive supernovae. At disk metallicities there are additional sources of Li-production, these are SN Ia and AGB stars. Some dispersion of Li at low $[Fe/H]$ nevertheless is observed. It can be due to intrinsic scatter of Li in ISM or presence of physical processes, what change the lithium abundance.

Carbon. The description of behaviour of carbon, as a whole, is unsatisfactory. The increasing $[C/Fe]$ with decreasing $[Fe/H]$ may be to explain by grow of the contribution from Supernovae type II and larger scatter at low metallicities may be due to unhomogeneous of early Galaxy.

Oxygen. The trend of $[O/Fe]$ with $[Fe/H]$ at $[Fe/H] < -2$ remains conflicting, as the observation data give not agree result through different indicators of oxygen. Probably, the main source of oxygen on early times of the Galaxy is the very massive stars (about 100 Msolar).

Sodium. The complicated model of Samland (1998) describes well the Na trend with $[Fe/H]$. This model uses the Na yields dependent from $[Fe/H]$ and it accounts of the large number of parameter appreciably changing distribution of chemical elements. The larger scatter of $[Na/Fe]$ at $[Fe/H] < -1$ than at $[Fe/H] > -1$ may be due to larger uncertainties of Na determination at $[Fe/H] < -1$ or intrinsic sodium dispersion at low metallicities.

Aluminium. The observation of Al is unsatisfactory. The resonance lines of Al I are affected by strong NLTE departures. The nucleosynthetic theories and chemical evolution models do not describe well the behaviour of aluminium.

α -elements. As a whole, the evolution of $[Si/Fe]$ and $[Ca/Fe]$ with $[Fe/H]$ is well described within the framework of various models of chemical evolution. The main sources of this element production are SN type II and, partially, SN Ia. The evolution of $[Mg/Fe]$ is less certain, because not all models describe well the trend Mg with $[Fe/H]$, though everyone accepts the same source of Mg production.

Neutron captures elements. R -process of the contribution of Ba abundance leaves from 8-10 M_{\odot} SN II and this component dominates on low metallicities. S -process becomes dominant above r -process only after 1 Gyr of galactic evolution

($[\text{Fe}/\text{H}]-1$) and it is connected to a long scale of evolution of stars of small weights and efficiency of s-production in AGB stars on different metallicities. The larger scatter of abundance at low metallicities is interpreted within the framework of unhomogeneous galactic models (Ba - Raiteri et al., 1999; Ba, Sr, Eu - Travaglio et al., 2000; Tsujimoto et al., 2000).

Cooper and zinc. Using our analysis the observation data, we have carried out the calculation of chemical evolution for Cu and Zn (Travaglio et al., 1999; Ferrini et al., 1992; Travaglio et al., 2001). The model of the Galaxy has three zones - halo, thick disk, and thin disk. We suggest that about 25% of Cu is produced by secondary phenomena in massive stars, and only 7-8% is due to primary phenomena in the same environment (either explosive or from a primary n-process). The bulk of Cu abundance (at least 62 - 65%) should be instead contributed on long time scales by type Ia supernovae. For Zn, its trend with respect to iron implies similar percentage yields for the two elements: 1/3 from primary processes in massive stars and 2/3 from type Ia supernovae. These rough indications were shown to roughly account for the Cu and Zn enrichment in the Galaxy. This approach was however found to be too schematic for interpreting the details of the database, including the scatter at very low metallicity. We argued that this last might be due to poorly mixed different contributions from massive stars in a non-homogeneous early stage (perhaps also complicated to the non-uniqueness of the r-process). A more quantitative analysis must therefore wait for a clarification of the underlying physical processes in evolved stars.

Examined element abundances show the scatter at low metallicities ($[\text{Fe}/\text{H}] < -2.0$). On the one hand it may be due to the low accuracy of the observational data, on the other hand it may be the evidence of the unhomogeneous of early Galaxy. The last may be due to the accretion of dwarf galaxies - satellites, or merging of separate fragments, on which has desintegrated primary uniform protogalaxy (Searle, Zinn, 1978). The scatter in element abundances in metal-poor stars may be also as result of small number supernovae (about 20), with various masses and, accordingly, different yields of heavy elements (Audouze, Silk, 1995) at earle Galaxy. The stochastic halo formation models (Argast et al., 2000) investigated the dispersion of the relative abundances as result of enrichment of ISM by single core-collapse supernovae. At $[\text{Fe}/\text{H}] < -3$, representative an early phase, the halo ISM is unmixed and dominated by local inhomogeneities caused by individual supernovae events. In the range $-3 < [\text{Fe}/\text{H}] < -2$ the dispersion noticeably decreases, ISM becomes better mixed and at $[\text{Fe}/\text{H}] > -2$ the halo ISM is well mixed.

The comparison of the trends of $[\text{El}/\text{Fe}]$ vs $[\text{Fe}/\text{H}]$ with calculations of the theories of chemical evolution and nucleosynthesis shows that many elements are described unsatisfactorily, it requires new investigations in the theories and the observations.

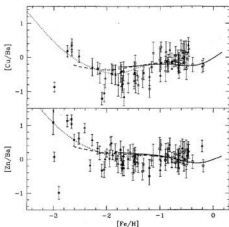


Figure 16: The same as Fig. 14 for the ratio $[\text{Cu}/\text{Ba}]$, and $[\text{Zn}/\text{Ba}]$. Symbols are the same as in Fig. 12.

lution and nucleosynthesis shows that many elements are described unsatisfactorily, it requires new investigations in the theories and the observations.

References

- Abia C., Rebolo R., 1989, *ApJ*, **347**, 186
 Abia C., Isern J., Canal R. 1995, *A&A*, **298**, 465
 Alonso A., Arribas S., Martinez-Roger, C., 1995, *A&A*, **297**, 197
 Argast D., Samland M., Gerhard O.E., Thielemann F.-K. 2000, *A&A*, **356**, 873
 Arlandini C., Kappeler F., Wisshak K., Gallino R., Lugaro M., Busso M., Straniero O. 1999, *ApJ*, **525**, 886
 Asplund M., Nordlund, Trampedach R., Stein R. F., 1999, *A&A*, **346**, L17
 Audouze J., Silk J. 1995, *ApJ*, **451**, L49
 Barbay B., 1988, *A&A*, **191**, 121
 Baumuller D., Gehren T., 1997, *A&A*, **325**, 1088
 Baumuller D., Butler K., Gehren T. 1998, *A&A*, **338**, 637
 Boesgaard A.M., King J.K., Deliyannis C.P., Vogt S.S. 1999, *AJ*, **117**, 492
 Bonifacio P., Molaro P. 1997, *MNRAS* **285**, 847
 Burbidge E.M., Burbidge G.R., Fower W.A., Hoyle F., 1957, *Rev.Mod.Phys.* **29**, 547
 Burris D.L., Pilachowski C.A., Armandroff T.E. et al. 2000, *ApJ* **544**, 302
 Castelli F., Gratton R.G., Kurucz R.L. 1997, *A&A*, **318**, 841
 Carlsson M. 1986, *Uppsala Obs. Rep.* 33
 Carlsson M., Rutten R.J., Bruls J.H.M.J., Shukina N.G. 1994, *A&A*, **138**, 860
 Carretta E., Gratton R.G., Sneden C. 2000, *A&A*, **356**, 238

- Cavallo R.M., Pilachowski C.P., Rebolo R. 1997, *PASP* **109**, 226
- Chaboyer B., Demarque P. 1994, *ApJ*, **433**, 510
- Chaboyer B., Fenton W.H., Nelson J.E., Patnaude D.J., Simon F. 2001, *ApJ*, **562**, 521
- Chang R.X., Hou J.L., Shu C.G., Fu C.Q. 1999, *A&A*, **350**, 38
- Chen Y. Q., Nissen P. E., Zhao G. et al. 2000, *A&A*, **S. 141**, 491
- Chiappini C., Matteucci F., Gratton R. 1997, *ApJ*, **477**, 765
- Conti P.S., Greenstein J.L., Spinrad H.E., Wallerstein G., Vardya M.S. 1967, *ApJ*, **148**, 105
- Cowan J., Thielemann F.-K., Truran J., et al. 1991, *Phys.Rep.*, **208**, 267
- Cowan J., Sneden C., Burles S., Ivans I.I., Beers T.C., Truran J., et al. 2002, *ApJ*, **572**, 861
- D'Antona F. 1991, *Mem.Soc.Astron.Italy* **62**, 165
- D'Antona F., Matteucci F. 1991, *A&A*, **247**, L37
- Denissenkov P.A. 1989, *Astrofizika* **31**, 223
- Edvardson B., Andersen J., Gustafsson B., Lambert D.L., Nissen P.E., Tomkin J., 1993, *A&A*, **275**, 101
- ESA, The Hipparcos and Tycho Catalogues. - 1997. - ESA
- Ferrini F., Matteucci F., Pardi C., Penco U. 1992, *ApJ*, **387**, 138
- Fulbright J.B., Kraft R.P. 1999, *AJ*, **118**, 527
- Galazutdinov G.A., 1992, *Preprint SAO RAS*, 92
- Gilroy K.K., Sneden C., Pilachowski C.A., Cowan J.J., 1988, *ApJ*, **327**, 298
- Goswami A., Prantzos N. 2000, *A&A*, **359**, 191
- Gratton R.G., Sneden C., 1994, *A&A*, **287**, 927
- Gratton R.G., Carretta E., Eriksson K., Gustafsson B., 1999, *A&A*, **350**, 955
- Gratton R.G., Sneden C., Carretta E., Bragaglia A. 2000, *A&A*, **354**, 169
- Gurtovenko E.A., Kostyk R.I., 1989, *Fraunhofer spectrum and system of solar Oscillators strengths*, *Naukova Dumka*, Kiev, p.200
- Gustafsson B., Karlsson T., Olsson E., Edvardsson B. 1999, *A&A*, **342**, 426
- Gustafsson B., Ryde N. 2000, in *IAU Symp.177, The carbon Star Phenomenon*, ed.R.F. Wing (Kluwer, Dordrecht), 481
- Heger A., Woosley S.E., Baraffe I., Abel T. 2002, (preprint), astro-ph/0112059
- Hill V., Plez B., Cayrel R., Beers T.C., et al. 2002, *A&A*, **387**, 560
- Hoffman R.D., Woosley S.E., Weaver T.A. 2001, *ApJ*, **549**, 1085
- Hollowell D., Iben I., Jr., 1989, *ApJ*, **340**, 966
- Hou J.L., Prantzos N., Boissier S. 2000, *A&A*, **362**, 921
- Iben I. Jr., 1965, *ApJ*, **142**, 1447
- Iben I., Jr. Renzini A. 1982, *ApJ*, **259**, L79
- Israelian G., Garcia Lopez R.G., Rebolo R. 1998, *ApJ*, **507**, 805
- Israelian G., Rebolo R., Garcia Lopez R.G., Bonifacio P., Molaro P., Basri G., Schukina N. 2001, *ApJ*, **551**, 833
- Kappeler F., Beer H., Wisshak K., 1989, *Rep.Prog.Phys.* **52**, 945
- Katz D., Soubiran C., Cayrel R., Adda M., Cautain R., 1998, *A&A*, **338**, 151
- King J.R. 1993, *AJ*, **106**, 1206
- King J.R. 1997, *AJ*, **113**, 2302
- King J.K. 2000, *AJ*, **120**, 1056
- Kiselman D. 1991, *A&A*, **245**, L9
- Korotin S.A., Mishenina T.V. 1999, *Astron Zh* **76**, 611
- Kraft R.P., Sneden C., Langer G.E., Prosser C.E. 1992, *AJ*, **104**, 645
- Kraft R.P., Sneden C., Langer G.E., Shetrone M., Bolte M. 1995, *AJ*, **109**, 2586
- Kurucz R.L., 1993, CD ROM n13
- Lamb S., Howard W.M., Truran J.W., Iben I., Jr., 1977, *ApJ*, **217**, 213
- Lee T., Papanastassiou D.A., Wasserburg G.R., 1977, *ApJ*, **211**, L107
- Liang Y.C., Zhao G., Shi J.R. 2001, *A&A*, **374**, 936
- Marigo P. 2001, *A&A*, **370**, 194-217
- Mashonkina L., Gehren T., Bikmaev I. 1999, *A&A*, **343**, 519
- Mashonkina L.I., Shimansky V.V., Sakhibullin N.A. 2000, *Astron. Zhurn.* **77**, 893
- Matteucci F., Raiteri C.M., Busso M., Gallino R., Gratton R. 1993, *A&A*, **272**, 421
- Matteucci F., D'Antona F., Timmes F.X. 1995, *A&A*, **303**, 460
- McWilliam A., Preston G.W., Sneden C., Searle L., 1995, *AJ*, **109**, 2757
- McWilliam A., 1998, *AJ*, **115**, 1640
- Mishenina T.V., Tsymbal V.V., 1997, *Pis'ma v AZh* **23**, 693
- Mishenina T.V., Korotin S.A., Klochkova V.G., Pan-chuk V.E. 2000, *A&A*, **353**, 978
- Mishenina T.V., Kovtyukh V.V., 2001, *A&A*, **370**, 951
- Mishenina T.V., Gorbaneva T.I., Kantsen L.E., Soubiran C. 2002, *Kinem. i fiz. Neb. Tel.*, accepted
- Mishenina T.V., Kovtyukh V.V., Soubiran C., Travaglio C., Busso M. 2002a, astro-ph/0209401
- Mishenina T.V., Kovtyukh V.V., Korotin S.A., Soubiran C. M. 2002b, *AnRep.* submitted
- Nissen P.E., Edvardsson B., 1992, *A&A*, **261**, 255
- Norris J., Ryan S., Beers T. 2001, *ApJ*, **561**, 1034-1059
- Oberhammer H., Csoto A., Schattl H. 2000, *Science* **289**, 88
- Pagel B.E.J., Tautvaisiene G., 1995, *MNRAS* **276**, 505
- Pagel B.E.J., Tautvaisiene G., 1997, *MNRAS*, **288**, 108
- Pilachowski C.A., Sneden C., Booth J. 1993, *ApJ*, **407**, 699
- Pilachowski C.A., Sneden C., Kraft R.P. 1996, *AJ*, **111**, 1689
- Pinsonneault M.H., Deliyannis C.P., Demarque P. 1992, *ApJ*, **S 78**, 181
- Portinari L., Chiosi C., Bressan A. 1998, *A&A*, **334**, 505
- Prantzos N., Vangioni-Flam E., Chauveau S. 1994, *A&A*, **285**, 132

- Prochaska J.X., Naumov S.O., Carney B.W., McWilliam A. Wolfe A.M. 2000, *AJ*, **120**, 2513
- Proffitt C.P., Michaud G. 1991, *ApJ*, **371**, 584
- Qian Y.-Z., Wasserburg G.J. 2001, *ApJ*, **549**, 337
- Raiteri C.M., Busso M., Gallino R., Picchio G., Pulone L., 1991, *ApJ*, **371**, 665
- Raiteri C.M., Gallino R., Busso M. 1992, *ApJ*, **387**, 263
- Raiteri C.M., Villata M., Gallino R., Busso M., Cravanzola A. 1999, *ApJ*, **518**, L91
- Rebolo R., Molaro P., Beckman J.E. 1988, *A&A*, **192**, 192
- Renzini A., Voli M. 1981, *A&A*, **94**, 175
- Romano D., Matteucci F., Molaro P., Bonifacio P. 1999, *A&A*, **352**, 117
- Ryan S.G., Norris J.E., Bessell M.S. 1991, *AJ* **102**, 303
- Ryan S.G., Norris J.E., Beers T.C. 1996, *ApJ*, **471**, 254
- Ryan S.G., T., Beers T.C., Suzuki T.K., Romano D., Matteucci F., Rosolankova K. 2001, *ApJ*, **549**, 55
- Samland M. 1998, *ApJ*, **496**, 155
- Schukina N.G., Bueno T. 1998, *Kinem. i Fiz. Neb. Tel* **14**, 315
- Searle L., Zinn R., 1978, *ApJ*, **225**, 357
- Shimanskaya N.N., Mashonkina L.I. 2001, *Astron Zhurn* **78**, 122
- Shustov B., Wiebe D., Tutukov A. 1997, *A&A*, **317**, 397
- Snedden C., Gratton R.G., Crocker D.A. 1991, *A&A*, **246**, 354
- Snedden C., Cowan J.J., Burris D.L., Truran J.W., 1998, *ApJ*, **496**, 235
- Soubiran C., Katz D., Cayrel R., 1998, *A&A*, **S 133**, 221
- Spiesman W.J., Wallerstein G. 1991, *AJ*, **102**, 1790
- Spite M., Spite F., 1978, *A&A*, **67**, 23
- Spite F., Spite M. 1982, *A&A*, **115**, 357
- Spite F., Spite M. 1986, *A&A*, **163**, 140
- Spite F., Spite M. 1991, *A&A*, **252**, 689
- Steffen M. 1985, *A&AS*, **59**, 403
- Stephens A. 1999, *AJ*, **117**, 1771
- Takeda Y. 1994, *PASJ* **46**, 53
- Thevenin F., Idiart T.P. 1999, *ApJ*, **521**, 753
- Thorburn J.A. 1994, *ApJ*, **421**, 318
- Timmes F.X., Woosley S.E., Weaver T.A., 1995, *ApJ*, **S 98**, 617
- Tomkin J., Lemke M., Lambert D.L., Sneden C. 1992, *AJ*, **104**, 1568
- Travaglio C., Gali D., Gallino R., Busso M., Ferrini F., Straniero O. 1999, *ApJ*, **521**, 691
- Travaglio C., Gali D., Burkert A. 2000, *astro-ph/0009165*
- Travaglio C., Gallino R., Busso M., Gratton R. 2001, *ApJ*, **549**, 346
- Truran J.W. 1981, *A&A*, **97**, 391
- Tsymbal V.V. 1996, *Model Atmospheres and Spectrum Synthesis, ASP Conf. Ser.* **108**, 198
- Tsujimoto T., Shigeyama T., Yoshii Y. 2000, 35th Liege Int.Astroph. Coll. The galactic halo: from globular clusters to field stars, Eds.A.Noels, P.Magain, D.Caro, E.Jehin, G Parmentier, A.Thoul. P. 51
- Walker T.P., Steigman G., Schramm D.N., Olive K.A., Kang H. 1991, *ApJ*, **376**, 51
- Westin J., Sneden C., Gustafsson B., Cowan J. 2000, *ApJ*, **530**, 783
- Woosley S.E., Weaver T.A. 1995, *ApJS* **101**, 181

INFREDED SPECTRA OF COOL STARS – NATURE AND MODELS (Review)

Ya.V. Pavlenko

Main Astronomical Observatory of National Academy of Sciences
Kyiv-127, 03680 Ukraine *E-mail:* yp@mao.kiev.ua

ABSTRACT. Problems of modeling of IR spectra of the cool stars are discussed. Some results for M-giants, C-giants, peculiar stars and brown dwarfs are shown.

Key words: Infrared spectra, M-dwarfs, L-dwarfs, synthetic spectra, Sakurai's spectra

1. Water spectra of M-dwarfs

More than 70% of stars in the vicinity of the Sun are M dwarfs. These numerous low-mass stars ($0.08 M_{\odot} \leq M < 0.6 M_{\odot}$), together with substellar objects - brown dwarfs ($M \leq 0.08 M_{\odot}$) can contain an appreciable amount of the baryonic matter in the Galaxy. Research of M dwarf spectra are of interest for many branches of modern astrophysics. Verification of the theory of stellar evolution and structure of stars, the detection among M dwarfs of a subset of young brown dwarfs, the physical state of plasma of their atmospheres at low temperatures, as well as the chemical and physical processes of dust formation are only a few of them.

The dominant opacity sources in the optical and IR spectra of M dwarfs are electronic band systems of diatomic molecules, such as TiO and VO, as well as rotational-vibrational bands of H₂O. H₂O provide special interest for modern astrophysics. Long history of H₂O band modelling in stellar spectra is described elsewhere (see Pavlenko 2002 and references therein).

Recently Jones et al. (2002) carried out a number of different tests on the fits of observed spectra of M-dwarf in order to find preferred model fits. For every spectrum they carry out the minimisation of a 3D function $S = f(x_s, x_f, x_w) = 1/N \times \sum (1 - F_{obs}/F_{syn})^2$, where F_{obs} , F_{syn} are observed and computed fluxes, N is the number of points in observed spectrum to be fitted, x_s , x_f , x_w are relative shift in wavelength scale, a normalisation factor which was used to coincide observed and computed spectra and parameter of instrumental broadening, respectively. As input data Jones et al. (2002) used AMES line lists of H₂O (Partridge & Schwenke 1998), CO (Goorvich 1984) and NEXTGEN model atmospheres of Hauschildt et al. (1999).

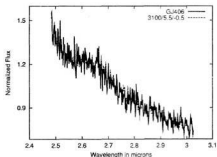


Figure 1: The observed spectrum of GJ 406 compared to a 3100 K, $\log g = 5.5$, solar metallicity synthetic spectrum. See Jones et al. (2002) for more details.

Fits to observed spectrum of late spectral type dwarf GJ 406 with strong water bands in the IR are shown in Fig. 1.

2. M-dwarfs. CO spectra

M dwarf infrared spectra additionally contain absorption bands of CO. One of most promising observational regions is located in the K band from 2.2 to 2.4 μm . Second overtone bands $^{12}\text{C}^{16}\text{O}$ and $^{13}\text{C}^{16}\text{O}$ are located here. As well as parameters such as effective temperature and gravity, they can be used for determination of carbon and oxygen abundances and the $^{12}\text{C}/^{13}\text{C}$ ratio in atmospheres of late-type stars. The determination of the $^{12}\text{C}/^{13}\text{C}$ ratio in M dwarf atmospheres is especially interesting. The ratio is a good age indicator for more massive ($M > 1 M_{\odot}$) late-type stars. Following the conventional theory of stellar evolution (see Aller & McLaughlin 1965), M dwarfs save their initial $^{12}\text{C}/^{13}\text{C}$ from their time of formation. Since the

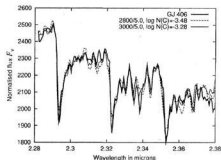


Figure 2: Fit to observed spectrum of GJ406. Synthetic spectra are shown for $T_{\text{eff}} = 2800$ and 3000 K for NEXTGEN model atmosphere (Haushildt et al 1999), line lists of H_2O (Partridge & Schwenke 1998), CO (Goorvich 1994) and VALD (Kupka et al. 1999).

galactic $^{12}\text{C}/^{13}\text{C}$ ratio is expected to change by around a factor of four over the lifetime of the galaxy, the determination of the $^{12}\text{C}/^{13}\text{C}$ ratio for M dwarfs potentially gives a strong constraint on their age. Then, atmospheric models need to include additional physical processes in their prescription for mixing between nucleosynthetic cores and observable atmospheres (Palla et al. 2000). On the other hand, M-dwarfs are not expected to modify their $^{12}\text{C}/^{13}\text{C}$ and are fully convective. Thus the $^{12}\text{C}/^{13}\text{C}$ ratios for a diverse sample of M dwarfs is expected to be a relatively straight-forward function of time and galactic location. However, determining the $^{12}\text{C}/^{13}\text{C}$ ratio is only a strong constraint on age if that ratio is a single-valued function of time and Galactic location. If that underlying assumption is not valid, any dispersion of $^{12}\text{C}/^{13}\text{C}$ in M-dwarf atmospheres might give for us some evidences about mixing processes inside our Galaxy. Unfortunately, due to the technical reasons we can carry out the analysis only for dwarfs of the solar vicinity.

Recently Pavlenko & Jones (2002) performed an extended study of formation of CO bands in atmospheres of late M-dwarfs. Namely, the best fit for M-dwarf GJ 406 was found for 2800 K for the solar abundance case, and 3000 K for $\log N(\text{C}) = -3.28$, Fig. 2. The new estimation of effective temperature corresponds better with empirical values for the effective temperature of the spectral class M6V than the Jones et al. (2002) analysis found using a similar technique but using a region dominated by water vapour. Best fits for GJ406 are found for solar metallicity rather than the metal poor result found by Jones et al. (2002).

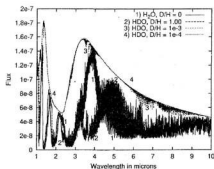


Figure 3: HDO and H_2O molecular bands computed for different D/H for $1200/5.0$ model atmospheres.

3. Brown dwarfs. Deuterium test

Lithium depletion takes place pre-main sequence stars and massive brown dwarfs when the temperature in the core is high enough ($T \sim 2.5 \cdot 10^6$ K) to produce the following reaction $\text{Li}(p,\alpha)^4\text{He}$. Less massive brown dwarfs ($M < 0.060 M_{\odot}$) are unable to reach these temperatures in their interior and this fact has been used to define a substellar criterion by the presence of Li in the atmosphere of these objects, the so called "Lithium test" (Rebolo et al. 1992). This test has been widely proved to determine the true substellar nature of several brown dwarfs (Rebolo et al. 1996, Ruiz et al. 1997, Martin et al. 1998). Additionally the frontier of objects which burn lithium and those less massive which have not yet depleted it (Lithium Depletion Boundary, LDB) provide an alternative method to date clusters younger than 150 Myr (Martin et al. 1998; Stauffer et al. 1998, 1999; Basri & Martin, 1999).

Deuterium is an element which can be depleted at lower temperatures than Lithium ($T \sim 8 \cdot 10^5$ K) in the fusion reaction $\text{D}(p,^3\text{He})$. That means that objects below a mass around $0.011-0.013 M_{\odot}$ (Saumon et al. 1996, Burrows et al. 1997, Chabrier et al. 2000) should preserve their deuterium from the time of formation. Those objects will never burn any element and several authors established at this frontier the separation between brown dwarfs and planets (Saumon et al. 1996). Following the same arguments than in the case of lithium, the "deuterium test" have been recently proposed (Béjar et al. 1999, Chabrier et al. 2000) to discriminate between substellar objects and stars which have burned their deuterium in less than $1-3$ Myr (D'Antona & Mazitelly 1998, Chabrier et al. 2000). This deuterium test, if applicable in practice,

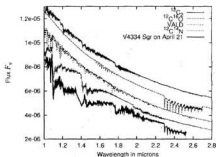


Figure 4: Strongest absorption features identifications in the 1.0-2.5 μm spectrum of Sakurai's Object spectra during 1997, computed for $T_{\text{eff}}/\log g = 5500/0.0$ model atmosphere of Asplund et al. (1999) abundances. Spectra are artificially shifted on the y-axis. See Pavlenko & Geballe for more details.

will provide a tool to date cluster younger than 50 Myr, including those younger than 7 Myr, in which the lithium dating is no longer valid, because all the stars preserve their initial content (D'Antona & Mazitella 1998, Chabrier et al. 2000).

In Fig.3 we show some spectral energy distributions of ultracool dwarf of $T_{\text{eff}} = 1200$ K, $\log g = 5.0$ from a grid of "dusty" C-models of Tsuji (1999) and Shchwenke and Partridge (1998) list of H_2O and HDO lines. Chemical equilibrium of HDO and H_2O were computed using information of molecular levels of H_2O in AMES database (Shchwenke and Partridge 1998). Synthetic spectra were computed by program WITA6 with step 0.05 nm and then convolved with gaussian of 1 nm. SEDs were computed for different D/O ratios (see Pavlenko 2002c for more details).

It's worth to note:

- Bands of HDO are shifted in the IR region in respect to H_2O bands.
- The best regions for D/H ratio determinations are 3.5-4, 6-7 microns as well as a region around 8 micron.

4. Sakurai's object

V4334 Sgr (Sakurai's Object), the "novalike object in Sagittarius" discovered by Y. Sakurai on February 20, 1996 (Nakano et al. 1996) is a very rare example of extremely fast evolution of a star during a very late final helium-burning event (Duerbeck & Benetti 1996). During the first few months after discovery,

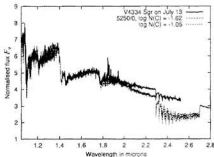


Figure 5: Fits to IR SEDs of V4334 Sgr in 1997.

Sakurai's Object increased in visual brightness to $V \sim 12^m$. In 1997 it increased further to $V \sim 11^m$. In March 1997 the first evidence of dust formation was seen (Kimeswenger et al. 1997, Kamath & Ashok 1999, Kerber et al. 2000). In early 1998 the optical brightness of Sakurai's Object decreased (dimming first reported by Liller et al. 1998), but then recovered. However, during the second half of 1998 an avalanche-like growth of the dusty envelope occurred, causing a rapid decrease in optical brightness and the complete visual disappearance of the star in 1999. At present essentially only thermal emission by dust can be observed (Geballe et al. 2002). Our view of the born again star has been completely obscured by the dust it has produced.

IR spectra of Sakurai's object is governed by absorption of a few molecules (4). Fits of theoretical SEDs to observed in 1997 - 1998 ones allow us to determine T_{eff} and $E_{\text{B-V}}$ of Sakurai's object at the latest stages of its evolution (Fig. 5 in the frame of self-consistent approach (Pavlenko et al. 2000, Pavlenko & Duerbeck 2001, Pavlenko & Geballe 2002). Fits to IR spectra allows to clearly determine an infrared excess due to emission of hot ($T > 1000$ K) dust (Fig.5. see Pavlenko & Geballe 2002 for more details).

Acknowledgements. I would like to thank Drs. Hugh Jones (Astrophysical Research Institute of Liverpool University) Rafael Rebolo and Victor Bejar (Instituto Astrofísica de Canarias), Thomas Geballe (Gemini Observatory), David Schwenke and David Goorvich (AMES) for fruitful collaboration.

References

- Aller, L.H., McLaughlin, D.B. (1965). *Stellar structure*. The University Chicago Press. Chicago and London. 1

- Asplund, M., Lambert, D.L., Kipper, T., Pollacco, D., Shetrone, M.D. (1999), *A&A* **343**, 507.
- Basri, G., Martín E.L. (1999) *ApJ* **510**, 266.
- Bejar, V.J.S., Zapatero Osorio, M.R., Rebolo, R. (1999) *ApJ*, **521**, 671.
- Burrows, A., Marley, Hubbard, W.B. et al. (1997) *ApJ* **491**, 856.
- Duerbeck, H.W. & Benetti, S. (1996), *ApJ*, **468**, L111.
- Chabrier, G., Baraffe, I., Allard, A., Hauschildt, P. (2000) *A&A*, **542**, L122.
- D'Antona, F., Mazzitelli, I. (1998) *Brown Dwarfs and Extrasolar Planets*, Eds. R. Rebolo, E. Martín, M.R. Zapatero Osorio (ASP Conference Series), 442.
- Geballe, T.G., Evans, A., Smalley, B., Eyres, S.P.S. (2002), *Astrophys. Space Sci.*, in press.
- Goorvitch, D. (1994), *Ap.J.Suppl.Ser.*, **95**, 535.
- Hauschildt, P., Allard, F., Baron, E. (1999) *ApJ*, **512**, 377.
- Jones, Hugh R.A., Pavlenko, Yakiv, Viti, Serena, Tenynson, Jonathan. (2002) *MNRAS*, **330**, 675.
- Kamath, U.S., Ashok, N.M. (1999), *MNRAS* **302**, 512.
- Kerber, F., Palsa, R., Köppen, J., Blöcker, T., Rosa, M.R. (2000), *ESO Messenger*, **101**, 212.
- Kimeswenger, S., Gratl, H., Kerber, F., Fouqué, P., Kohle, S. Steele, S. (1997), *IAU Circ.*, 6608.
- Kupka, F., Piskunov, N., Ryabchikova, T. A., Stempels, H. C., Weiss, W. W. (1999), *Astron. & Astroph. Suppl.* **138**, 119.
- Liller, W., Janson, M., Duerbeck, H.W., van Genderen, A.M. (1998), *IAU Circ.*, 6825.
- Martín, E.L., Basri, G., Gallegos, J.E. et al. (1998) *ApJ*, **499**, L61.
- Nakano, S., Sakurai, Y., et al. (1996) *IAU Circ.* 6322.
- Pall, F., Bachiller, R., Stanghellini, L., Tosi, M., Galli, D., (2000) *A&A*, **355**, 69.
- Partridge, H., Schwenke, D.J. (1997) *Chem. Phys.* **106**, 4618.
- Pavlenko, Ya.V., Yakovina, L.A., Duerbeck, H.W. (2000), *it A&A* **354**, 229.
- Pavlenko, Ya.V. & Duerbeck, H.W. (2001), *A&A*, **367**, 933.
- Pavlenko, Ya.V. & Geballe, T. (2002), *A&A*, **390**, 621.
- Pavlenko, Ya.V. (2002) *Astron. Rept.* **46**, 567.
- Pavlenko, Ya.V. & Jones, H.R.A. (2002) *A&A*, accepted (astro-ph 0210017).
- Rebolo, R., Martín, E.L., Magazzù, A. (1992) *Ap.J.* **389**, L83.
- Rebolo, R., Martín, E.L., Basri, G., Marcy, G.V., Zapatero Osorio, M.R. (1996) *ApJ* **469**, L53.
- Ruiz, M.T., Leggett, S.K., Allard, F. (1997) *ApJ* **491**, L107.
- Saunon, D., Hubbard, W.B., Burrows, A., Gulliot, T., Lunine, J.I., Chabrier, G., (1996), *ApJ* **460**, 999.
- Stauffer, J., Schultz, G., Kirkpatrick, J.D. (1998) *ApJ* **499**, L199.
- Stauffer, J. Barrado y Navascues, D. Bouvier, J. et al., 1999 *ApJ* **527**, 219.

SOME FEATURES OF roAp STARS SPECTRUM

A.V. Shavrina¹, N.S. Polosukhina², V.V. Tsymbal³,
Ya.V. Pavlenko⁴, A.V. Yushchenko⁴, V.F. Gopka⁵, A.A. Veles¹

¹Main Astronomical Observatory of NAS of Ukraine
Golosiivo, 03650, Kyiv, Ukraine, *shavrina@mao.kiev.ua*

²Crimean Astrophysical Observatory, Nauchnyj, Crimea, Ukraine

³Tavrian National University, Simferopol, Ukraine

⁴Astronomical observatory, Odessa National University
65014, park Shevchenko, Odessa, Ukraine;
Chonbuk National University, (South) Korea

⁵Astronomical observatory, Odessa National University
65014, park Shevchenko, Odessa, Ukraine

ABSTRACT. We have shown the possibility for modelling Li blend 6708 Å for two roAp stars, HD83368 and HD60435, taking into account lithium spots on the surfaces of these rotating stars. REE spots were also included in calculations. Slow rotating star HD101065 (Przybyslski's star) give the possibility of scrupulous identification of REE lines blending Li line and estimation of 6Li/7Li ratio.

Key words: Stars: chemically peculiar; individual: HD83368, HD60435, HD101065 stars: individual: HD83368, HD60435, HD101065.

1. Introduction

The chemically peculiar stars possess unusual individual characteristics, first of all, such chemical anomalies as high abundance of heavy elements, particularly of rare elements, sufficiently strong magnetic field, unhomogenous distribution of chemical elements on the star surface. The method of Doppler imaging, applied to some stars, shows that chemical anomalies are distributed in spots, rings, connected apparently with magnetic field structure (Hatzes, 1991). Some of these roAp stars are characterized by non-radial pulsations on time scale of minutes, tens of minutes (Kurtz, 1990).

The big range of the lithium line intensity in the spectra of CP stars (Faraggiana et al., 1996; Hack et al., 1997) is an evidence of the complexity of the physical nature of these stars. Until now there is no theory which can explain this phenomenon. The behaviour of the Li line at 6708 Å in spectra of several magnetic CP stars is studied in the framework of international project "Lithium in CP stars".

2. Lithium spots in two roAp stars: HD83368 and HD60435.

A different behaviour of the 6708 Å line can be explained in terms of the oblique rotator model and occurrence of Li spots at the magnetic poles. In general, the line profile variations seen in CP stars are due to abundance inhomogeneities on the surface of a rotating star.

We calculated the synthetic spectra in the range 6675–6735Å and 6112–6174 Å with the help of "STARSP" and "ROTATE" code developed by V. Tsymbal (see Tsymbal, 1994; Shavrina et al., 2000). The last code was modified by A. Yushchenko. The Kurucz's model atmospheres were used (Kurucz, 1993). We carried out the model calculation of lithium line 6708 Å forming in two lithium spots, using observed by P. North (see Shavrina et al. 2000) spectra for different rotation phases (7 phases for HD 60435 and 8 phases for HD 83368) with spectral resolution 100000. We used a method of direct modelling, based on Doppler variations of the Li line profile at 6708 Å for rotating star. Computations of spots' parameters (size, location and elemental abundance) were performed with Tsymbal's ROTATE code (see Polosukhina et al. 2000), which allows to calculate the photosphere plus spots line profiles for rotating star.

Preliminary consideration of Li profile changes with phases and further modelling shows that while the behaviour of the Li line for HD 83368 we can describe with two spots, of the same size, near the magnetic poles and at opposite places of the star's surface, the spots on the surface of HD 60435 do not lie on the opposite sides and/or are not of the same size. The next results are obtained for HD83368 using the atmo-

sphere model with $T_{eff} = 7750K$, $\log g = 4.0$ and values of parameters: $i = 90^\circ$, $v_e = -35km s^{-1}$,

- the spot 1: $l = 337^\circ$, $\varphi = 0^\circ$, $R = 35^\circ$, $\varepsilon_{Li} = -7.23$;
- the spot 2: $l = 173^\circ$, $\varphi = 0^\circ$, $R = 33^\circ.5$, $\varepsilon_{Li} = -7.13$.

The resulting lithium spots parameters for HD60435 are:

- spot 1: $l_1 = 205 \pm 10^\circ$, $\varphi = 15 \pm 5^\circ$, $R = 40 \pm 7^\circ$, $\log(N_{Li}/N_H) = -9.3 \pm 0.2$.
- spot 2: $l_2 = 11 \pm 6^\circ$, $\varphi = -15 \pm 5^\circ$, $R = 44 \pm 3^\circ$, $\log(N_{Li}/N_H) = -8.2 \pm 0.2$.

The observed and calculated Li line profiles with parameters given above are shown in Fig.1. Fig.2 shows observed and calculated spectra for one phase for each star when calculation included REE spots, parameters of which were also found. We also have calculated the profiles of Pr III lines 6160 Å 6161 Å (Fig.3) and Eu II 6645 Å (Fig.4). Spot parameters obtained from these lines are agreed good with results of REE lines, blending Li doublet line 6708 Å as it is seen from the table.

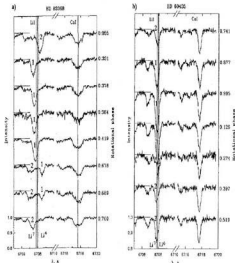


Figure 1: Observed (dots) and computed (solid curves) profiles at (a) eight rotational phases for HD 83368 and (b) seven rotational phases for HD 60435.

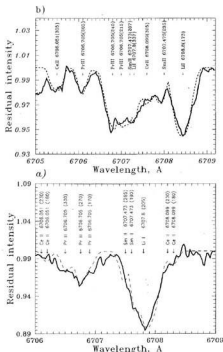


Figure 2: Observed and computed Li I 6708Å profiles for (a) HD 60435 (phase 0.743) and (b) HD 83368 (phase 0.689).

3. Przybylski's star (HD101065)

Following Cowley & Mathys (1998) and Cowley et al. (2000) we have undertaken the analysis of the spectrum near 6708Å of Przybylski's star (HD 101065, V816 Cen), which has the most unusual of all stellar spectra (Wegner et al. 1974; 1983). As it was noted by its discoverer, A. Przybylski (1961; 1966; 1977), the strongest spectral lines in the spectrum of HD 101065 generally belong to lanthanides. The strong complicated spectral feature at λ 6708Å in the observable spectra creates the problem of correct line identification in this region. The comprehensive analysis of REE lines was performed and the main contribution of lithium was shown for this blend. We have calculated the model atmosphere with $T_{eff} = 6600$ K and $\log g = 4.0$ and abundances from Cowley et al. (2000) with modified Kurucz's code ATLAS12 (Kurucz, 1999). The line opacity was accounted by "opac-

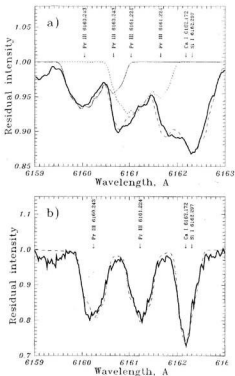


Figure 3: Observed (thick solid curves) and computed profiles of the Pr III 6160.2 Å and 6161.2 Å lines (a) for HD 83368 (phase 0.320), dotted and dashed lines correspond to contributions of two main spots, visible in this phase; (b) for HD 60435 (phase 0.005), here spot components are not resolved.

ity sampling" method using VALD (Kupka et al. 1999) and DREAM (Biemont et al.) line lists. The Kurucz's model of $T_{\text{eff}} = 6750$, $\log g = 4.0$ (Kurucz, 1993) was also used in calculations of synthetic spectra. The rotation line profile with $v \sin i = 3.5 \pm 0.5 \text{ km s}^{-1}$ and microturbulence velocity $V_{\text{micro}} = 2 \text{ km s}^{-1}$ were applied. T-P dependence for used models is shown in Fig.5 (upper).

We calculated the synthetic spectra in the range 6705.8-6708.7 Å with the help of "STARSP" and "ROTATE" (Tsymbal, 1994). Line list consisting of VALD (Kupka et al. 1999) and DREAM (for REE, Biemont et al.) lines and chemical element abundances from (Cowley, 2000) were used in synthetic spectra simulations. Some REE element abundances were changed for better agreement with observed spectrum, using pure

Table 1: REE spots data derived from line profiles for HD 83368

El, $\lambda_{\text{lab}}, \text{Å}$	$\lambda_{\text{obs}}, \text{Å}$	long, l_{sp}	R, R_{sp}	$\log N_{\text{El}},$ dex
Phase = 0.689 (248° .04)				
Ce II	6705.5	$305 \pm 10^\circ$	$30 \pm 10^\circ$	-8.5 ± 0.3
6706.051	6706.1	$240 \pm 10^\circ$	$10 \pm 10^\circ$	-8.1 ± 0.3
Ce II	6707.6	$305 \pm 10^\circ$	$26 \pm 10^\circ$	-8.5 ± 0.3
6708.099	6708.0	$250 \pm 10^\circ$	$15 \pm 10^\circ$	-8.2 ± 0.3
Pr III	6706.1	$305 \pm 10^\circ$	$15 \pm 10^\circ$	-8.8 ± 0.3
6706.705	6706.8	$240 \pm 10^\circ$	$30 \pm 10^\circ$	-8.5 ± 0.3
	6707.3	$195 \pm 10^\circ$	$15 \pm 10^\circ$	-8.0 ± 0.3
Sm II	6707.6	$235 \pm 10^\circ$	$20 \pm 10^\circ$	-8.2 ± 0.3
6707.473	6708.0	$207 \pm 10^\circ$	$20 \pm 10^\circ$	-7.8 ± 0.3
Phase = 0.768 (276° .48)				
Eu II	6644.5	$310 \pm 10^\circ$	$40 \pm 10^\circ$	-9.8 ± 0.3
6645.064	6645.2	$272 \pm 10^\circ$	$15 \pm 10^\circ$	-8.9 ± 0.3
	6645.5	$228 \pm 10^\circ$	$27 \pm 10^\circ$	-8.9 ± 0.3
Phase = 0.320 (115° .2)				
Pr III	6160.0	$145 \pm 10^\circ$	$25 \pm 10^\circ$	-8.0 ± 0.3
6160.243	6160.2	$120 \pm 10^\circ$	$15 \pm 10^\circ$	-8.0 ± 0.3
	6160.8	$65 \pm 10^\circ$	$20 \pm 10^\circ$	-8.3 ± 0.3
	6160.9	$45 \pm 10^\circ$	$20 \pm 10^\circ$	-8.3 ± 0.3
Pr III	6160.9	$145 \pm 10^\circ$	$25 \pm 10^\circ$	-8.0 ± 0.3
6161.224	6161.1	$120 \pm 10^\circ$	$15 \pm 10^\circ$	-8.0 ± 0.3
	6161.7	$65 \pm 10^\circ$	$20 \pm 10^\circ$	-8.3 ± 0.3
	6161.8	$45 \pm 10^\circ$	$20 \pm 10^\circ$	-8.3 ± 0.3

lines with known gf values. We calculated positions of additional REE lines on the base of NIST energy levels (<http://physics.nist.gov/cgi-bin/AtData>). Gf-values for such lines, which are rather distant from Li lines, were matched for better agreement with observed spectrum. Gf-values for 2 nearest to Li 6708 Å line, Nd II 67067.755 and Nd II 6708.03 were estimated by P. Quinet with Cowan's code. The line of Sm II, λ 6707.779 Å coincides almost with the centre of lithium blend, but unfortunately, the calculations for Sm II are not possible due to fact that the energy matrix dimensions exceed the permitted values. We tried to calculate the blend 6708 Å with SmII line absorption instead of Li lines, choosing gf values for Sm II line. Result fitting was bad (see Fig.2). Only the inclusion of ^7Li and ^6Li lines with ratio $^6\text{Li}/^7\text{Li} = 0.3$ allowed us to represent the observed blend profile rather well (see Fig.6).

We have considered the possibility to model the remarkable spectral feature 6708 Å for HD 101065 (Przybylski's star) in two ways - as a blend of Li and REE lines and as blend of REE lines only. We show by model calculations that Li lines absorb significantly in the range 6707.72 - 6708.02 Å and resulting Li abundance is 3.1 dex (in the scale $\lg N(\text{H})=12.0$), isotopic ratio $^6\text{Li}/^7\text{Li}$ is near to 0.3.

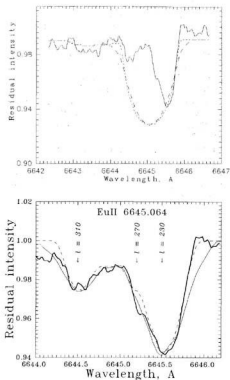


Figure 4: Eu II 6645.06A profiles for HD 83368 (phase 0.768); solid curve - the observed spectrum, dashed and dotted curves - the calculated spectra for 11 and 2 kG; upper - calculated profiles for all photosphere, $v_{\text{ sini}}=34$ km/s; lower - for two spots

Conclusion

Our line profile computation with Tsymbal's code ROTATE for a spotted stellar surface allowed us to derive the lithium and REE spot parameters: location, size, element abundance. As a rule it results in a good agreement between calculated and observed profiles for subsolar position of lithium spots. When the spots lie near the limb, however, it is difficult to achieve a good agreement due to a complicated blending with lines of other elements (mainly REE) and the weakness of the Li line. A similar problem was mentioned in other papers too with Piskunov's code (Kuschnig et al., 1999). Taking into calculations the REE spots we achieved a better representation of observed spectra for rotating roAp stars HD83368 ($V_{\text{ sini}}=34$ km/sec) and HD60435(11 km/sec).

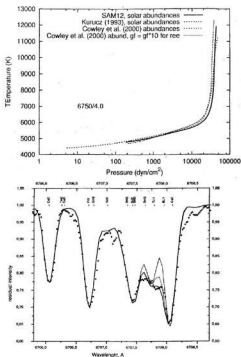


Figure 5: Upper: T-P dependence for model atmospheres, calculated by us and Kurucz's model from (Kurucz, 1993); lower: Li blend profiles, the dots - observed spectrum, dashed curve - calculated with 7Li only, thick curve - with ratio of $6\text{Li}/7\text{Li} = 0.33$. Thin curve - calculated spectrum without Li - with Sm II line 6707.799Å.

We have considered the possibility to model the remarkable spectral feature 6708Å for HD 101065 (Przybylski's star) in two ways - as a blend of Li and REE lines and as blend of REE lines only. We show by model calculations that Li lines absorb significantly in the range 6707.72 - 6708.02Å and resulting Li abundance is 3.1 dex (in the scale $\lg N(\text{H})=12.0$), isotopic ratio $^6\text{Li}/^7\text{Li}$ is near to 0.3. Our calculations and identifications of REE lines, additional to VALD and DREAM lists, demonstrate the necessity of gf values for them.

Acknowledgements. We are grateful to P. North for observed spectra, P. Quinet for calculated gf values for two lines of Nd II. The data from Kurucz's CDROM 23, ADC NASA, VALD, NIST, DREAM were used and we thank the administrations of these databases, obtainable through INTERNET. This work was partially supported by the grant of PostDoc Program, Chonbuk National University (Korea).

References

- Biemont E., Palmeri P. and Quinet P.: D.R.E.M. Database on Rare Earth at Mons. Univ., <http://www.umh.ac.be/astro/dream.shtml>.
- Cowley C.R., Mathys G.: 1998, *A&A*, **339**, 165.
- Cowley C.R., Ryabchikova T., Kupka F., Bord J.D., Mathys, G., Bidelman, W.P.: 2000, *MNRAS*, **317**, 299.
- Faraggiana R., Gerbaldi M., Delmas F.: 1996, *Ap&SS*, **238**, 169.
- Hack M., Polosuchina N.S., Malanushenko V., Castelli F.: 1997, *A&A*, **319**, 637.
- Hatzes A. P.: 1991, *MNRAS*, **253**, 89.
- Kupka F., Piskunov N.E., Ryabchikova T.A., Stempels H.C., Weiss W.W.: 1999, *A&AS*, **138**, 119.
- Kuschnig R., Ryabchikova T.A., Piskunov N.E., Weiss W.W., Gelbman M.J.: 1999, *A&A*, **348**, 924.
- Kurtz D.W.: 1990, *ARA&A*, **28**, 607.
- Kurucz R.L.: 1993, *CDROM13*, *CDROM23*.
- Kurucz R.: <http://cfaku5.harvard.edu>.
- <http://physics.nist.gov/cgi-bin/AtData>.
- Polosuchina N.S., Kurtz D., Hack M., North P., Ilyin I., Zverko J., Shakhovskoy D.: 1999, *A&A*, **351**, 283.
- Polosuchina N.S., Shavrina A.V., Hack M., Khalack V., Tsymbal V., North P.: 2000, *A&A*, **357**, 920.
- Przybylski A.: 1961, *Nature*, **189**, 739.
- Przybylski A.: 1966, *Nature*, **210**, 20.
- Przybylski A.: 1977, *MNRAS*, **178**, 71.
- Shavrina A.V., Polosuchina N.S., Tsymbal T., Khalack V.R. Quantitative analysis of the spectra of magnetic roAp star HD 83368 with "lithium" spots // *Astronomy Reports*: 2000, **44**, N 4, 235.
- Tsymbal V.V.: 1994, *Odessa Astron. Publ.*, **7**, part 2, 146.
- Wegner, G., Petford A.D.: 1974, *MNRAS*, **168**, 557.
- Wegner G., Cummins D., Burne P., Stickland D.: 1983, *Ap.J.*, **272**, 646.

GALAXIES AND THE INTERGALACTIC MEDIUM: EVOLUTIONARY INTERRELATIONS

B.M. Shustov

Institute of Astronomy of the RAS, Pyatnitskaya str. 48, Moscow, 119017, Russia
bshustov@inasan.ru

ABSTRACT. During their life galaxies exchange in matter and energy with the intergalactic medium (IGM). This complex process is a most important factor in galactic evolution as well in evolution of the IGM. In this paper recent progress in the IGM studies and mechanisms of mass gain and mass loss from galaxies are briefly reviewed. Using a model of chemo-dynamical evolution of galaxies I discuss enrichment of the IGM with metals and origin of the radial gradients of chemical composition in disk galaxies as possible consequence of heavy elements loss. The general conclusion is simple: many problems remain unsolved but we are under way to understanding of consistent evolution of galaxies – IGM system.

1. Introduction:

One of the most fundamental questions of galactic evolution can be formulated very simply – “what are main features of evolutionary interrelations galaxies – intergalactic medium?” This question is addressed to both groups of experts: cosmologists and astrophysicists. From the commonly used terminology the galactic history is divided in two eras (Hensler, 1987):

- the time before and during protogalactic clouds on galactic mass scale grow. In this era the matter can be considered as primordial gas that is a building material for the future (clusters of) galaxies;

- the time after these protogalactic clouds have commenced to collapse as isolated systems (in this era galaxies become a dominant baryonic structures in the Universe which strongly influence on the IGM).

First item is a subject of cosmological studies. The second one – lies mostly in the domain of astrophysics. Martin Rees noted (1985) that “galaxy formation straddles the interface between cosmology an astrophysics”. Recent observations and theoretical models brought valuable data about galactic evolution and arguments for considering the galactic evolution in consistence with evolution of the intergalactic medium (IGM). In this paper I

briefly review this issue drawing special attention to chemical evolution.

In Sect. 2 I introduce some general facts about the intergalactic medium. Mechanisms of interaction between galaxies and IGM are discussed in Sect. 3. In Sect. 4, a simple though powerful model of chemo-dynamical evolution of (disk) galaxies is introduced and two problems related to chemical interrelations between the IGM and galaxies: enrichment of the IGM and radial gradients of chemical abundances in disk galaxies are discussed.

2. Intergalactic medium before and after galaxy formation

2.1. IGM before formation of galaxies

With the expression “intergalactic medium” one indicates the material other than ordinary galaxies. This is some analogy between stars – interstellar medium (ISM) and galaxies – IGM. Astrophysicists do not classify the ISM in the stellar clusters as separate object though detailed classification of various circumstellar structures (shells, outflows etc.) is elaborated. In the case of IGM inside clusters of galaxies (remember that most of galaxies belong to some cluster, and in contrary most of stars in galaxies are those of field) we use the expression “intracluster medium” (ICM). The properties of the IGM drastically changed in the process of evolution of the Universe. I sketch the evolution just to introduce main ingredients of the IGM and their general interrelations with galactic evolution.

According to the conventional picture of Creation Myth (see Fig. 1) the smooth baryonic plasma consisted of hydrogen, helium and light elements, produced in the first three minutes after the Big Bang, and hot black body radiation filled the expanding Universe. After few hundreds thousands of years at epoch corresponding to $z \sim 1000$, the black-body radiation cooled below 3000 K and the plasma (primordial IGM) is expected to recombine and remain neutral until sources of radiation develop that are capable of reionizing it. Primordial IGM in this

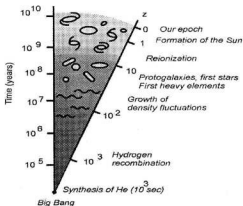


Figure 1: History of the Universe

epoch ("dark ages") consists of cool gas filled with ever-faded cosmic background radiation.

Information of great importance about this primordial IGM is coming from observation of cosmic microwave background. The observed features, imprinted at $z \sim 1000$, enable direct investigation of the formation of structure of the Universe as well as constraining the values of basic cosmological quantities such as the amounts of various forms of matter and vacuum energy in the Universe. The currently most favored theoretical model for describing our Universe is based on idea of inflation, which provides a natural mechanism for producing initial density fluctuation described by power-law spectrum and also predicts the Universe to be spatially flat. The initial spectrum of adiabatic density fluctuations is modulated through acoustic oscillations in the plasma phase prior to recombination and the resulting inhomogeneities are then imprinted as anisotropies in the CMB. In the inflationary scenario the CMB temperature anisotropies are predicted to follow a multivariate Gaussian distribution and so may completely described in terms of their angular power spectrum. Recent observation (Taylor et al. 2002) with the Very Small Array (a 14-element interferometer array installed at the Teide Observatory, Tenerife) at frequency 34 GHz on angular scales 3.6–0.4 degrees ($l = 150 - 900$) brought new confirmation of this theory. The power spectrum obtained (Scott et al. 2002) is in a very good agreement with the results of the BOOMERANG, DASI and MAXIMA telescopes. Combining the results obtained with all other CMB experiments and assuming the HST key project limits for H_0 Rubino-Martin et al. (2002) obtained the tight constraints for fundamental cosmological parameters.

In most of current models the contents of the Universe are divided into three components: ba-

ryonic (ordinary) matter, cold dark matter (CDM), which interacts with baryonic matter solely through its gravitational effect, and intrinsic vacuum energy. Some presence of so called warm dark matter is not excluded. Major difference between warm and cold dark matter is related to ability of weakly interacting particles, which the CDM or warm dark matter consists of, to wipe out part of the initial density fluctuations. For warm dark matter this scale of wiping out is much larger than for CDM. Durer&Novosyadly (2001) constructed a mixed dark matter model with some addition of massive neutrinos, which are assumed to be particles of warm dark matter. The general consensus is now almost universal that some variant of CDM including mixed models is probable. The present day contributions of these components to the overall density of the Universe are usually expressed in terms of the "omega parameter" $\Omega = \rho / \rho_{crit}$, where $\rho_{crit} = 3H_0^2 / (8\pi G) = h^2 1.88 \times 10^{-29} \text{ g cm}^{-3}$ is the critical density with H_0 the present day Hubble constant $H_0 = h \cdot 100 \text{ km s}^{-1} \text{ Mpc}^{-1}$ (most estimates of h lie in the range of 0.5–0.8). For our flat Universe $\Omega = 1$. Fundamental parameters of cosmological models are contribution in Ω by vacuum energy Ω_Λ , and matter Ω_m , which consists of contribution of baryonic matter Ω_b and cold dark matter Ω_{cdm} . Rubino-Martin et al (2002) derived: $\Omega_m = 0.28 (+0.07)$ and $\Omega_\Lambda = 0.72 (+0.07 - 0.13)$. Durer&Novosyadly (2001) give similar estimates, except additional term – the density of massive neutrinos $\Omega_\nu = 0.03 (+0.07 - 0.03)$.

The evolution of the primordial IGM up to the end of "dark ages" is characterized by growth of the density fluctuations that eventually brings to formation of (cluster of) protogalaxies. Due to progress in numerical and analytical modeling in last decade (see e.g. review of Bertschinger 1998) most of researchers accept that clustering of small scale CDM fluctuations leads in a natural way to formation of so called "dark matter haloes", which are spheroidal non-dissipative CDM structures, governing by their gravitation the evolution (gathering and virialization) of dissipative baryonic matter in the central areas of the haloes. In such a scenario diffusely distributed baryonic material responds to the gravitational influence of the underlying dark matter. The most overdense regions collapse first to form the earliest galaxies. This leaves the remaining gas as the IGM. Rather than being a uniform medium filling the space between galaxies, the IGM itself should show structure on scales larger than that of individual galaxies. (Clusters of) galaxies are forming in the central parts of the haloes. At the heart of the hierarchical clustering process lies the fact that galaxies tend to form first near high peaks of the density field because these are the first to collapse at any given epoch. This is known as "biased galaxy formation", because the

distribution of galaxies offers a biased view of the underlying distribution of mass. An important consequence of biased galaxy formation is that bright galaxies tend to be born in a highly clustered state that is strongly supported by observation (Benson et al. 2000, 2001).

It is a great challenge for scientists to find "exact" value of Ω_b , i.e. to estimate amount of ordinary (baryonic) matter. This value can be estimated for a given cosmological model by measuring of primordial abundance ratio D/H. Standard nucleosynthesis models together with recent observations of deuterium yield $Y=0.247\pm 0.02$ and $\Omega_b h^2=0.0193\pm 0.0014$ (Burles&Tytler 1999). As some of the baryons had already collapsed into galaxies at $z=2-10$, the value of $\Omega_b h^2=0.019$ should strictly be considered as an upper limit to the intergalactic density parameter.

More direct way is to estimate relevant contributions from observations of all baryonic components. The problem is that we can only observe part of baryonic matter. The cosmic density distribution of galaxies is related to the measured luminosity density $(1.7\pm 0.6)\times 10^7 L_{\odot} \text{Mpc}^{-3}$ in V-band. From mass-luminosity relation for galaxies the luminous matter density is estimated as $\Omega_{\text{gal}} h=0.002-0.006$ (Carr 1994). Other forms of baryonic matter are believed to be:

- Intergalactic gas
- Hot gas in the ICM observed in X-ray domain
- Dim stars (only low mass first generation stars can be considered), small planet- or comet-like bodies and cloudlets.

I briefly describe first two constituents of the IGM.

2.2. Intergalactic gas

According to results of Burles and Tytler (1999) the proper mean density of hydrogen nuclei at redshift z may be expressed in standard cosmological terms as $n_p=1.6\times 10^{-7} \text{cm}^{-3} (\Omega_b h^2/0.019)(1+z)^3$. Cosmological models predict that most of the intergalactic hydrogen was reionized by the first generation of stars or quasars at $z=7$ or larger (this is considered as a workable definition of the "end of dark ages"). The process of reionization began as individual sources started to generate expanding HII regions surrounding IGM. As more and more sources of ultraviolet radiation switched on, the ionized volume grew in size. The reionization ended when the cosmological H II regions overlapped and filled the intergalactic space. The lack of smooth Ly-alpha absorption by HI in quasar spectra (Gunn&Peterson, 1965) led to the conclusion that diffusely distributed hydrogen is totally ionized at relevant z . From other side numerous absorption features ("Lyman alpha forest") clearly evidence for existence of clouds of neutral hydrogen in all range of z for quasars.

The term 'Ly-alpha forest' is used to denote the huge amount of narrow absorption lines whose

measured equivalent widths imply N_{HI} ranging from $\sim 10^{17} \text{cm}^{-2}$ down to 10^{21}cm^{-2} . A comprehensive review of properties of these absorbers is given by Rauch (1988). (An example of hydrogen Ly- α forest, observed with Keck telescope is shown below in Fig. 3.) Other class of intervening absorbers having a neutral hydrogen column density exceeding $2\times 10^{21} \text{cm}^{-2}$ are optically thick to photons having energy greater than 13.6 eV and produces a discontinuity at the hydrogen Lyman limit, i.e. at an observed wavelength of $912(1+z)\text{\AA}$. These scarcer objects (Lyman Limit Systems -LLS) are associated with the extended gaseous haloes of bright galaxies near the line of sight. It is a reasonable approximation to use for the distribution of absorbers along the line of sight: $f(N_{\text{HI}},z)=A\cdot N_{\text{HI}}^{-1}\cdot(1+z)^{\gamma}$. The function of column density appears to provide at high redshift a surprisingly good description over 9 decades in N_{HI} , i.e. from 10^{17} to 10^{21}cm^{-2} . The γ is different for Ly- α clouds ($\gamma=2.8$) and for LSS ($\gamma=1.5$). Typical normalization value $\alpha A=4\times 10^7$ per unit redshift at $z=3$ produces 3 LLSs and ~ 150 forest lines above $N_{\text{HI}}=10^{21}\text{cm}^{-2}$. In "Damped Ly-alpha Systems" (DLA) the HI column density is so large ($N_{\text{HI}}\rightarrow 10^{20} \text{cm}^{-2}$, comparable with the interstellar surface density of spiral galaxies today) that the radiation damping wings of the Ly- α line profile become detectable. While relatively rare, damped systems account for most of the neutral hydrogen seen at high redshifts.

All Ly- α absorbers observed up to redshifts larger than 5 are believed to trace the potential wells of the dark matter. Except at the highest column densities, discrete absorbers are inferred to be strongly photoionized.

The most important outstanding issue regarding the DLA concerns their relationship with galaxies, though it is open question. Lanzetta et al. (1995) noted that while it is known that at least some DLA systems arise in galaxies, it is not known what range of properties (in terms, for example, of morphological type, luminosity, and surface brightness) are spanned by the absorbing galaxies, or even whether all DLAs arise in galaxies. Part of the difficulty is that the high neutral hydrogen column densities of damped Ly- α absorption systems imply small impact parameters to the lines of sight, and it is difficult to identify faint galaxies at small angular separations to bright quasars.

Pichon et al. (2001) analyzed the structure of the IGM using information on Ly- α forest from the spectra of QSO HE1122-1628 obtained with VLT/UVES and new inversion method. This method was applied to recover the temperature of the gas and underlying density field and to obtain 3D spatial distribution of the IGM from 1D information along grid of lines of sight. To test the method Pichon et al. (2001) simulated 3D distribution of

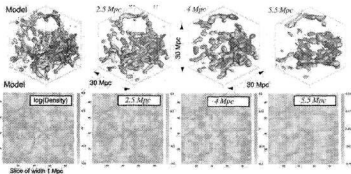


Figure 2: Top panels: the model of the IGM and the reconstructed density for distances between lines of sight 2.5, 4 and 5.5 Mpc. Bottom panels – a slice of $1 \times 80 \times 80$ Mpc across the simulation and the reconstructed fields (the scale on the panels is in pixels) (from Pichon et al. 2001).

CDM and used the restoring technique (see Fig. 2). The technique seems to be tested successfully.

Helium is probably not reionized until $z \sim 3$, as inferred from the strong HeII Ly- α absorption depressions due to Gunn-Peterson effect at $(304 \text{ \AA})(1+z)$ in the UV spectra of high- z QSOs. This absorption was first observed (Heap et al. 1999) with HST spectrometer STIS along line of sight to the quasar Q0302-003 ($z=3.29$) (see Fig. 3).

It is an interesting discussion (see in Kriss et al. 2001) if HeII is smoothly distributed over the IGM or the depression at $(304 \text{ \AA})(1+z)$ in the UV spectra of this and other quasars is caused by HeII

located in HI Ly- α absorbers and not resolved in spectra as HeII Ly- α forest only because of poor spectral resolution of UV telescopes. Kriss et al. (2001) probably elucidated the problem. They presented the FUSE observations of the line of sight to the quasar HE2347-432 in 1000-1187 \AA band at a resolving power 15000 (Fig. 4). The HeII Ly- α absorption was resolved as discrete forest of absorption lines at redshift range 2.3 to 2.7. About half of these features have HI counterparts with column densities $N_{\text{HI}} > 10^{21.5} \text{ cm}^{-2}$. The HeII to HI column density ratio ranges from 1 to >1000 with an average ~ 80 . These data strongly support models of photoionization mechanism of reionization of the IGM by integrated light from quasars propagated through the IGM (Madau et al., 1999; Fardal et al. 1998), which predict values of $N_{\text{HeII}}/N_{\text{HI}} \sim 30-100$ for quasar spectra with the spectral indices $q=1.5$ to 2.1 ($f_{\text{UV}} \sim v^q$). Intrinsic spectral indices for quasars (as measured down to $\sim 350 \text{ \AA}$) lie in this range (Zheng et al. 1997). Recently Telfer et al. (2002) used a sample of 332 HST of 184 QSOs with $z > 0.33$ to study the typical ultraviolet spectral properties of QSOs, with emphasis on the ionizing continuum. The sample is nearly twice as large as that from work by Zheng et al. (1997) and provides much better spectral coverage in the extreme-ultraviolet (EUV). The overall composite continuum can be described by a power law with index $\gamma_{\text{EUV}} = -1.76 \pm 0.12$ ($f_{\nu} \sim \nu^{-\gamma}$) between 500 and 1200 \AA . Ratios >100 (about 40%) indicate that localized regions of the IGM are photoionised by softer spectra. This may be additional contributions from starburst galaxies or heavily filtered quasar radiation. The 304 \AA (Ly- α) lines of He II can be used to probe low-density regions of the IGM, particularly the void-like gaseous structures in the baryon distribution that develop in concert with

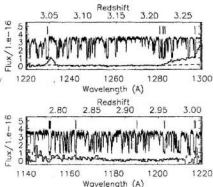


Figure 3: The HST/STIS spectrum (solid line at bottom) of the quasar Q0302 shows HeII absorption shortward of 1300 \AA (Heap et al. 1999) with superposed higher resolution spectrum of HI Ly- α from Keck/HIRES. The HI Ly- α were normalized and multiplied by 0.25 in wavelength to match the HeII wavelength scale (from Shull et al. 1999).

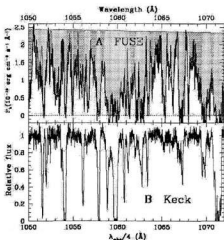


Figure 4: The upper part is a portion of the FUSE spectrum of HE2347-4342. The smooth curve across the top is the extrapolated continuum. The light-shaded area shows the fraction of the HeII opacity due to absorption features that correspond to HI absorption lines identified in the Keck spectrum (bottom). The area shaded in green shows the fraction of the opacity due to additional HeII absorption features that have no HI counterparts in the Keck spectrum. (Kriss et al. 2001).

the large-scale structures in dark matter and the reionization. The presence of HeII Ly- α absorbers with no HI counterparts indicates that that structure is common even in low-density regions. This is consistent with hydrodynamic models that predict density fluctuations due to gravitational instabilities on all scales, from the high density peaks that form galaxies to the distribution of gas in low-density voids (Hui&Gnedin 1997, Cen&Ostriker 1999).

The cloud structure is seen not only for HI and HeII but also for some highly ionized ions (e.g. OVI). Tripp et al. (2000) observed OVI absorption lines in spectrum of quasar H1821+643 (Fig. 5). The number density of OVI absorbers with rest equivalent width >30 mÅ in the H1821+643 spectrum is remarkably high (>17). The cosmological mass density of the hot matter (under assumption that metallicity is of 1/10 solar and the fraction of oxygen in the OIV ionization stage is 0.2) is estimated as $\Omega_b h^2 = 0.003$. This is comparable to the combined cosmological mass density of stars and cool gas in galaxies and X-ray emitting gas in galaxy clusters at low redshift.

Establishing the epoch of reionization and reheating is crucial for determining its impact on several key cosmological issues, from the role reionization plays in allowing protogalactic objects to cool and make stars to determining the small-scale structure in the temperature fluctuations of the cosmic background radiation. Conversely, probing the reionization epoch may provide a means for constraining competing models for the formation of cosmic structures and for detecting the onset of the first generation of stars, galaxies and black holes in the Universe.

The metallicity of the IGM is not unified. The typical metallicities range from 0.3% to 1% of solar values as derived from observations of Ly- α forest absorbers (Rauch 1998). It can be measured from the strong UV resonance lines such as CIV $\lambda 1549$, Si IV $\lambda 1400$, CIII $\lambda 977$, SiIII $\lambda 1206$, OVI $\lambda 1035$. Shull et al. (1999) remark that these UV resonance lines are the most sensitive abundance indicators available in astrophysics, and they are widely used as abundance indicators in stars, in the low-redshift interstellar medium, and in the high-redshift IGM. Current evidence at high redshift suggests that C IV/Si IV abundance ratios shift at $z \sim 3$, possibly due to a spectral renaissance stimulated by the breakthrough

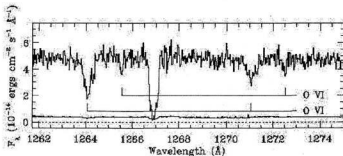


Figure 5: Spectrum of quasar H1821+643 showing the strong OVI absorption lines at $z = 0.22497$ and the weaker absorber at $z = 0.22637$. The calibrated flux is plotted vs. observed heliocentric wavelength, and the solid line near zero is the 1s flux uncertainty (Tripp et al., 2000).

and overlap of the cosmological He II ionization fronts from QSOs and starburst sources (Giroux & Shull 1997). Songaila (2001) using observation of 32 quasars with emission redshift in range 2.31–5.86 studied evolution of the intergalactic metal density at high z . The CIV column density distribution function appeared to be invariant throughout the whole z -range. The metallicity at $z=5$ exceeds 3.5×10^{-4} , which in turn implies that massive star formation took place beyond this redshift.

Important property of the damped Ly- α absorption systems is that they are predominantly neutral (neutral hydrogen and singly-ionized heavy elements are the dominant ionization species), allowing for heavy element abundances to be measured without the need of applying large ionization corrections. Absorption lines from low-abundance singly-ionized species, including transitions of Ti II, Cr II, Ni II and Zn II, are of particular importance because they are usually unsaturated (or only mildly saturated), allowing accurate column densities to be measured. The typical metallicities for DLA systems are about 10% of solar and do not evolve significantly over a redshift interval $0.5 < z < 4$ during which most of today's stars were actually formed (Lanzetta et al. 1995). Clearly, these metals were produced in stars that formed in a denser environment; the metal-enriched gas was then expelled from the regions of star formation into the IGM but it is striking that there is no pronounced trend for heavy element abundances to increase with decreasing redshift, and in particular no trend for heavy element abundances to approach solar values at redshifts $z=0$, as would be expected under scenarios of chemical evolution due to the conversion of gas into stars. It is not yet clear how to interpret these results.

2.3. Hot gas and other constituents of the ICM

It is well established (see e.g. White et al. 1993, David 1997), that the x-ray hot gas is the main "visible" component of clusters of galaxies, its total mass varies from 1 (groups) to 7 (rich clusters) times the stellar mass present in cluster galaxies and it can reach up to 30% of the total cluster mass: "visible" plus dark matter (see Fig. 6). Such a high gas mass fraction has been deemed "the baryon catastrophe" (White et al. 1993), since it is inconsistent with $\Omega_m = 1$ and Big Bang nucleosynthesis calculations (Walker et al. 1991). However, if $\Omega_m = 0.2$, then the inferred baryon density is 6% of the critical density, which is consistent with Big Bang nucleosynthesis. ROSAT observations have shown that groups of galaxies contain significantly less hot gas than rich clusters (Mulchaey et al. 1996). In general, the mass fraction of hot gas increases from 2% in ellipticals, to 10% in groups, and up to 30% in rich

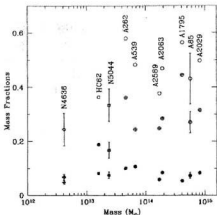


Figure 6: Mass fraction of stars ($M_{\text{stars}}/M_{\text{tot}}$; filled symbols), stars plus gas ($(M_{\text{stars}} + M_{\text{gas}})/M_{\text{tot}}$; crosses in open symbols), and stars plus gas plus MACHOs ($(M_{\text{stars}} + M_{\text{gas}} + M_{\text{MACHO}})/M_{\text{tot}}$; open symbols). Ellipticals are indicated by diamonds, groups of galaxies by squares, and rich clusters of galaxies by circles. Errors are shown at 68% confidence (David, 1997).

clusters. The gas mass in the ICM is also highly correlated with the luminosity from ellipticals and lenticulars present in the cluster. The total mass in the hot-gas component of the ICM ranges from 2×10^{13} to 5.2×10^{14} solar masses within a 3 Mpc radius: this corresponds very roughly to a gas density of 10^{-3} atoms cm^{-3} . If one includes the X-ray emitting gas in groups and clusters in the luminous mass, the ratio of total gravitating mass to luminous mass decreases significantly between galaxies and rich clusters. This has the unexpected result that a greater fraction of the gravitating mass is observable in rich clusters than in individual galaxies. David (1993) showed, by including the mass of MACHOs in galaxies in the baryonic mass, that the baryon-mass fraction is essentially consistent among galaxies, groups, and clusters.

Studies of the effect of clumpiness of the ICM suggests clumping only overestimates ICM gas fraction $< 20\%$ (Mathiesen et al. 1999).

The x-ray emission from galaxy clusters is generally interpreted as due to thermal bremsstrahlung in hot gas (gas temperature within 10^7 – 10^8 K); the observations of the temperature profiles of the hot gas are consistent with the gas itself being in hydrostatic equilibrium. Poor clusters have low central density, low gas mass and low temperature, whereas rich clusters have high central density, high gas mass and high temperature. The ICM mass-temperature $M_{\text{ICM}} - < T_x >$ relations was derived by Mohr et al. (1999) for a sample of 45 galaxy clusters. It is a mild dependence of ICM mass

fraction f_{ICM} on $\langle T_x \rangle$, the clusters with ICM temperatures below 5 keV have a mean ICM mass fraction $\langle f_{\text{ICM}} \rangle = 0.160 \pm 0.008$, which is significantly lower than that of the hotter clusters $\langle f_{\text{ICM}} \rangle = 0.212 \pm 0.006$ (90% confidence intervals).

The hot diffuse component of the ICM peaks at the center of the cluster and falls off with distance from the center, and the x-ray emission can be traced out to a distance of 3 Mpc. It is enriched with heavy elements: x-ray satellite observations done in the late 1970s revealed the presence of heavy-element emission lines in the x-ray emission associated with clusters. The elemental abundances of O, Ne, Mg, Si, S, Ca, Ar, and Fe for four clusters of galaxies (Abell 496, 1060, 2199, and AWM 7) were determined by Arnaud et al. (1996) from X-ray spectra derived from ASCA. Since the gas in the outer parts of the cluster is optically thin and virtually isothermal, the abundance analysis is very straightforward compared to the analysis of stellar or H II region spectra. Arnaud et al. (1996) found that the abundance ratios of all four clusters are very similar. The mean abundances of O, Ne, Si, S, and Fe are 0.48, 0.62, 0.65, 0.25, and 0.32, respectively, relative to solar. The abundances of Si, S, and Fe are unaffected by the uncertainties in the atomic physics of the Fe L shell. The abundances of Ne and Mg and to a lesser extent O are affected by the present uncertainties in Fe L physics and are thus somewhat more uncertain. The Fe abundances derived from the Fe L lines agree well with those derived from the Fe K lines for these clusters. The observed ratio of the relative abundance of elements is consistent with an origin of all the metals in Type II supernovae. More recent results (Dupke et al. 1999) of spatially resolved ASCA spectral analysis of A496, A2199, A3571 and Perseus. Mild, but significant, central abundance enhancements are found in each. The analysis of an ensemble of individual elemental abundance ratio indicates that ~50% of the intracluster iron near the centers of these clusters is from Type Ia supernovae.

It is a challenge for theory of enrichment of the ICM with products of stellar evolution. The iron yield needed to reproduce the typical observed iron mass over stellar mass ratio in a typical cluster turns out to be 5×10^3 which is 5 times larger than that measured for the Milky Way galaxy. The conclusion is that one cannot account for the iron mass in the ICM using standard iron mass yield, i.e. that of our Galaxy. This implies that there was a high supernova activity in cluster galaxies in the past, either a much higher past average SNI rate as compared with the present value observed in ellipticals (at least a factor 10) or a high SNII rate (Arnaboldi, 2000). The presence of large numbers of Type II supernovae during the early stages of evolution of

cluster galaxies is a very strong constraint on all models of galaxy and chemical evolution and implies either a very flat initial mass function or bimodal star formation during the period when most of the metals were created.

Chemical evolution models, which make use of bimodal star formation or a higher SNII rate, are able to predict the iron masses (typically of the order of 10^{12} solar masses) in the ICM, but the total ejected masses of gas are always an order of magnitude smaller than the observed ones (Matteucci & Vettolani, 1988). This would imply that the bulk of gas observed in the hot x-ray emitting component of the ICM has a primordial origin, i.e. it is pristine material produced during the big bang and was never used to form stars. The agreement between the prediction of the chemical evolution model for early-type galaxies and the observed heavy element content of the ICM is based on the assumption that there had been a complete mixing of the galactic heavy-element-enriched gas with the unprocessed ICM gas on a time scale shorter than the age of the Universe.

Another constraints comes from the observed trend of increasing gas mass fraction between groups (poor clusters) and rich clusters. The efficiency of galaxy formation could not be greater in groups compared to rich clusters since groups and clusters produce the same light per unit mass (David & Blumental, 1992). If groups and clusters are closed systems (i.e., they retain all gas shed by evolving stars), then $M_{\text{gas}}/M_{\text{stars}}$ should be a constant. Since this is contrary to observations, groups cannot be closed systems and must have experienced significant gas loss. (David 1997).

Very recent observations (see e.g. Arnaboldi et al. 2002) have shown that direct detection of individual stars in the ICM is possible. Studies of the ICM in the Virgo and Fornax clusters have detected several hundreds of point-like emissions from individual stars in their post-AGB phase of planetary nebulae. The planetary nebulae are very easy to detect because their nebular outer shell encircling the central star emits nearly 15% of the total energy from the central star in the [O III] emission line at 5007 Å: by simply taking an image through a narrow-band filter centered at the planetary nebulae redshifted [O III] emission and in its adjacent continuum, it has been possible to identify nearly a hundred planetary nebulae emissions in nearby clusters. Simulations based on the overall number of detected planetary nebulae emissions and the properties of their luminosity function in early-type galaxies indicate that the diffuse stellar component in the ICM can contribute up to 50% of the total light emitted by galaxies in the Virgo and Fornax clusters. The detailed spatial distribution of this diffuse stellar component

is not known yet on the Mpc scale, and its distribution may be related to the origin of this ICM component itself. Tidal interactions between galaxies in a cluster are expected to be frequent and cause galaxies to lose a substantial fraction, 30–70%, of their stars to the cluster potential where they become the stellar component of the ICM. Because this diffuse component would then originate from tidal tails, one expects its spatial distribution to be quite inhomogeneous. The debris can be relaxed in the cluster core but the further out one goes, the more unrelaxed the population might become.

3. Mechanisms of interaction of galaxy and IGM

Galaxies and pregalactic stars (if they exist) and IGM are closely evolutionary interrelated. Mechanisms responsible for interrelations can be separated in two groups according to the "direction" of influence: galaxies \rightarrow IGM and IGM \rightarrow galaxies. In first group I include ionization of the IGM by stellar radiation and massive black holes in central parts of galaxies, heating of the IGM (not only by ionization but also via hot wind), and replenishment the IGM with (chemically processed) matter (accretion, infall). In second group there are processes of providing galaxies with (chemically different) matter, dynamical stripping of gaseous component of galaxies and dynamical friction that could play significant role in structural evolution of clusters of galaxies (e.g. formation of gravitational leader in a clusters – cD galaxy (Gorbatskii, 1984)). I do not consider violent exchange processes during the close galactic encounters (collisions). In this section I only discuss mechanisms important for chemical evolution of galaxies and the IGM: galactic wind, expelling of dust and briefly comment on other mass loss and mass gain mechanisms.

3.1. Galactic wind

The galactic wind is believed to be produced by multiple supernovae events in galaxies. Galactic winds in elliptical galaxies play an important role in the evolution of the interstellar medium in these systems. According to conventional theory at early stages massive SN explosions lead to sweeping out of remaining gas and stopping star formation. High intensity rate of the outflow will pollute the surroundings with metals. The impact of supernova-driven galactic winds on the formation and evolution of galaxies depends on how well the high-velocity gas in the wind can couple to the rest of the gas in the galaxy and its halo. Numerical simulations demonstrate that this coupling will generally be rather poor, as the wind tends to follow the shortest path to vacuum. As a result, winds will

generally not carry off great amounts of mass from a galaxy, but may carry substantial amounts of kinetic energy and metals generated in the supernova explosions driving them. If galactic winds escape their host galaxies and impact the intergalactic medium (IGM) then probes of the diffuse IGM, such as the Lyman-alpha forest, should reflect this tremendous energy input. Surprisingly, simulations that do not include winds accurately reproduce the observed Lyman-alpha absorption properties. On the other hand, metal-line observations indicate that the low-density IGM has been polluted with metals (presumably via galactic outflows).

There are numerous observations of the galactic wind. I just mention one, which evidences for galactic wind developing at very early stages of galactic evolution. Dawson et al (2002) report the serendipitous detection in high-resolution optical spectroscopy of a strong, asymmetric Ly β emission line at $z=5.190$. The detection was made in a 2.25 hr exposure with the Echelle Spectrograph and Imager on the Keck II telescope through a spectroscopic slit of dimensions $1 \times 20''$. The progenitor of the emission line lies in the Hubble Deep Field-North northwest flanking field, where it appears faint and compact. The Ly-alpha line profile shows the sharp blue cutoff and broad red wing commonly observed in star-forming systems and expected for radiative transfer in an expanding envelope. The Ly α profile is consistent with a galaxy-scale outflow with a velocity of $v > 300 \text{ km s}^{-1}$. This value is consistent with wind speeds observed in powerful local starbursts (typically $10^2 - 10^3 \text{ km s}^{-1}$).

Most authors are dealing with the galactic winds from ellipticals, starburst galaxies (wind is expected to be very might from these) and dwarf galaxies. Dwarf galaxies are very numerous and low gravitational potential makes easier the expelling of hot metal enriched material into the IGM. In next section we will discuss the role of disk galaxies in enrichment of the IGM with heavy elements. These will be based on the model of blow-out presented by Igumenshchev et al. (1990). Based on this model we estimated metal mass loss rate due to wind as $-0.01 M_{\odot} \text{ yr}^{-1}$ (Shustov et al., 1997). Relative efficiency of loss strongly depends on the mass of galaxy. The dependence on mass of galaxy is presented in Fig. 7 from paper of Wiebe et al. (1999), in which oxygen and iron mass loss rate are compared with estimates of David et al. (1991) and Matteucci & Gibson (1995) for ellipticals. As we see metal mass loss rate from spiral galaxies is quite comparable with that from ellipticals. It is important that according to our model the mass loss rate from unit of the disk area for same galaxy varies depending on radial distance. In outer part of disk galaxies it is higher. Observationally it is supported by larger radii of supershells at

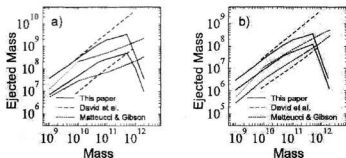


Figure 7: Dependence of theoretical oxygen (a) and iron (b) ejected masses on the mass of a galaxy for spirals (Wiebe et al 1999) and ellipticals (David et al. 1991, Matteucci et al. 1995).

larger distances from galactic center. However for some galaxies decrease of star formation activity in galactic outskirts can reduce this effect.

3.2. Dust expelling from galaxies

Recent studies have proven that dust is an important constituent of intergalactic matter. In particular, the emission spectra of quasars have been found to exhibit intergalactic absorption bands that are also typical of the interstellar extinction curve and that are commonly explained by the presence of graphite grains in the interstellar medium (Chens et al. 1991). Data on a few clouds of intergalactic dust obtained from direct observations of grain infrared radiation are presented by Wszolek & Rudnicki (1990).

Outside galaxies the conditions necessary for dust to be formed – low temperature and high gas density – are not fulfilled. Therefore, one has to assume that dust produced in galaxies is brought to the intergalactic space by one or several mechanisms. The sweeping of dust out of galaxies as they move through the intergalactic gas or dust motion driven by the intergalactic wind have been proposed for such mechanisms. The latter is discussed by Faber and Gallagher (1976) who argued that this mechanism can be efficient only in elliptical galaxies. Alton et al. (2000) observed dust outflows from quiescent spiral disks. They have conducted a search for «dust chimneys» in a sample of 10 highly-inclined galaxies. They have procured B-band CCD images for this purpose and employed unsharp-masking techniques to accentuate the structure of the dust lane. Three of these galaxies possess numerous curvi-linear chimney structures stretching up to 2 kpc from the midplane and the fraction of total galactic dust contained in such structures is of order 1%. Optical extinction offers a lower limit to the amount of dust contained in the extraplanar layer but, by examining the transparent sub-mm thermal emission from NGC 891 the limit was fixed of 5%. These results are consistent with a similar recent study by Howk & Savage (1999) which

indicates that about half of quiescent spiral disks possess detectable dust chimneys.

Starburst galaxies also reveal the presence of dust in circumgalactic vicinity. Alton et al. (1999) presented SCUBA images of the nearby, starburst galaxies NGC 253, NGC 4631 and M82 (primarily at wavelengths of 450 and 850 μm). The existence of a dust outflow along the minor axis of M82 and make a similar (but somewhat more tentative report) for the other two galaxies NGC 253 and NGC 4631. The scale-size of the «vertical» features is 0.7–1.2 kpc. A mass of $10^{6-7} M_{\odot}$ is inferred for the outflowing grains in M82. This amount of grain material could either have accrued from an inflow along the disk (e.g. a bar) or, if the lower mass limit applies, have been synthesized by massive stars in the starburst. The ejected grains are probably travelling close to the escape velocity of the host galaxy and assuming, hypothetically, that they do manage to breach the halo Alton et al. (1999) expect superwinds to expel up to 10% of the dust residing in interstellar disks into the intergalactic medium.

The motion of dust under the action of radiation pressure is most commonly considered in the vicinity of individual stars, notably the Sun. Only a few authors have explored the possibility of large-scale motion of dust caused by this mechanism. The problem of the possible blowing of dust out of galaxies by radiation pressure from stars is raised by Pecker (1974) who concluded that the radiative force on dust does not exceed the gravitational attraction and cannot result in large-scale sweeping of dust out of galaxies. Having considered this possibility, Chiao et al (1972) reached an opposite conclusion; however, they used a simplified galaxy model. This process has been more thoroughly studied in Ferrara et al. (1991). The authors considered the motion of graphite and silicate grains under the effect of the total radiation field and the gravitational field of a spiral galaxy. It was important results of their calculations that dust grains can be raised by this mechanism to a considerable height above the galactic

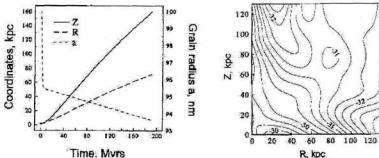


Figure 8: Left panel: Evolution of radius a , radial distance R and height Z of silicate grain; right panel – density distribution of silicate grains (Shustov&Wiebe 1995).

disk in a time of the order of 10^6 yr, virtually escaping into the intergalactic space. However, many important points are only outlined in this paper or are not treated at all. The entire study was carried out for a single dust grain, and no detailed analysis of the motion of dust as an assembly of grains characterized by a size distribution and an initial number-density distribution was given. Furthermore, underestimated values of the interstellar gas density (0.1 cm^{-3} at the Galactic center) were used to integrate the equation of motion of the grain, resulting in the effects of braking processes and dust destruction being underestimated. Shustov and Wiebe (1995) improved this approach and included all considered factors. They calculated the density distribution of dust near a spiral galaxy (for definiteness, near the Milky Way) established as a result of its sweeping by radiation pressure from stars. This mechanism is most efficient for grains with radii of $(0.7-2) \times 10^{-3}$ cm, which escape into the intergalactic space mainly with velocities of the order of $1000-2000 \text{ km s}^{-1}$. Grains with smaller radii also leave the disk but are completely destroyed at distances of the order of $30-70$ kpc. Graphite grains are swept out of the Galaxy more effectively, because they are less prone to destruction. In Fig. 8 evolution of silicate dust grain and dust density field at high z are shown. The rate of mass loss from the Galaxy in the form of dust is estimated for the Milky Way as $-0.04 M_{\odot} \text{ yr}^{-1}$. This value should be decreased (3-5 times) because of Lorenz force in magnetic field of the Milky Way. The role of magnetic field is hard to estimate because of poorly known structure of the field. The latter conclusion is confirmed by the fact that our values of dust density ($10^{-22}-10^{-21} \text{ g cm}^{-3}$) in the circumgalactic space are consistent with observations.

It is important that effectiveness of dust expelling depends on the galactic mass similar to that for the wind. For low mass galaxy $5 \times 10^9 M_{\odot}$ it is 5 times relatively higher while for massive galaxy $10^{11} M_{\odot}$ becomes negligible.

3.3. Other mechanisms

Ram pressure by ICM causes stripping of interstellar matter from galaxies. Since Gunn&Gott (1972) introduced the concept of ram pressure stripping this mechanism has been invoked to explain different observational phenomena, such as HI deficiency of spiral galaxies in clusters (Giovanelli & Haynes, 1985) and low star formation activity (Dressler et al. 1999). Many theoretical studies of this process were made e.g. Farouki&Shapiro (1980), Kritsuk (1984). A comprehensive analysis of physical processes of interaction of galaxies with IGM was done by Gorbatskii (1986) and I will comment only on some recent results. Vollmer et al. (2001) investigated the role of ram pressure stripping in the Virgo Cluster using N -body simulations. Radial orbits within the Virgo Cluster's gravitational potential are modelled and analyzed with respect to ram pressure stripping. The N -body model consists of 10,000 gas cloud complexes that can have inelastic collisions. Ram pressure is modeled as an additional acceleration on the clouds located at the surface of the gas distribution in the direction of the galaxy's motion within the cluster. Several simulations were made, changing the orbital parameters in order to recover different stripping scenarios using realistic temporal ram pressure profiles. It was demonstrated that ram pressure can lead to a temporary increase of the central gas surface density. In some cases a considerable part of the total atomic gas mass (several $10^9 M_{\odot}$) can fall back onto the galactic disk after the stripping event. A quantitative relation between the orbit parameters and the resulting HI deficiency is derived containing explicitly the inclination angle between the disk and the orbital plane. It is concluded that the scenario in which ram pressure stripping is responsible for the observed HI deficiency is consistent with all HI 21 cm observations in the Virgo Cluster.

Gas flows in galaxies are fundamental ingredients for studying their chemical evolution. More-

over the formation of galaxy itself in accretion mode can be considered as intensive infall. There are direct observations of infall of HI clouds onto galaxies. Oort in 1970 first (see in Matteucci 2001) discussed the possibility of matter infalling onto the disks of spiral galaxies. He envisioned that the penetration into the Galaxy of extragalactic neutral gas clouds with very high velocities ($V_{\text{VHVC}} > 140 \text{ km-sec}^{-1}$) can trigger the formation of high velocity clouds (HVC; $80 < V_{\text{VHVC}} < 140$) when they interact with galactic matter and suggested that the present time infall rate onto the Galaxy should be of the order of $1 M_{\odot} \text{ yr}^{-1}$. Mirabel and Morras (1990) presented observations at 21 cm of HI in the direction of the galactic anticenter showing that a stream of VHVC has reached the outer Galaxy and is interacting with galactic matter. Their HI survey provided evidence for the accretion of gas onto the Galaxy at very high velocities: more than 99% of the VHVC in the direction of the galactic anticenter and 84% of the VHVC in the inner Galaxy have negative (approaching) velocities. Mirabel and Morras (1990) derived from a survey of VHVC a total infall rate onto the galactic disk of $0.2-0.5 M_{\odot} \text{ yr}^{-1}$. Estimates of the infall rate should be regarded as still uncertain. Chemical composition of the high velocity in models is typically assumed to be primordial.

4. Modeling galactic evolution

In recent years, various models have been widely used for the study of the evolution of galaxies (see a comprehensive book of Matteucci (2001). Basic equations of any model include the conservation laws of mass of gas and mass of i -th element. Four basic processes are used to be taken into account: star formation, the return of gas to the interstellar medium by evolved stars, the accretion of intergalactic gas, and the ejection of matter into the intergalactic space. For multi-zone models additional terms describing transfer and interaction between zones should be added.

I will not analyze all model approaches. Modern numerical models are complex codes, which include to some extent all the approaches (stellar dynamics, gas dynamics, chemical evolution) and are able to produce impressive evolutionary scenario. Very impressive is quick progress in N-body and SPH technique is developing quickly (see e.g. Klypin et al. 1999, Berzik 1999, Westera et al. 2002). Nevertheless basic principles of all models are same and for quick look some simple and clear model remains a useful instrument. Below I demonstrate some results, obtained with a simple model ("our model") which includes most important ingredients of chemo-dynamical evolution of the galaxy. For details see Shustov et al.(1997) and Wiebe et al.(1998). The dynamic basis of the

model is the idea proposed by Firmani and Tutukov (1992), who assumed that the thickness of the gaseous disk is determined by two competing processes: the input of energy from supernova explosions and the dissipation of energy in cloud-cloud collisions. This assumption makes it possible to obtain the halo-disk transition in a self-consistent manner and to avoid artificial assumptions about the character and rate of accretion onto the gaseous disk from the halo. Later basic improvements to the model were the inclusion of galactic mass loss in the form of stellar wind and due to the sweeping out of dust grains by stellar radiation pressure as it was described in the previous section.

All models typically have a large number of free parameters. It is desirable to check the agreement with observations of «final» (current) characteristics of a galaxy, and data on evolution of similar galaxies with time. In studies of our Galaxy, it is customary to use G-dwarf problem and

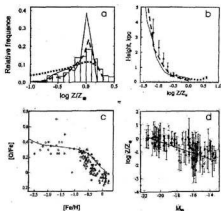


Figure 9: General test results obtained with model (Shustov et al.(1997) and Wiebe et al.(1998) for the Galaxy: a) The calculated metallicity distribution for stars (dashed curve) compared to the data of the catalog of Cayrel de Strobel (1992), estimates for Simple close model (dots) an close model with dynamically changing half thickness of the disk (solid line); b) The observed metallicity (filled circles) as a function of height above the disk plane (Grenon 1990). The calculated dependence is shown by the solid line – for closed model, dashed line – for our model; c) The observed $[O/Fe]$ - $[Fe/H]$ relations from (Barbuy 1988, 1989) (circles) and (Edvardson (1988) (triangles). The solid line corresponds to the chemical composition obtained in our model; d) Dependence of iron abundance on galactic luminosity. Observations – from Brodie&Huchra (1991); our model is shown by solid line.

the «age-metallicity» relation for this purpose. However, the latter test is not conclusive: the wide spread of age and metallicity determinations for galactic objects makes it impossible to sufficiently constrain the choice of model parameters. In Fig. 9 some general test results obtained with our model for the Galaxy are shown.

As it can be seen from Fig. 9, our model reasonably well passed the tests. Now I briefly comment some items related to the topic of the paper: enrichment of the IGM and radial gradients of chemical composition in the disk galaxies.

5. Enrichment of the IGM with heavy elements by galaxies

As it was discussed above the studies of quasar absorption lines reveal that the low-density intergalactic medium (IGM) at $z \sim 3$ is enriched to between 10^3 and 10^2 solar metallicity. This enrichment may have occurred in an early generation of Population III stars at redshift $z > 10$, by protogalaxies at $-6 < z < -10$, or by larger galaxies at $-3 < z < -6$. One introduces the episodes of pre-galactic star formation as a possible explanation for the widespread existence of heavy elements (such as carbon, oxygen and silicon) in the IGM. Evolution of massive PopIII stars is now popular subject to investigate. In our Galaxy we never observed such stars, though this research direction seems to be promising. Nevertheless galaxies remain to be believed as the most effective producers of metals.

It is recent tendency that model appear in which chemical evolution of galaxies and the IGM are followed in consistent way starting from cosmological simulations. Aguirre et al. (2001) constructed a model (cosmological simulation), to which they add a prescription for chemical evolution and metal ejection by winds, assuming that the winds have properties similar to those observed in local starbursts and Lyman break galaxies. Aguirre et al (2001) found that winds of velocity $v > 200-300 \text{ km s}^{-1}$ are capable of enriching the IGM to the mean level observed, although many low-density regions would remain metal free. Calibrated by observations of Lyman break galaxies, their calculations suggest that most galaxies at $z > 3$ should drive winds that can escape and propagate to large radii. The primary effect limiting the enrichment of low-density intergalactic gas in their scenario is then the travel time from high- to low-density regions, implying that the metallicity of low-density gas is a strong function of redshift.

As we discussed in Section 2.2 measurements of the chemical compositions of distant objects-quasars and galaxies-show that their heavy element abundances are high and do not increase appreciably as z decreases, i.e. with approach to the current epoch (Pettini et al. 1997). This is usually taken as

evidence that most of the heavy elements in galaxies were synthesized shortly after the formation of the galaxies, on a very short timescale of the order of 10^3-10^6 yr . The high rates of heavy-element formation at high z should correspond to high SFRs ($> 100 M_{\odot} \text{ yr}^{-1}$ for a massive galaxy) and large bolometric luminosities exceeding the current luminosities by an order of magnitude or more.

The early activity of star forming galaxies: heating and outflows from dwarf galaxies can substantially influence on the subsequent formation of larger galaxies and on chemical evolution of the IGM. E.g. Scannapieco (2001) using semianalytic and numerical techniques, showed that the winds identified with high-redshift low-mass galaxies may strongly affect the formation of stars in more massive galaxies that form later. Winds typically strip baryonic material out of pre-virialized intermediate mass halos, suppressing star formation. More massive halos trap the heated gas but collapse later, leading to a larger characteristic metallicity. This scenario accounts for the observed bell-shaped luminosity function of early-type galaxies, explains the small number of Milky-Way satellite galaxies relative to standard CDM prescriptions, and provides a reasonable explanation for the lack of metal-poor disk stars in the Milky Way and in other massive galaxies.

Elliptical galaxies are widely assumed to be the primary source of heavy elements in the intracluster medium (ICM), with a role of other morphological types being negligible. In this paper we argue that contribution of spiral galaxies into the chemical evolution of the ICM is also important. This statement rests upon our recent calculations of the heavy element loss from a disk galaxy, invoking two mechanisms: hot steady-state galactic wind and dust expulsion by the stellar radiation pressure. This model reproduces main properties of our Galaxy and, being applied to galaxies of various masses, describes well the observed correlation between spiral galaxy mass (luminosity) and metallicity. In our model this correlation develops as a result of the mass dependence of both loss mechanisms, in the sense that less massive galaxies lose metals more efficiently. We showed that a typical disk galaxy is nearly as effective in enriching the ICM as an elliptical galaxy of the same mass.

We calculated integrated mass of O and Fe ejected by spiral galaxies in a galactic cluster (Fig. 10). To assess the overall production of O and Fe in disk galaxies one has to integrate mass of the element ejected from a single galaxy over the galactic mass function. It is now widely assumed that the present galactic luminosity function (LF) can be described by Schechter (Schechter 1976) law with reasonable accuracy. We take Schechter function in its original form, assuming that the spiral luminosity function

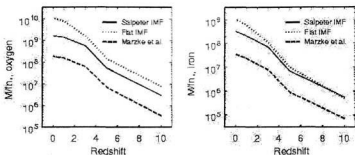


Figure 10: Integrated oxygen (a) and iron (b) ejected mass vs. redshift for different choices of stellar and galactic mass function: f – share of spirals, n , – richness of cluster according Schechter (1996). From Wiebe et al. (1999).

is proportional to it (universality of LF for all morphological types was recently argued by Andreon (1998) and Marzke et al. (1998)).

We demonstrated that "effective" loss (per unit luminosity) from spiral galaxies is only slightly lower than loss from ellipticals. The dominant role of early-type galaxies in rich clusters is caused by that they outnumber spirals. We present some observational arguments to this point, based on recent determinations of the ICM abundances, emphasizing the fact that the ratio of total iron mass to cluster luminosity does not depend on the fraction of cluster spirals in a wide range of the latter, contrary to what one might expect if they do not contribute into the ICM heavy element abundance.

In recent years the problem of mixing attracts attention of researchers. Ferrara et al. (2000) emphasized that from one side galaxies are believed to be primary sources of heavy elements injected into the IGM, however from the other side it remains still far from being clearly understood what mechanisms spread metals over Mpc scales from parent galaxies. Many open questions related to a production of heavy elements and enrichment of the IGM with them are discussed by Shchekinov (2002).

6. Radial gradient in the Galaxy

In most disk galaxies, negative radial gradients of abundances of heavy elements are observed. This has been the subject of many observational and theoretical studies (see reviews of Pagel (1977), Henry&Wortney 1999)). In the disk of our Galaxy, all the most abundant elements (C, N, O, Ne, S, Fe, Ar, Al) show radial gradients (see e.g. Fig. 11) The gradients for many types of objects with ages from 10 to 10⁸ Myr within R–5–15 kpc of the Galactic center (open clusters, HII regions, planetary nebulae, B stars) have similar values of -0.04 to -0.08 dex kpc⁻¹. However, the uncertainties are fairly high, even if we consider a single element and

type of object. For example, estimates of the oxygen abundances in HII regions vary from -0.13 to -0.05. Nevertheless, it can be considered well established that heavy element abundances are a factor of two to five higher in the central part of the Galaxy than at its periphery. The similarity between the gradients inferred from young and old objects indicates that they do not depend significantly on age, at least during most of the Galaxy's lifetime. For other disk galaxies gradients of about -0.03 to -0.1 dex kpc⁻¹ are typical (Kennicutt & Garnett 1994, Garnett et al 1997, van Zee et al. 1998), so that the Milky Way is typical in this respect. Recent results of Andrievski et al. (2002a) of determination the galactic abundance gradient in the range 6-11 kpc using most accurate data on 77 galactic Cepheids brought similar estimates though even more recent determination of metallicity using Cepheids at galactocentric distances 4–6 kpc (of Andrievski et al. (2002b)) revealed that radial metallicity distribution is more likely bimodal: it is flatter in the solar neighbourhood and steepens to the center starting from -6.5 kpc.

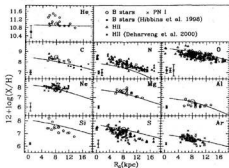


Figure 11: Chemical gradients in MW disk (from Hou et al. 2000)

There have been many attempts to explain the origin of radial gradients of chemical composition. The «static» models (i.e., including only star formation and the return of gas to the interstellar medium by evolved stars) fail to reproduce the gradients: it is necessary to take into account gas motions in one way or another. The dynamical factors involved can be subdivided into two groups: (1) accretion at a rate that depends on time and galactocentric distance and (2) radial gas flows in the galactic disk.

The first hypothesis is especially popular, since introducing accretion makes it possible to simultaneously resolve the "G-dwarf problem". To reproduce the observed gradients, we must assume that the time scale for accretion depends on galactocentric distance R , so that gas accumulates at the center of a galaxy and heavy elements are produced at a higher rate there (Portinari&Chiosi 1999, Chiappini et al. 1997, Pranzos&Boissier 2000). The accreting gas could originate from (1) the galactic halo (in this case, accretion corresponds to the ongoing formation of the disk) and (2) matter swept up by the galaxy as it moves through the intergalactic medium. Kennicutt (1996) summarized arguments against sustained gas infall onto the Galactic disk. Modern observational data can be reconciled with the accretion scenario only if the accretion rate is much lower than the current star-formation rate. Direct observations of gas accretion onto the Galactic disk are available only for individual high-velocity clouds and say nothing about the role in the disk's evolution played by the periodic accretion of such clouds. Even if these clouds provide an infall of intergalactic gas onto the disk at a mean rate of $0.5M_{\odot}\text{yr}^{-1}$, due to its episodic nature, this process cannot produce a regular and sustained heavy-element distribution across the disk. Moreover, the typical sizes of high-velocity intergalactic clouds (up to 25 kpc) substantially exceed the interval of Galactocentric distances where the gradient is observed (about 10 kpc). Another argument against a radial dependence of the accretion rate is that the accumulation of gas by a galaxy can be a self-regulating process. An enhanced accretion rate in the central region of a galaxy should lead to more active star formation and, consequently, to more intense energy release by young stars. This energy (e.g., in the form of galactic fountains and wind) can act against the infall of gas onto the disk, weakening the dependence of the accretion rate on R .

A possible alternative scenario to radially dependent accretion could be radial gas flows in the galactic disk. Lacey and Fall (1985) identified three main origins for the development of radial gas motions in a galactic disk: (1) infall onto the disk of a material with low angular momentum; (2) viscos-

ity of the gaseous disk; (3) gravitational interaction between the gas and spiral density waves. It has been shown that taking these processes into account together with radially dependent accretion can explain the development of chemical-composition gradients. However, thus far, radial gas flows lack a sound theoretical basis and must be artificially added to models. Moreover, to equalize the radial gas distribution and solve the G-dwarf problem, a model must include radially dependent accretion even if radial inflows are present.

We (Wiebe et al. 2001) used our model in two-zone modification. The galactic disk was divided in two parts (zones): zone A: $R=5$ kpc $M=0.5\times 10^{11}M_{\odot}$ and zone B: $R=5-15$ kpc $M=1.5\times 10^{11}M_{\odot}$. Four variants (models) were calculated:

- closed model (just to compare with, we name it standard or reference model),
- closed with dark matter as a parameter (just to try to stop some discussion concerning possible role of dark matter),
- open with radially dependent accretion (in zone A $M_{\text{infall}}=0$, in zone B $M_{\text{infall}}=2M_{\odot}/\text{yr}$. Such accretion rates are expected for a galaxy moving at a velocity of 100-300 km/s through intergalactic space of density $10^{-3}-10^{-4}\text{cm}^{-3}$, with capture efficiency 1). We assumed lowest metallicity $Z(\text{O,N})=0$ of accreted material. Note - extreme values were chosen. This was to make most favorable environment for this hypothesis)
- open with loss of heavy elements up to 30%, depending on radial distance.

Results are shown in Fig. 12., that presents its main characteristics: star formation rate (SFR) and abundances of oxygen Z_{O} and nitrogen Z_{N} as functions of time for the four variants of model. At the initial stage of the Galaxy's life, the gradient of the oxygen and nitrogen abundances is about 0.05 kpc^{-1} . This gradient arises because the initial density in the inner regions is a factor of three higher than in the outer regions. Combined with the adopted of the SFR on the gas density (Smidt law), this means that the time scale for star formation at the Galactic center is shorter than at the periphery, implying a faster accumulation of heavy elements at the center. Therefore, the closed model can adequately explain the chemical-composition gradient for old objects. However, the O-gradient disappears by the time the Galaxy reaches an age of $t\sim 3\times 10^9$ yr. The situation is similar for nitrogen; however, since this element is synthesized in long-lived, intermediate-mass stars, the nitrogen abundances in the outer and inner regions equalize at a later stage, when the Galaxy is $t\sim 5\times 10^9$ yr old. This absence of a gradient is typical of models in which the star-formation parameters (and the rate of gas accretion onto the disk) are independent of R (Portinari&Chiosi 1999).

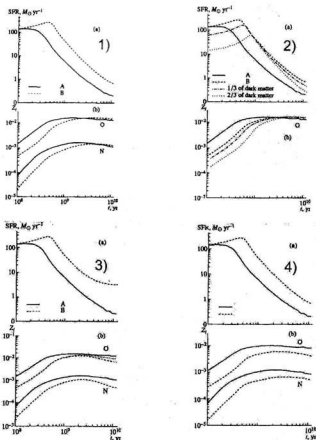


Figure 12: Star formation rate: panels (a) and abundance distributions for O and N: panel (b) for different variants of the evolutionary model (Wiebe et al. 2001 - 1) closed model; 2) closed model with dark matter; 3) model with radially dependent accretion; 4) standard model. The solid and dashed curves correspond to zone A and B respectively. See explanations in text.

A decrease in the gradient with time was also noted in models with radially varying accretion, such as those in paper of Pranzos&Boissier (2000).

The absence of any significant dependence of Z_O and Z_N on time in our model is due to the fact that we take into account the finite lifetime of stars. When the star formation rate decreases with time, the enrichment of the ISM with heavy elements synthesized in massive stars at late stages of the Galaxy's evolution is compensated by the supply to the ISM of gas with low Z ejected by long-lived, low-mass stars formed during the main episode of star formation and whose lifetimes are shorter than the age of the Galaxy. As a result, Z is maintained at an approximately constant level. The "asym-

ptotic" values Z_N and Z_O are determined by fixed parameters of stellar evolution and the shape of the IMF and are, accordingly, virtually the same in outer and inner regions. Evolution of of galaxy whose outer regions contain some mass fraction of dark matter is shown in panel 2). We considered two cases, with the dark mass fractions equal to one-third and two-thirds of the initial mass of the zone B. It is evident from the figure that the gradient increases during the initial evolution of the Galaxy; however, even in this case, it eventually levels off. Note that the adopted dark mass fractions for the disk are probably strongly overestimated and that, in reality, dark matter accounts for a much smaller fraction of the disk mass.

Results for the model with radially dependent accretion are shown in panel 3). In this case, the negative abundance gradients of both oxygen and nitrogen vary little throughout the evolution of the Galaxy, in agreement with observations. However, there are two arguments against this possibility. First, it is not obvious why accretion of intergalactic gas should be more efficient at the periphery than at the center of the Galaxy. Second, the metallicities of intergalactic gas (and of high-velocity clouds) are lower than the solar value but are not equal to zero. The dashed curve in Fig. 12 corresponds to the case when the value of Z_{in} and Z_{O} of the accreted gas is one-third of the current oxygen abundance in the ISM at any time. We can see that the gradient levels off with time, even if accretion is present. In panel 4) the curves for zone A again correspond to the standard case, while Model B assumes that 30% of the heavy elements synthesized in the disk of the Galaxy are ejected into the surrounding space via Galactic wind and the expulsion of dust by stellar radiation pressure. It is evident that these models are characterized by very constant gradients. This is due to the fact that a fixed fraction of heavy elements is ejected from the Galaxy at any given time.

Possible explanations of the negative gradient of chemical composition are not confined to accretion of gas and loss of heavy elements by the Galaxy. A similar gradient also develops if radially dependent star formation parameters are introduced into the model. For example, the IMF and the coefficient of proportionality in Schmidt law could depend on R . However, issues connected with quantitative estimates of these parameters are not sufficiently well understood to be included in realistic evolutionary models of the Galaxy and we, accordingly, do not discuss them further here.

Conclusion

Let me conclude very generally. Many problems remain still unsolved, new will appear, but we are under way to understanding of consistent evolution of galaxies – IGM system.

References

- Aguirre A., Hernquist L., Schaye J., Weinberg D.H., Katz N., Gardner J., 2001, *ApJ*, **560**, 599
- Alton P. B., Rand R. J., Xilouris E. M., Bevan S., Ferguson A. M., Davies J. I., Bianchi S., 2000, *A&AS*, **145**, 83
- Alton P. B., Davies J. I., Bianchi S., 1999, *A&A*, **343**, 51
- Andreon S., 1998, *A&A*, **336**, 98
- Andrievsky M., Kovtyukh V.V., Luck R.E., Lepine J.R.D., Bersier D., Maciel W.J., Barbuy, B., Klochkova V.G., Panchuk V.E., Karpishek R.U., *A&A*, **381**, 32
- Andrievsky M., Bersier D., Kovtyukh V.V., Luck R.E., Maciel W.J., Lepine J.R.D., Beletsky Yu.V., *A&A*, **384**, 140
- Barbuy B., 1988, *A&A*, **191**, 121.
- Barbuy, B. and Erdelyi-Mundes, M., 1989, *A&A*, **214**, 239
- Benson A. J., Cole S., Frenk C. S., Baugh C. M., Lacey C., 2000, *MNRAS*, **311**, 793
- Benson A. J., Pearce F. R., Frenk C. S., Baugh C., Jenkins A., 2001, *MNRAS*, **320**, 261
- Bertschinger E., 1998, *Ann.Rev.A&A*, **36**, 599
- Berzick P., 1999, *A&A*, **348**, 371
- Brodie J.P., Huchra J.P., 1991, *ApJ*, **379**, 157
- Burles S., Tytler D., 1999, *ApJ*, **499**, 699
- Carr B., 1994, *Ann.Rev.A&A*, **32**, 531
- Carr B.J., Rees M.J., 1984, *MNRAS*, **206**, 315
- Cayrel de Strobel G., Hauck B., Francois P., Thevenin F., Friel E., Mermilliod M., and Borde S., 1992, *A&AS*, **95**, 273
- Cen R., J. P. Ostriker J. P., 1999, *ApJ*, **514**, 1
- Chens F.H., Gaskell C.M., Koratkar A.R., 1991, *ApJ*, **370**, 487
- Chiao R.Y. and Wickramasinghe, N.C., 1972, *MNRAS*, **159**, 361
- Chiappini C., Matteucci F., Gratton R., 1997, *ApJ*, **477**, 765
- David L.P., 1997, *ApJ*, **484**, L11
- David L.P., Forman W., Jones C., 1991, *ApJ*, **380**, 39
- David, L. P., Blumenthal, G., 1992, *ApJ*, **389**, 510
- Dawson S., Spinrad H., Stern D., Dey A., van Breugel W., de Vries W., Reuland M., 2002, *ApJ*, **570**, 92
- Dressler A., Smail I., Poggianti B.M., Butcher H., Couch W.J., Ellis R.S., Oemler A.Jr., 1999, *ApJS*, **122**, 51
- Dupke R.A. White R. E. III, Arnaud, K. A. 1999, *Bulletin of the American Astronomical Society*, **31**, 700
- Durrer R., Novosyadly B., 2001, *MNRAS*, **324**, 560
- Edvardsson B., Andersen J., Gustafsson B., Lambert D.L., Nissen P.E., Tomkin J., 1988, *A&AS*, **102**, 603
- Faber S.M., Gallagher J.S., 1976, *ApJ*, **204**, 365
- Faruoki R., Shapiro, S.L., 1980, *ApJ*, **241**, 928
- Fardal M. A., Giroux M. L., Shull J. M., 1998, *Astron.J*, **115**, 2206
- Ferrara A., Ferrini F., Franco J., Barsella, B., 1991, *ApJ*, **381**, 137
- Ferrara A., Pettini M., Shchekinov Yu., 2000, *MNRAS*, **319**, 539
- Firmani C., Tutukov A., 1992, *A&A*, **264**, 37

- Fukugita M., Hogan C.J., Peebles P.J.E., 1998, *ApJ*, **503**, 518
- Garnett D.R., Shields G.A., Skillman E.D., Sagan S.P., Dufour R.J., 1997, *ApJ*, **489**, 63
- Gronen M., 1990, *Chemical and Dynamical Evolution of Galaxies*, Pisa: ETS Editrice, p. 26
- Giovaneli R., Haynes M.P., 1985, *ApJ*, **292**, 404
- Giroux M.L., Shull J.M., 1997, *Astron. J.*, **113**, 1505
- Gorbatskiy V.G., 1986, *Introduction in Physics of Galaxies and Cluster of Galaxies*, Nauka, Moscow, 256p
- Gunn J.E., Gott J.R.III, 1972, *ApJ*, **176**, 1
- Gunn J., Peterson B., 1965, *ApJ*, **142**, 1633
- Haardt F., Madau P., 1996, *ApJ*, **461**, 20
- Henry R.B.C., Worthey G., *Publ. Astron. Soc. Pacif.*, 1999, **111**, 919
- Hensler G., 1987, *Mitt. Astron. Ges.*, **70**, 141
- Hou, J. L.; Prantzos, N.; Boissier, S., 200, *A&A*, v. **362**, 921
- Howk J.C., Savage B.D., 1999, *Astron. J.*, **117**, 2077
- Hui L., Gnedin N.Y., 1997, Zhang Y, *ApJ*, **486**
- Igumenshchev I.V., Shustov B.M., Tutukov A.V., 1990, **234**, 396
- Kennicutt R.C., Garnett D.R., 1996, *ApJ*, **456**, 504
- Kennicutt R.C., 1996, *Proc. IAU Symp. No 171.*, Eds R. Bender, R.L. Davies. Dordrecht: Kluwer. p.11
- Klypin A., Kravtsov A.V., Valenzuela O., Prada F., 1999, *ApJ*, **52**, 82
- Kriss G.A., Shull J.M., Oegerle W., Zheng W., Davidsen A. F.; Songaila A.; Tumlinson J.; Cowie L. L.; Deharveng J.-M.; Friedman S. D.; Giroux M. L.; Green R. F.; Hutchings J. B.; Jenkins E. B.; Kruk J. W.; Moos H. W.; Morton D. C.; Sembach K. R.; Tripp T. M., 2001, *Science*, **293**, 1112
- Kritsuk A.G., 1984, *Astrophysics*, **19**, 263
- Lacey C.G., Fall S.M., 1985, *ApJ*, **290**, 154
- Lanzetta K.M., Wolfe A.M., Turnshek D.A., 1995, *ApJ*, **440**, 435
- Madau P., Haardt F., Rees M.J., 1999, *ApJ*, **514**, 648
- Marzke R.O., da Costa L.N., Pellegrini P.S., Willmer C.N.A., Geller M.J., 1998, *ApJ*, **503**, 617
- Mohr J.J., Mathiesen B., Evrard A.E., 1999, *ApJ*, **517**, 627
- Mathiesen B., Evrard A.E., Mohr J.J., 1999, *ApJ*, **520**, L21
- Matteucci F., Vettolani G., 1988, *A&A*, **202**, 21
- Matteucci F., Gibson B.K., 1995, *A&A*, **304**, 11
- Matteucci F., 2001, *The Chemical Evolution of the Galaxy*, Kluwer Academic Publisher
- Mirabel I.F., Morris R., 1990, *ApJ*, **356**, 130
- Mulchaey J. S., Davis D. S., Mushotzky R. F., Burstein D. 1996, *ApJ*, **456**, 80
- Pagal B.E.J., 1997, *Nucleosynthesis and Chemical Evolution of Galaxies*, Cambridge: Cambridge University Press
- Pecker J.C., 1974, *A&A*, **35**, 7
- Pettini M., Smith L.; King D. L.; Hunstead R.W., 1997, *ApJ*, **486**, 665
- Pichon C., Vergely, J.L., Rollinde, E., Colombi, S. Petitjean, P., 2001, *MNRAS*, **326**, 597
- Portinari L., Chiosi C., 1999, *A&A*, **350**, 827
- Prantzos N., Boissier S., 2000, *MNRAS*, **313**, 338
- Rauch M., 1988, *Ann. Rev. A&A*, **36**, 267
- Rees M.J., 1985, in "Cosmological Processes", eds, W.D.Arnett et al., *VNU Science Press Utrecht*, p.44
- Rubino-Martin J.A., Rebolo R., Carierra P., Clearly K., et al, 2002 astro-ph/0205367
- Scannapiesco E., 2001, *AAS*, **198**, 2001S
- Scott P.F., Cariera P., Clearly K., Davies R.D., et al, 2002 astro-ph/0205380
- Shchekinov Yu.A., 2002, Astro-ph/0205320
- Schechter P., 1976, *ApJ*, **203**, 297
- Shull J.M., Savage B.D., Morse J.A., Neff S.G., Clarke J.T., Heckman T., Kinney A.L., Jenkins E.B., Dupree A.K., Baum S.A., Hasan H., 1999, "The Emergence of the Modern Universe: Tracing the Cosmic Web (White paper of the UV-Optical Working Group (UVOWG))
- Shustov B., Wiebe D., 1995, *Astronomy Reports*, **39**, 650
- Shustov B., Wiebe D., Tutukov A., 1997, *A&A*, **317**, 397
- Taylor A.C., Carierra P., Clearly K., Davies R.D., et al, 2002 astro-ph/0205381
- Telfer R.C., Zheng W., Kriss G.A., Davidsen A.F. 2002, *ApJ*, **565**, 773
- Tripp T.M., Savage B.D., Jenkins E.B., 2000, *ApJ*, *Letts.*, **534**, L1
- van Zee L., Salzer J.J., Haynes M.P., O'Donoghue A.A., Balonek Th.J., 1988, *Astron. J.*, **116**, 2805
- Vollmer B., Cayatte V., Balkowski C., Dushl W.J., 2001, *ApJ*, **561**, 708
- Walker T. P., Steigman G., Schramm D. N., Olive K. A., Kang H., 1991, *ApJ*, **378**, 186
- Westera P., Samland R., Buser R., Gerhard O.E., 2002, *A&A*, **348**, 371
- Wiebe D.S., Tutukov A.V., Shustov B., 1998, *Astron. Zh.*, **75**, 1
- Wiebe D.S., Shustov B.M., Tutukov A.V., 1999, *A&A*, **345**, 93
- Wiebe D.S., Tutukov A.V., Shustov B.M., 2001, *Astronomy Report*, **45**, 854
- White S.D.M., Navarro J.F., Evrard A.E., Frenk C.S., 1993, *Nature*, **366**, 429
- Wzoielik B. and Rudnicki K., 1990, *The Galactic and Extragalactic Background Radiation*, *Proc. IAU Symp. No. 139*, 385
- Zheng W., Kriss G.A., Telfer R.C., Grimes J.P., Davidsen A.F., 1997, *ApJ*, **475**, 469

Наукове видання

Вісті Одеської астрономічної обсерваторії

Том 16 (2003)

Англійською мовою

Технічний редактор М. І. Кошкін

Підписано до друку 15.12.03. Формат 60x84/8.

Друк офсетний. Папір офсетний. Ум. друк. арк. 9,77. Тираж 300 прим. Зам. 528.

Видавництво і друкарня «Астропринт»

65026, м. Одеса, вул. Преображенська, 24.

Тел.: +38 (0482) 26-96-82, 26-98-82, 37-14-25.